Trade-offs of induced herbivore defense in *Nicotiana attenuata*: the role of early signaling and defense metabolite biosynthesis

by Lynn Ullmann-Zeunert

Gutachter:
1. Prof. Dr. Ian T. Baldwin, Jena

2. Prof. Dr. Ralf Oelmüller, Jena

3. Prof. Dr. Nicole van Dam, Nijmegen, Niederlande

Verteidigungstermin: 7.3.13 in Jena

Für meinen Mann und meine Eltern

Trade-offs of induced herbivore defense in *Nicotiana attenuata*: the role of early signaling and defense metabolite biosynthesis

Dissertation
zur Erlangung des akademischen Grades
doctor rerum naturalium (Dr. rer. nat.)

vorgelegt dem
Rat der Biologisch-Pharmazeutischen Fakultät
der Friedrich-Schiller-Universität Jena

von
Dipl. Biol. Lynn Ullmann-Zeunert
geboren am 20.02.1985, in Langenfeld

Table of Content

1. General Introduction

Induced herbivore defense

Herbivores and plants have co-evolved for 350 million years (Karban, 1997). During that time two main anti-herbivore defense strategies in plants developed: constitutive and inducible defense. Constitutive defenses are permanent independent of the presence of a herbivore, while induced defenses are only activated when herbivory occurs. Examples for constitutive defenses are physical barriers (thorns, cuticles, trichomes), while the reduction of photosynthesis (Kerchev, 2011), protein degradation (Brütting, 2012; Wünsche, 2005), reallocation of resources (Orians et al., 2011), biosynthesis and activation of trypsin-proteinase-inhibiores (TPIs) (Zavala and Baldwin, 2004), and the biosynthesis of several secondary defense metabolites (Jansen et al., 2009) are induced after herbivore attack. Plants produce an enormous variety of secondary defense metabolites after herbivore attack (Mendelsohn and Balick, 1995), such as terpenes, phenolics and N containing compounds (alkaloids, cyanogenic glycosides and glycosinolates). Metabolites which function as a repellent or toxin, are a direct defense, while volatile organic compounds (VOC) are mostly an indirect defense (Kant et al., 2009) strategy against herbivores because they attract the herbivores' enemies (Kessler and Baldwin, 2001).

The biosynthesis of many secondary defense metabolites is induced by jasmonic acid (JA), a phytohormone that accumulates rapidly directly after herbivore attack (JA-burst). JA triggers the activation of a complex signal transduction cascade leading to the transcriptional activation of several defense responses (Koo and Howe, 2009). The JA-induced responses are fine-tuned by other phytohormones such as ethylene (ET) and salicylic acid (SA) (Pieterse et al., 2009). In *Arabidopsis thaliana* ethylene treatment resulted in a transient increase of JA (Laudert and Weiler, 1998) and in *N. attenuata* ET suppressed the JA-induced nicotine production (Kahl et al., 2000; Winz and Baldwin, 2001). In contrast, SA acts antagonistic on JA-induced herbivore responses likely in a dose-dependent manner (Doares et al., 1995; Doherty et al., 1988; Pena-Cortes et al., 1993). This phytohormone is usually well known for its regulatory role in pathogen resistance, but many insects also induce JA and SA-related responses (Kant et al., 2008). Recent studies provide evidence for an ET-SA cross-talk after herbivore attack: ET suppressed SA accumulation in *N. attenuata* (Diezel et al., 2009a) and SA mediated signaling in Arabidopsis (Leon-Reyes et al., 2009). However, phytohormone signaling is more complex as other phytohormones such as abscisic acid, auxin, cytokinins,

brassinosteroids and gibberellins regulate parts of the herbivore defense signaling network (Erb et al., 2012; Pieterse et al., 2009).

Herbivores are perceived by plants through insect-derived elicitors such as fatty acid-amino acid conjugates (FACs) (Halitschke et al., 2001; Pohnert et al., 1999; Spiteller et al., 2004; Yoshinaga et al., 2007), inseptins (Schmelz et al., 2006; Schmelz et al., 2007) or caeliferins (Alborn et al., 2007). After herbivore perception, mitogen-activated protein kinases (MAPKs) are one of the earliest activated proteins. In *N. attenuata* (Wu, 2007), tomato and potato (Karban and Baldwin, 1997; Li, 2006) the salicylic-acid protein kinase (SIPK) and the wound-induced protein kinase (WIPK) or their homologues are at the end of this MAPK kinase cascade. In *N. attenuata* SIPK and WIPK activate a glycerolipase that produces free fatty acids which are the substrate of JA biosynthesis (Kallenbach et al., 2010). The following JA-burst induces changes in gene activity through a gene regulatory protein complex (Chini et al., 2007; Thines, 2007; Yan et al., 2009). One of the jasmonate induced defense genes is the well known transcription factor MYB8 that activates phenolamide biosynthesis.

In addition to the activation of herbivore defense in attacked leaves (local), plants also accumulate defensive compounds in non-attacked distal leaves (systemic). A signal transmits the "information of an herbivore attack" to the intact parts of the plant and activates a systemic response. Although the systemic response has been studied for 40 years, the mobile signal itself remains unidentified (Green and Ryan, 1972; Karban and Baldwin, 1997).

Costs of induced herbivore defense

Defense is costly for the plant because the plant invests limited resources into defense that would otherwise be available for growth or reproduction. Therefore, induced defense has been postulated to have evolved as a cost-saving strategy (Simms and Fritz, 1990) as resources are only invested when needed. Nevertheless, induced defense has been shown to reduce the plant's fitness in an herbivore free environment (Baldwin, 1998). Furthermore, several studies demonstrated the impact of herbivore density, presence of competitors and resource availability on the costs of defense (Agrawal et al., 2006; Baldwin, 1998; Baldwin and Hamilton, 2000; van Dam and Baldwin, 1998).

These costs are likely due to changes in resource allocation in response to herbivory because the plant's fitness optimization is a process of resource allocation (Baldwin, 2001). Therefore, several plant defense theories explain fitness-growth-defense trade-offs by predicting the method of resource allocation to different plant functions (reviewed (Stamp, 2003)). Recent studies have already shown a herbivory-induced resource reallocation (Gomez

et al., 2012; Schwachtje et al., 2006) to protect resources from herbivores. Nevertheless, the benefits and costs of this allocation are dependent on environmental conditions, and they are predicted to be related to life history, ontogeny and phonology of a plant (Orians et al., 2011).

Previous studies showed costs of induced defense mainly by manipulating JA-levels and measuring the impact on plant's seed production and biomass accumulation. Therefore, fitness effects induced by JA are well studied. For example, in Arabidopsis and tomato the application of JA reduced seed number (Cipollini, 2007; Redman et al., 2001) and also biomass accumulation in tomato. In *N. attenuata* and *Nicotiana sylvestris* the costs of JA induced defenses were more pronounced in plants grown in competition (Baldwin and Hamilton, 2000; van Dam and Baldwin, 1998), demonstrating that the competition for limited-resources has a high impact. JA-induced defenses are also mediated by resource availability within the plant. For example, protein biosynthesis that is important for growth competes with alkaloid biosynthesis for their common amino acid precursors (Hegnauer, 1988; Lindsey and Yeoman, 1983). Furthermore, JA downregulates genes expressing growth related proteins such as ribulose-bisphosphate-carboxylase-oxygenase (RuBisCO) or photosystem II (PSII) (Halitschke et al., 2003), which reduces photosynthesis capacity and thus available resources.

Studying the effect of defense on plant's fitness by manipulating JA levels only takes into account the costs caused by defense signaling and the responses downstream, but costs induced by earlier signaling are not considered. Furthermore, costs of single defense traits downstream of JA cannot be separated from effects caused by JA. Earlier studies have explored the costs of single defense traits by crossing cultivars that varied in their defense traits (Krischik and Denno, 1983), or by using wild plants with different genetically based defense levels (Berenbaum et al., 1986). Zavala and Baldwin (2004) were one of the first who studied the costs of a specific plant defense trait by manipulating a specific gene (Zavala and Baldwin, 2004; Zavala et al., 2004). Within this thesis, I used a variety of transgenic plants impaired in herbivory-induced defense responses to analyze the costs caused by JA signaling and a single plant trait (Manuscript III). Furthermore, I used plants silenced in *SIPK* and *WIPK* signaling to study their impact on plant's fitness (Manuscript I).

Quantifying the cost of defense for growth by measuring biomass accumulation does not discriminate between investments into storage, litter or even defense related processes (Chapin et al., 1990). Therefore, compounds of biomass that directly promote resource availability for growth, such as photosynthetic proteins, would be a better measure for

investment into this plant trait (Chapin et al., 1990). Already Mole (1994) outlined the difficulties to demonstrate resource based growth-defense trade-offs and recommended quantifying the allocation of a fitness-limiting resource to different plant traits (growth, reproduction and defense). Although a few studies addressed the problem by quantifying the allocation of nitrogen (N) to seeds, biomass and defense (Baldwin and Hamilton, 2000; Ohnmeiss and Baldwin, 1994; Van Dam and Baldwin, 2001), they did not take into account that the resource allocation to biomass does not discriminate between different plant functions. Furthermore, they only focused on the impact of a single defense metabolite, and did not consider the possible influence of different defense traits on resource allocation. In contrast, I analyzed the influence of different secondary metabolites on resource allocation and by using a photosynthetic protein as a measure for growth I was further able to quantify the direct resource allocation to plant growth (Manuscript III).

Nitrogen (N) as currency

N is a fitness-limiting resource for plants. It is needed for the biosynthesis of amino acids, proteins, nucleic acids and secondary metabolites. Plants store N in vacuoles in the form of nitrate, but they can also store the nutrient in the form of proteins. The enzyme essential for CO_2 fixation ribulose-1,5-bisphosphatecarboxylase/oxygenase (RuBisCO), which is build out of 8 large (LSU) and 8 small (SSU) subunits, is considered as a N storage protein (Millard, 1988) because it is the most abundant protein in plant leaves (Ellis, 1979), and its content correlates with N availability (Garciaferris and Moreno, 1994; Imai et al., 2008; Makino et al., 1984; Millard and Catt, 1988). Herbivory decreases levels of RuBisCO (Giri et al., 2006) which suggests the remobilization of N from RuBisCO after elicitation. Since RuBisCO expression additionally influences growth (Stitt and Schulze, 1994), RuBisCO is a good proxy to measure effects of defense on growth.

Since N intensive metabolites have a high N demand (Baldwin et al., 1994a) and JA decreases a plant's competitive ability for N assimilation (van Dam and Baldwin, 1998), N reserves contained in the plant after herbivore attack can be limited and makes a N allocation from N storage, such as RuBisCO, to defense likely. Furthermore, the N allocation within the plant is influenced by the N availability in the soil: In *Eucalyptus cladocalyx* the N allocation to cyanogenic glycosides, N containing defense metabolites, correlated with the N availability (Simon et al., 2010) and in the wild tobacco an increased N availability decreased the biosynthesis of N-intensive metabolites (Lou and Baldwin, 2004). Since N is an essential resource, plants have additionally evolved strategies to protect this limiting resource from

herbivores by allocating it to roots and storage tissues (Frost, 2008; Hanik et al., 2010; Meloni et al., 2012).

Due to the importance of N for plant growth and defense, it is a good fitness limiting resource to study growth-defense trade-offs in a common currency. I compared the N demand of defense with the N amount not available for growth by comparing the N-investment into both plant functions. Therefore, I defined N-intensive defense metabolites as a measure for defense and total soluble protein (TSP), with a special focus on RuBisCO, as a measure for growth. A ^{15}N-labeling experiment helped to study N partitioning between growth and defense within a defined N pool (Manuscript III).

Methods used for N quantification

In order to study growth-defense trade-offs in the common N currency, methods for simultaneous quantification of N and ^{15}N in N-intensive metabolites and proteins are required. Isotope-ratio mass-spectrometry combined with an elemental analyzer is a classical method for high precision quantification of isotope ratios and total N contents in plant tissues (Brand, 1996; Brenna et al., 1997). As this method requires 20 µg N for accurate measurements (micromass, datasheet 501 of Micromass IsoPrime^{TM} Stable Isotope Ratio Mass Spectrometer), it is less suitable for measuring samples with a low mass or low N content. It is highly suitable for the analysis of tissue samples, but has limited applicability to measure ^{15}N and total N in a single secondary metabolite or protein.

Small metabolites can be quantified on a UPLC-UV-Tof-MS (Gaquerel et al., 2010) that also allows the determination of total N by using the metabolite's specific N %, but not a direct ^{15}N-determination. The MS-spectrum dependents on the isotope composition of the corresponding compound, so that variations in isotope ratios cause shifts in the isotope pattern of a spectrum. Different approaches have been developed to determine the ^{15}N-incorporation in peptides based on the spectrum patterns (Jehmlich et al., 2008; MacCoss et al., 2005; Pan C., 2011; Snijders et al., 2005). One of them was recently modified to extend its applicability to the ^{15}N-determination of metabolites (Taubert et al., 2011).

Although methods for the quantification of ^{15}N-incorporation of peptides/proteins are available, a suitable MS-based method for the absolute quantification of ^{15}N-labeled protein has been lacking. Most existing MS-based quantification methods only allow the relative quantification of proteins because they compare peptide intensities of an unlabeled and a labeled sample set (Gouw et al., 2010; Kline and Sussman, 2010; Schaff, 2008; Schulze and Usadel, 2010). Available methods for absolute quantification are based on the intensity ratio

of the monoisotopic peak of a synthetically labeled standard peptide, which was spiked into the sample in known amounts, and the corresponding peptide of the protein of interest. In labeled samples, the peak intensities of the monoisotopic peak of a spectrum are altered, resulting in incorrect protein quantification. Therefore, the development of a method for absolute protein quantification in ^{15}N-labeled samples was required. In Manuscipt II, I describe the development of such a method.

Nicotiana attenuata, a model plant for studying trade-offs in a common N currency

The wild tobacco *N. attenuata* (Torr. Ex Watscon) is an annual plant germinating in a post fire inorganic N-rich environment in response to smoke-derived signals (Baldwin and Morse, 1994; Baldwin et al., 1994b). After a fire the wild tobacco produces monocultures in which the competition for N is high and even increases with time because 3 years after a fire the N supply in the soil decreases dramatically (Lynds and Baldwin, 1998). Therefore, the plants are highly selected for competitive ability for N assimilation. Furthermore, the monocultures are often the first food source for herbivores appearing after a fire, such as the solanaceous specialist *Manduca sexta*. The plants have developed sophisticated defense responses to quickly detect and prevent herbivore feeding (reviewed in (Wu and Baldwin, 2010)). In addition to the biosynthesis of C-rich compounds such as volatiles or diterpene glycosides (DTGs) (Heiling et al., 2010), the plant synthesizes N-rich secondary metabolites such as nicotine (Steppuhn et al., 2004), caffeoylputrecine (CP) and dicaffeoylspermidine (DCS) (Kaur et al., 2010) and invests N into TPIs (Zavala and Baldwin, 2004; Zavala et al., 2004) which inhibit proteases in the caterpillar's midgut. Field studies demonstrated the costs caused by the biosynthesis of N-intensive defenses (Abiko et al., 2010; Steppuhn et al., 2004; Zavala and Baldwin, 2004; Zavala et al., 2004). As N is a limited resource for the wild tobacco's growth and defense, and its defense signaling is well studied, this plant is the ideal model to study growth-defense trade-offs in a common N currency.

Aim of this thesis

As outlined above, induced defense reduces the plant's growth and fitness mainly due to the allocation of fitness-limiting resources to defense, reallocation of resources to roots and the downregulation of photosynthetic genes. Although the costs downstream and those mediated through JA are well studied, costs induced by early defense signaling upstream of JA still need to be explored. Furthermore, little is known about the regulation of fitness reduction after herbivory through early defense signaling and defense metabolite biosynthesis.

Resource based trade-offs are optimally studied by quantifying the partitioning of a fitness-limiting resource into the different plant functions. N is the optimal nutrient for such studies because it is essential for plant growth and defense. In this thesis, I explored the costs of early signaling and studied the regulation of resource allocation to growth and defense. I used transgenic plants impaired in defense signaling and N as common currency to answer the following questions:

- (Manuscript I) Does early herbivore defense signaling, specifically SIPK and WIPK, reduce the plants fitness? If yes, what are the growth-defense trade-off underlying mechanisms?
- (Manuscript II) How can N-investment and ^{15}N-incorporation into RuBisCO be quantified accurately similar to existing methods for defense metabolites? In this manuscript I describe the development of a method to quantify simultaneously ^{15}N-labeled proteins, their N content and ^{15}N-incorporation which is a necessary tool to answer the questions in Manuscript III.
- (Manuscript III) What is the role of N allocation in mediating trade-offs between growth and defense? Does the biosynthesis of N-intensive metabolites, such as phenolamides, influence this allocation? How high are the costs of N-intensive metabolite biosynthesis quantified in a common N currency compared to costs for growth?

2. Overview of Manuscripts

Manuscript I

BMC Plant Biology: accepted on 11.09.12, in press

MAPK-dependent JA and SA signaling in *Nicotiana attenuata* affects plant growth and fitness during competition with conspecifics

Stefan Meldau[1], Lynn Ullman-Zeunert[1], Geetha Govind, Stefan Bartram and Ian T. Baldwin

[1] These authors contributed equally.

In this manuscript, we analyzed the costs caused by early defense signaling by growing plants silenced in SIPK and WIPK in competition with WT. The data demonstrate that SIPK and WIPK mediate defense trade-offs by the regulation of JA and SA, whereby higher SA-levels partially masked the benefits caused by lower JA-level in SIPK-silenced plants. The plant performances, which were related to alteration in phytohormone levels, could not be explained by changes in photosynthesis or N assimilation. We concluded that early defense signaling is associated with large fitness costs, which are mediated by changes in phytohormone levels.

Meldau, S. designed and performed field experiments and one glasshouse experiments (Figure 1), drafted the introduction and main part of the discussion and submitted the manuscript. Ullmann-Zeunert, L. designed and performed the other glasshouse experiments, did all statistical analysis, prepared IRMS measurements, drafted the method and results part and the discussion about nitrogen assimilation and photosynthesis of the manuscript. Govind, G. established and performed *in vitro* seedling competition assays. Bartram, S. processed IRMS measurements. Baldwin, IT. designed field experiments and the seedling competition assay and revised the manuscript.

Manuscript II

Journal of Proteome Research (2012), 11, 4947-4960

Determination of ^{15}N-incorporation into plant proteins and their absolute quantitation: a new tool to study nitrogen flux dynamics and protein pool sizes elicited by plant-herbivore interactions

Lynn Ullmann-Zeunert, Alexander Muck, Natalie Wielsch, Franziska Hufsky, Mariana A. Stanton, Stefan Bartram, Sebastian Böcker, Ian T. Baldwin, Karin Groten and Aleš Svatoš

In this manuscript the development of a new LC-MS^E based method for simultaneous determination of ^{15}N-incorporation into proteins and their absolute quantification is described. We demonstrate that this approach has a high accuracy and precision, and it enables studying plant stress under ecologically relevant growth conditions. This method enables N flux studies and protein dynamic analysis in response to herbivory which are necessary to explore defense trade-offs in a common N currency.

Ullmann-Zeunert, L. designed and performed the experiments, prepared IRMS measurements, did protein analysis and drafted the manuscript, Muck, A. established the LC-MS^E measurements and processed half of the MS measurements. Wielsch, N. revised the manuscript and processed the second half of the MS measurements. Hufsky, F. programmed MoLE, and processed the extracted MS-spectra for further analysis. Stanton, M. designed and performed experiments. Bartram, S. processed IRMS measurements and gave helpful comments. Böcker, S. gave helpful comments for additional experiments and developed the final formula for protein quantitation. Baldwin, IT revised the manuscript and helped with design of the experiments. Groten, K. designed experiments, supported method development, and helped with the manuscript preparation. Svatoš, A. helped with method development, revised and submitted the manuscript.

Manuscript III

submitted to The Plant Journal at 30.10.2012

Quantification of growth-defense trade-offs in a common nitrogen currency: phenolamide production mediates herbivory-induced nitrogen reallocation to proteins in wild tobacco

Lynn Ullmann-Zeunert[1], Mariana Stanton[1], Natalie Wielsch, Stefan Bartram, Christian Hummert, Aleš Svatoš, Karin Groten, Ian T. Baldwin

[1] These authors contributed equally

In this manuscript we examined the influence of N-intensive metabolite biosynthesis on N allocation in response to herbivory by using transgenic lines impaired in JA defense signaling and phenolamide biosynthesis. N was used as common currency to measure growth-defense trade-offs at the same scale. The total N contents of the shoots indicated a N transport from the shoot to the roots influenced by phenolamide biosynthesis. A detailed analysis of N pools in systemic and local leaves of different age revealed a phenolamide biosynthesis mediated N allocation to proteins which is additionally influenced by the leaf type and age. A ^{15}N-pulse experiment revealed that N used for phenolamide biosynthesis in not coming from the putative N storage protein, ribulose-1,5-bisphosphatecarboxylaseoxygenase (RuBisCO).

Ullmann-Zeunert, L. designed and performed experiments, prepared IRMS measurements and did protein analysis; did statistical analysis and drafted the figures, methods, results and discussion of the manuscript and revised the introduction; Stanton, M. designed and performed experiments, prepared IRMS measurements and metabolite analysis; drafted the introduction and revised all other parts of the manuscript; Bartram, S. processed IRMS measurements; Wielsch, N. processed MS^E analysis. Hummert C. did correlation analysis and drafted heatmaps (Figure 4); Svatoš, A. helped with the MS^E measurements; Groten, K. designed experiments, and helped with manuscript preparation; Baldwin, I.T. helped with the design of experiments, preparing the manuscript and gave helpful comments.

2.1 Manuscript I

MAPK-dependent JA and SA signaling in *Nicotiana attenuata* affects plant growth and fitness during competition with conspecifics.

Stefan Meldau[1,2,3*], Lynn Ullman-Zeunert[1,2.3], Geetha Govind[2,3,5], Stefan Bartram[2,3,4] and Ian T. Baldwin[2*]

In press at BMC Plant Biology

[1]These authors contributed equally.
[*]To whom correspondence should be addressed.

[2]Max Planck Institute for Chemical Ecology
Hans-Knöll-Str.8
D-07745 Jena, Germany

[3]Department of Molecular Ecology,
[4]Department of Bioorganic Chemistry

[5]current address: Leibniz Institute of Plant Genetics and Crop Plant Research
Department of Molecular Genetics
Corrensstr.3
D-06466 Gatersleben, Germany

Short title: Costs of defenses in *Nicotiana attenuata*

Co-corresponding authors:
Stefan Meldau: Email: smeldau@ice.mpg.de; Phone: +49 (0)3641 57 1134
Ian T. Baldwin: Email: baldwin@ice.mpg.de; Phone: +49 (0)3641 57 1100

Abstract

Background: Induced defense responses to herbivores are generally believed to have evolved as cost-saving strategies that defer the fitness costs of defense metabolism until these defenses are needed. The fitness costs of jasmonate (JA)-mediated defenses have been well documented. Those of the early signaling units mediating induced resistance to herbivores have yet to be examined. Early signaling components that mediate herbivore-induced defense responses in *Nicotiana attenuata*, have been well characterized and here we examine their growth and fitness costs during competition with conspecifics. Two mitogen-activated protein kinases (MAPKs), salicylic acid (SA)-induced protein kinase (SIPK) and wound-induced protein kinase (WIPK) are rapidly activated after perception of herbivory and both kinases regulate herbivory-induced JA levels and JA-mediated defense metabolite accumulations. Since JA-induced defenses result in resource-based trade-offs that compromise plant productivity, we evaluated if silencing *SIPK* (ir*SIPK*) and *WIPK* (ir*WIPK*) benefits the growth and fitness of plants competiting with wild type (WT) plants, as has been shown for plants silenced in JA-signaling by the reduction of *Lipoxygenase 3* (*LOX3*) levels.

Results: As expected, ir*WIPK* and *irLOX3* out-performed their competing WT plants. Surprisingly, ir*SIPK* plants, which have the largest reductions in JA signaling, did not. Phytohormone profiling of leaves revealed that ir*SIPK* plants accumulated higher levels of SA compared to WT. To test the hypothesis that these high levels of SA, and their presumed associated fitness costs of pathogen associated defenses in ir*SIPK* plants had nullified the JA-deficiency-mediated growth benefits in these plants, we genetically reduced SA levels in ir*SIPK* plants. Reducing SA levels partially recovered the biomass and fitness deficits of ir*SIPK* plants. We also evaluated whether the increased fitness of plants with reduced SA or JA levels resulted from increased nitrogen or CO_2 assimilation rates, and found no evidence that greater intake of these fitness-limiting resources were responsible.

Conclusions: Signaling mediated by WIPK, but not SIPK, is associated with large fitness costs in competing *N. attenuata* plants, demonstrating the contrasting roles that these two MAPKs play in regulating the plants' growth-defense balance. We discuss the role of SIPK as an important regulator of plant fitness, possibly by modulating SA-JA crosstalk as mediated through ethylene signaling.

Key words: fitness costs, induced defense, MAPK, herbivory, *Nicotiana attenuata*, salicylic acid, jasmonic acid, ethylene, nitrogen, photosynthesis

Background

Plants have evolved effective defense strategies to ward off natural enemies, including pathogens and herbivores. Allocation of fitness-limiting resources to anti-pathogen and anti-herbivore resistance frequently imposes costs on plants, which are readily seen as reductions in plant growth and fitness. These fitness costs of defense production play a fundamental role in most plant defense theories (reviewed in Herms and Mattson, 1992). Instead of producing costly defense metabolites permanently, plants often activate defense pathways only in response to signals that implicate the presence of attackers. Such plastic defense pathways, so called induced defenses, are generally believed to have evolved as a resource-saving strategy (reviewed in Heil and Baldwin, 2002).

Fitness costs of induced resistance pathways are frequently evaluated by manipulating defense hormone levels, such as jasmonic acid (JA) and salicylic acid (SA), two hormones which respectively regulate major anti-herbivore and anti-pathogen defense responses (reviewed in Heil and Baldwin, 2002; Glazebrook, 2005; Boss et al., 2010). SA mediates plant resistance to biotrophic, hemibiotrophic pathogens and some piercing/sucking herbivores (Walling, 2009). Priming of SA-related defense responses increases disease resistance and plant fitness in the field (Traw et al., 2007). However, under pathogen-free conditions, maintaining the SA-pathway imposes a trade-off for plant growth and fitness when compared to plants with genetically reduced SA levels (Abreu and Munne-Bosch, 2009).

The jasmonate signaling cascade, including the wound hormone JA-isoleucine (JA-Ile), is widely considered to be a master regulator of plant resistance to arthropod herbivores as well as various pathogens (reviewed in Howe and Jander, 2008). Fitness costs imposed by the activation of JA-mediated defense pathways have been measured by treating plants with JA or by using plants altered in JA production or perception. Application of JA and SA reduces seed production and mutants with reduced sensitivity to these hormones tend to have higher fitness correlates in *Arabidopsis thaliana* grown under controlled conditions in a glasshouse experiment (Cipollini, 2002). When native populations of Coyote tobacco (*Nicotiana attenuata*) plants were treated with JA, the JA-mediated resistance traits proved to be costly for seed production in the absence of herbivore attack, but benefited plant fitness when plants were attacked by herbivores (Baldwin, 1998).

Upon herbivore or pathogen attack, endogenous SA and JA levels are strongly regulated by upstream signaling units that mediate defense responses to various attackers. To

understand if the ability to be inducible *per se* can result in fitness costs, we need to analyze the trade-offs in biomass and fitness correlates associated with the signaling units upstream of these phytohormone pathways. Following this approach, in *A. thaliana*, a single *R* gene (*RPM1*), which is involved in bacterial pathogen recognition, was demonstrated to result in large fitness costs to plants grown in the field (Tian et al., 2003). Similarly, it was shown that natural variation at a single genomic locus, involved in regulating SA and JA levels, can explain growth and resistance phenotypes of a large number of *A. thaliana* accessions (Todesco et al., 2010). Therefore, analyzing costs of such upstream regulators can help explain growth and defense polymorphism in natural populations. While these studies describe costs of *R* genes involved in resistance to pathogens, the costs of perception and signaling units mediating resistance to herbivores upstream of hormonal sectors remain unexplored.

In *N. attenuata,* one of its main natural defoliators, the lepidopteran larvae *Manduca sexta*, is perceived through fatty acid-amino acid conjugates (FACs) present in the insect's oral secretions (reviewed in Bonaventure et al., 2011). It was reported recently that FAC perception results in growth reductions in *N. attenuata* (Hummel et al., 2009), but the underlying mechanisms remain elusive. One of the earliest molecular events in FAC perception is the activation of mitogen-activated protein kinases (MAPK, Wu et al., 2007). MAPK activity is important for the induction of plant defense responses upon herbivore attack, including the regulation of various hormonal pathways (Figure 1). In *N. attenuata*, salicylic acid-induced protein kinase (SIPK) and wound-induced protein kinase (WIPK), as well as their homologues in tomato (*Lycopersicum esculentum*), cultivated tobacco (*N. tabacum*) and *A. thaliana* mediate the activation of defense-related hormonal responses in herbivory-induced tissues (Kandoth et al, 2007; Seo et al., 2007; Wu et al, 2007; Schäfer et al., 2011). Both, SIPK and WIPK, regulate wound and herbivory-induced JA and JA-Ile levels, whereas only SIPK regulates herbivory-induced ethylene (ET) levels in *N. attenuata* (Wu et al, 2007). LecRK1, which is an important negative regulator of herbivory-induced SA levels is also regulated by SIPK and WIPK (Gilardoni et al., 2011; Fig.1).

N. attenuata is an annual plant that grows in the immediate post-fire environment in the Great Basin Desert (Utah, USA) where it occurs in monoculture-like populations, surrounded by conspecific competitors. Because this environment is characterized by highly reduced nitrogen availability, synchronized seed germination and intense intra-specific competition, it represents the primordial agricultural niche. In such transiently resource-rich

environments, plants are strongly selected for competitive abilities which depend on maximizing the acquisition and the efficient use of acquired resources. In other words, plants are selected to maximize, and not to optimize, resource acquisition. In this manuscript, we analyzed the costs of maintaining and activating herbivory-induced signaling pathways when plants are grown under the intense resource competition conditions that the plants commonly germinate into in nature, using *SIPK* and *WIPK*-silenced *N. attenuata* plants.

We grew plants transformed with inverted repeat (ir) constructs for *SIPK* (ir*SIPK*) and *WIPK* (ir*WIPK*) in competition with wild type (WT) plants and analyzed plant growth and fitness parameters, with and without simulated herbivory. Quantifying true plant fitness requires the meaurements of reproductive success over multiple generations and is therefore difficult to assess. Here we measured flower and seed capsules numbers of plants competing with each other as parameters to assess the fitness consequences defense signaling pathways for plant fitness. Our data reveal that although both MAPK-silenced lines accumulated less JA after herbivory, only ir*WIPK* plants benefited from the reduced defensive state with higher biomass and fitness. Ir*SIPK* plants accumulated higher levels of SA and when these plants were crossed with oe*NahG* plants that overexpress bacterial salicylate hydroxylase (NahG), to lower free SA levels, we could partially recover growth and fitness parameters caused by SIPK silencing. Although both kinases are frequently reported to regulate common defense pathways, our data demonstrate that SIPK and WIPK regulate different signaling systems that regulate *N. attenuata*'s physiological reconfiguration after herbivore attack and its resulting fitness parameters.

Results

Silencing two herbivory-responsive MAPKs differentially affects plant growth under field and glasshouse conditions

Two mitogen-activated protein kinases, SIPK and WIPK, in *N. attenuata* have been shown to regulate herbivory-induced defense responses (Meldau et al., 2009). As defenses are costly and thought to incur trade-offs for plant growth and reproduction (Herms and Mattson, 1992), we evaluated if silencing *SIPK* and *WIPK* benefited plant growth and fitness. Growth was first analysed in transgenic ir*SIPK* and ir*WIPK* plants in a paired design with WT in their natural habitat in the Great Desert Basin in Utah, USA. Although both transgenic plants have similar reductions in their direct and indirect defenses in comparison to WT plants (Meldau et al, 2009), surprisingly, ir*SIPK* plants were significantly smaller than WT (Figure 2A, Welch

two sample t-test, p = 0.049), whereas ir*WIPK* plants grew similarly to competing WT plants (Welch two sample t-test, p-value = 0.17; Figure 2A). A table with all additional statistical values is provided in the supplemental material (Supplemental Table 1).

A similar experiment was carried out in the glasshouse under controlled conditions. Defense-related trade-offs in *N. attenuata* were only found when plants were growing in competition with conspecifics (Heil and Baldwin, 2002). Thus, we used a paired design of size-matched plants competing for the same resources in individual pots to analyze plant growth and fitness. As MAPK activity and JA-levels are highly induced during herbivore attack (Wu et al., 2007), we assumed that differences in growth and fitness would be more pronounced when the competing plants were elicited by a simulated herbivory treatment (wouding and application of *M. sexta* oral secretions, W+OS, see Material and Methods). In addition to ir*SIPK* and ir*WIPK*, we used JA deficient plants (as*LOX3*) (Halitschke and Baldwin, 2003, Meldau et al., 2009) with lower levels of anti-herbivory defense metabolites as "positive controls" as these plants should perform better in comparison to competing WT plants. The results of the glasshouse experiments were comparable with the results from the field. Independent of treatment, ir*SIPK* plants were smaller than WT and produced fewer capsules (Figure 2B), whereas ir*WIPK* plants and as*LOX3* plants produced significantly more dry mass and greater capsule numbers after treatments (Figure 2B). Although MAPK activity and JA levels are highly induced by W+OS treatments, the growth benefits in *WIPK* and *LOX3*-silenced plants were also observed in the absence of W+OS treatments, which suggests that plants are continuously challened by various environmental stresses that activate JA signaling (Fig. 2B).

In *N. attenuata*, simulated herbivory can already inhibit growth of seedlings (Hummel et al., 2009). To assess growth effects of *SIPK* and *WIPK*-silenced plants at the seedling stage, we performed an *in vitro* seedling competition assay (Additional Figure 1). Under untreated conditions, we did not find growth difference of seedlings (data not shown), whereas wound-induced *WIPK* (ANCOVA, $F_{5,344} = 20.79$, p = 0.049) and *LOX3* (ANCOVA, $F_{5,344} = 20.79$, p = $3.72e^{-07}$) grew faster than WT, while *SIPK*-silenced seedlings grew similarly (ANCOVA, $F_{5,344} = 20.79$ p = 0.95; Figure 2C). The biomass accumulation of *WIPK*- and *SIPK*-silenced seedlings reflected the trend found in the seedling root growth assay (Welch two sample t-test, p = 3.3e-04; Figure 2C). In summary, our data from three different growth assays demonstrated that silencing *WIPK* benefits plant growth and fitness, but that ir*SIPK* plants did not benefit from their JA deficiency.

Ir*SIPK* plants accumulate more SA in leaf tissues

SA is known to negatively influence plant growth and development (Vicente and Plasencia, 2011). A previous study demonstrated that leaves of ir*SIPK* plants grown in individual pots have higher basal SA-levels than do WT plants (see Supplemental Figure 4 in Kallenbach et al., 2010,). To test, if *SIPK*, *WIPK* or *LOX3*-silenced plants also have altered SA-levels when grown in experimental designs that included an intra-specific competitor, SA-levels were measured in untreated leaf tissues and 1 h after W+OS treatments. We found significantly higher SA-levels for ir*SIPK* plants independent of treatment (Welch two sample t-test, control: p =0.002; W+OS: p = 0.048) (Figure 3A). Of the other transgenic lines tested, only ir*WIPK* plants accumulated slightly less SA after W+OS treatments when compared to competing WT plants (Welch two sample t-test, p = 0.037). However, JA-levels of ir*SIPK*, ir*WIPK* and ir*LOX3* lines were greatly reduced after W+OS treatments compared to the corresponding WT (Figure 3B). We thus hypothesized that higher SA-levels may influence the growth and fitness phenotype of these JA-deficient plants. To test this hypothesis, ir*SIPK* plants were crossed with an overexpression (oe) salicylic acid hydroxylase (NahG) line (oe*NahG*; Hettenhausen et al, 2012). The crossed line, *SxN*, had SA-levels similar to WT (Figure 3A) and lower JA-levels when compared to the corresponding WT plants (Welch two sample T-test, p = 0.004; Figure 3B). Notably, JA levels were also reduced in oe*NahG*, when compared to the corresponding WT plants (Figure 3B). A previous report showed that oeNahG plants grown in single pots did not show any difference in JA levels 1h after W+OS treatments (Gilardoni et al., 2012) and we hypothesize that different growth conditions in our competition setup might have caused the altered accumulation of JA in the oeNahG line.

Reducing SA levels in ir*SIPK* plants partially restores the JA deficiency-mediated growth promotion found in JA-deficient plants

To investigate the influence of SA on ir*SIPK's* growth and reproduction, additional competition experiments including *SxN* and oe*NahG* plants were carried out. To combine the results of several experiments in a single graph, we calculated the relative differences between the two competing plants in one pot and expressed them relative to the WT plants used in the individual experiments (Figure 4A). Crossing ir*SIPK* with oe*NahG* resulted in a phenotype similar to plants deficient in JA and JA-mediated defenses (ir*WIPK* and ir*LOX3*). *SxN* plants had greater biomass (ANOVA, $F_{2,97}$=11.12, p =4.5e^{-05}; Figure 4B), a higher capsule count (ANOVA; Line: $F_{1,58}$ = 21.18, p = 2.32e^{-05}; Treatment: $F_{1,58}$ = 8.08, p = 0.006; Figure 4C) and

higher number of flowers (ANOVA; Line: $F_{1,58}$ = 45.90, p = $7e^{-09}$; Figure 4D) than their corresponding WT, whereas ir*SIPK* plants did not, indicating that higher SA levels are fitness-limiting factors in ir*SIPK* plants. Since *SxN* acccumulates less JA than oe*NahG* plants, we speculated that the cross would realize greater fitness benefits than the oe*NahG* plants. However, independent of treatment, *SxN* had a similar increase in growth and fitness when compared to their corresponding WT, as did oe*NahG* plants (Figure 4), indicating that silencing *SIPK* impairs growth and fitness in *N. attenuata* also via SA-independent pathways and that *SIPK*-silencing does not effect the *oeNahG*-mediated growth and fitness promotion.

In comparison to the data presented in Figure 2B, where ir*WIPK* plants accumulated significantly more biomass when plants were treated with W+OS, the experiments presented in Figure 4 revealed a constitutively higher biomass in ir*WIPK* plants, when compared to WT plants. In addition, the reduced biomass and seed capsule number is also less pronounced for ir*SIPK* plants, when data from both experiments are compared. These effects could be due to slightly different soil conditions between the two experimental set-ups (see Material and Methods).

Differences in photosynthetic rates do not explain growth and fitness differences of ir*SIPK*, ir*WIPK* and ir*LOX3* plants

Silencing of ribulose-1,5-bisphosphate carboxylase/oxygenase (RuBisCO) in *N. attenuata* leads to a decrease in photosynthetic rate and reduced plant growth and lower amounts of defense metabolites after treatment with simulated herbivory (Mitra and Baldwin, 2008). Photosynthetic rates are also influenced by herbivory (Kerchev et al., 2011), biotic stress (Bilgin et al., 2010) and plant hormone levels In particular exogenous SA application was shown to reduce photosynthetic activity by altering chloroplast structure (Uzunova and Popova, 2000), RuBisCO activity (Pancheva and Popova, 1998) and transcript levels of photosynthetic genes (Heidel and Baldwin, 2004). Thus, we hypothesized, that ir*SIPK* plants would show reduced growth and fitness compared to ir*WIPK,* ir*LOX3* and WT plants as a result of lower photosynthetic rates mediated presumably by its higher SA levels. However, ir*SIPK* plants had a similar or even higher photosynthetic rates than WT and the other transgenic plants (ANOVA, $F_{2,56}$=15.7, p = $3.9e^{-06}$) (Figure 5). Consistent with these results, reduced SA levels in *SxN* plants also did not result in increased photosynthetic rates compared to ir*SIPK* plants. These data indicate that 1) photosynthetic rates under these growth

conditions are independent of SA levels and 2) lower amounts of photosynthetic products can not explain why ir*SIPK* plants did not benefit from reduced JA-mediated defenses.

JA has been shown to down-regulate photosynthesis-related gene expression (Halitschke and Baldwin, 2003). Therefore, higher photosynthetic activity might support the growth and fitness of *WIPK* and *LOX3* silenced plants. But ir*WIPK* and ir*LOX3* plants – though they had similar reductions in JA levels compared to WT (Figure 3B) - showed the opposite patterns of photosynthetic rates (Figure 5), and even had a lower photosynthetic activity compared to WT. Therefore, we conclude that the growth promotion of ir*WIPK* and ir*LOX3* plants is not mediated by improved CO_2 assimilation.

Leaf JA and SA-levels do not influence competitive ability for nitrogen aquisition

In addition to photosynthetic rates, the availability of nitrogen influences growth and defense of plants. Under low nitrogen regimes, *N. attenuata* plants grew slower and had lower levels of nitrogen-intensive defense compounds than plants grown under high nitrogen levels (Lou and Baldwin, 2004). Furthermore, when grown in competition, plants impaired in the production of trypsin proteinase inhibitors (TPIs), a JA-induced nitrogen-intensive defense, produced more seed capsules and were taller than their neighbouring WT plants (Zavala and Baldwin, 2004). Based on these results, ir*SIPK*, ir*WIPK* and ir*LOX3* plants were expected to forgo the costs nitrogen investments in nitrogen-intensive defense metabolites (Halitschke et al, 2003, Meldau et al, 2009). Several lines of evidence suggest that JA (van Dam and Baldwin, 1998) and SA (Nazar et al, 2011, Sarangthem and Singh, 2003) can influence the plant's nitrogen assimilation and metabolism. Based on these findings, we evaluated if the differences in growth of the three transgenic lines compared to WT were due to altered competitive availabilities for nitrogen acquisition. We grew the three transgenic lines and WT in competition pairs and pulse-labeled the pots with nitrogen in form of $K^{15}NO_3$. Although ir*WIPK* and ir*LOX3* plants showed higher total nitrogen content than WT plants before wounding (ANOVA, $F_{2,102}$=29.25, p = 9.1e^{-11}; Figure 6A), after this treatment they showed a similar nitrogen content as WT. In addition, all transgenic lines incorporated similar amounts of ^{15}N compared to their corresponding WT plants (ANOVA, $F_{5,94}$ = 0.98, p = 0.44; Figure 6B) and only *SxN* showed a treatment effect (Welch two sample t-test, p= 0.009). Moreover, seeds of all transgenic lines had similar total N and ^{15}N contents (Supplemental Figure 2). Therefore, we conclude that JA and SA levels in leaves do not correlate with nitrogen uptake and content under these growth conditions. However, we cannot exclude that the growth and

fitness phenotype of ir*WIPK*, ir*LOX3* and ir*SIPK* was influenced by an altered nitrogen allocation towards growth and reproduction, once the nitrogen was incorporated by the plant.

Discussion

Activation of MAPKs is one of the earliest molecular events in response to herbivore perception (Wu et al., 2007). In this study, a reversed genetics approach was used to analyse if maintaining two herbivory-induced MAPKs, namely NaSIPK and NaWIPK, confer fitness costs to a native tobacco species. Our data show that, although silencing these two MAPKs abolished herbivory-induced JA production, which is known to impose fitness costs on plants, only *WIPK*-silenced plants benefited from these reductions in terms of increased growth and fitness. These results suggest that in addition to JA signaling and JA-associated defenses, SIPK and WIPK regulate different suits of physiological responses after the perception of herbivory, responses that have profound effects on a plant's ability to maximize their fitness. One of these responses is SA signaling.

SIPK and WIPK silencing differentially effects SA levels

SIPK and WIPK have frequently been shown to regulate similar responses to biotic and abiotic stresses (Tena et al., 2011). Both MAPKs redundantly regulate defense responses and wound and herbivory-induced JA/JA-Ile levels in tomato and *N. attenuata* (Kandoth et al., 2007; Wu et al., 2007; Meldau et al., 2008). In *N. attenuata*, both kinases regulate transcript levels of genes important for defense against herbivores (Wu et al., 2007) including LecRK1, which is crucial for herbivory-induced downregulation of SA (Gilardoni et al., 2011). Interestingly, only SIPK-, but not WIPK-, silencing led to elevated SA levels; WIPK even accumulated slightly less SA in leaves after simulated herbivory, suggesting that regulation of LecRK1 transcripts is not responsible for the differential accumulations of SA levels (Fig. 3B). Silencing *SIPK*, but not *WIPK*, impaires herbivory-induced ET levels in *N. attenuata*. Similarily, only plants deficient in MPK6, the homologue of SIPK in *A. thaliana*, but not MPK3 (WIPK homologue)-deficient plants show reduced herbivory-induced ET levels (Wu et al., 2007; Schäfer et al., 2011). Diezel and colleagues demonstrated that *N. attenuata* plants impaired in ET biosynthesis or perception accumulated higher levels of herbivory-induced SA; similarily, SA-mediated signaling is suppressed by ET in *A. thaliana* (Diezel et al., 2009; Leon-Reyes et al., 2009).Collectively, these results suggest that the increased SA levels in SIPK silenced plants are a result of impaired ET signaling. Future

experiments designed to recover ET emissions in SIPK silenced plants will help to understand the role of ET in mediating the SA phenotype in ir*SIPK* plants.

Can increased SA mask JA-mediated trade-offs in ir*SIPK* plants?

JA- and methyl-JA-induced responses were reported to negatively affect growth and fitness in several plant species (Redman et al., 2001, Cipollini 2007, Baldwin 1998) and plant productivity was enhanced when JA levels or JA/JA-Ile sensitivity were genetically reduced (Cipollini 2002, Royo et al., 1999). Reducing JA levels also increased plant growth and fitness in *WIPK*- and *LOX3*-silenced *N. attenuata* plants (Figure 2 and 4). In contrast, ir*SIPK* plants which showed the highest reductions in herbivory-induced JA levels (Figure 3), did not benefit in terms of growth and fitness. Inhibition of JA-induced defense responses by negative crosstalk through higher SA levels has been intensively studied (reviewed in Pieterse et al., 2009). In *N. attenuata*, elevated SA levels were found to strongly suppress defense responses to herbivores (Gilardoni et al., 2011, Diezel et al., 2009). Although oe*NahG* plants did not show differences in basal SA levels, which is consistant with data presented in Gilardoni et al., 2012, the oe*NahG* plants still produced more biomass and fitness when compared to competing WT plants. It is possible that SA levels in other tissues than leaves might be reduced in oe*NahG* plants. Future experiments designed to analyze the SA levels in other tissues, such as roots, might shed light on this phenomenon. By crossing ir*SIPK* with oe*NahG* plants, we tested if higher SA levels could mask the JA deficiency-mediated growth benefits in SIPK silenced plants. Although *SxN* plants showed similar SA levels when compared to oe*NahG*, the cross accumulated significantly less JA (Figure 3). However, the elevated biomass and fitness of oe*NahG* plants was not further increased by JA-deficiency in *SxN*, demonstrating that SA-independent pathways might also be involved in suppressing growth benefits in JA-deficient ir*SIPK* plants. Although we did not observe developmental abnormalities in response to *SIPK*-silencing, these plants might also have other pleiotropic effects, which may influence plant growth and fitness. For example, it was shown that silencing the NaSIPK-homolog MPK6 in Arabidopsis effects stomata patterning (Bush and Krysan, 2007; Wang et al., 2007, 2008). In *N. attenuata*, stomata size and density of ir*SIPK* plants are similar to that of WT plants (data not shown). Future studies designed to identify specific phosphorylation targets regulated by SIPK will help to elucidate its important role in plant growth and fitness regulation.

Mechanisms of JA- and SA-mediated plant growth suppression

Contrasting effects of SA on photosynthesis have been described (Pancheva et al., 1996; Pancheva and Popova, 1998; Slaymaker et al., 2002; Fariduddin et al., 2003; Abreu et al., 2009), whereas JA is thought to affect photosynthesis-related gene expression negatively (Halitschke and Baldwin, 2003). We did not find a clear correlation between SA or JA levels and photosynthetic rates using our set-up (Figure 5). Since our measurements are just spatiotemporal snapshots, we cannot rule out that photosynthesis and SA or JA levels are correlated at other growth stages or in different tissues.

Another important trait for plant growth under resource-limited conditions is the ability to assimilate nitrogen, a trait that was shown to be altered by JA-treatments in competing *N. sylvestris* plants (Baldwin and Hamilton, 2000). However, similar to our photosynthesis measurements, we did not find clear patterns of nitrogen uptake that would explain the growth phenotypes of all JA and SA deficient lines (Figure 6, Supplemental Figure 2). Our data do not exclude changes in nitrogen metabolism as a growth promoting factor. All transgenic lines with reduced JA-signaling showed lower levels of nitrogen-intensive defense metabolites than did WT (Halitschke and Baldwin, 2003, Meldau et al., 2009) which may allocate nitrogen resources towards growth and reproduction. Baldwin (2001) discussed fitness optimization as a process of resource allocation and demonstrated that the biosynthesis of nicotine, a JA-induced nitrogen-intensive defense metabolite, can slow growth (Baldwin et al, 1998). JA-induced partitioning of newly fixed carbon and nitrogen into additional secondary metabolite pathways was recently described in *N. tabacum* (Hanik et al, 2010a,b) which may lead to an additional reallocation of resources. Further experiments with detailed analysis of different nitrogen pools are required to fully understand the role of nitrogen partitioning in mediating growth and fitness of plants with and without JA and SA perturbations.

In addition to the regulation of metabolite fluxes, SA and JA can also affect developmental processes through the regulation of hormonal pathways. SA can regulate growth through modulation of cell expansion, probably via auxin, (Scott et al., 2004; Xia et al., 2009) and might regulate the cell cycle through its crosstalk with cytokinin and brassinosteroid pathways (Riou-Khamlichi et al., 1999; Hu et al., 2000). JA was also shown to effect plant growth through the regulation of the cell cycle and cell number in *Arabidopsis* (Zhang et al., 2008). Thus, the alteration of other hormonal pathways might also influence the growth patterns reported here for *N. attenuata* plants with altered MAPK, JA and SA levels.

Costs of inducibility

We hypothesized that growth and fitness trade-offs imposed by MAPK signaling will only occur when plants were elicited by simulated herbivory since this treatment highly activates SIPK and WIPK. With the exception of *SIPK*-silenced plants, all other transgenic lines, including *LOX3*-silenced and oe*NahG* plants, produced more dry mass and capsules even without simulated herbivory (Figure 2 and 3). These data demonstrate that basal levels of WIPK activity, JA or SA impairs growth and fitness of competing *N. attenuata* plants. In their natural enviroment, the synchronized germination of *N. attenuata* plants in the first growing season following fires, which in turn results from the detection of smoke-derived germination cues, leads to high intraspecific competition (Baldwin et al. 1994) and our growth setup was designed to capture this natural environmental stress. However, competition with conspecifics may have induced WIPK activity, JA or SA levels in other tissues than leaves, such as their root systems. Therefore the reduced levels of defense traits in other tissues might have caused increased growth and fitness in the control, unelicted plants. Comparing defense traits in different tissues, such as roots, of *N. attenuata* plants grown in single pots with plants in competition will help to answer these questions.

Several studies have demonstrated that herbivore attack changes a plant's photosynthetic capacity (Baldwin and Ohnmeiss, 1994; Walling, 2000, Hermsmeier et al, 2001; Kessler and Baldwin 2002, Halitschke et al., 2011), and that photosynthetic proteins are commonly downregulated (Giri et al, 2006). Our data suggest that the JA and SA mediated costs for growth and fitness are independent of photosynthetic regulation, but we can not exclude that WIPK activity directly influences photosynthetic activity, as our data have shown lower photosynthesis in unelicited ir*WIPK* plants (Figure 6). Furthermore, ir*SIPK*, ir*LOX3* and ir*WIPK* plants showed a treatment effect on their photosynthetic activity (Figure 5). Therefore, LOX3, SIPK and WIPK activities likely play multiple roles in the regulation of herbivory-induced photosynthesis.

In contrast to their photosynthetic rates, control ir*WIPK* plants as well as ir*LOX3* plants had significantly higher total nitrogen contents in their rosette leaves compared to their corresponding WT plants (Figure 6). These findings indicate, that costs of basal levels of WIPK and LOX3 activity may be amortized by increases in nitrogen resources.

The life history of *N. attenuata* plants may necessitate basic levels of SA, JA and WIPK activity, which come with the cost of reduced growth and capsule production. WIPK and JA-mediated defenses are elicited by attack from the multitude of herbivores that feed on

this plant in nature and these defenses use fitness-limiting resources for their production. However, the importance of SA-mediated defense responses in *N. attenuata* are only poorly understood. Our study suggests that maintaining the SA sector must play an important role for fitness of *N. attenuata* not only by moderating JA induced responses, and that SIPK joins two other components shown to suppress SA responses during OS elicitation, response that allow for unfettered JA-mediated defense production: the ethylene burst (Diezel et al. 2009) and LecRK1 (Gilardoni et al., 2011). Analyzing the performance of *N. attenuata* plants with different levels of SA under natural conditions are needed to identify the fitness enhancing factors require the clearly costly SA pathway.

Conclusions

In this study, we analyzed the fitness consequences of maintaining signaling elements that mediate early herbivory-induced defense responses in native tobacco, *Nicotiana attenuata*. Our data demonstrate that two herbivory-induced MAPKs, NaSIPK and NaWIPK, show strongly diminished JA levels, but only *NaWIPK*-silenced plants benefited from these reduced defense responses with increased growth and fitness levels during our competition experiments. We demonstrate that *irSIPK*-plants do not realize the fitness benefits that are commonly enjoyed by JA-deficient plants, partially because Na*SIPK*-silencing leads to higher levels of SA. Photosynthesis and nitrogen acquisition rates can not explain the growth differences in our setup, indicating that the observed growth phenotypes are rather mediated by resource allocations or signaling mediated growth reductions. Future experiments are needed to identify the specific metabolic pathways by which SA- and JA-signaling divert resources from growth and reproduction. For this analysis identifying the other regulatory targets of SIPK will be essential. Herbivory-induced MAPK activity and JA signaling was shown to vary in natural accessions of *N. attenuata* (Wu et al., 2008; Schuman et al., 2009; Kallenbach et al., 2012) and the natural variation in the SA pathway is currently being analyzed. Determining the costs of the MAPK, JA and SA-mediated pathways for plant growth and fitness contributes to our understanding of the ecological mechanisms behind the genetic variation in these induced defense signaling systems.

Acknowledgements

We thank Shiva Jung Pandey and Willi Brand for technical support; Karin Groten, Matthias Erb, Dorothea Meldau and Michael R. Zeunert for helpful comments on the manuscript,

Brigham Young University for use of its awesome field station, the Lytle Ranch Preserve, and the Max Planck Society for funding.

Material and Methods

Plant growth conditions

Germination: Wild-type *Nicotiana attenuata* Torr. Ex. Watson seeds of the 30th (field and first glasshouse experiment, Figure 1) and 31th (other experiments) inbred generations of an accession which originated from seeds that were collected at the Desert Inn Ranch in Utah 1988 (Baldwin et al., 1998) and seeds of different transgenic lines, were sterilized and germinated on Gamborg's 5 media according to Kruegel et al. (2002). For each of the constructs, several independently transformed, homozygous lines harboring single insetions with similar phenotypes, are available and have been fully characterized. For practical reasons, we only used one of the previously described ransgenic lines. The transformed lines used in this study have been previously characterized in the following publications: ir*SIPK* (A-109) and ir*WIPK* (A-56) were described in Meldau et al., 2009; oe*NahG* (A-481) in Meldau et al., 2011, Hettenhausen et al., 2012 and Gilardoni et al., 2012; as*LOX3*(A-300) in Halitschke and Baldwin, 2003; ir*LOX3* (A-562), in Allmann et al., 2010. After using as*LOX3* plants in the first experiments, we used newly generated ir*LOX3* plants, because of their more pronounced reduction in JA levels (22-50% reduction of the OS-elicited JA burst in as*LOX3* (Halitschke and Baldwin, 2003), 81-83% in ir*LOX3* (Allmann et al., 2010, as compared to WT plants).

Glasshouse: For glasshouse experiments the plants were transferred to Teku pots ten days after germination. Ten days later the plants were planted into 2L competition pots. A transgenic plant was always paired with a WT plant. Pots with two WT plants were used as comparison. Plants were grown at 26–28 °C under 16 h of light as described by Kruegel et al. (2002). The glasshouse experiment in 2010 was performed with the following modifications: Frühsdorfer Nullerde was used as substrate with additional 0.5 g/L PG Multimix (14, 16 and18 days after transfer to 2L pots), 0.85 g/L phosphate, 0.05 g/L Micromax (Scotts), 0.35 g/L$MgSO_4 7H_2O$ added to the soil. As fertilizer, Peters Allrounder (Scotts) was added (20 g/400 L day7-14, 40 g/400 L day 14-21, 15-30 g/400L after day 21) with an additional amount of Borax (3 g/400 L day 1-7, 2 g/400 L day 7-14, 1 g/400 L after day 14). To perform the experiments under nitrogen-limiting conditions, external nitrogen supplementations were stopped after plants were transferred to 2L pots in all experiments.

Field: Field experiments were carried out as described by Meldau et al. (2009). In brief: seedlings were transferred into hydrated peat pellets fifteen days after germination. After gradual adaption to the local environmental conditions over 14 days, ir*SIPK* and ir*WIPK*, each paired with one size-matched WT plant, were transplanted into an irrigated field plot at the Lytle Ranch Preserve. The release of transgenic plants was carried out under APHIS notification (06-242-101 n). Growth was measured 30 days after transplantation to the field.

Plant treatment and performance measurements

Eight days after transfer to 2L competition pots, each plant pair was pulse-labelled with 10.2 mg (5.1 mg ^{15}N and 5.1 mg ^{14}N) nitrogen as KNO_3 (Chemotrade, Leipzig; Merck). Three days later- giving the plants time to assimilate the labeled nitrogen- the oldest sink leaf, youngest source leaf and transition leaf, were wounded (W) with a pattern wheel and the puncture wounds immediately treated with 10 µL 1:5 diluted *Manduca sexta* oral secretion (OS) (W+OS) over 3 consecutive days in order to simulate continuous herbivore feeding damage. This treatment effectively mimics herbivore attack and allows for uniform induction kinetics (Halitschke et al., 2001).

The oldest sink leaf at the time of labeling was harvested 8 days after the first treatment, while samples of untreated plants were used as controls. When all plants were elongated and prior to bud formation (6 days after the last treatment), S1 leaves were wounded and treated as described for rosette leaves. The flowers, both open and closed, and capsules were then counted between day 63 and 65 after germination. The plants were harvested 12 days later and oven dried for 3 days to determine the dry mass.

In vitro seedling growth assay

WT and transgenic lines (ir*WIPK*, ir*SIPK* and ir*LOX3*) of *N. attenuata* used in the glasshouse experiments were used for seedling growth assays. The seeds were sterilized and germinated (Kruegel et al., 2002) on full strength media consisting of H_3BO_3 10 µM, $MnSO_4$ 0.5 µM, $ZnSO_4$ 0.5 µM, $CuSO_4$ 0.1 µM $(NH_4)_6Mo_7O_{24}$ 0.01 µM, Fe-EDTA 15 µM, KH_2PO_4 0.5 mM, $MgSO_4$ 1.2 mM, $CaCl_2$ 2.0 mM. Nitrogen was supplied as KNO_3 at a concentration of 2 mM nitrogen (Matt et al., 2001). The seedlings were transferred to $1/4^{th}$ strength media for competition assay when the root length was approximately 1 cm. Special square petri dishes (120 X 120 X 17 mm) for competition experiment were made by cutting the solidified

1/4th strength media into blocks of 1cm wide with 0.5 cm space between blocks; and approximately upper 2 cm was cut. On each block, wild type seedling was paired with uniform length seedling of either irWIPK or irSIPK or irLOX3 (see also Additional Figure 1). The shoots were placed in the upper air filled portion of the block. After transfer to blocks, one of the cotyledonary leaves of each seedling was wounded with the tips of bent forceps (making three pin holes). The petri dishes were wrapped with a layer of fabric tape (Micropore 3M Health Care, Neuss, Germany) to allow for gas exchange and were placed vertically in a growth chamber (Kruegel et al., 2002) to ensure that roots grew to the bottom. The shoots grew in the air filled volume of the upper portion of the blocks. The seedlings were allowed to adjust to the transfer shock for one day after which the growth of roots was monitored on a daily basis. At the end of the 7 day competition experiment, the fresh mass of the roots and shoots of both members of the competing pair was determined: the wild type and its competing transformed line.

Phytohormone analysis

For phytohormone analysis, plants were grown as described above. The plants were used only for phytohormone analysis and not included into the other analyses. The youngest source leaves were harvested as a control 10 days after transfer to 2L competition pots, and then transition leaves were wounded and treated with 20 µL 1:5 diluted *M. sexta* oral secretion. The treated leaves were harvested an hour later after removal of the midrib and immediately frozen in liquid nitrogen. After extraction, phytohormones were analysed on an LC-MS⁄MS system (Varian 1200 Triple-Quadrupole-LC-MS system; Varian, Palo Alto, CA, USA according to Schäfer et al., 2011).

Photosynthesis measurement

Photosynthesis was measured indirectly by determining CO_2 assimilation rates. At least 5 replicates were used to analyze photosynthesis using a LI-COR 6400 portable photosynthesis system (LI-COR Bioscience) with 400 µmol/mol CO_2 concentration and light intensity of 1200 µmol/m^2/s for measurements.

Sample preparation for isotope ratio mass spectrometry

^{15}N-incorporation of seed and leaves was analyzed by an elemental analyzer – continuous flow – isotope ratio mass spectrometry (EA–CF–IRMS). One capsule per plant

was harvested 71 days after germination. The capsules were harvested when they showed the first signs of opening. Seeds were dried for 2 weeks at room temperature before measurement. The leaf blades of the oldest sink leaf at time point of labeling were harvested 5 days after the last treatment, dried at 60 °C for 48 h and homogenized before analysis.

In order to accomodate the high sensitivity of the IRMS, samples were diluted to a final labeling of about 1 atom% ^{15}N by adding a standard (acetanilide; alice-1) to the sample. Seeds weighing 0.3 mg ± 20% (approximately two seeds), were placed in 40 µL tin capsules together with 0.7819 mg ± 20% of the standard. Roughly 0.1250 mg ± 20% of the homogenized and dried plant material was diluted with 0.8325 ± 20% mg of the standard. The exact sample and dilution masses were determined and used to calculate ^{15}N abundance. Three technical replicates of each sample were analyzed.

Isotope ratio mass spectrometry analysis

The tin capsules were sealed and combusted (oxidation at 1020 °C, reduction at 650 °C in a constant helium stream (80 mL min^{-1}) quantitatively to CO_2, N_2 and H_2O in an elemental analyzer (EuroEA CN2 dual, Hekatech, Wegberg, Germany). After passing a CO_2/water trap ($NaOH/MgClO_4$) and a chromatographic CN-column at 85 °C, the remaining N_2 was transferred via an open split to a coupled isotope ratio mass spectrometer (IsoPrime, Micromass, Manchester, UK). The laboratory working standard was calibrated using IAEA-N-1 reference material with a $\delta^{15}N$ value of +0.43‰. A caffeine standard (cafice-1) was analyzed together with the samples as quality analysis reference material for long-term performance monitoring of the entire analytical procedure (for details see Werner et al., 2001).

Isotopic ratios of nitrogen

$$R_{^{15}N} = \frac{[^{15}N]}{[^{14}N]} \qquad (1.3)$$

are expressed in δ notation versus the international standard N_2(Air) with $^{15}R_{std} = 0.0036765$.

$$\delta^{15}N_{sa} = \frac{^{15}R_{sa} - ^{15}R_{std}}{^{15}R_{std}} \qquad (1.4)$$

Usually given in ‰ (per mil)

$$\delta^{15}N_{sa}(‰) = \left(\frac{^{15}R_{sa}}{^{15}R_{std}} - 1\right) \cdot 1000 \qquad (1.5)$$

Based on the δ notation, isotope abundance ^{15}N (%) was calculated with 1.6.

$$^{15}N_{sa}(\%) = \frac{100}{\left(1 \Big/ \left(\frac{\delta^{15}N_{pt}(‰)}{1000} + 1\right) \cdot {}^{15}R_{std}\right) + 1} \quad (1.6)$$

based on the following equations

$$^{15}N_{sa}(\%) = \frac{^{15}R_{sa}}{1 + {}^{15}R_{sa}} \cdot 100 \quad (1.7)$$

$$^{15}R_{sa} = \left(\frac{\delta^{15}N_{sa}(‰)}{1000} + 1\right) \cdot {}^{15}R_{std} \quad (1.8)$$

for labeled plant tissue diluted with acetanilide (alice-1, $\delta^{15}N_{alice\text{-}1}$ = -1.36, 10.36% N) calculations were based on the following relations:

$$\delta^{15}N_{pt}(‰) = \frac{\delta^{15}N_{sa}(‰) - \delta^{15}N_{alice\text{-}1}(‰) \cdot x_{alice\text{-}1}}{x_{pt}} \quad (1.9)$$

$$x_{alice\text{-}1} = \frac{\%N_{alice\text{-}1} \cdot m_{alice\text{-}1}}{totN_{alice-1} + totN_{pt}} \text{ and } x_{pt} = \frac{\%N_{pt} \cdot m_{pt}}{totN_{alice-1} + totN_{pt}}$$

$$\text{with } \%N_{pt} = \frac{\%N_{sa} \cdot m_{sa} - \%N_{alice\text{-}1} \cdot m_{alice\text{-}1}}{m_{pt}} \quad (1.10)$$

With $^{15}N(\%)$ = atom percent of ^{15}N; R_{St} = isotope ratio of standard; alice-1 = acetanilid used for dilution; sa = measured sample; m = mass; %N = total nitrogen percentage; pt = plant tissue sample; totN = total nitrogen mass

Statistical analysis

All statistical analyses were performed using the software program R (R Developmental Core (Team, 2009) and the libraries therein (http://www.r-project.org/). For ANOVA analysis, if the assumption of homoscedasticity of variances was violated or the residuals did not follow a normal distribution, the response variables were transformed prior to the analyses using Box-Cox transformation (Sakia, 1992). The Box-Cox-lambda was estimated using Venables' and Ripley's MASS library for R. All models were simplified to the minimum adequate model using Akike's information criterion (Ronchetti, 1985). The

Welch two sample T-test was used, in order to account for heteroscedasticity in some data sets. To facilitate comparisons of all statistical analysis, this test was used in all cases.

Conflict of interest

The authors declare that they have no conflict of interest.

Authors' contributions

S.M. and I.T.B did field experiments; S.M. and L.UZ. performed glasshouse experiments; G.G. and I.T.B.established and G.G. performed *in vitro* seedling competition assays; S.B., S.M and L. UZ. performed the IRMS measurements; S.M. and L.UZ. prepared the manuscript, G.G., S.B. and I.T.B. edited the manuscript; L.UZ. conducted statistical analyses; S.M., L.UZ., G.G. and I.T.B. designed experiments.

Figure legends

Figure 1 Herbivory-induced signaling in *N. attenuata*.

Oral secretions of *Manduca sexta* contain fatty acid-amino acid conjugates (FACs), which are perceived by *Nicotiana attenuata* through an unknown perception event (black filled box with question mark), leading to the activation of salicylic acid-induced protein kinase (SIPK) and wound-induced protein kinase (WIPK). SIPK and WIPK regulate transcripts of LecRK1, which is a negative regulator of SA. SIPK and WIPK regulate biosynthesis of jasmonic acid (JA) and its isoleucine conjugate (JA-Ile). SIPK, but not WIPK, also regulates ethylene (ET) emissions, possibly leading to suppressed SA levels, thereby allowing unfettered JA/JA-Ile-mediated defense responses. Growth and fitness consequences of SIPK and WIPK-regulated signaling are unknown (red box).

Figure 2: Growth and fitness of *N. attenuata* plants impaired in herbivory-induced defense signaling.

(A) Mean (± SE, n ≥ 9) stalk length of ir*SIPK* and ir*WIPK* plants grown for 44 days in the plant`s natural habitat (Utah, USA) compared to size-matched wild type (WT) plants. **(B)** Mean (± SE) dry mass (n ≥ 3, pooled samples, each containing 5 biological replicates) and total capsule number (n ≥ 19) of transgenic plants (ir*SIPK*, ir*WIPK*) grown in competition with wild type (WT) plants. To simulate herbivory, three rosette leaves of each plant were wounded with a pattern wheel (W) and treated with 10 µL 1:5 diluted *Manduca sexta* oral

secretions (OS). Untreated plants served as controls. **(C)** Mean (± SE , n ≥ 16.) relative root growth difference to WT in wounded seedlings grown in competition (asteriks indicate significant differences between ir*LOX3* and ir*WIPK* when compared to ir*SIPK* plants (ANCOVA, $F_{2,344} = 13.46$, $p < 0.001$)) and mean (± SE, n = 8) seedling fresh mass grown under low nutrient conditions. Asteriks indicate significant differences between a transgenic line and WT in one pot (Welch two sample T-test;***: p<0.001; **: p<0.01; *: p<0.05).

Figure 3 Phytohormones in leaves of competing *N. attenuata* plants. Mean (± SE, n ≥ 4) of **(A)** jasmonic acid (JA) and **(B)** salicylic acid (SA) levels of transgenic plants grown in competition with WT plants in 2L pots. SxN plants are crosses between ir*SIPK* and oeNahG plants. Ten days after transfer to 2L pots, the youngest source leaf of each plant was harvested as a control and the source-sink transition leaves were wounded with a pattern wheel (W) and treated with 20 µL 1:5 diluted *Manduca sexta* oral secretion (OS) and harvested 1h after elicitation. Asteriks indicate significant differences between transgenic line and WT in one pot. (Welch two sample T-test;***: p < 0.001; **: p < 0.01; *: p < 0.05)

Figure 4: Reducing SA levels in *SIPK*-silenced plants restores growth.
(A) Scheme of the exerimental approach. The transgenic lines (respectively WT plants) were grown with size matched WT plants in competition in one pot. One half of the plants was wounded with a pattern wheel and treated with *Manduca sexta*'s oral secretion (W+OS), the other half was kept as untreated controls. During the experiment, drymass ("DM"), capsule ("C") and flower ("F") number were determined. For comparison between treatments, the difference between the two plants (Line-WT) in one pot was calculated for each treatment and expressed in % of the individual WT of that specific pot (see formula in graphic). Differences in **(B)** dry mass, **(C)** capsule number and **(D)** flower number of transgenic lines (ir*SIPK*, ir*WIPK*, ir*LOX3*, *oeNahG*, *SxN*) compared to competing wild type (WT) plants. Ten days after transfer to 2L pots, rosette leaves of transgenic and WT plants were wounded with a pattern wheel (W) and treated with 10 µL 1:5 diluted *Manduca sexta* oral secretion (OS). Treatment was repeated for two consecutive days. At the stalk elongation stage, W+OS treatment was repeated with expanded S1 leaves. Non-elicited plants were used as controls. The minimum adequate model is represented through small letters (a, b; ANOVA, dry mass: Line: $F_{2,97} = 11.12$, $p < 0.001$, capsule number: Line: $F_{1,58} = 21.18$, $p < 0.001$, Treatment: $F_{1,58} = 8.08$, $p < 0.01$; flower number: Line $F_{1,58} = 45.90$, $p < 0.001$). Asterics indicate significant

differences between control and W+OS treatment (Welch two sample t-test, *: P<0.05, n.s. = no significant difference)

Figure 5: Growth differences of transgenic plants are not correlated with CO_2 assimilation rates.

Differences (mean ± SE, n ≥ 4) in photosynthesis rates between transgenic lines (ir*SIPK,*ir*WIPK*, ir*LOX3*, oe*NahG*, *SxN*) compared to competing wild type (WT) plants (calculated as described in Figure 4A). Rosette leaves were OS-elicited as described in Figure 4. Photosynthesis rate was measured at the youngest treated rosette leaf 1 day after the last treatment. The minimum adequate model is represented through small letters (a, b, c; ANOVA, $F_{2,56} = 15.70$, $p < 0.001$).

Figure 6: Growth differences in transgenic plants are not correlated with nitrogen uptake. Differences (mean ± SE, n ≥ 5) in **(A)** total nitrogen and **(B)** ^{15}N-incorporation between transgenic lines (ir*SIPK*, ir*WIPK*, ir*LOX3*, oe*NahG*, *SxN*) compared to competing wild type (WT) plants (calculated as described in Figure 4A). 7 days after transfer to 2L pots, the oldest sink leaf was marked and each plant pair was pulse-labeled with 5.1 mg nitrogen delivered as $K^{15}NO_3$. Three days later, rosette leaves of transgenic plants and WT were OS-elicited as described for Figure 4. Leaves were harvested five days after last treatment. Total nitrogen and ^{15}N-incorpration were determined by IRMS (see Material and Methods). The minimum adequate model is represented through small letters (a, b, c; total nitrogen: ANOVA, $F_{2,102} = 29.251$, $p < 0.001$;^{15}N-incorporation). Asterics indicate significant differences between control and W+OS treatment (Welch two sample t-test, $p < 0.01$, n.s. = no significant difference)

Literature

Abreu, M.E., and Munne-Bosch, S. (2009). Salicylic acid deficiency in NahG transgenic lines and sid2 mutants increases seed yield in the annual plant *Arabidopsis thaliana*. J Exp Bot **60,** 1261-1271.

Allmann, S., Halitschke, R., Schuurink, R.C., and Baldwin, I.T. (2010). Oxylipin channelling in *Nicotiana attenuata*: lipoxygenase 2 supplies substrates for green leaf volatile production. Plant Cell Environ **33,** 2028-2040.

Baldwin, I.T., Ohnmeiss, T.E. (1994) Coordination of photosynthetic and alkaloidal responses to damage in uninducible and inducible *Nicotiana sylvestris*. Ecology **75 (4)** 1003-1014

Baldwin, I.T. (1998). Jasmonate-induced responses are costly but benefit plants under attack in native populations. P Natl Acad Sci USA **95,** 8113-8118.

Baldwin, I.T., Gorham, D., Schmelz, E.A., Lewandowski, C.A., and Lynds, G.Y. (1998). Allocation of nitrogen to an inducible defense and seed production in *Nicotiana attenuata*. Oecologia **115,** 541-552.

Baldwin, I.T., Hamilton, W. (2000). Jasmonate-induced responses of *Nicotiana sylvestris* results in fitness costs due to impaired competitive ability for nitrogen. Journal of Chemical Ecology **26(4),** 915-952.

Baldwin, I.T. (2001). An ecologically motivated analysis of plant-herbivore interactions in native tobacco. Plant Physiology **127(4)**, 1449-1458.

Bilgin D.D., Zavala J.A., Zhu J., Clough S.J., Ort D.R., DeLucia E.H. (2010). Biotic stress globally downregulates photosynthesis genes. Plant Cell Environ **33**(10), 1597-613.

Bonaventure, G., van Doorn, A., Baldwin, I.T. (2011). Herbivore associated elicitors: FAC signaling and metabolism. Trends in Plant Science **16,** 294-299.

Boss, W.F., Sederoff, H.W., Im, Y.J., Moran, N., Grunden, A.M., and Perera, I.Y. (2010). Basal signaling regulates plant growth and development. Plant Physiol **154,** 439-443.

Bush, S.M., and Krysan, P.J. (2007). Mutational evidence that the Arabidopsis MAP kinase MPK6 is involved in anther, inflorescence, and embryo development. J Exp Bot **58,** 2181-2191.

Cipollini, D. (2007). Consequences of the overproduction of methyl jasmonate on seed production, tolerance to defoliation and competitive effect and response of *Arabidopsis thaliana*. New Phytol **173,** 146-153.

Diezel, C., von Dahl, C.C., Gaquerel, E., and Baldwin, I.T. (2009). Different lepidopteran elicitors account for cross-talk in herbivory-induced phytohormone signaling. Plant Physiol **150,** 1576-1586.

Fariduddin, Q., Hayat, S., and Ahmad, A. (2003). Salicylic acid influences net photosynthetic rate, carboxylation efficiency, nitrate reductase activity, and seed yield in *Brassica juncea*. Photosynthetica **41,** 281-284.

Gilardoni, P.A., Hettenhausen, C., Baldwin, I.T., and Bonaventure, G. (2011). *Nicotiana attenuata* Lectin Receptor Kinase1 suppresses the insect-mediated inhibition of induced defense responses during *Manduca sexta* herbivory. Plant Cell **23,** 3512-3532.

Giri, A.P., Wuensche, H. , Mitra, S., Zavala, J.A., Muck, A., Svatos, A., Baldwin, I.T.(2006). Molecular interactions between the specialist herbivore *Manduca sexta* (Lepidoptera, Sphingidae) and its natural host *Nicotiana attenuata* VII. Changes in the plant's proteome. Plant Physiol **142**. 1621-1641

Glazebrook, J. (2005). Contrasting mechanisms of defense against biotrophic and necrotrophic pathogens. Annu Rev Phytopathol **43,** 205-227.

Halitschke, R., Schittko, U., Pohnert, G., Boland, W., Baldwin, I.T. (2001). Molecular interactions between the specialist herbivore *Manduca sexta* (Lepidoptera, Sphingidae) and its natural host *Nicotiana attenuata*. III. Fatty acid-amino acid conjugates in herbivore oral secretions are necessary and sufficient for herbivore-specific plant responses. Plant Physiol, **125(2)**, 711-717.

Halitschke, R., Gase, K., Hui, D.Q., Schmidt, D. D., Baldwin, I.T. (2003). Molecular interactions between the specialist herbivore *Manduca sexta* (Lepidoptera, Sphingidae) and its natural host *Nicotiana attenuata*. VI. Microarray analysis reveals that most herbivore-specific transcriptional changes are mediated by fatty acid-amino acid conjugates. Plant Physiol **131(4)**, 1894-1902

Halitschke, R., and Baldwin, I.T. (2003). Antisense LOX expression increases herbivore performance by decreasing defense responses and inhibiting growth-related transcriptional reorganization in *Nicotiana attenuata*. Plant J **36,** 794-807.

Halitschke, R., Hamilton, J.G., and Kessler, A. (2011) Herbivore-specific elicitation of photosynthesis by mirid bug salivary secretions in the wild tobacco *Nicotiana attenuata*. New Phytol **191,** 528-535

Hanik, N., Gomez, S., Schueller, M., Orians, C.M., and Ferrieri, R.A. (2010a). Use of gaseous 13NH(3) administered to intact leaves of *Nicotiana tabacum* to study changes in nitrogen utilization during defence induction. Plant Cell Environ **33,** 2173-2179.

Hanik, N., Gomez, S., Best, M., Schueller, M., Orians, C.M., and Ferrieri, R.A. (2010b). Partitioning of new carbon as ^{11}C in *Nicotiana tabacum* reveals insight into methyl jasmonate induced changes in metabolism. J Chem Ecol **36,** 1058-1067.

Heidel, A.J., Baldwin, I.T. (2004). Microarray analysis of salicylic acid- and jasmonic acid-signalling in responses of *Nicotiana attenuata* to attack by insects from multiple feeding guilds. *Plant Cell Environ*, **27(11)**, 1362-1373.

Heil, M., Baldwin, I.T. (2002). Fitness costs of induced resistance: emerging experimental support for a slippery concept. Trends in Plant Science **7(2)**, 61-67

Herms, D.A., Mattson, W.J. (1992). The dilemma of plants: To grow or defend. Qarterly Rev of Biol **67 (3),** 283-335

Hermsmeier, D., Schittko, U. Baldwin, I.T.(2001). Molecular interactions between the specialist herbivore *Manduca sexta* (Lepidoptera, Sphingidae) and its natural host *Nicotiana attenuata*. I. Large-scale changes in the accumulation of growth- and defense-related plant mRNAs. Plant Physiol **125,** 683-700

Hettenhausen, C., Baldwin, I.T., and Wu, J. (2012). Silencing MPK4 in *Nicotiana attenuata e*nhances photosynthesis and seed production but compromises abscisic acid-induced stomatal closure and guard cell-mediated resistance to *Pseudomonas syringae* pv tomato DC3000. Plant Physiol **158,** 759-776.

Howe, G.A., and Jander, G. (2008). Plant immunity to insect herbivores. Annu Rev Plant Biol **59,** 41-66.

Hu, Y.X., Bao, F., and Li, J.Y. (2000). Promotive effect of brassinosteroids on cell division involves a distinct CycD3-induction pathway in *Arabidopsis*. Plant J **24,** 693-701.

Hummel, G.M., Schurr, U., Baldwin, I.T., and Walter, A. (2009). Herbivore-induced jasmonic acid bursts in leaves of *Nicotiana attenuata* mediate short-term reductions in root growth. Plant Cell Environ **32,** 134-143.

Kallenbach, M., Alagna, F., Baldwin, I.T., and Bonaventure, G. (2010). *Nicotiana attenuata* SIPK, WIPK, NPR1, and fatty acid-amino acid conjugates participate in the induction of jasmonic acid biosynthesis by affecting early enzymatic steps in the pathway. (vol 152, pg 96, 2010). Plant Physiol **152,** 1760-1760.

Kallenbach, M., Bonaventure, P., Gilardoni, P., Wissgott, A., Baldwin, I.T. (2012) Empoasca leafhoppers attack wild tobacco plants in a jasmonate-dependent manner and identify jasmonate mutants in natural populations. P Natl Acad Sci USA, in print

Kandoth, P.K., Ranf, S., Pancholi, S.S., Jayanty, S., Walla, M.D., Miller, W., Howe, G.A., Lincoln, D.E., and Stratmann, J.W. (2007). Tomato MAPKs LeMPK1, LeMPK2, and LeMPK3 function in the systemi n-mediated defense response against herbivorous insects. P Natl Acad Sci USA **104,** 12205-12210.

Kerchev, P.I., Fenton, B., Foyer C.H., Hancock R.D. (2011). Plant responses to insect herbivory: interactions between photosynthesis, reactive oxygen species and hormonal signalling pathways. *Plant Cell Environ* **35**(2), 441-53.

Kessler, A. and Baldwin, I.T. (2002). Plant responsens to insect herbivory: the emerging molecular analysis. Annu Rev Plant Biol **53**. 299-328

Krügel, T., Lim, M., Gase, K., Halitschke, R., and Baldwin, I.T. (2002). Agrobacterium-mediated transformation of *Nicotiana attenuata*, a model ecological expression system. Chemoecology **12,** 177-183.

Leon-Reyes, A., Spoel, S.H., De Lange, E.S., Abe, H., Kobayashi, M., Tsuda, S., Millenaar, F.F.,Welschen, R.A.M., Ritsema, T., Pieterse, C.M.J. (2009) Ethylene modulates the role of nonexpressor of pathogenesis-related genes1 in cross-talk between salicylate and jasmonate signaling. Plant Physiol **149**, 1797–1809

Lou, Y. G., Baldwin, I. T. (2004). Nitrogen supply influences herbivore-induced direct and indirect defenses and transcriptional responses to *Nicotiana attenuata*. Plant Physiol **135**, 496-506.

Matt, P., Geiger, M., Walch-Liu, P., Engels, C., Krapp, A., and Stitt, M. (2001). Elevated carbon dioxide increases nitrate uptake and nitrate reductase activity when tobacco is growing on nitrate, but increases ammonium uptake and inhibits nitrate reductase activity when tobacco is growing on ammonium nitrate. Plant Cell Environ **24,** 1119-1137.

Mitra, S. and Baldwin, I.T. (2008). Independently silencing two photosynthetic proteins in *Nicotiana attenuata* has different effects on herbivore resistance, Plant Physiol **148**,1128-1138

Meldau, S., Wu, J.Q., and Baldwin, I.T. (2009). Silencing two herbivory-activated MAP kinases, SIPK and WIPK, does not increase *Nicotiana attenuata*'s susceptibility to herbivores in the glasshouse and in nature. New Phytol **181,** 161-173.

Meldau, S., Baldwin, I.T., and Wu, J.Q. (2011). SGT1 regulates wounding- and herbivory-induced jasmonic acid accumulation and *Nicotiana attenuata*'s resistance to the specialist lepidopteran herbivore *Manduca sexta*. New Phytol **189,** 1143-1156.

Nazar, R., Iqbal, N., Syeed, S., and Khan, N.A. (2011). Salicylic acid alleviates decreases in photosynthesis under salt stress by enhancing nitrogen and sulfur assimilation and antioxidant metabolism differentially in two mungbean cultivars. J Plant Physiol **168,** 807-815.

Pancheva, T.V., and Popova, L.P. (1998). Effect of salicylic acid on the synthesis of ribulose-1,5-bisphosphate carboxylase/oxygenase in barley leaves. J Plant Physiol **152,** 381-386.

Pancheva, T.V., Popova, L.P., and Uzunova, A.N. (1996). Effects of salicylic acid on growth and photosynthesis in barley plants. J Plant Physiol **149,** 57-63.

Pieterse, C.M.J., Leon-Reyes, A., Van der Ent, S., and Van Wees, S.C.M. (2009). Networking by small-molecule hormones in plant immunity. Nat Chem Biol **5,** 308-316.

Redman, A.M., Cipollini, D.F., and Schultz, J.C. (2001). Fitness costs of jasmonic acid-induced defense in tomato, *Lycopersicon esculentum*. Oecologia **126,** 380-385.

Riou-Khamlichi, C., Huntley, R., Jacqmard, A., and Murray, J.A.H. (1999). Cytokinin activation of Arabidopsis cell division through a D-type cyclin. Science **283,** 1541-1544.

Ronchetti, E. (1985). Robust Model selection in regression. Statistics & Probability Letters **3,** 21-23.

Royo, J., Leon, J., Vancanneyt, G., Albar, J.P., Rosahl, S., Ortego, F., Castanera, P., and Sanchez-Serrano, J.J. (1999). Antisense-mediated depletion of a potato lipoxygenase reduces wound induction of proteinase inhibitors and increases weight gain of insect pests. P Natl Acad Sci USA **96,** 1146-1151.

Sakia, R.M. (1992) The Box-Cox transformation technique: a review, The Statistician **41**, 169-178

Sarangthem,K. and Singh, N. (2003) Efficacy of salicylic acid on growth, nitrogen metabolism and flowering of *Phaseolus vulgaris*, Crop Res. **26(2)**, 355-360

Schäfer, M., Fischer, C., Meldau, S., Seebald, E., Oelmuller, R., and Baldwin, I.T. (2011). Lipase Activity in Insect Oral Secretions Mediates Defense Responses in *Arabidopsis*. Plant Physiol **156,** 1520-1534.

Schuman, M. C., Heinzel, N., Gaquerel, E., Svatos, A., Baldwin, I. T. (2009). Polymorphism in jasmonate signaling partially accounts for the variety of volatiles produced by *Nicotiana attenuata* plants in a native population. New Phytol, 183, 1134-1148.

Scott, I.M., Clarke, S.M., Wood, J.E., and Mur, L.A.J. (2004). Salicylate accumulation inhibits growth at chilling temperature in *Arabidopsis*. Plant Physiol **135,** 1040-1049.

Seo, S., Katou, S., Seto, H., Gomi, K., and Ohashi, Y. (2007). The mitogen-activated protein kinases WIPK and SIPK regulate the levels of jasmonic and salicylic acids in wounded tobacco plants. Plant J **49,** 899-909.

Slaymaker, D.H., Navarre, D.A., Clark, D., del Pozo, O., Martin, G.B., and Klessig, D.F. (2002). The tobacco salicylic acid-binding protein 3 (SABP3) is the.chloroplast carbonic anhydrase, which exhibits antioxidant activity and plays a role in the hypersensitive defense response. P Natl Acad Sci USA **99,** 11640-11645.

Tena, G., Boudsocq, M., Sheen, J. (2011) Protein kinase signaling networks in plant innate immunity. Curr Opin Plant Biol **14**, 519-529

Team, R.D.C. (2009). R: A language and environment for statistical computing (Vienna: R Foundation for Statistical Computing).

Tian, D., Traw, M.B., Chen, J.Q., Kreitman, M., and Bergelson, J. (2003). Fitness costs of R-gene-mediated resistance in *Arabidopsis thaliana*. Nature **423,** 74-77.

Todesco, M., Balasubramanian, S., Hu, T.T., Traw, M.B., Horton, M., Epple, P., Kuhns, C., Sureshkumar, S., Schwartz, C., Lanz, C., Laitinen, R.A.E., Huang, Y., Chory, J., Lipka, V., Borevitz, J.O., Dangl, J.L., Bergelson, J., Nordborg, M., and Weigel, D. (2010). Natural allelic variation underlying a major fitness trade-off in *Arabidopsis thaliana*. Nature **465,** 632-U129.

Traw, M.B., Kniskern, J.M., and Bergelson, J. (2007). SAR increases fitness of *Arabidopsis thaliana* in the presence of natural bacterial pathogens. Evolution; international journal of organic evolution **61,** 2444-2449.

Uzunova, A.N., and Popova, L.P. (2000). Effect of salicylic acid on leaf anatomy and chloroplast ultrastructure of barley plants. Photosynthetica **38,** 243-250.

van Dam, N.M., and Baldwin, I.T. (1998). Costs of jasmonate-induced responses in plants competing for limited resources. Ecol Lett **1,** 30-33.

Vicente, M.R.S., and Plasencia, J. (2011). Salicylic acid beyond defence: its role in plant growth and development. J Exp Bot **62,** 3321-3338.

Walling, L.L., (2000). The myriad plant responses to herbivores. Journal of Plant Growth Regul **19**, 195-216

Walling, L.L. (2009). Adaptive Defense Responses to Pathogens and Insects. Adv Bot Res **51,** 551-612.

Wang, H., Ngwenyama, N., Liu, Y., Walker, J.C., and Zhang, S. (2007). Stomatal development and patterning are regulated by environmentally responsive mitogen-activated protein kinases in *Arabidopsis*. Plant Cell **19,** 63-73.

Wang, H., Liu, Y., Bruffett, K., Lee, J., Hause, G., Walker, J.C., and Zhang, S. (2008). Haplo-insufficiency of MPK3 in MPK6 mutant background uncovers a novel function of these two MAPKs in *Arabidopsis* ovule development. Plant Cell **20,** 602-613.

Werner, R.A., and Brand, W.A. (2001). Referencing strategies and techniques in stable isotope ratio analysis. Rapid Communications in Mass Spectrometry **15,** 501-519.

Wu, J.Q., Hettenhausen, C., Meldau, S., and Baldwin, I.T. (2007). Herbivory rapidly activates MAPK signaling in attacked and unattacked leaf regions but not between leaves of Nicotiana attenuata. Plant Cell **19,** 1096-1122.

Wu, J.Q., Hettenhausen, C., Schuman, M.C., Baldwin, I.T. (2008). A comparison of two *Nicotiana attenuata* accessions reveals large differences in signaling induced by oral secretions of the specialist herbivore *Manduca sexta*. Plant Physiology, **146**(3), 927-939.

Xia, J.C., Zhao, H., Liu, W.Z., Li, L.G., and He, Y.K. (2009). Role of cytokinin and salicylic acid in plant growth at low temperatures. Plant Growth Regul **57,** 211-221.

Zavala, J. A., Baldwin, I. T. (2004). Fitness benefits of trypsin proteinase inhibitor expression in *Nicotiana attenuata* are greater than their costs when plants are attacked. BMC Ecology **4**, 11

Zhang, Y., and Turner, J.G. (2008). Wound-induced endogenous jasmonates stunt plant growth by inhibiting mitosis. PLoS ONE **3** (11): e3699. doi:10.1371/ journal.pone.0003699

Figure titles

Figure 1 Herbivory-induced signaling in *N. attenuata*.

Figure 2: Growth and fitness of *N. attenuata* plants impaired in herbivory-induced defense signaling.

Figure 3 Phytohormones in leaves of competing *N. attenuata* plants.

Figure 4: Reducing SA levels in *SIPK*-silenced plants restores growth.

Figure 5: Growth differences of transgenic plants are not correlated with CO_2 assimilation rates.

Figure 6: Growth differences in transgenic plants are not correlated with nitrogen uptake.

Figures

Figure 1

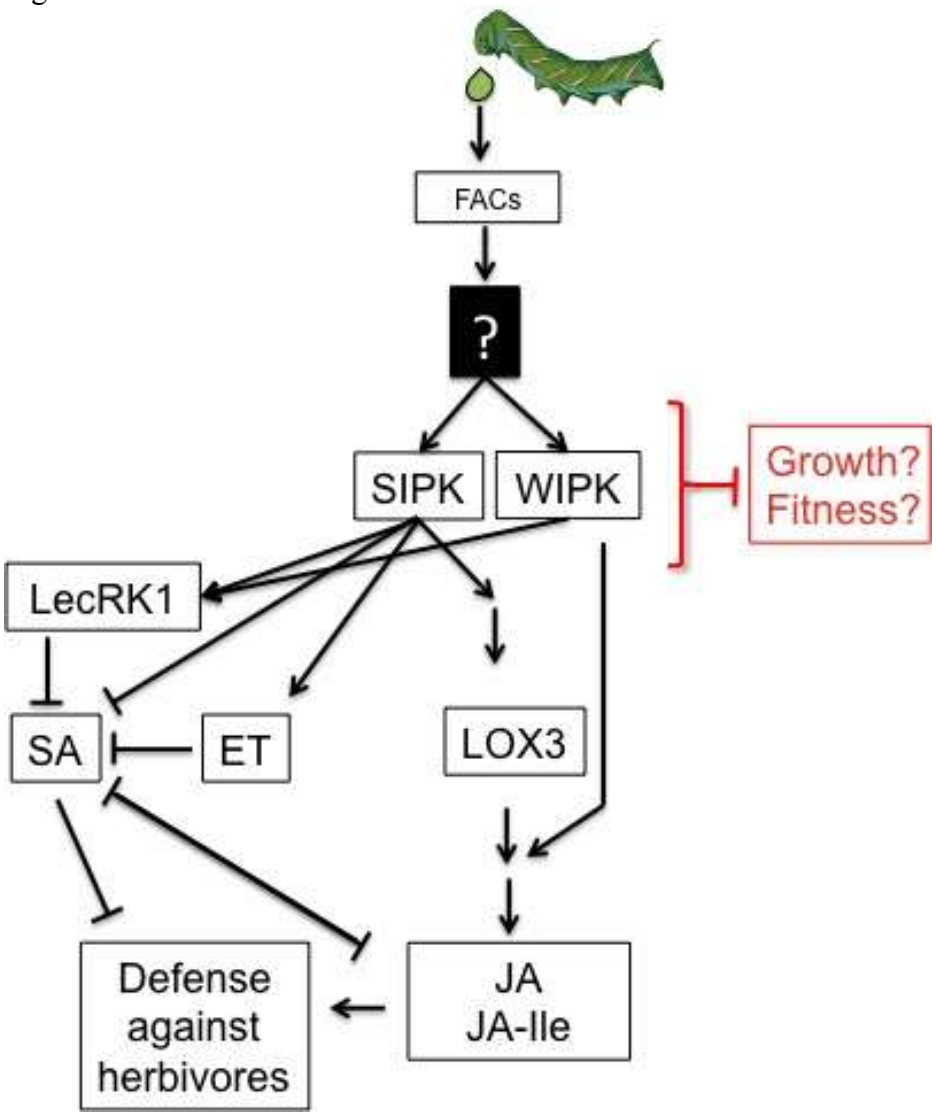

Figure 2

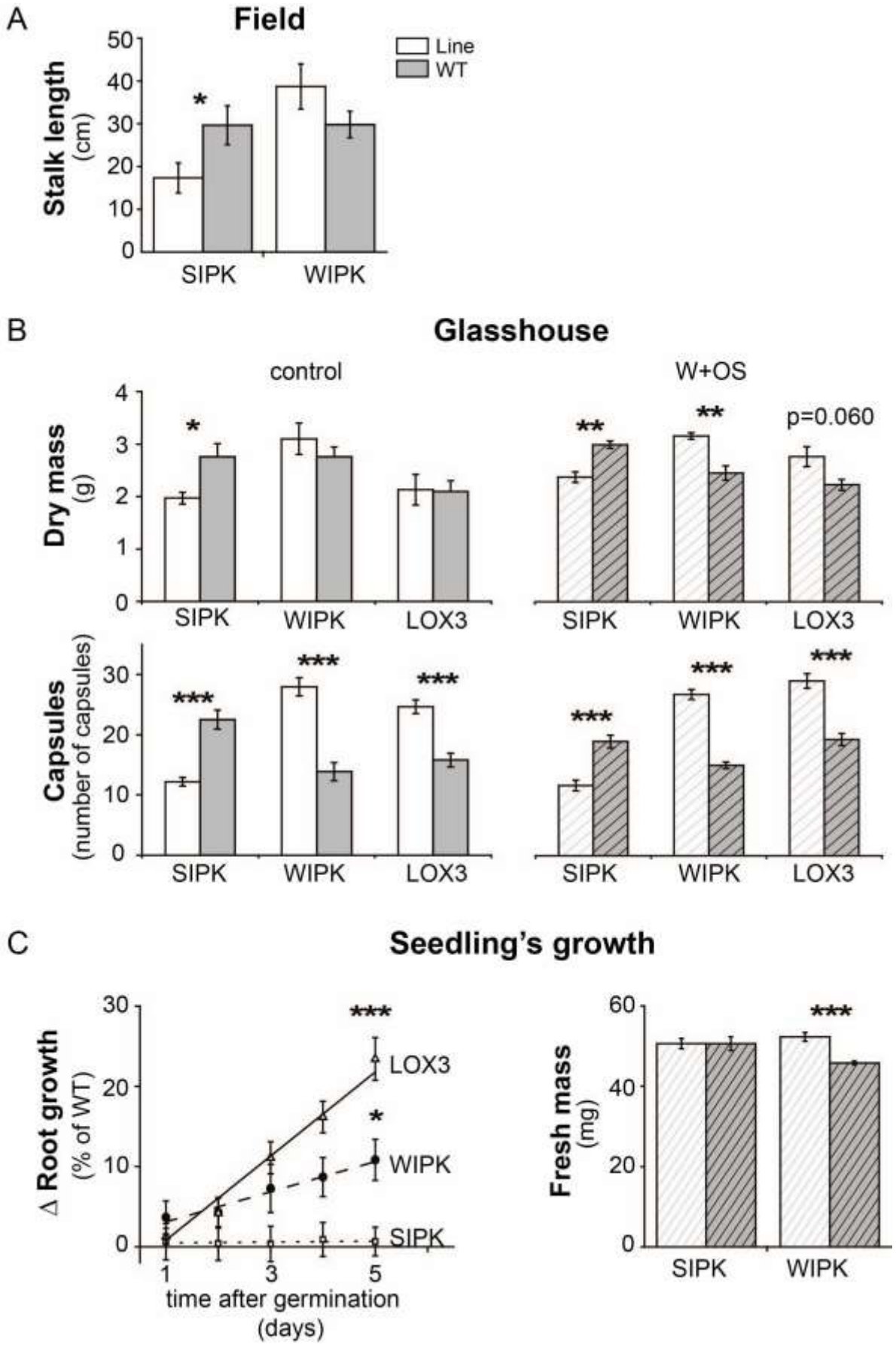
A
Field
Line
WT
Stalk length (cm)
SIPK
WIPK
B
Glasshouse
control
W+OS
Dry mass (g)
p=0.060
Capsules (number of capsules)
SIPK
WIPK
LOX3
C
Seedling's growth
Δ Root growth (% of WT)
time after germination (days)
Fresh mass (mg)

Figure 3

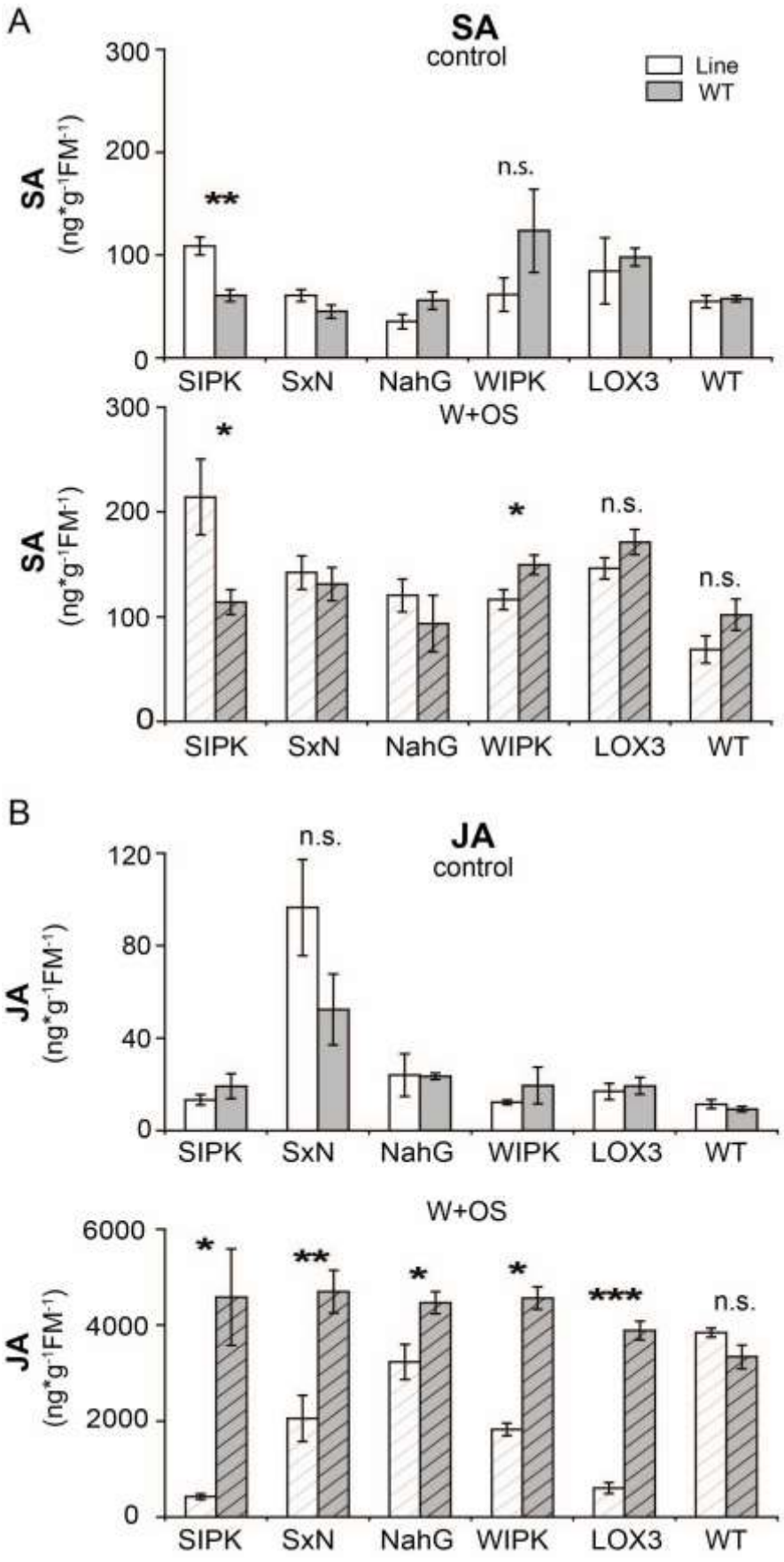
A
SA
control
Line
WT
SA (ng*g-1FM-1)
300
200
100
0
**
n.s.
SIPK
SxN
NahG
WIPK
LOX3
WT
W+OS
*
*
n.s.
n.s.
B
JA
control
JA (ng*g-1FM-1)
120
80
40
n.s.
W+OS
6000
4000
2000
*
**
*
*
***
n.s.

Figure 4

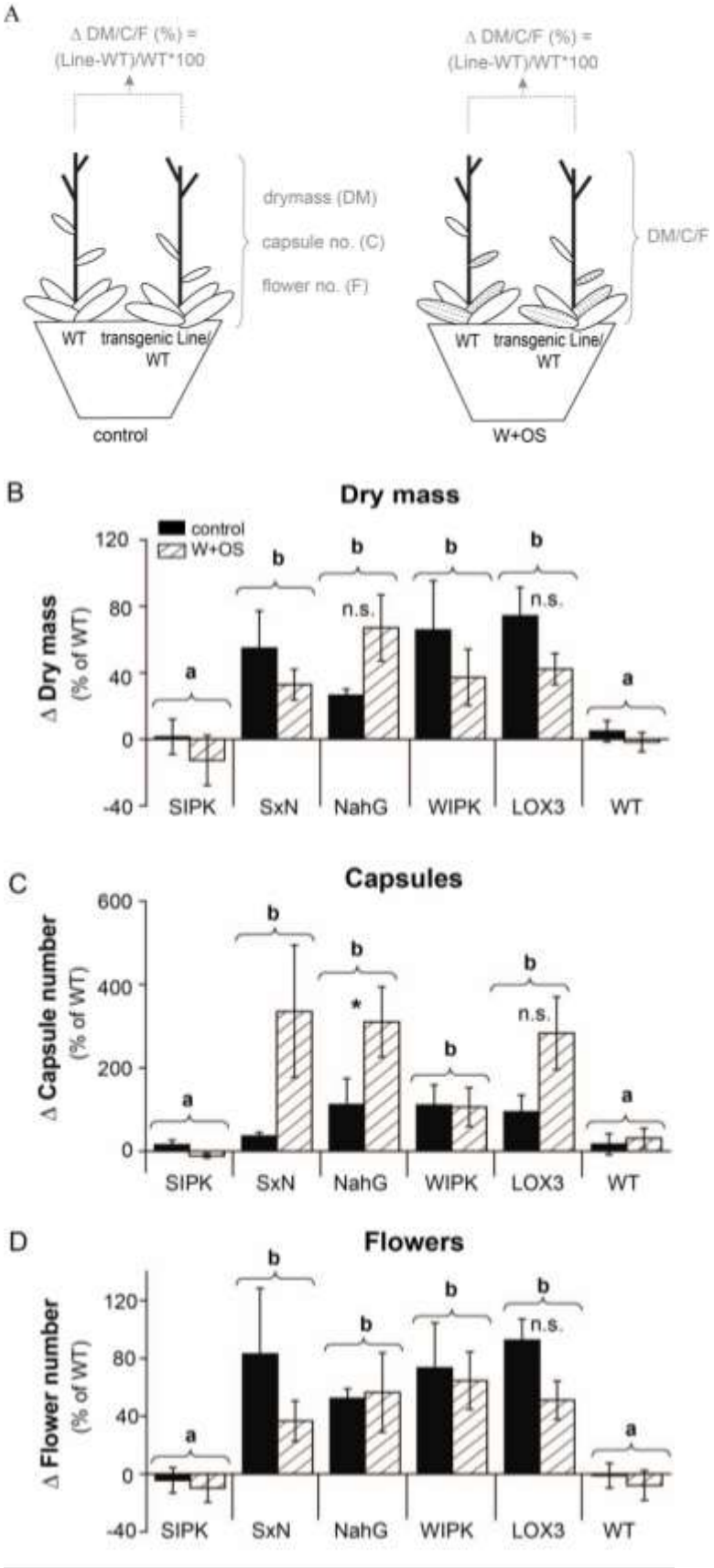
A
Δ DM/C/F (%) =
(Line-WT)/WT*100
drymass (DM)
capsule no. (C)
flower no. (F)
DM/C/F
WT transgenic Line/ WT
control
W+OS
B
Dry mass
control
W+OS
Δ Dry mass (% of WT)
SIPK
SxN
NahG
WIPK
LOX3
WT
C
Capsules
Δ Capsule number (% of WT)
D
Flowers
Δ Flower number (% of WT)
n.s.
*

Figure 5

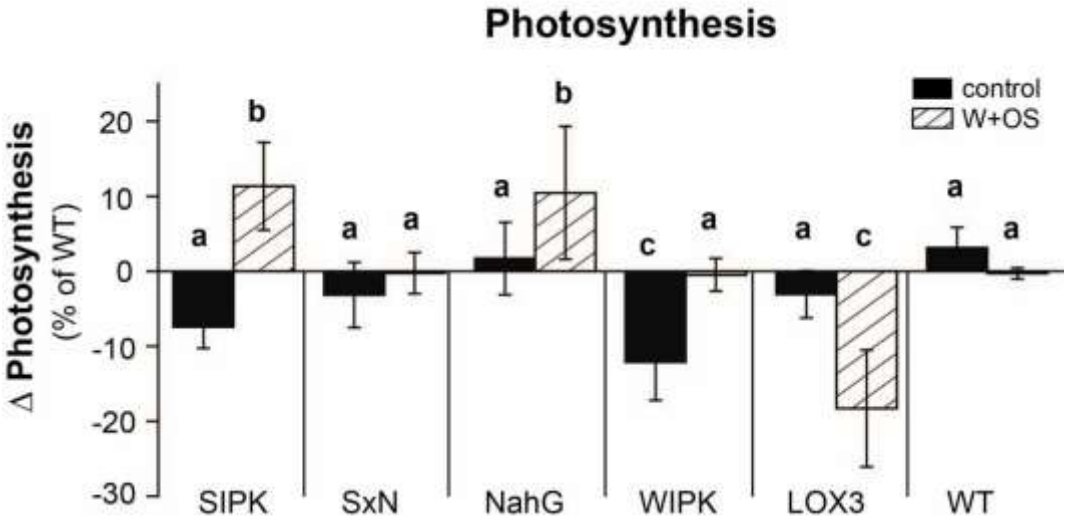
Photosynthesis
control
W+OS
Δ Photosynthesis
(% of WT)
20
10
0
-10
-20
-30
a
b
a
a
a
b
c
a
a
c
a
a
SIPK
SxN
NahG
WIPK
LOX3
WT

Figure 6

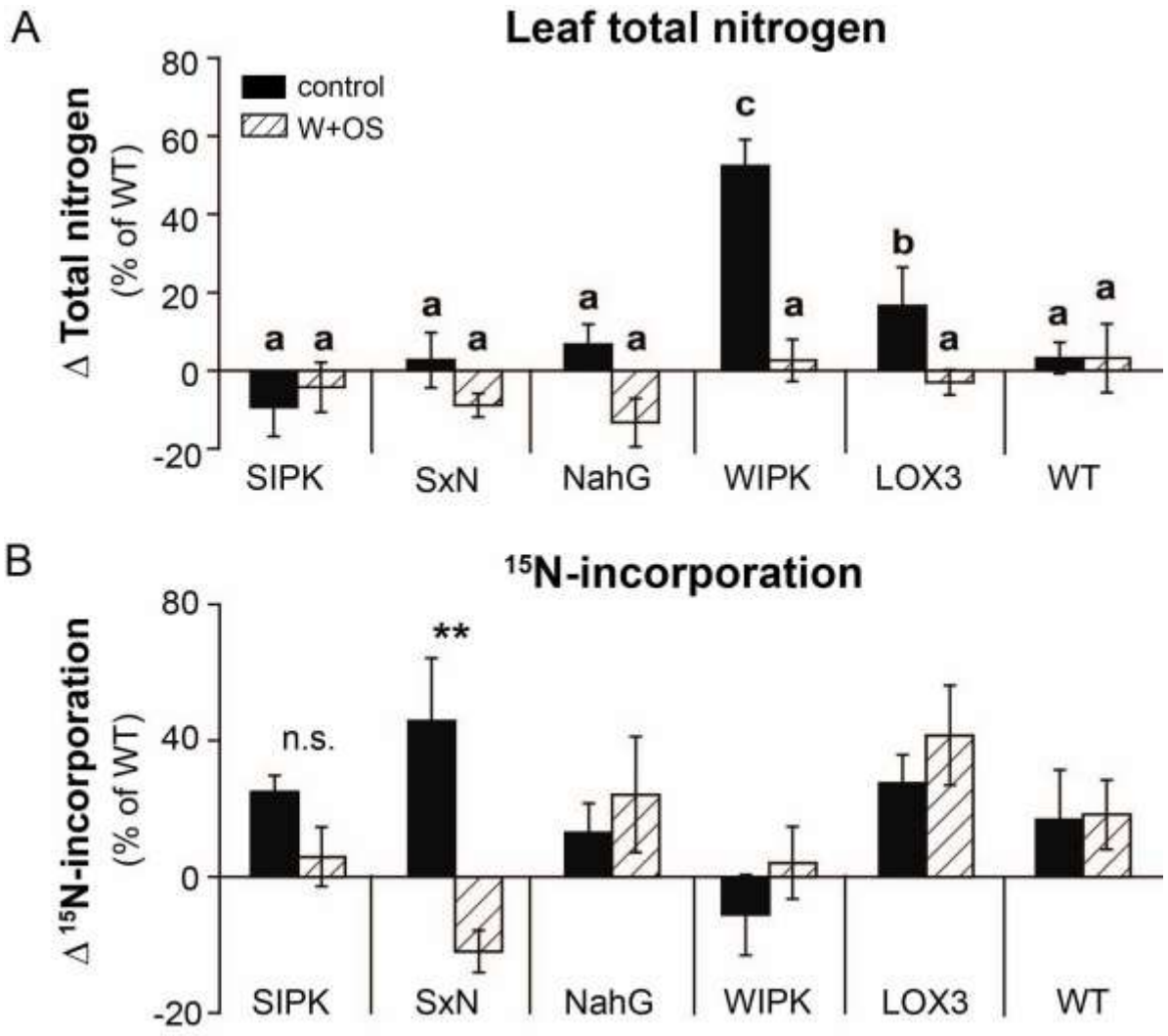
A
Leaf total nitrogen
control
W+OS
Δ Total nitrogen
(% of WT)
80
60
40
20
0
-20
a a
a a
a a
c
a
b
a
a a
SIPK
SxN
NahG
WIPK
LOX3
WT
B
15N-incorporation
Δ 15N-incorporation
(% of WT)
80
40
0
-20
n.s.
**
SIPK
SxN
NahG
WIPK
LOX3
WT

Additional Material

Figure A1

Additional Figure1(A) Representative picture of the *in-vitro* seedling assay system. Wounded seedlings of transgenic lines (ir*WIPK* or ir*SIPK* or ir*LOX*3; left side) competing with wounded WT (wild type; right side) seedlings under low nutrient conditions. **(B)** Representative picture of two WT plants grown in competition in a 2L pot.

Figure A2

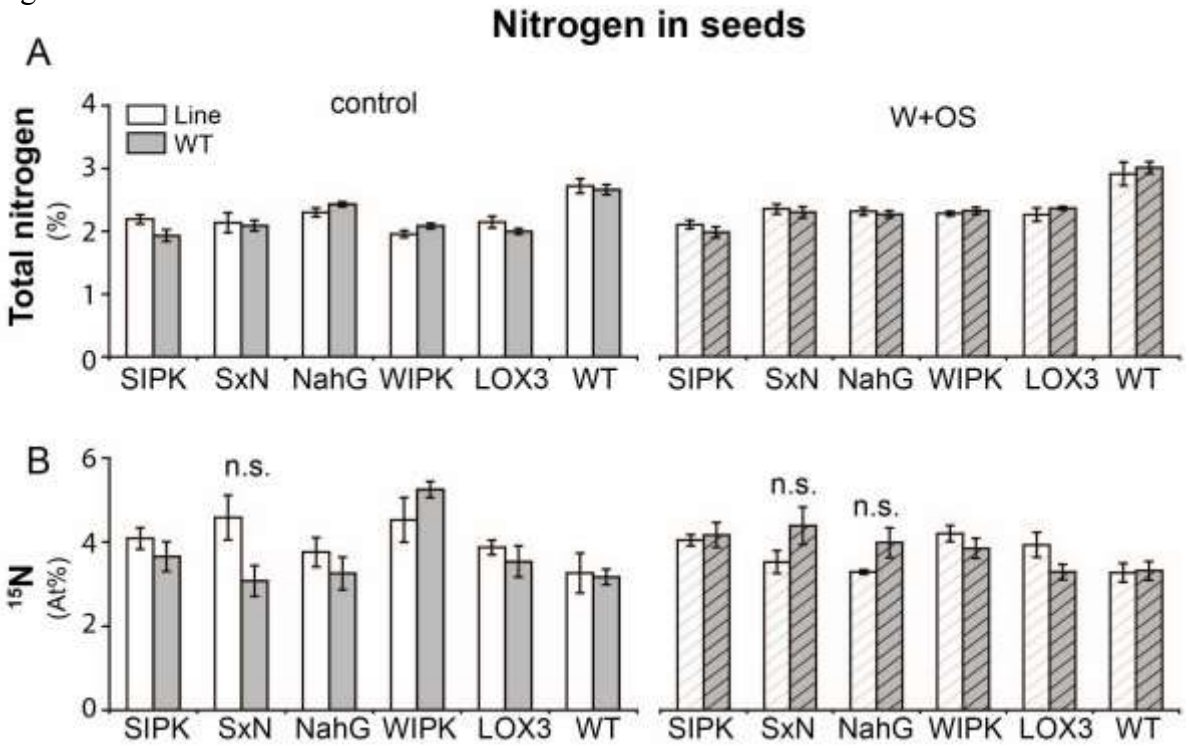

Additional Figure 2 (A) Total nitrogen content and **(B)** ^{15}N-incorporation of transgenic lines with impaired defense (ir*SIPK*,ir*WIPK*) or modified phytohormone levels (ir*LOX3*, oe*NahG*, *SxN*). Mean (± SE, n ≥ 3) grown in competition with WT after simulated herbivory. 7 days after transfer to 2L pots the oldest sink leaf was marked and each plant pair was pulse-labeled with 5.1 mg nitrogen in $K^{15}NO_3$. 3 days later the three rosette leaves of transgenic plants and WT were wounded three days in a row with a pattern wheel (W) and treated with 10 µL 1:5 diluted *Manduca sexta* oral secretion (OS). After all plants were elongated and had firt buds or started flowering,the expanded S1 leaves were treated in a similar way. Non elicited plants were used as controls. One capsule per plant was harvested 70 days after germination. Total nitrogen and ^{15}N-incorpration were determined by IRMS (see Material and Methods). Stars indicate significant differences between transgenic line and WT in one pot, and WT and WT respectivley (Welch two sample T-test;***: $p < 0.001$; **: $p < 0.01$; *: $p < 0.05$)

2.2 Manuscript II

Determination of ^{15}N-incorporation into plant proteins and their absolute quantitation: a new tool to study nitrogen flux dynamics and protein pool sizes elicited by plant-herbivore interactions

Lynn Ullmann-Zeunert, Alexander Muck, Natalie Wielsch[1], Franziska Hufsky[1,3], Mariana A. Stanton[1], Stefan Bartram[1], Sebastian Böcker[3], Ian T. Baldwin[1], Karin Groten[1], Aleš Svatoš[1*]

Journal of Proteome Research **(2012), 11, 4947-4960**

Journal of proteome research

Article

pubs.acs.org/jpr

Determination of ^{15}N-Incorporation into Plant Proteins and their Absolute Quantitation: A New Tool to Study Nitrogen Flux Dynamics and Protein Pool Sizes Elicited by Plant–Herbivore Interactions

Lynn Ullmann-Zeunert,[†] Alexander Muck,[†,‡] Natalie Wielsch,[†] Franziska Hufsky,[†,§] Mariana A. Stanton,[†] Stefan Bartram,[†] Sebastian Böcker,[§] Ian T. Baldwin,[†] Karin Groten,[†] and Aleš Svatoš*[,†]

[†]Max Planck Institute for Chemical Ecology, Jena, Germany

[§]Friedrich Schiller University, Jena, Germany

Supporting Information

ABSTRACT: Herbivory leads to changes in the allocation of nitrogen among different pools and tissues; however, a detailed quantitative analysis of these changes has been lacking. Here, we demonstrate that a mass spectrometric data-independent acquisition approach known as LC–MS^E, combined with a novel algorithm to quantify heavy atom enrichment in peptides, is able to quantify elicited changes in protein amounts and ^{15}N flux in a high throughput manner. The reliable identification/quantitation of rabbit phosphorylase b protein spiked into leaf protein extract was achieved. The linear dynamic range, reproducibility of technical and biological replicates, and differences between measured and expected ^{15}N-incorporation into the small (SSU) and large (LSU) subunits of ribulose-1,5-bisphosphate-carboxylase/oxygenase (RuBisCO) and RuBisCO activase 2 (RCA2) of *Nicotiana attenuata* plants grown in hydroponic culture at different known concentrations of ^{15}N-labeled nitrate were used to further evaluate the procedure. The utility of the method for whole-plant studies in ecologically realistic contexts was demonstrated by using ^{15}N-pulse protocols on plants growing in soil under unknown ^{15}N-incorporation levels. Additionally, we quantified the amounts of lipoxygenase 2 (LOX2) protein, an enzyme important in antiherbivore defense responses, demonstrating that the approach allows for in-depth quantitative proteomics and ^{15}N flux analyses of the metabolic dynamics elicited during plant–herbivore interactions.

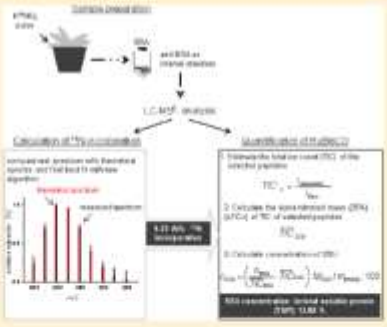

KEYWORDS: *LC–MS^E, ^{15}N-incorporation, absolute protein quantification, Nicotiana attenuata, herbivory, soil-grown plants*

INTRODUCTION

Plants fundamentally depend on inorganic nitrogen (N) for growth, reproduction, storage and defense, but N-resources in the natural environment are limited and set limits to the fitness of many plants. Thus, the production of N-containing metabolites used by plants for defense against herbivores competes with the other N pools.[1,2] A number of studies have estimated the costs of herbivore-induced defenses by tracking the N-allocation to specific secondary metabolites, and also the total N content of leaves, roots and seeds using pulse-chase labeling with ^{15}N.[3−5] However, a major source of nitrogen in plants are proteins, so that the analysis of changes in protein abundance is crucial for a better understanding of N-flux after herbivore attack. Large-scale changes in protein abundance after simulated herbivory have been measured by two-dimensional (2D) gel-electrophoresis combined with mass spectrometry (MS) for protein identification,[6,7] but the sensitivity and reproducibility of gels is limited. 2D-gels only allow for the quantitation and identification of the most abundant proteins in a complex sample[8] and is a procedure difficult to automate.[9] A high throughput quantitative method that would enable the simultaneous absolute quantitation of protein pool sizes and tracking of N-flux through the plant under ecologically relevant conditions by ^{15}N labeling has not yet been developed. The aim of our study was to develop such a method that is applicable to studying protein changes in plants elicited by herbivores.

Most modern quantitative proteomic strategies rely on stable isotope labeling and MS analysis to determine the relative quantity of a protein based on peptide abundances.[10−13] Except for one study,[14] all were performed with cell cultures, on agar plates or on hydroponically grown plants, and required a set of fully labeled and unlabeled tissues for the relative quantitation and peptide identification.[15−21] The only method available using soil-grown plants also requires a set of ^{14}N- and ^{15}N-labeled plants, which excludes the possibility of tracking nitrogen. Furthermore, the approach only allows a relative quanitification of proteins.[14] For absolute quantitation purposes, synthetically labeled standard peptides are usually added as internal standards after extraction and enzymatic digestion.[22] However, this approach requires at least one reference prototypic peptide for each protein of interest so that it is not only cost-intensive and can only be applied to a relatively low number of proteins but also

Received: May 23, 2012
Published: August 20, 2012

limited to organisms that have been characterized by reliable peptide sequences.

Furthermore, it has been shown that only approximately 16% of all tryptic peptides in complex digests are accessible by data-dependent scanning modes (DDA).[23] Therefore, the absolute quantitation of proteins by a data-independent approach (DIA) was the method of choice for our study. Such a data acquisition algorithm has been developed by Silva et al. and implemented in the parallel MS^E acquisition workflow.[24] It makes use of high-resolution, accurate mass data acquired on a hybrid time-of-flight mass spectrometer that operates in alternating low energy (MS) and elevated energy (MS^E) full scan acquisition.[25] MS^E-based absolute quantitation of proteins is based on the finding that the average MS signal response of the three most intense tryptic peptides per mole of a protein is constant.[24] This fact allows for the absolute simultaneous quantitation of many proteins at once using a universal signal response factor (counts/mol) calculated in a defined dynamic range from the known amount of unlabeled protein from an evolutionary unrelated organism added prior to tryptic digestion as an internal standard. Thus, a large number of samples or conditions may be analyzed at a low cost in a high through put fashion.

Combining LC−MS^E with pulse-chase metabolic labeling with ^{15}N to track N-flux leads to unknown ^{15}N-incorporation levels in peptides. Thus, a method for the calculation of ^{15}N-incorporation levels was required for the analysis of the LC−MS^E data. Several methods for the calculation of ^{13}C and ^{15}N heavy isotope incorporation levels have been reported over the last years.[13,26−30] The general approach of these methods is to compare high-resolution peptide mass spectra with theoretical mass spectra at different incorporation levels. Except for an excel sheet published by Taubert et al.,[13] all other approaches were not suitable for our data set produced by LC−MS^E, and the excel sheet does not allow a high-throughput analysis. Therefore, we developed a novel method called MoLE (Molecule Labeling Estimator) that allows a rapid analysis of multiple spectra for determining ^{15}N-incorporation levels of peptides.

The protein quantitation approach based on LC−MS^E-data published by Silva et al.[24] relies on the intensities of the monoisotopic peak. However, increasing levels of ^{15}N-incorporation of peptides leads to a decline in the intensity of the monoisotopic peak resulting in an underestimation of the amount of the proteins of interest. We solved this problem by establishing a new approach for absolute protein quantitation based on the alpha trimmed mean of robust estimations of the total (isotope) ion count (TIC) taking the ratio of the measured to the theoretical intensity of a peak in a spectrum at its calculated ^{15}N-incorporation. This quantitation strategy is applicable to labeled proteins.

We used *Nicotiana attenuata*, an annual plant that germinates in a postfire inorganic nitrogen-rich environment in response to smoke-derived signals,[31] to validate our method. It seemed to be an ideal ecological model for protein quantitation and protein-metabolites crosstalk studies because (a) although it is a nonsequenced organism, a large number of protein sequences of closely related species (e.g. *N. tabacum* and the two important sequenced crops potato[32] and tomato[33] are available and (b) its general trade-offs between growth and defense are well-studied but a detailed analysis of these trade-offs at the protein level is still missing.

RuBisCO and RuBisCO activase 2 (RCA2) were used as example proteins because both proteins are crucial for photosynthesis and both were shown to play a role in herbivory; thus, they are ideal example proteins to study trade-offs between growth and defense.[34] Additionally, with concentrations up to 50% of total soluble protein, RuBisCO is the most abundant protein in plants and is thought to be an important N storage protein, thus playing a central role in N-metabolism. It is constructed of 16 subunits, 8 identical large ones and 8 identical small ones. RCA modulates the activity of RuBisCO by dissociating the inhibitory sugar phosphates from the active site of the enzyme independent of carbamylation and is known to influence RuBisCO amounts.[35]

We also studied a lipoxygenase (LOX) enzyme, which plays a central role in the production of signaling and defense metabolites in plants by catalyzing the dioxygenation of linolenic and linoleic acid leading to fatty acid hydroperoxides (HPs). In *Nicotiana attenuata*, NaLOX2 specifically supplies HPs for the production of so-called green leaf volatiles (GLVs) and is involved in the recycling of C_{12} derivatives,[36] while another LOX isoform, NaLOX3, catalyzes the first step in the biosynthesis of jasmonic acid (JA), a key element of plant-defense signaling.[37] GLVs and JA are induced rapidly by damage and herbivory. Interestingly, an increase in transcript levels of LOX occurs later than the maximum increase in JA and GLVs. It is thought that the initial bursts are produced by constitutive enzyme pools that are rapidly activated upon attack.[38]

Furthermore, an initial herbivore attack alters the plants ability to resist a subsequent attack. Again, it was hypothesized that inactive or active enzyme pools increase after herbivory to allow the plant to respond more rapidly to future attacks.[39] However, little is known about the enzyme pools of LOX2 and LOX3 available in the plant. Therefore, our objectives were to quantify the pools of LOX2 and LOX3 proteins in plants before and at later time-points (1−7 days) after repeated herbivory.

Thus, in this study we successfully addressed the need for a new quantitative proteomics approach enabling the determination of ^{15}N incorporation levels and protein pool sizes based on LC−MS^E data. We demonstrate that the method is applicable to soil-grown plants which received a ^{15}N pulse for tracking of changes in N-flux and elicited by simulated herbivory.

■ EXPERIMENTAL PROCEDURES

Chemicals

All chemicals were from commercial sources and were used directly without further purification.

Plant Germination, Growth Conditions and Treatment

Plants. *Nicotiana attenuata* Torr. ex. Wats (Solanaceae) seeds of an inbred line's 30th generation, whose first generation was originally collected in Utah, were sterilized and germinated on Gamborg B5 media (Duchefa) according to Kruegel et al.[40] The plants were incubated in a growth chamber at 26 °C with an 11/13 h day/night cycle. After transfer to single pots, plants were cultivated in a glasshouse at 16/8 h day/night cycle with 26− 31 °C during the day and about 20 °C during the night and 45−55% humidity. Daily conditions slightly changed depending on season.

Unlabeled Plants for Phosphorylase b Quantitation and Linear Dynamic Range Analysis. Ten days after germination, the plants were transferred to Teku pots, and 10 days later to 1 L single pots with soil. To determine the linear dynamic range, three leaves of five rosette-stage plants were pooled after the harvest. The leaves were chosen randomly.

Permanent Labeling Experiment (for the setup see also Figure S1a, Supporting Information). For the

dx.doi.org/10.1021/pr300465n | J. Proteome Res. 2012, 11, 4947−4960

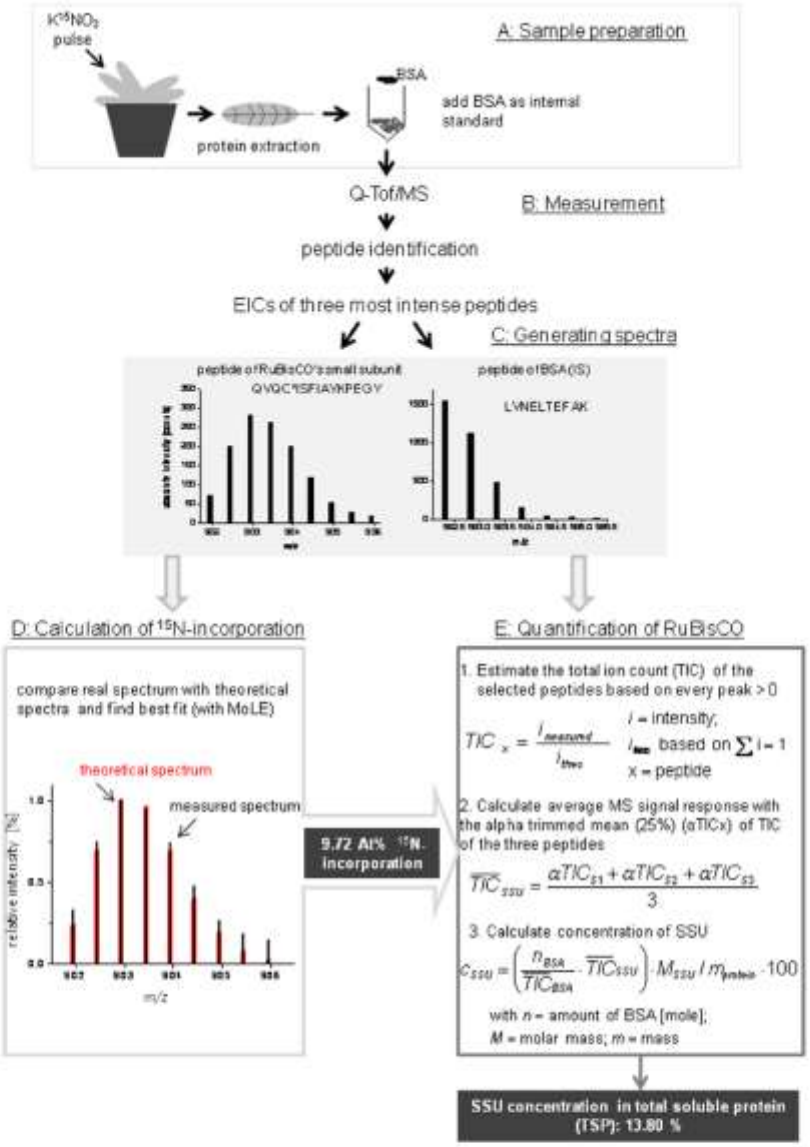

Figure 1. Experimental workflow using ribulose-1,5-bisphosphate-carboxylase/oxygenase small subunit (RuBisCO SSU) as an example. (A) Twenty-seven days after germination *Nicotiana attenuata* plants were labeled with a $K^{15}NO_3$ pulse and the oldest sink leaf was marked. Seven days later, this leaf was harvested. After the extraction of total soluble protein, bovine serum albumin (BSA) was added as an internal standard before tryptic digestion. (B) Samples were analyzed on a LC−MS^E system. The three most intense peptides of RuBisCO SSU and of BSA (Table 1) were identified by their retention time (RT), mass and charge. Extracted ion chromatograms (EIC) of each peptide were generated. (C) Spectrum of 5 scans around the maximal intensity of the three selected peptides of RuBisCO SSU was created and used for ^{15}N-incorporation calculation. For quantitation, a spectrum of the scan with the highest absolute intensity was produced for the 3 selected peptides of SSU and of BSA. (D) ^{15}N-Incorporation was determined with a novel algorithm (MoLE) by comparing the pattern of the spectrum of each peptide to theoretical patterns in a library. (E) For quantitation, the total ion count (TIC) of all peaks of a spectrum was estimated by taking the ratio of the measured intensity to the theoretical intensity (derived from the theoretical spectrum of ^{15}N-incorporation) (1). On the basis of all individual TICs of a peptide, the alpha trimmed mean (25%) was calculated (2). The TIC alpha trimmed means of the three peptides of RuBisCO SSU and the internal standard BSA were averaged and used to calculate the percentage of RuBisCO SSU in total soluble protein (TSP, determined by the Bradford method) (3).

permanent labeling experiment, the plants were transferred after 12 days into 50 mL hydroponic culture single pots containing different concentrations of ^{15}N-labeled $Ca(NO_3)_2$ (0, 1, 5, 10, 50, 100 At%), and 10 days later to 1 L hydroponic culture pots with the same $^{15}NO_3^-$ concentrations in the form of KNO_3 and kept in the glasshouse. For the first 12 days in hydroponic culture, the plants were fertilized with 0.210 g Flory P/K (Euflor, Munich, Germany), 0.0536 g $MgSO_4$, 0.455 mL Fe-diethylenetriamine-pentaacetic acid (Fe-DTPA) solution (2.78 g $FeSO_4 \cdot 7H_2O$ and 3.93 g $C_{14}H_{23}N_3O_{10}$ per L) and 2 mmol $Ca(NO_3)_2$ per L. After transfer to 1 L single pots, they were fertilized with 0.123 g $MgSO_4 \cdot 7H_2O$, 0.129 g $CaSO_4 \cdot H_2O$, 0.048 g K_2HPO_4, 0.031 g KH_2PO_4, 0.5 mL micronutrient solution (2.533 g H_3BO_3, 1.634 g $MnSO_4 \cdot 2H_2O$, 0.151 g Na_2MoO_4 $2H_2O$, 0.440 g $ZnSO_4 \cdot 7H_2O$,

0.080 g $CuSO_4 \cdot 5H_2O$, 0.020 g $CoCl_2 \cdot 6H_2O$ per L H_2O), 0.5 mL Fe·DTPA and 1 mmol KNO_3 per L until harvest. This fertilization regime resulted in 0.37, 1.35, 5.28, 10.19, 49.49, and 98.16 At% in the plants if the natural abundance of ^{15}N is considered. Once per week, all pots received 1 mmol KNO_3 per L with the same concentrations of $^{15}NO_3^-$ they received when still in 50 mL pots, and the pots were filled up to 1 L with water. Labeled media were prepared by substituting $^{14}NO_3^-$ for $^{15}NO_3^-$ at appropriate concentrations without consideration of the natural abundance of ^{15}N. The plants were harvested 10 days after transfer to 1 L pots. All analyses were carried out with −2 sink leaves at the time of harvest.[41]

Pulse Labeling Experiments (see also Figure 1 for the experimental workflow and Figure S1, Supporting Information, for the setup). For the pulse labeling experiment 27-day-old plants were labeled with 5.1 mg nitrogen in the form of $K^{15}NO_3$ and the oldest sink (−1) leaf was marked. For a kinetic analysis, the oldest sink leaf at the time of labeling was harvested 3, 4, 6, 7, and 10 days after the $K^{15}NO_3$-pulse. Three reference plants received the same amount of unlabeled fertilizer.

To study the role of LOX2 and LOX3 after repeated herbivory, a transgenic line which has reduced expression of NaLOX3 (*irLOX3*; A-03-562-2,[36]) and a co silencing of NaLOX2 was used in addition to *N. attenuata* WT and germinated as described above for a further validation of our approach. Three days after pulse labeling the oldest sink leaf, youngest source leaf and transition leaf (0) at the time-point of labeling plants were wounded (W) with a pattern wheel and treated with 10 μL 1:5 diluted *Manduca sexta* oral secretion (OS) (W+OS) on three consecutive days. The time-shift between labeling and treatment was used because in a preliminary experiment ^{15}N incorporation in leaves reached its maximum three days after labeling. At this time-point there were not significant differences in amino acid residues ^{15}N-labeling pattern (calculated from CID-fragmentation spectra of individual peptides, data not shown). Untreated plants were used for control. The oldest sink leaves were harvested 0, 1, 3, 4, and 7 days after the first treatment.

Total Protein Extraction and Quantitation

To extract the soluble proteins, the leaf tissue was homogenized by GenoGrinder2000 (SpexCertiPrep, Middlesex, U.K.) in 200 μL 0.1 M Tris-HCl (pH 7.6) per 100 mg leaf tissue. The tissue was completely suspended by Vortex and the samples shaken for 2 min. After centrifugation for 25 min at 16100× *g* at 4 °C, the supernatant was transferred to a fresh tube. The protein concentration was measured using a Bio-Rad protein assay kit (Biorad, Hercules, CA) with bovine serum albumin (BSA) as standard.

Sample Preparation for LC−MS^E Analysis

Sample Preparation for Phosphorylase b Quantitation. Five micrograms of total soluble protein and 0.498 μg (7.5 pmol) BSA as internal standard were combined with different amounts (3 samples per concentration: 5, 10, 20, 40, 50 pmol) of phosphorylase b from rabbit (Sigma Aldrich, Germany) in a total volume of 60 μL 0.1 M Tris-HCl-buffer (pH 7.6). Phosphorylase b (1 pmol/μL) dissolved in 25 mM ammonium bicarbonate buffer was used as stock solution. The samples were further prepared as described below.

Preparation of All Other Samples. Five micrograms of total soluble protein and 0.334 μg (5 pmol) BSA as internal standard were combined in a total volume of 20 μL 0.1 M Tris-HCl-buffer.

Reduction, Alkylation and Digestion of All Samples. The samples were reduced by the addition of an equal volume of 20 mM DTT (final concentration of DTT: 10 mM). The samples were incubated at 80 °C for 20 min, cooled to room temperature (RT) and 1 volume of 55 mM iodoacetamide was added to alkylate the reduced cysteines by incubation at 4 °C in the dark for 2 h. The proteins were then precipitated by adding 0.25 times the volumes of 50% TCA (final concentration 10% w/v) at 4 °C for 45 min. After centrifugation for 15 min at 4 °C with 16100× *g*, the precipitates were washed with 80% acetone, centrifuged again at 4 °C with 16100× *g* for 5 min and dried afterward. Proteolysis was initiated by dissolving the dry protein pellet in 25 μL of 50 mM ammonium bicarbonate containing 65 ng of sequencing grade porcine trypsin (Promega, Madison, WI) to each sample and digestion was carried out overnight at 37 °C. After being vacuum-dried to remove any remaining liquid and ammonium bicarbonate, the dried and digested proteins were kept at −20 °C. Prior to further analysis, the samples were redissolved in 0.1% formic acid containing 3% acetonitrile.

Chromatographic and Mass Spectrometry Conditions

Samples were separated using a nanoAcquity nanoUPLC system (Waters, Manchester, UK). A mobile phase of 0.1% aqueous formic acid was used to concentrate and desalt the sample on a Symmetry C18 trap-column (20 × 0.18 mm, 5 μm particle size) at a flow rate of 15 μL min^{-1}. Subsequently, peptides were eluted onto a nanoAcquity C18 column (200 mm × 75 μm ID, C18 BEH 130 material, 1.7 μm particle size) using an increasing acetonitrile gradient in 0.1% aqueous formic acid at a flow rate of 0.350 μL min^{-1}. Buffers A (0.1% FA in H_2O) and B (100% MeCN, 0.1% FA) were linearly mixed in a gradient from 1% to 45% phase B over 60 min, increased to 95% B over 5 min, held at 95% B for 5 min and decreased to 1% B over 1 min. The analytical column was immediately re-equilibrated for 9 min.

The eluted peptides were transferred to the nanoelectrospray source of a Synapt HDMS tandem mass spectrometer (Waters, Manchester, U.K.) equipped with a metal-coated nanoelectrospray tip (Picotip, 50 × 0.36 mm, 10 μm internal diameter, New Objective, Woburn, MA). The source temperature was set to 80 °C, cone gas flow 20 L/h, and the nanoelectrospray voltage was 3.2 kV. For all measurements, the mass spectrometer was operated in V-mode with a resolving power of at least 10000 fwhm. All analyses were performed in positive ESI mode. A 650 fmol/μL human Glu-fibrinopeptide B in 0.1% formic acid/acetonitrile (1:1 v/v) was infused at a flow rate of 0.5 μL min^{-1} through the reference NanoLockSpray source every 30 s to compensate for mass shifts in MS and MS/MS fragmentation mode.

LC−MS data were collected using alternating low energy (MS) and elevated energy (MS^E) modes of acquisition over 1.5 s intervals in the range m/z 50−1700 with an interscan delay of 0.2 s. In low energy mode, data were collected at constant collision energy of 4 eV set on the trap T-wave device and ramped during scan from 15 to 40 eV in elevated MS^E mode. The chromatographic and mass spectrometry performances of the system were regularly checked using tryptically digested BSA and *N. attenuata* wild type samples.

Data Processing and Protein Identification

The LC−MS^E data of unlabeled samples from a continuum were collected using MassLynx v4.1 software and processed by ProteinLynx Global Server Browser v.2.4 software (Waters, Manchester, U.K.) under baseline subtraction, smoothing, deisotoping, lockmass-correction and alignment according to

Table 1. Peptides of Ribulose-1,5-bisphosphate-carboxylase/oxygenases (RuBisCO) Large (L) and Small (S) Subunit and RuBisCO Activase 2 (RCA2) (R) from *Nicotiana attenuata* and of BSA (B) Used for Absolute Protein Quantitation and for Calculation of the ^{15}N-Incorporation of Hydroponically-grown Plants[a]

no	calc. $[MH]^+$	exp. $[MH]^+$	Δ ppm[b]	Rt [min]	Rt RSD [%]	sequence	sumformula
L1	1021.5313	1021.5313	0.0	41.05	0.7	DTDILAAFR	$C_{45}H_{72}N_{12}O_{15}$
L2	1261.7150	1261.7148	0.2	51.09	0.4	DITLGFVDLLR	$C_{58}H_{96}N_{14}O_{17}$
L3	1579.8367	1579.8376	0.6	47.94	0.5	EIVFNFAAVDVLDK	$C_{74}H_{114}N_{16}O_{22}$
S1	2069.0437	2069.0519	4.0	45.13	0.5	YETLSYLPDLSEEQLLR	$C_{93}H_{145}N_{21}O_{32}$
S2	1802.8781	1802.8848	3.7	39.66	1.1	QVQC*ISFIAYKPEGY	$C_{83}H_{123}N_{19}O_{24}S_1$
S3	933.5152	933.5128	2.7	33.78	2.4	IIGFDNVR	$C_{42}H_{68}N_{12}O_{12}$
B1	1163.6306	1163.6395	7.7	35.98	1.6	LVNELTEFAK	$C_{53}H_{86}N_{12}O_{17}$
B2	1479.7954	1479.7966	0.8	41.37	2.5	LGEYGFQNALIVR	$C_{68}H_{106}N_{12}O_{19}$
B3	1567.7427	1567.7454	1.7	47.87	1.0	DAFLGSFLYEYSR	$C_{74}H_{102}N_{16}O_{22}$
R1	1214.6263	1214.6298	2.9	28.17	1.0	TDNVPEEAVIK	$C_{52}H_{87}N_{15}O_{20}$
R2	1706.7980	1706.8067	5.1	36.37	2.7	GLVQDFSDDQQDIAR	$C_{71}H_{111}N_{21}O_{28}$
R3	1332.6794	1332.6839	3.4	33.61	1.8	WVSGTGIEAIGDK	$C_{59}H_{93}N_{15}O_{20}$

[a]Three most intense peptides were taken, except from RuBisCO LSU where the 4th, 5th and 7th most intense peptides were used. The table includes the average mass and retention time (Rt) calculated from triplicate analysis. Carbamido methylated methionine is denoted as C*. [b]Δ ppm = $10^6(M_{in} - M_{exp})M_{in}^{-1}$

the ion accounting algorithm.[42] The processed data were searched against the Uniprot *"Nicotiana tabacum"* subdatabase (downloaded 6 January 2009) to which sequences from BSA, trypsin and phosphorylase b from rabbit were appended. The search parameters were set as follows: mass accuracy of 10 ppm for precursor ions and 15 ppm for product ions, a minimum of 2 peptide matches per protein, with a minimum of 3 consecutive fragment ions each. The maximum false positive rate (FDR) against the randomized database was set to 2%. Further settings were one possible missed tryptic cleavage site, a fixed carboxymethylation of cysteines, variable deamidation of asparagine/glutamines and variable oxidation of methionines. On the basis of our database search of unlabeled wild type samples, on average 90 proteins were found in the protein extracts, and about half of those could be identified.

N. attenuata's RuBisCO LSU consists of 477 amino acids and has a mass of 52.90 kDa, RuBisCO SSU of 180 with a mass of 20.35 kDa and RCA2 of 439 with a mass of 48.28 kDa, respectively.

Data Processing of ^{15}N-Labeled Samples

Extracted ion chromatograms (EIC) of the light form of three peptides of the protein of interest (phosphorylase b, BSA, RuBisCOactivase 2 (RCA2), RuBisCO large (LSU) and small subunit (SSU) and lipoxygenase 2 (LOX2) (Tables 1, S2, S3, Supporting Information) were generated from the full scan mass spectra based on their m/z of the identified peptides and their retention time. The peptides were chosen based on three criteria: (1) most intense peptides, (2) peptides that showed analytical reproducibility, and (3) no overlap in spectra. As the most intense peptides of the proteins of interest varied between experiments, they were determined individually for each experiment by peptide lists generated with PLGS v2.4 of unlabeled samples (Tables 1, S2, S3). For ^{15}N-incorporation estimations, average spectra were generated from 5 scans at the top of the chromatographic peak, and for quantitation, one spectrum was generated of the scan at the top. They were baseline subtracted, smoothed and centroided manually in MassLynx v4.1 software. The following settings were used: Baseline subtraction, polynomial order 20, below curve 5%, tolerance 0.010 Da; smoothing, Savitzky-Golay with smooth window of 3 channels, applied twice to each spectrum; Centroid calculation, minimum peak width at half height of 4 channels and centering at peak width at 35% from the top. Subsequently, the masses were lockmass-corrected by the same software. For lockmass, a correction factor was calculated based on the ratio of the measured mass to the theoretical mass of the lockmass substance 785.8426 Da. To determine the measured mass, a spectrum of the calibration trace was created in a mass window of 30 min. During this period of time, all intense peptides were detected. The correction factor was applied as follows:

$$\textbf{correction factor} = \frac{\text{theoretical mass}_{785.8426}}{\text{measured mass}_{785.8426}} \quad (1.1)$$

The measured monoisotopic masses were multiplied with this factor.

Quantitation of Phosphorylase b from Rabbit, RuBisCO, RCA2, and LOX2

The absolute quantity of each protein of interest (calc_c) (phosphorylase b, RuBisCO SSU, RuBisCO LSU, RCA2, LOX2) was calculated based on the relation between the average of the robust estimations of total ion count (TIC) of the three most intense peptides of internal standard (IS, BSA) and the three most intense peptides of the protein of interest (Table 1, S2, S3, Supporting Information): First the TIC of each peptide was estimated based on the measured intensity ($ix_{measured}$) of every peak (x) > 0 of the spectrum and its ratio to its theoretical intensity (ix_{theo}) at its individual ^{15}N-incorporation level. The theoretical intensity is the relative intensity of a peak based on a theoretical spectrum at its ^{15}N-incorporation. Then the alpha trimmed means of TIC of the selected peptides (px, p = kind of protein) (αTIC_{px}), calculated based on all robust TIC estimations of this peptide, were averaged to get the average total ion count ($\overline{TIC}$) (Figure 1). We used the alpha trimmed mean to minimize the influence of outliers, which often result in inaccurate results from nonrobust estimators such as the mean, or simply using the sum of peak intensities as TIC. Finally, the average total ion count estimates of all charge states of a peptide were added. The calculation is shown for RuBisCO SSU (RUB−SSU=S) as example:

$$TIC_x = \frac{ix_{measured}}{ix_{theo}} \text{ with } \sum ix_{theo,i} = 1 \quad (1.2)$$

dx.doi.org/10.1021/pr300465n | J. Proteome Res. 2012, 11, 4947−4960

$$\overline{\mathrm{TIC}}_{\mathrm{RUB-SSU}} = \frac{\alpha\mathrm{TIC}_{S1} + \alpha\mathrm{TIC}_{S2} + \alpha\mathrm{TIC}_{S3}}{3} \quad (1.3)$$

$$\mathrm{calcc}_{\mathrm{RUB-SSU}} = \left(\frac{n_{\mathrm{BSA}}}{\overline{\mathrm{TIC}}_{\mathrm{BSA}}} \times \overline{\mathrm{TIC}}_{\mathrm{RUB-SSU}}\right) \times M_{\mathrm{RUB-SSU}}/m_{\mathrm{protein}} \times 100 \quad (1.4)$$

With n = amount of BSA (mole), M = molar mass of protein of interest, m = mass of total soluble protein on column.

MoLE: Molecule Labeling Estimator

To estimate the ^{15}N-incorporation, we developed a new method implemented in the program MoLE "Molecule Labeling Estimator". It requires a list of masses $M_0;\ldots;M_K$ with intensities $f_0;\ldots;f_K$ normalized such that $\sum_i f_i = 1$ as input. The isotope pattern of the sample molecule is extracted from the mass spectrum based on the sum formula of the molecule (peptide) and its charge. The basic concept of the algorithm is to simulate the isotope pattern of the sample molecule for different incorporations and to match those with the isotope pattern of the measured sample. The predicted isotope distribution is based on all natural-abundance isotopes, except the element that is selected to be enriched. The simulation of the isotope pattern with masses $m_0;\ldots;m_K$ and intensities $p_0;\ldots;p_K$ is computed by deconvoluting the isotope distributions of the individual elements of the molecule.[43] All possible incorporation rates between 0 and 100% are tested in steps size 10. After the best initial scoring incorporation ratio r has been determined, the second phase of the algorithm is started, where the ratio is varied between $r - 10$ and $r + 10$ with step size 1. In subsequent phases, additional digits of the ratios can be determined.

To score each incorporation ratio, the statistical model introduced in Böcker et al.[43] is used. This score is based on Bayesian statistics and the maximum likelihood framework. The likelihood is computed to observe the data $\mathcal{D}$ under the model $\mathcal{M}$ of a particular incorporation ratio and the background model $\mathcal{B}$ that one of the incorporation ratios is correct:

$$\mathbb{P}(\mathcal{D}|\mathcal{M}, \mathcal{B}) = \prod_i \mathbb{P}(M_i|m_i) \prod_i \mathbb{P}(f_i|p_i) \quad (1.5)$$

Here the independence of the individual probabilities is assumed, where $\mathbb{P}(M_i|m_i)$ is the probability of observing a peak with mass M_i when the true mass of the ion is m_i and $\mathbb{P}(f_i|p_i)$ is the probability of observing a peak with intensity f_i when the true intensity of the ion is p_i.

The ^{15}N-incorporations were calculated based on the more relevant ^{13}C isotope abundance of 1.096%, instead of the carbonate specific abundance of 1.112%, since this appears to be more appropriate in biological studies.[44]

The program also allows scoring incorporation ratios using mass differences instead of masses; therefore, we could calibrate using the monoisotopic peak; or to ignore masses, so that the score is based solely on intensities. As we have observed that peaks of low intensity often show high variations in the measured intensity, the program offers the option to remove all such peaks from the analysis. Furthermore, to counter the effect of an imprecise baseline correction, there is an additional option to subtract the median intensity of the removed peaks from the intensity of each of the remaining peaks. To account for modifications such as carbamidomethylation, carboxylation and hydroxylation MoLE offers the option of entering the molecular formula of the modification where the enrichment is not taken into account and the natural ^{15}N/^{14}N ratio is used.

The program is freely available and can be downloaded from http://bio.informatik.uni-jena.de/software/mole/.

Calculation of ^{15}N-Incorporation

The processed spectra of the three chosen peptides of the protein of interest (RCA2, RuBisCO SSU and LSU, LOX2) (Table 1, S2, S3, Figure S2, Supporting Information) were used for the calculation of the ^{15}N-incorporation of the protein. The program MoLE (see above) and the script published by Taubert et al.[13] were used to calculate the ^{15}N-incorporation for each peptide. The average ^{15}N-incorporation of the three peptides was then defined as the overall ^{15}N-incorporation of the protein.

For the calculation of the ^{15}N-incorporation by MoLE, we used intensities only, since the results for our data set were not improved by using additional settings. First, all peaks of the averaged spectra with relative intensities between 0 and 2% were removed, and the median of the intensities of the removed mass peaks was subtracted from the intensities of the remaining peaks. This step was necessary to adjust the unequal impact of baseline correction on peaks of different intensities. Furthermore, peaks below 3 and 7% relative intensity were not scored, because small peaks were often less precise. This adjustment was applied so that unlabeled samples were close to the natural ^{15}N abundance of 0.3677 At%. If peptides had modifications which were added to the peptide during the sample preparation, they were defined as naturally labeled parts of the molecular formula. For unlabeled samples, ^{15}N abundance was set to 0.3677 At%.

Sample Preparation for Isotope Ratio Mass Spectrometry

To reconfirm the ^{15}N-labeling calculated from LC–MS^E data, the labeling of total soluble protein was also analyzed by an elemental analyzer–continuous flow–isotope ratio mass spectrometry (EA–CF–IRMS). Three hundred micrograms of dissolved protein was filled into 40 μL tin capsules for liquid samples (IVA Analysentechnik, Meerbusch, Germany) and dried before analysis. To accommodate the high sensitivity of the IRMS, samples were diluted to a final labeling of about 1 At% ^{15}N by adding a 5 μg/μL solution of unlabeled BSA to the tin capsules.

For the determination of ^{15}N-incorporation in leaves, the plant tissue was dried at 60 °C for 48 h and homogenized before analysis. About 0.125 ± 20% mg of the homogenized and dried plant material was put into 40 μL tin capsules together with 0.8325 ± 20% mg of working standard (acetanilide) to ensure that the labeling did not exceed about 1 At% ^{15}N (and thus avoid detector saturation). The exact plant sample weights were measured and used for calculation of ^{15}N abundance. Three technical replicates for each sample were analyzed.

Isotope Ratio Mass Spectrometry Analysis

The IRMS analysis and the calculation of ^{15}N-incorporation were carried out as described by Meldau et al.[45]

Evaluation of ^{15}N-Incorporation over Time

The increase in labeling over time was characterized by a sigmoidal regression analysis using the Gompertz function with the software Origin 8G (Originlab, Northampton, MA). Based on the function:

$$y = ae^{-e^{[-k\cdot(x-t_i)]}} \quad (1.6)$$

with a representing the horizontal asymptote, t_i the time-point of inflection and k a constant related to the increase in labeling. We

dx.doi.org/10.1021/pr300465n | J. Proteome Res. 2012, 11, 4947−4960

calculated the maximal slope s as an indicator of ^{15}N incorporation per day as follows:

$$s = \frac{a \cdot k}{e} \quad (1.7)$$

RESULTS AND DISCUSSION

The aim of this study was to develop a new strategy for the absolute quantitation of proteins with unknown ^{15}N-incorporation levels which would enable us to study changes in the protein pools and ^{15}N flux after herbivore attack of plants in detail. Robustness and reliability of the strategy was analyzed thoroughly before applying it to soil-grown elicited plants with simulated herbivory.

Quantitation Strategy

Our quantitation strategy is based on Silva et al.[24] who established a data-independent approach (DIA) for absolute quantitation of proteins in complex leaf samples, also known as LC−MS^E. The approach uses a universal signal response factor of a single internal standard for protein quantitation. To calculate the universal signal response factor the authors summed the intensity of the deisotoped monoisotopic peak over the whole chromatographic peak of all charge stages for each of the three most intense peptides of the internal standard. The averaged intensity of those three peptides divided by the quantity of the internal standard was defined as the universal signal response factor. The average signal response of the protein of interest was calculated as described for the internal standard and used with the universal signal response factor for quantification. This method was not suitable for our samples because plants were labeled with ^{15}N, and increasing ^{15}N-incorporation decreases the intensity of the monoisotopic peak as a function of the sum formula of the peptide and its labeling. Therefore, we developed a new strategy and calculated the universal signal response factor based on the robust estimations of total ion count (TIC) of the three most intense peptides as shown in Figure 1E (see also Experimental Procedures, eqs 1.2−1.4). In brief, we defined the signal response of a peptide as alpha trimmed mean of TIC. The alpha trimmed mean of TIC was calculated from a set of robust TIC estimations which are based on the ratio of measured intensity and theoretical intensity of every peak of a spectrum >0 at the top of the chromatographic peak. As defined above, the theoretical intensity is the relative intensity of a peak based on a theoretical spectrum at its specific ^{15}N-incorporation level. On the basis of the alpha trimmed mean of TIC of the three most intense peptides of the internal standard, its average signal response was determined. By dividing it through the quantity of internal standard, we obtained the universal signal response factor. The average signal response of the protein of interest was calculated in the same way and quantified based on the universal signal response factor of the internal standard. This strategy for protein quantitation is independent of the isotopic distribution and the sum formula of a peptide, so that it is applicable to all labeled proteins.

Validation of the Quantitation Approach with Phosphorylase b

To test the applicability of here developed LC−MS^E-based quantitation strategy in our complex leaf samples, we added different amounts of phosphorylase b from rabbit to internal standard-spiked unlabeled total soluble protein extracts. We chose BSA as internal standard because it is a midsized protein (585 amino acids) similar to the studied ones and cannot be synthesized by plants. The tryptic digests of these extracts were analyzed using an alternate scanning mode of data acquisition (LC−MS^E) on a Q-Tof mass spectrometer. Based on the LC−MS^E data we generated peptide lists with PLGS v2.4. Peptides corresponding to the studied proteins were identified by searching with an MS-Blast homology-based searching algorithm[46] against a subdatabase downloaded from Uniprot (see Material and Methods). We used the peptide list to determine the three most intense peptides of BSA and phosphorylase b (Table S2, Supporting Information). For peptide selection, in addition to the signal intensity, we also used further criteria. Some of the peptides were not detectable in all analyzed samples due to isotopic overlap in spectra with other peptides. Therefore, we selected only those peptides for quantitation that could be reproducibly detected and did not overlap with other peptides.

Phosphorylase b was quantified based on its average signal responses and the universal signal response factor of BSA (Figure 1E, Figure 2) as described above. We conducted triple measurements of each sample to analyze the technical reproducibility. Phosphorylase b could be reliably quantified up to an amount of 300 fmol on the column with a maximal relative deviation of 20.18%, which is equivalent to 38.8% in total soluble protein (TSP). Samples with concentrations lower than 300 fmol could be measured with a reproducibility of 10%. For higher injected amounts (up to 750 fmol on the column; ~97% in TSP) the amounts of proteins determined was lower than expected and the deviation of determination increased significantly (34.27%). It is probably related to an oversaturation of the ion detector in the used instrumentation (see later for detailed explanation). Silva et al.[24] showed a deviation in a similar range (15%) after applying six exogenous proteins in varying concentrations to samples of the human serum. The data demonstrate that a reliable quantitation of proteins in our complex leaf extracts is

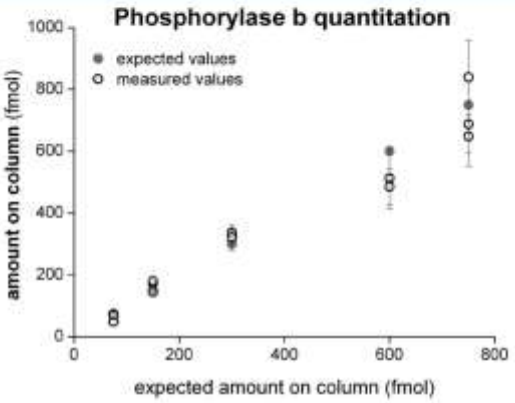

Figure 2. Calculated and expected amounts of phosphorylase b after addition of different known amounts to complex leaf samples. Five μg of total soluble protein (TSP) of *Nicotiana attenuata* (three independent samples per concentration) were spiked with different amounts of phosphorylase b from rabbit muscle and a standard amount of BSA as internal standard prior sample preparation for LC−MS^E measurement (see Figure 1). The protein quantity of phoshorylase b was calculated based on the universal response factor of BSA and the robust estimations of the total ion counts (TIC) of the three most intense peptides of phosphorylase b (Table S1, Supporting Information). Each sample was measured three times. The variability of technical replicates of each sample is indicated by the error bars.

dx.doi.org/10.1021/pr300465n | J. Proteome Res. 2012, 11, 4947−4960

possible using LC−MS^E data and the estimation of the universal response factor based on TIC.

Peptide Identification of RuBisCO LSU and SSU and RCA2 of *N. attenuata*

To further validate the applicability of our approach for leaf proteins, two important proteins of plants, RuBisCO and RuBisCO activase (RCA), which are regulated by herbivory[34] and involved in regulation of nitrogen dynamics in leaves[47,48] were chosen as model proteins for quantitation and nitrogen flux studies. As *N. attenuata* is an a nonsequenced organism, and the protein sequences of *N. attenuata* were not available at the beginning of our study, we used peptide sequences of *N. tabacum* and *N. sylvestris* for peptide identification, because the phylogenetic distance of *N. attenuata* to *N. tabacum* and *N. sylvestris* is close.[49] In fact, the very recently obtained complete mRNA sequences of *N. attenuata* in our laboratory showed for RuBisCO LSU (JF419563) 99% identity to *N. tabacum* (NP_054507), and for SSU (JF419564) 96% identity to *N. sylvestris* (P22433) after translation to the protein sequence. From three RCA isoforms occurring in *N. attenuata* (JF419565, JF419566, JF419567), the most abundant isoform, RCA2, showed a 99% identity to *N. tabacum* RCA2 (Q40565). These data demonstrate that our approach also allows absolute protein quantitation of nonsequenced organisms, as long as a close related sequenced species are available whose genome can be used for peptide identification.

We found a concentration-dependent protein sequence coverage from 23.9 to 48.2% for RuBisCO LSU, 29.3 to 59.7% for RuBisCO SSU and 18.2 to 58.5% for RCA2 (data not shown). Accurate measurements with a relative standard deviation (RSD) of retention time less than 2.7% and a highest mass precision error of 5.1 ppm (expect for one peptide, Table 1 and S3) allowed a precise peptide identification. Independent experiments showed similar intense peptides, while order of the most intense peptides varied (data not shown), so that different peptides for quantitation were selected for the different experiments (Table 1 and S3). We further observed that LC−MS^E data for RuBisCO LSU resulted in peptides whose intensity was significantly higher compared to the internal standard BSA and other model proteins. LSU has many basic sites which might result in a better ionization and consequently higher intensities of these peptides. To avoid detector oversaturation that might result in (a) incorrect calculations of ^{15}N-incorporation levels and (b) a quantitation error, we chose peptides with a maximum intensity lower than 2000 counts for RuBisCO LSU quantitation. This may lead to a small underestimation of the average signal response of RuBisCO LSU, but for all other evaluated proteins, the data-independent acquisition approach was fully applicable.

Determination of the Linear Dynamic Range (LDR)

For the sample analysis we used a microchannel plate detector of ions (MCP) equipped with a time-to-digital data converter. These detectors provide high sensitivity, high speed (in picoseconds) and low background noise, but MCPs have certain limitations due to their inability to count precisely if more than one ion simultaneously hits the detector. This lowers MCP linear dynamic ranges at high intensities of ions (linearity approximately 2.5 orders of magnitude) compared to other types of detectors, such as photomultipliers in tandem quadrupoles or the novel hybrid detectors.[50]

Our complex leaf samples contain unknown amounts of RuBisCO LSU and SSU and RCA2. To determine the linear dynamic range (LDR) of the detector for quantitation and the optimal amount of protein required for their LC−MS^E analyses, different amounts of total protein were analyzed. The average MS signal defined as the average of alpha trimmed mean of TIC of the three chosen peptides (Table 1) of RuBisCO LSU, RuBisCO SSU and RCA2 (example proteins) and BSA (internal standard) were calculated. The total amount of protein (total soluble protein (TSP) on column) injected ranged from 15.6 to 500 ng. Figure 3 represents the relationship between the amount of protein loaded onto the column and the average signal response: BSA was linear in the full range tested with a correlation coefficient of 0.9911, whereas RuBiSCO SSU and LSU ranged between 15.6 to 125 ng (R^2 SSU: 0.9928 and LSU: 0.9750) RCA2 from 15.6 to 250 ng (R^2 RCA2: 0.9911) (Figure 3), giving an average linear dynamic range of about 1.5 orders of magnitude.

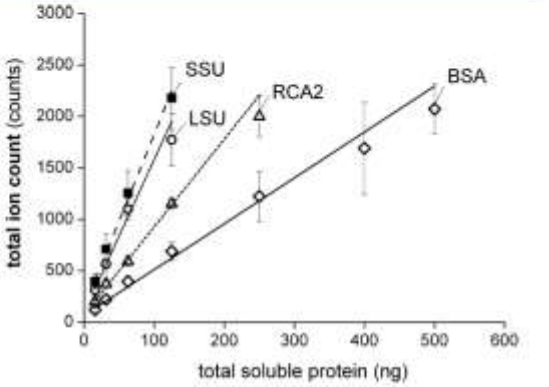

Figure 3. Linear dynamic range of LC−MS^E measurements. Signal response for RuBisCO large (LSU) and small subunit (SSU), RuBisCO activase 2 (RCA2) (R) and BSA plotted against the amount of the analyzed total soluble protein (TSP). The averaged total ion count (mean ± SE, n = 3) for each protein was calculated using selected peptides (Table 1, L1−3; S1−3; R1−3; B1−3). Data were analyzed by a linear regression (R^2: LSU = 0.9750; SSU = 0.9928; RCA2 = 0.9911; BSA = 0.9741).

Most proteins in the sample are less abundant than RuBisCO SSU and LSU, so that initially an amount of 250 ng of TSP was chosen for analysis. However, for our three studied proteins it was sufficient to use 75 ng as optimal protein amount for the LC−MS^E analysis in the given dynamic range of protein concentration.

Labeled Peptide Identification and Determination of ^{15}N-Incorporation

The aim of our study is not only the absolute quantitation of proteins, but to study N-flux in plants after herbivore attack which requires labeling of plants with ^{15}N. However, ^{15}N-incorporation into proteins causes shifts in the isotope pattern of mass spectra of peptides used for protein identification and quantification. Thus, two additional challenges had to be faced: Identification of labeled peptides and determination of ^{15}N-incorporation of each peptide, which is a prerequisite for protein quantification.

Peptide identification algorithms applied in conventional database searching software are well established for peptides of natural isotopic distribution, but metabolic ^{15}N-labeling of plants never reaches 100% and results in ubiquitous labeling which dramatically reduces the efficiency of peptide identification by

database searching.[51] Therefore, here, we harvested for each experiment three untreated plants per time point, extracted proteins and generated peptide lists with PLGS v2.4 as described above. The peptide lists were used to identify peptides for quantitation (Table 1, Table S3, Supporting Information). Based on this information, peptides of the labeled samples were identified manually according to their identical retention times and identified m/z values of the unlabeled peptide to demonstrate the proof of principle. Upon software modifications, such identification/quantitation should be possible in an automated manner.

For our protein quantitation approach, we used the robust estimation of TIC which requires the theoretical intensity of each peak of a spectrum (see above and Experimental Procedures). As the spectrum is influenced by the level of ^{15}N labeling the individual ^{15}N-incorporation had to be determined for each peptide. To estimate the isotope enrichment of labeled peptides, we developed a program, called MoLE "Molecule Labeling Estimator", which simulates different ^{15}N-incorporations of a sample molecule and matches them with the isotope pattern of the measured samples using the best probable fit to determine the ^{15}N-incorporation.

Previous approaches used the mean square error[13,26,29] or the Pearson correlation coefficient[27] of peak intensities to score incorporation ratios. Jehmlich et al.[52] proposes to use the accurate mass of the most intense peak to determine this ratio. Pan et al.[28] combine peptide identification and determination of ^{15}N-incorporation in a single analytical step. MoLE uses both intensities and mass shifts, integrated into a single probabilistic model of the data. This statistical model was originally introduced by Böcker et al.[43] for molecular formula identification using isotope patterns. It is based on a Bayesian probabilistic model in combination with a maximum likelihood estimation which has proven to be beneficial in numerous areas of data analysis. Unlike the approach of Böcker et al.,[43] MoLE uses additional parameters for peak list processing and additional information for the molecular formula, to estimate heavy isotope enrichments of molecules. In addition, MoLE comes with an easy-to-use graphical user interface, and allows batch processing of mass spectra. It could be easily modified to be applicable for other heavy nuclide isotopes (^{2}H, ^{18}O, ^{13}C) enrichment calculations.

To assess the accuracy of ^{15}N level calculations, plants with different constant ^{15}N-labeling from natural abundance to almost 100 At% were cultured, and the ^{15}N-incorporations of RuBisCO LSU's and SSU's peptides (Table S1, Supporting Information) were determined for 5 biological replicates. The difference from the expected ^{15}N-incorporation was for all peptides and labeling levels, except two peptides at 49.49 At%, less than 1 At% (Figure 4). To validate the program MoLE, the ^{15}N-incorporation for LSU and SSU was also calculated with a previously published macro Excel sheet.[13] The values obtained with the macro Excel sheet were similar to those obtained with MoLE and showed similar deviations from the expected values (Figure S3, Table S1). However, MoLE has the advantage that peaks are identified automatically and the ^{15}N-incorporation of multiple spectra can be calculated at the same time. The larger error for 49.49 At% incorporation was found with both programs, and is caused by the increasing complexity of the spectra. As discussed by MacCoss et al.,[27] the width of the isotope distribution is broadest near 50 At% and narrowest at 0 and 100 At%, so that precision is higher in samples with more compact isotope distributions.

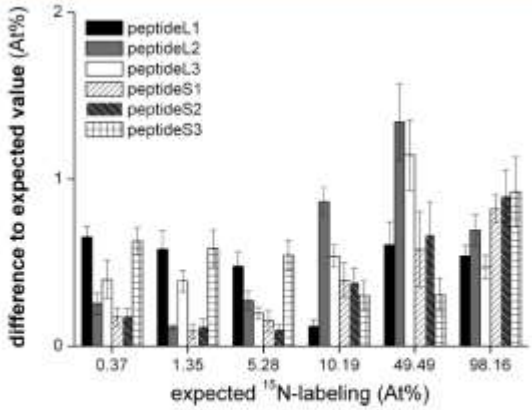

Figure 4. Absolute differences between calculated (MoLE) and expected ^{15}N-incorporation of RuBisCO from leaf extracts of plants grown at different concentrations of partial permanent ^{15}N-labeling. Mean ± SE ($n = 5$) of three peptides of RuBisCO LSU(L1−3) and SSU (S1−3) (for peptides see Table 1).

To further assess the quality of our measurements, we calculated the differences between two injections for five biological replicates using MoLE (Figure S4, Supporting Information). For low levels of labeling (<10.19 At%), these technical differences were less than 0.4 At%. At higher levels, the differences reached 1.0 At% (Figure S4). Overall, our data demonstrates, that ^{15}N-incorporation of the proteins can be reliably determined by MoLE.

Comparison of LC−MS^E and IRMS

The classical method to study nitrogen partitioning in plants is isotope ratio mass spectrometry (IRMS). IRMS measurements have a high precision (SD ≤ 0.3 % for ^{15}N) and instruments are usually optimized to natural abundance variations of isotopes.[53,54] We compared the ^{15}N-incorporation of RuBisCO LSU and SSU estimated by the program MoLE from LC−MS^E data and the ^{15}N-incorporation of total soluble protein (TSP) measured by elemental-analyzer continuous-flow IRMS (EA-CF-IRMS) with the expected values (Figure 5). Both approaches showed a clear linear relationship ($R^2 = 0.9998$) to the expected values, confirming the precision of our estimations.

However, for our research question, the analysis of ^{15}N-incorporation of proteins by LC−MS^E measurements has clear advantages. Samples for IRMS measurement with a labeling higher than 5 At% had to be diluted with unlabeled BSA to remain in the linear dynamic range of the IRMS instrument, and samples with a labeling of more than 10 At% could not be measured accurately by IRMS (data not shown). The difference from the expected value (Figure S5, Supporting Information) and the variability between the technical replicates (Figure S6) increased with the labeling, due to the difficulty of exact weighing in the submicrogram range during dilutions with BSA. Furthermore, IRMS requires tedious sample preparation in order to measure the ^{15}N-incorporation of individual proteins, and requires at least 300 ng of protein for accurate measurements which can only be extracted from multiple samples. Summarizing, in comparison with the IRMS, our approach demonstrated a high precision for ^{15}N-incorporation determination. IRMS is suitable for the determination of ^{15}N-incorporation in tissues or total soluble protein with a higher precision at lower ^{15}N-abundance, while our method also allows calculating ^{15}N-

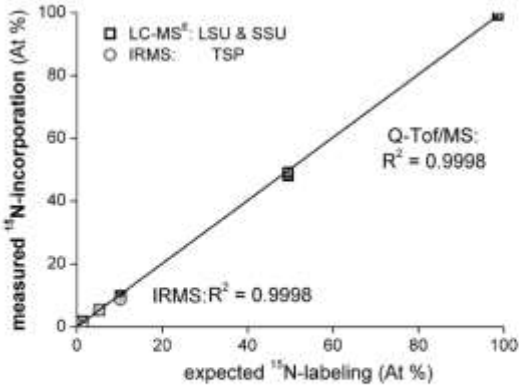

Figure 5. Correlation of calculated and expected ^{15}N-incorporation levels at different concentrations of partial permanent ^{15}N-labeling determined by two different methods. ^{15}N-incorporation of RuBisCO LSU and SSU (mean ± SE, n = 5) was calculated by MoLE algorithm from data measured by LC−MS^E and of total soluble protein it was determined by isotope ratio mass spectrometry (IRMS). Linear curve fit between expected and calculated ^{15}N-incorporation was 0.9998 for both methods.

incorporations of a large number of single proteins in complex mixtures also with high ^{15}N-abundances.

Quantitation of Isotopically Labeled Proteins after *in vivo* Pulse Labeling of Whole Plants Grown in Soil

Many previously published MS-based methods for quantitation of plant proteins were performed with plant cell suspension cultures,[16,17] hydroponic culture[51] or solid culture media.[21] However, plants grown in hydroponic culture have a limited value in studying ecological interactions;[55] and for the study of changes in protein pool sizes in plant-herbivore interactions a soil-based method is required. SILIP is the only MS proteomics method available for soil-grown plants,[14] but it requires a set of fully labeled and unlabeled plants which does not allow tracking of ^{15}N-flux and quantitation of proteins with unknown amounts of labeling. Therefore, we adapted the experimental design of van Dam and Baldwin,[4] who pulse-labeled plants grown in soil to study nitrogen acquisition after leaf removal and methyl jasmonate treatment.

Nicotiana attenuata plants grown in soil received a $K^{15}NO_3$ pulse of 5.1 mg nitrogen and were harvested at the indicated time-points after treatment (see also Materials and Methods) leading to different unknown levels of ^{15}N-incorporation. Three plants per time point received an unlabeled KNO_3 pulse to generate peptide lists with PLGS. On the basis of these peptide lists, we identified the most intense peptides of the proteins of interest (Table S3, Supporting Information) and determined the ^{15}N-incorporation of our three example proteins with MoLE algorithm.

A kinetic analysis revealed that the increase in labeling in the three analyzed proteins over time was exponential, and the best fit for describing the increase was obtained with a three parametric Gompertz function with a coefficient of correlation higher than 0.93 (Figure 6a). This relationship was also described for the increase in labeling of bacteria (*Pseudomonas putida*)[13] and for plant growth.[56] The maximal labeling (asymptote) was slightly different between the three proteins used in this study, but not statistically significant (data not shown). The slope for RCA2 was higher than for RuBisCO LSU and SSU (Figure 6a). The slope can be considered as measure for ^{15}N- incorporation

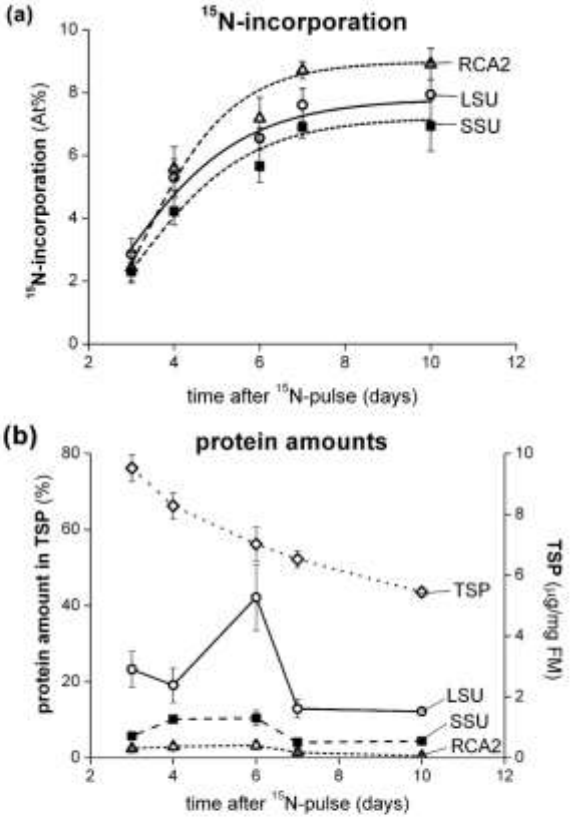

Figure 6. (a) ^{15}N-Incorporation and (b) protein amount in TSP of RuBisCO LSU and SSU and RCA2 over time from rosette leaves of soil-grown *N. attenuata* plants after *in vivo* labeling with $K^{15}NO_3$. The oldest sink leaves at the time-point of labeling were harvested at indicated time points (n = 5). Total soluble protein (TSP) extracts were measured by LC−MS^E. ^{15}N-Incorporation was determined with MoLE (R^2: RCA2 = 0.9650, LSU = 0.9262, SSU = 0.9695). The regression analysis was performed with Origin 8G. For ^{15}N-incorporation calculation and quantitation the most intense peptides (Table 1) were used. Mean ± SE are shown.

(metabolic turnover)[13] and gives a first hint that the turnover of RCA2 is faster than for RuBisCO. This result might be explained by the relationship between the proteins: RuBisCO can be activated very rapidly by RCA,[35] so that a faster fine-tuning of the amount of the activator is probably more important than the regulation of the RuBisCO amounts.

On the basis of the individual labeling of each peptide, we calculated the theoretical intensities of each peak of a spectrum of the peptides used for quantitation (Table S3, Supporting Information) and used them to estimate the TICs of the peptides. The average signal response calculated from the alpha trimmed means of the set of TICs of the peptides was used to quantify the three example proteins based on eq 1.2−1.4.

As expected, RCA2 was with values ranging from 0.45 to 3.28% of TSP less abundant than LSU (12.22 to 42.17% of TSP) and SSU (4.05 to 10.45% of TSP) (ANOVA, $F_{2,69}$ = 111.69, p < 0.001) which corresponds to ratios of RCA/RuBisCO between 0.03 and 0.1. This result is consistent with the findings for *N. tabacum* showing ratios of RCA/RuBisCO between 0.03 and 1.5.[48,57] Considering a limited amount of resources in plants, it is

sensible that the activator is available in lower amounts than the enzyme to be activated.

The time-course of the amounts of the three proteins in TSP showed different patterns (ANOVA, $F_{2,69} = 4.40$, $p < 0.05$), and did not correlate with the TSP per mg fresh mass which decreased with leaf age. The amount of RCA2 and RuBisCO SSU slightly decreased over time, while RuBisCO LSU showed a distinct increase 6 days after application of the ^{15}N-pulse (Figure 6b). In rice leaves RuBisCO contents have been shown to be dependent on the developmental stage of the leaf and to follow a log-normal curve,[58] thus, the increase in RuBisCO LSU might reflect the highest amount of RuBisCO at the full expansion of the leaf before senescence. This hypothesis is supported by Suzuki et al.,[59] who found maximal RuBisCO levels just before a rapid decline at full leaf expansion of *Eucalyptus globulus* seedlings. As climate and light conditions can only be partly regulated in the glasshouse and the increase in RuBisCO preceded a hot, sunny day, RuBisCO LSU amounts could have also been influenced by environmental conditions.[60] The amount of RuBisCO SSU did not show the transient increase supporting the findings in expanded tobacco leaves for which an SSU-independent control of LSU translation has been proposed,[61] we also cannot rule out that we missed an increase of RuBisCO SSU due to sampling times and the faster degradation of RuBisCO SSU compared to LSU.[62]

Overall our data confirm that enzyme pools and ^{15}N-incorporation levels can be reliably quantified after pulse-labeling of soil-grown plants enabling us to study further proteins relevant for plant-herbivore interactions. In contrast to other previously published MS-based methods for quantitation[14,16,17,21,51] the total number of samples is cut into half because the approach does not require the mix of an unlabeled and labeled sample. It only requires a single set of samples and three unlabeled samples per time point for peptide identification.

Quantitation of LOX2 Protein after Repeated Simulated Herbivory

As proof of principle of our approach and to demonstrate its applicability for ecological studies we analyzed the dynamics of LOX2 protein, an important enzyme for antiherbivore defense responses, after repeated herbivore treatment. During their lifetime, plants are often repeatedly challenged by herbivores, and the same herbivore usually feeds repeatedly on the same leaf or on different leaves of the same plant. It is known that an initial herbivore attack alters the plants ability to resist subsequent attacks.[39,63] It was hypothesized that a first attack leads to the accumulation of inactive forms of signaling proteins which are rapidly activated upon a subsequent attack.[39] However, little is known about the enzyme pools available in the plant after repeated herbivore feeding. In the past, identification and quantitation of the different LOX isoforms was mainly based on gene transcript data.[37,64] LOX proteins, in particular the JA-related LOX isoform (see Figure 7a), were primarily detected and quantified by antibodies,[65−67] but the use of antibodies only allows a limited throughput of samples and specificity has to be carefully evaluated. Additionally, in some studies, LOX activity was determined,[65,66] but this approach does not allow a distinction between different LOX isoforms.

Here we show for the first time the absolute quantitation of LOX2 protein in TSP. We treated wild tobacco leaves with standardized mechanical wounding and oral secretions from *Manduca sexta*, to simulate herbivory, and quantified LOX2 protein at different time-points after treatment. We elicited the plants every 24 h three times in a row. In addition to wild type plants we used plants impaired in JA-defense signaling (ir*LOX3*) in our analysis because gene expression of LOX2 in ir*LOX3* lines

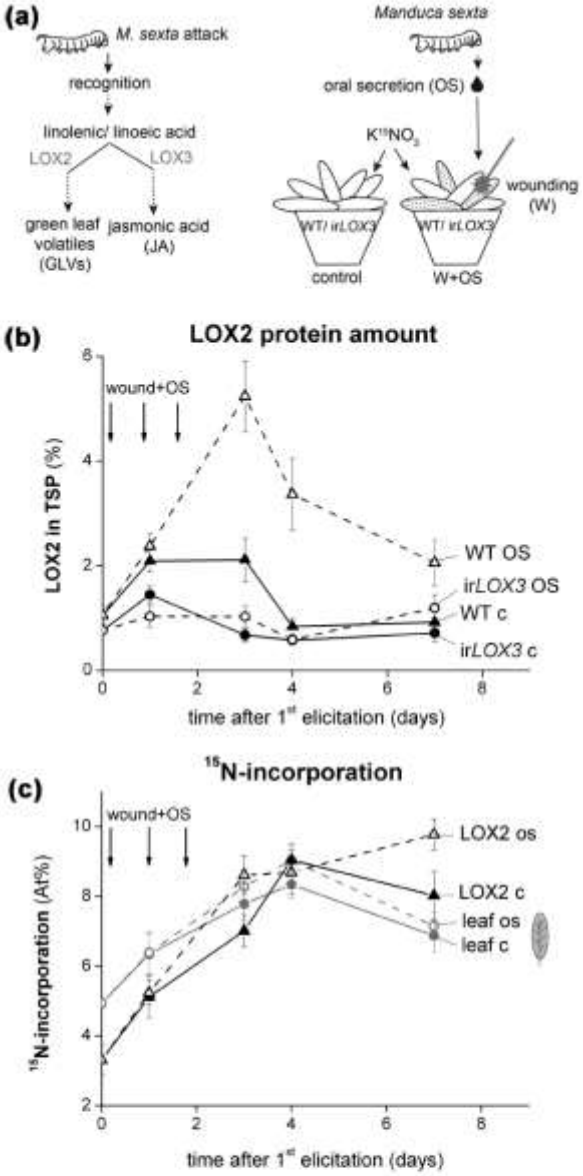

Figure 7. Role of lipoxygenase 2 (LOX2) after repeated herbivory. (a) Current simplified model of the role of LOX2 and a second LOX isoform, LOX3, after herbivory, and scheme of the experimental approach: Plants were pulse labeled with K^{15}NO$_3$ 7 days after transfer to 1 L pots and 3 days before wounding. The same three rosette leaves of ir*LOX3* and WT plants were wounded (W) with a pattern wheel and treated with 10 μL 1:5 diluted *Manduca sexta* oral secretion (OS) (W +OS) 3 days in a row. Untreated plants were taken as control. (b) LOX2 protein amounts in total soluble protein (TSP) (mean ± SE, $n = 5$) were measured by LC−MS^E and calculated based on the most intense peptides (Table S3, Supporting Information) as described for Figure 1. (c) ^{15}N-Incorporation of LOX2 protein in leaves of WT plants determined with MoLE and total ^{15}N-incorporation of the same leaf measured by IRMS. Arrows indicate days of treatment. Oldest sink leaves at time point of labeling were harvested at indicated time points.

dx.doi.org/10.1021/pr300465n | J. Proteome Res. 2012, 11, 4947−4960

is reduced by 90% compared to WT plants after elicitation.[38] Thus, ir*LOX3* plants seemed to be the perfect tool for the validation of our quantitation approach.

LOX2 protein could be clearly identified on average with 17 peptides and a sequence coverage rate of 25.5%, while LOX3 protein could not be detected, neither in untreated nor in treated samples. We assume that the LOX3 protein is less abundant than LOX2. Peptides used for quantitation of LOX2 are shown in Table S3 (Supporting Information). All peptide sequences were carefully checked against the NCBI database to confirm their identity. LOX2 protein accounts for about 0.83 −2.1% of TSP in untreated WT plants (Figure 7b), while ir*LOX3* plants had in average significantly lower levels (59.3%) than WT (ANOVA, $F_{1,93} = 42.98$, $p < 0.001$, Figure 7b). The results clearly show that untreated plants already contain a substantial amount of the enzyme, and confirm the hypothesis that pre-existing enzyme pools are responsible and sufficient for the initial, rapid burst of GLV production after elicitation (20 min[38]).

LOX2 protein expression transiently increased 4 days after the first treatment (Figure 7b). This is first evidence, that plants are primed for the next attack by increasing basal enzyme levels. The increase only occurred after several treatments, consistent with the idea of Stork at al.[39] that after repeated herbivore feeding baseline levels of defense increase in discrete steps depending on the pattern of attack.

On the basis of our results we do not know if LOX2 protein accumulates in an active or inactive form. For AtLOX2, the NaLOX3 homologue in *Arabidopsis*, it was shown that untreated plants had an additional 26 amino acid transcript peptide compared to wound and salivary-treated plants.[68] In our data set we could not find an additional peptide sequence. Nevertheless, NaLOX2 might have to be activated by Ca^{2+} or by changing its phosphorylation status as assumed for AtLOX2 activity.[68,69]

In addition to the total protein amounts, we were interested in the ^{15}N-incorporation over time. We determined the ^{15}N-incorporation in the whole leaf by IRMS and in LOX2 protein by MoLE algorithm (Figure 7c). The values are in a similar range, but there was a time-shift. The overall uptake of ^{15}N into the leaf is faster than its incorporation into proteins. Furthermore, ^{15}N is more rapidly incorporated into LOX2 after attack than in control plants, indicating that the newly acquired nitrogen is partly channeled into LOX2 production. In ir*LOX3* plants the time-course of ^{15}N-incorporation in leaves and LOX2 protein was similar to WT plants, but the increase in LOX2 protein 7 days after simulated herbivory compared to control plants was more pronounced than in WT (Figure S7, Supporting Information).

■ CONCLUSION

These experiments demonstrate that our LC−MS^E-based approach allows a reliable quantitation of the leaf proteome with unknown ^{15}N incorporation levels based on the use of a single unlabeled internal standard. In comparison to other methods, ours is less expensive and generally applicable, because only one internal standard is used and moreover the internal standard BSA can be purchased in high quality and quantity at a low price, thus an experiment-specific synthesis, for example, of standard peptides, is not necessary. Sample preparation is easy and fast, and a high sample through-put is possible. Further automation to search for individual heavy peptides in spectra after bioinformatic identification of their natural forms is desirable, including spectral processing and output to MoLE.

We now have a tool at hand that enables us to compare in-depth the effects of herbivory on nitrogen distribution and protein pool sizes, broadening our picture of how silencing of specific genes relates to metabolism and defense.

■ ASSOCIATED CONTENT

Supporting Information

Supplemental Tables 1−3 and Supplemental Figures 1−7. This material is available free of charge via the Internet at http://pubs.acs.org.

■ AUTHOR INFORMATION

Corresponding Author

*[1] MS Spectrometry Group, Max Planck Institute for Chemical Ecology, Hans-Knoell-Str. 8, 07745 Jena, Germany, svatos@ice.mpg.de, Tel. +493641571700, Fax +493641571701.

Present Address

[‡]Waters GmbH, Eschborn, Germany.

Notes

The authors declare no competing financial interest.

■ ACKNOWLEDGMENTS

We thank Matthias Schöttner for his technical and Emily Wheeler for her editorial support. Financial support by Max Planck Society and a grant from the International Max Planck Research School "The Exploration of Ecological Interactions with Molecular and Chemical Techniques" to F.H. and M.A.S. are gratefully acknowledged.

■ REFERENCES

(1) Bazzaz, F. A.; Chiariello, N. R.; Coley, P. D.; Pitelka, L. F Allocating rescources to reproducation and defense. *Bioscience* **1987**, *37*, 58−67.

(2) Baldwin, I. T. An ecologically motivated analysis of plant-herbivore interactions in native tobacco. *Plant Physiol.* **2001**, *127*, 1449−1458.

(3) Baldwin, I. T.; Gorham, D.; Schmelz, E. A.; Lewandowski, C. A.; Lynds, G. Y. Allocation of nitrogen to an inducible defense and seed production in *Nicotiana attenuata*. *Oecologia* **1998**, *115*, 541−552.

(4) Van Dam, N. M.; Baldwin, I. T. Competition mediates costs of jasmonate-induced defences, nitrogen acquisition and transgenerational plasticity in *Nicotiana attenuata*. *Funct. Ecol.* **2001**, *15*, 406−415.

(5) Frost, C. J.; Hunter, M. D. Herbivore-induced shifts in carbon and nitrogen allocation in red oak seedlings. *New Phytol.* **2008**, *178*, 835−845.

(6) Giri, A. P.; Wunsche, H.; Mitra, S.; Zavala, J. A.; Muck, A.; Svatos, A.; Baldwin, I. T. Molecular interactions between the specialist herbivore *Manduca sexta* (Lepidoptera, Sphingidae) and its natural host *Nicotiana attenuata*. VII. Changes in the plant's proteome. *Plant Physiol.* **2006**, *142*, 1621−1641.

(7) Chen, Y.; Panga, Q.; Daia, S.; Wanga, Y.; Chenb, S.; Yana, X. Proteomic identification of differentially expressed proteins in Arabidopsis in response to methyl jasmonate. *J. Plant Physiol.* **2011**, *168*, 995−1008.

(8) Gygi, S. P.; Corthals, G. L.; Zhang, Y.; Rochon, Y.; Aebersold, R. Evaluation of two-dimensional gel electrophoresis-based proteome analysis technology. *Proc. Natl. Acad. Sci. U.S.A.* **2000**, *97*, 9390−9395.

(9) Turck, C. W.; Falick, A. M.; Kowalak, J. A.; Lane, W. S.; Lilley, K. S.; Phinney, B. S.; Weintraub, S. T.; Witkowska, H. E.; Yates, N. A. The association of biomolecular resource facilities proteomics research group 2006 study - relative protein quantitation. *Mol. Cell. Proteomics* **2007**, *6*, 1291−1298.

(10) Gouw, J. W.; Krijgsveld, J.; Heck, A. J. R. Quantitative proteomics by metabolic labeling of model organisms. *Mol. Cell. Proteomics* **2010**, *9*, 11−24.

(11) Kline, K. G.; Sussman, M. R. Protein quantitation using isotope-assisted mass spectrometry. *Annu. Rev. Biophys.* **2010**, *39*, 291−308.

(12) Schulze, W. X.; Usadel, B. Quantitation in mass-spectrometry-based proteomics. *Annu. Rev. Plant Biol.* **2010**, *61*, 491−516.
(13) Taubert, M.; Jehmlich, N.; Vogt, C.; Richnow, H. H.; Schmidt, F.; von Bergen, M.; Seifert, J. Time resolved protein-based stable isotope probing (Protein-SIP) analysis allows quantification of induced proteins in substrate shift experiments. *Proteomics* **2011**, *11*, 2265−2274.
(14) Schaff, J. E.; Mbeunkui, F.; Blackburn, K.; Bird, D. M.; Goshe, M. B. SILIP: a novel stable isotope labeling method for in planta quantitative proteomic analysis. *Plant J.* **2008**, *56*, 840−854.
(15) Bindschedler, L. V.; Palmblad, M.; Cramer, R. Hydroponic isotope labelling of entire plants (HILEP) for quantitative plant proteomics; an oxidative stress case study. *Phytochemistry* **2008**, *69*, 1962−1972.
(16) Engelsberger, W. R.; Erban, A.; Kopka, J.; Schulze, W. X. Metabolic labeling of plant cell cultures with $K15NO_3$ as a tool for quantitative analysis of proteins and metabolites. *Plant Methods* **2006**, *2*, 14.
(17) Gruhler, A.; Schulze, W. X.; Matthiesen, R.; Mann, M.; Jensen, O. N. Stable isotope labeling of *Arabidopsis thaliana* cells and quantitative proteomics by mass spectrometry. *Mol. Cell. Proteomics* **2005**, *4*, 1697−1709.
(18) Huttlin, E. L.; Hegeman, A. D.; Harms, A. C.; Sussman, M. R. Comparison of full versus partial metabolic labeling for quantitative proteomics analysis in *Arabidopsis thaliana*. *Mol. Cell. Proteomics* **2007**, *6*, 860−881.
(19) Lanquar, V.; Kuhn, L.; Lelievre, F.; Khafif, M.; Espagne, C.; Bruley, C.; Barbier-Brygoo, H.; Garin, J.; Thomine, S. N-15-Metabolic labeling for comparative plasma membrane proteomics in Arabidopsis cells. *Proteomics* **2007**, *7*, 750−754.
(20) Palmblad, M.; Bindschedler, L. V.; Cramer, R. Quantitative proteomics using uniform N-15-labeling, MASCOT, and the trans-proteomic pipeline. *Proteomics* **2007**, *7*, 3462−3469.
(21) Skirycz, A.; Memmi, S.; De Bodt, S.; Maleux, K.; Obata, T.; Fernie, A. R.; Devreese, B.; Inze, D. A Reciprocal N-15-labeling proteomic analysis of expanding Arabidopsis leaves subjected to osmotic stress indicates importance of mitochondria in preserving plastid functions. *J. Proteome Res.* **2011**, *10*, 1018−1029.
(22) Ong, S. E.; Foster, L. J.; Mann, M Mass spectrometric-based approaches in quantitative proteomics. *Methods* **2003**, *29*, 124−130.
(23) Michalski, A.; Cox, J.; Mann, M. More than 100,000 detectable peptide species elute in single shotgun proteomics runs but the majority is inaccessible to data-dependent LC−MS/MS. *J. Proteome Res.* **2011**, *10*, 1785−1793.
(24) Silva, J. C.; Gorenstein, M. V.; Li, G. Z.; Vissers, J. P. C.; Geromanos, S. J. Absolute quantification of proteins by $LCMS^E$ - A virtue of parallel MS acquisition. *Mol. Cell. Proteomics* **2006**, *5*, 144−156.
(25) Geromanos, S. J.; Vissers, J. P. C.; Silva, J. C.; Dorschel, C. A.; Li, G. Z.; Gorenstein, M. V.; Bateman, R. H.; Langridge, J. I. The detection, correlation, and comparison of peptide precursor and product ions from data independent LC-MS with data dependant LC-MS/MS. *Proteomics* **2009**, *9*, 1683−1695.
(26) Jehmlich, N.; Schmidt, F.; Hartwich, M.; von Bergen, M.; Richnow, H. H.; Vogt, C. Incorporation of carbon and nitrogen atoms into proteins measured by protein-based stable isotope probing (Protein-SIP). *Rapid Commun. Mass Spectrom.* **2008**, *22*, 2889−2897.
(27) MacCoss, M. J.; Wu, C. C.; Matthews, D. E.; Yates, J. R. Measurement of the isotope enrichment of stable isotope-labeled proteins using high-resolution mass spectra of peptides. *Anal. Chem.* **2005**, *77*, 7646−7653.
(28) Pan, C.; Fischer, C. R.; Hyatt, D.; Bowen, B. P.; Hettich, R. L.; Banfield, J. F. Quantitative tracking of isotope flows in proteomes of microbial communities. *Mol. Cell. Proteomics* **2011**.
(29) Snijders, A. P. L.; de Vos, M. G. J.; Wright, P. C. Novel approach for peptide quantitation and sequencing based on N^{-15} and C^{-13} metabolic labeling. *J. Proteome Res.* **2005**, *4*, 578−585.
(30) Sperling, E.; Bunner, A. E.; Sykes, M. T.; Williamson, J. R Quantitative analysis of isotope distributions in proteomic mass spectrometry using least-squares Fourier transform convolution. *Anal. Chem.* **2008**, *80*, 4906−4917.
(31) Baldwin, I. T.; Staszakkozinski, L.; Davidson, R. Up in smoke 0.1. smoke-derived germination cues for postfire annual, *Nicotiana attenuata* Torr ex Watson. *J. Chem. Ecol.* **1994**, *20*, 2345−2371.
(32) Xu, X.; Pan, S.; Cheng, S.; Zhang, B.; Mu, D.; Ni, P.; Zhang, G.; Yang, S.; Li, R.; Wang, J.; Orjeda, G.; Guzman, F.; Torres, M.; Lozano, R.; Ponce, O.; Martinez, D.; De la Cruz, G.; Chakrabarti, S. K.; Patil, V. U.; Skryabin, K. G.; Kuznetsov, B. B.; Ravin, N. V.; Kolganova, T. V.; Beletsky, A. V.; Mardanov, A. V.; Di Genova, A.; Bolser, D. M.; Martin, D. M. A.; Li, G.; Yang, Y.; Kuang, H.; Hu, Q.; Xiong, X.; Bishop, G. J.; Sagredo, B.; Mejia, N.; Zagorski, W.; Gromadka, R.; Gawor, J.; Szczesny, P.; Huang, S.; Zhang, Z.; Liang, C.; He, J.; Li, Y.; He, Y.; Xu, J.; Zhang, Y.; Xie, B.; Du, Y.; Qu, D.; Bonierbale, M.; Ghislain, M.; del Rosario Herrera, M.; Giuliano, G.; Pietrella, M.; Perrotta, G.; Facella, P.; O'Brien, K.; Feingold, S. E.; Barreiro, L. E.; Massa, G. A.; Diambra, L.; Whitty, B. R.; Vaillancourt, B.; Lin, H.; Massa, A.; Geoffroy, M.; Lundback, S.; DellaPenna, D.; Buell, C. R.; Sharma, S. K.; Marshall, D. F.; Waugh, R.; Bryan, G. J.; Destefanis, M.; Nagy, I.; Milbourne, D.; Thomson, S. J.; Fiers, M.; Jacobs, J. M. E.; Nielsen, K. L.; Sonderkaer, M.; Iovene, M.; Torres, G. A.; Jiang, J.; Veilleux, R. E.; Bachem, C. W. B.; de Boer, J.; Borm, T.; Kloosterman, B.; van Eck, H.; Datema, E.; Hekkert, B. T. L.; Goverse, A.; van Ham, R. C. H. J.; Visser, R. G. F.; Potato Genome Sequencing Consortium. Genome sequence and analysis of the tuber crop potato. *Nature* **2011**, *475*, 189−194.
(33) Fei, Z. J.; Joung, J. G.; Tang, X. M.; Zheng, Y.; Huang, M. Y.; Lee, J. M.; McQuinn, R.; Tieman, D. M.; Alba, R.; Klee, H. J.; Giovannoni, J. J. Tomato functional genomics database: a comprehensive resource and analysis package for tomato functional genomics. *Nucleic Acids Res.* **2011**, *39*, D1156−D1163.
(34) Mitra, S.; Baldwin, I. T. Independently silencing two photosynthetic proteins in *Nicotiana attenuata* has different effects on herbivore resistance. *Plant Physiol.* **2008**, *148*, 1128−1138.
(35) Andersson, I. Catalysis and regulation in Rubisco. *J. Exp. Bot.* **2008**, *59*, 1555−1568.
(36) Allmann, S.; Halitschke, R.; Schuurink, R. C.; Baldwin, I. T. Oxylipin channeling in *Nicotiana attenuata*: Lipoxygenase 2 supplies substrates for green leaf volatile production. *Plant, Cell Environ.* **2010**, *33*, 2028−2040.
(37) Halitschke, R.; Baldwin, I. T. Antisense LOX expression increases herbivore performance by decreasing defense responses and inhibiting growth-related transcriptional reorganization in *Nicotiana attenuata*. *Plant J.* **2003**, *36*, 794−807.
(38) Allmann, S.; Halitschke, R.; Schuurink, R. C.; Baldwin, I. T. Oxylipin channelling in *Nicotiana attenuata*: lipoxygenase 2 supplies substrates for green leaf volatile production. *Plant Cell Environ.* **2010**, *33*, 2028−2040.
(39) Stork, W.; Diezel, C.; Halitschke, R.; Galis, I.; Baldwin, I. T. An ecological analysis of the herbivory-elicited JA burst and its metabolism: plant memory processes and predictions of the moving target model. *PLoS One* **2009**, *4*(3)e4697.
(40) Kruegel, T.; Lim, M.; Gase, K.; Halitschke, R.; Baldwin, I. T. Agrobacterium-mediated transformation of *Nicotiana attenuata*, a model ecological expression system. *Chemoecology* **2002**, *12*, 177−183.
(41) Pluskota, W. E.; Qu, N.; Maitrejean, M.; Boland, W.; Baldwin, I. T. Jasmonates and its mimics differentially elicit systemic defence responses in *Nicotiana attenuata*. *Journal . Exp. Bot.* **2007**, *58*, 4071−4082.
(42) Li, G. Z.; Vissers, J. P. C.; Silva, J. C.; Golick, D.; Gorenstein, M. V.; Geromanos, S. J. Database searching and accounting of multiplexed precursor and product ion spectra from the data independent analysis of simple and complex peptide mixtures. *Proteomics* **2009**, *9*, 1696−1719.
(43) Böcker, S.; Letzel, M. C.; Liptak, Z.; Pervukhin, A. SIRIUS: decomposing isotope patterns for metabolite identification. *Bioinformatics (Oxford)* **2009**, 25 (2), 218−224.
(44) Beavis, R. C. Chemical mass of carbon in proteins. *Anal. Chem.* **1993**, *65*, 496−497.
(45) Meldau, S.; Ullmann-Zeunert, L.; Govind, G.; Bartram, S.; Baldwin, I. T. Basal and herbivory-induced defense trade-offs are mediated by mitogen-activated protein kinases, jasmonic acid and

salicylic acid in the native tobacco, *Nicotiana attenuata*. *BMC Plant Biol.* **2012**, in press.
(46) Shevchenko, A.; Sunyaev, S.; Loboda, A.; Shevchenko, A.; Bork, P.; Ens, W.; Standing, K. G. Charting the proteomes of organisms with unsequenced genomes by MALDI-quadrupole time of flight mass spectrometry and BLAST homology searching. *Anal. Chem.* **2001**, *73*, 1917−1926.
(47) He, Z. L.; von Caemmerer, S.; Hudson, G. S.; Price, G. D.; Badger, M. R.; Andrews, T. J. Ribulose-1,5-bisphosphate carboxylase/oxygenase activase deficiency delays senescence of ribulose-1,5-bisphosphate carboxylase/oxygenase but progressively impairs its catalysis during tobacco leaf development. *Plant Physiol.* **1997**, *115*, 1569−1580.
(48) Mate, C. J.; vonCaemmerer, S.; Evans, J. R.; Hudson, G. S.; Andrews, T. J. The relationship between CO_2-assimilation rate, Rubisco carbamylation and Rubisco activase content in activase-deficient transgenic tobacco suggests a simple model of activase action. *Planta* **1996**, *198*, 604−613.
(49) Clarkson, J. J.; Knapp, S.; Garcia, V. F.; Olmstead, R. G.; Leitch, A. R.; Chase, M. W. Phylogenetic relationships in Nicotiana (Solanaceae) inferred from multiple plastid DNA regions. *Mol. Phylogenet. Evol.* **2004**, *33*, 75−90.
(50) de Hoffmann, E., S. V. E. Section 3.3 Data Acquisition. *Mass Spectrometry: Principles and Applications*; Wiley: Chichester, 2007; p 183.
(51) Nelson, C. J.; Huttlin, E. L.; Hegeman, A. D.; Harms, A. C.; Sussman, M. R. Implications of N^{-15}-metabolic labeling for automated peptide identification in *Arabidopsis thaliana*. *Proteomics* **2007**, *7*, 1279−1292.
(52) Jehmlich, N.; Schmidt, F.; Taubert, M.; Seifert, J.; Bastida, F.; von Bergen, M.; Richnow, H. H.; Vogt, C. Protein-based stable isotope probing. *Nat. Protoc.* **2010**, *5*, 1957−1966.
(53) Brand, W. A. High precision isotope ratio monitoring techniques in mass spectrometry. *J. Mass Spectrom.* **1996**, *31*, 225−235.
(54) Brenna, J. T.; Corso, T. N.; Tobias, H. J.; Caimi, R. J. High-precision continuous-flow isotope ratio mass spectrometry. *Mass Spectrom. Rev.* **1997**, *16*, 382−382.
(55) Ferrario-Méry, S.; Thibaud, M. C.; Betsche, T.; Valadier, M. H.; Foyer, C. H. Modulation of carbon and nitrogen metabolism, and of nitrate reductase, in untransformed and transformed *Nicotiana plumbaginifolia* during CO_2 enrichment of plants grown in pots and in hydroponic culture. *Planta* **1997**, *202*, 510−512.
(56) Yin, X. Y.; Goudriaan, J.; Lantinga, E. A.; Vos, J.; Spiertz, H. J. A flexible sigmoid function of determinate growth. *Ann. Bot.* **2003**, *91*, 361−371.
(57) Yamori, W.; von Caemmerer, S. Effect of rubisco activase deficiency on the temperature response of $CO(_2)$ assimilation rate and rubisco activation state: insights from transgenic tobacco with reduced amounts of rubisco activase. *Plant Physiol.* **2009**, *151*, 2073−2082.
(58) Irving, L. J.; Robinson, D. A dynamic model of Rubisco turnover in cereal leaves. *New Phytol.* **2006**, *169*, 493−504.
(59) Suzuki, Y.; Kihara-Doi, T.; Kawazu, T.; Miyake, C.; Makino, A. Differences in Rubisco content and its synthesis in leaves at different positions in *Eucalyptus globulus* seedlings. *Plant Cell Environ.* **2010**, *33*, 1314−1323.
(60) Feller, U.; Anders, I.; Mae, T. Rubiscolytics: fate of Rubisco after its enzymatic function in a cell is terminated. *J. Exp. Bot.* **2008**, *59*, 1615−1624.
(61) Ichikawa, K.; Miyake, C.; Iwano, M.; Sekine, M.; Shinmyo, A.; Kato, K. Ribulose 1,5-bisphosphate carboxylase/oxygenase large subunit translation is regulated in a small subunit-independent manner in the expanded leaves of tobacco. *Plant Cell Physiol.* **2008**, *49*, 214−225.
(62) Cohen, I.; Knopf, J. A.; Irihimovitch, V.; Shapira, M. A proposed mechanism for the inhibitory effects of oxidative stress on rubisco assembly and its subunit expression. *Plant Physiol.* **2005**, *137*, 738−746.
(63) Bricchi, I.; Leitner, M.; Foti, M.; Mithoefer, A.; Boland, W.; Maffei, M. E. Robotic mechanical wounding (MecWorm) versus herbivore-induced responses: early signaling and volatile emission in Lima bean (*Phaseolus lunatus* L.). *Planta* **2010**, *232*, 719−729.
(64) Chen, G. P.; Hackett, R.; Walker, D.; Taylor, A.; Lin, Z. F.; Grierson, D. Identification of a specific isoform of tomato lipoxygenase (TomloxC) involved in the generation of fatty acid-derived flavor compounds. *Plant Physiol.* **2004**, *136*, 2641−2651.
(65) Avdiushko, S.; Croft, K. P. C.; Brown, G. C.; Jackson, D. M.; Hamiltonkemp, T. R.; Hildebrand, D. Effect of volatile methyl jasmonate on the oxylipin pathway in tobacco, cucumber, and arabidopsis. *Plant Physiol.* **1995**, *109*, 1227−1230.
(66) Feussner, I.; Hause, B.; Voros, K.; Parthier, B.; Wasternack, C. Jasmonate-induced lipooxygenase forms are localized in chloroplasts of barley leaves (*Hordeum vulgare* cv Salome). *Plant J.* **1995**, *7*, 949−957.
(67) Royo, J.; Leon, J.; Vancanneyt, G.; Albar, J. P.; Rosahl, S.; Ortego, F.; Castanera, P.; Sanchez-Serrano, J. J. Antisense-mediated depletion of a potato lipoxygenase reduces wound induction of proteinase inhibitors and increases weight gain of insect pests. *Proc. Natl. Acad. Sci. U.S.A.* **1999**, *96*, 1146−1151.
(68) Thivierge, K.; Prado, A.; Driscoll, B. T.; Bonneil, E. r.; Thibault, P.; Bede, J. C. Caterpillar- and salivary-specific modification of plant proteins. *J. Proteome Res.* **2010**, *9*, 5887−5895.
(69) Bonaventure, G.; Gfeller, A.; Rodriguez, V. M.; Armand, F.; Farmer, E. E. The fou2 gain-of-function allele and the wild-type allele of two pore channel 1 contribute to different extents or by different mechanisms to defense gene expression in Arabidopsis. *Plant Cell Physiol.* **2007**, *48*, 1775−1789.

SUPPLEMENTAL MATERIAL

Lynn Ullmann-Zeunert[1], Alexander Muck[2±], Natalie Wielsch[1±], Franziska Hufsky[1,3], Mariana A. Stanton[1], Stefan Bartram[1], Sebastian Böcker[3], Ian T. Baldwin[1], Karin Groten[1], Aleš Svatoš[1*]

Table S1: ^{15}N-incorporation of the selected peptides of RuBisCO large (L1-3) and small subunit (S1-3) (Table 1) with different permanent ^{15}N-labeling of plants (value ± standard error (SE)); ^{15}N-incorporation was calculated A) with MoLE and B) with the excel sheet from (Taubert et al [19]); L1-3 and S1-3 are numbers of peptides (Table 1).

A

expected ^{15}N labeling [At%]	^{15}N-incorporation ± SE [At%] calculated by MoLE					
	0.37	1.35	5.28	10.19	49.49	98.61
L1	1.01 ± 0.06	1.93 ± 0.12	5.76 ± 0.09	10.11 ± 0.06	48.88 ± 0.14	99.15 ± 0.06
L2	0.61 ± 0.07	1.46 ± 0.01	5.01 ± 0.06	9.33 ± 0.09	48.15 ± 0.23	99.30 ± 0.09
L3	0.76 ± 0.11	1.74 ± 0.06	5.33 ± 0.10	9.65 ± 0.07	48.35 ± 0.21	99.08 ± 0.07
S1	0.53 ± 0.05	1.42 ± 0.05	5.16 ± 0.08	9.80 ± 0.10	49.03 ± 0.29	99.43 ± 0.08
S2	0.54 ± 0.04	1.47 ± 0.05	5.18 ± 0.03	9.81 ± 0.08	48.91 ± 0.25	98.96 ± 0.44
S3	0.99 ± 0.08	1.94 ± 0.11	5.82 ± 0.09	9.89 ± 0.09	49.39 ± 0.18	99.53 ± 0.21

B

expected ^{15}N labeling [At%]	^{15}N-incorporation ± SE [At%] calculated according to Taubert et al.					
	0.37	1.35	5.28	10.19	49.49	98.61
L1	0.87 ± 0.06	1.83 ± 0.09	5.47 ± 0.06	10.14 ± 0.04	48.89 ± 0.17	99.12 ± 0.07
L2	0.58 ± 0.06	1.41 ± 0.02	4.86 ± 0.21	9.30 ± 0.09	48.27 ± 0.21	99.07 ± 0.07
L3	0.46 ± 0.06	1.39 ± 0.02	4.91 ± 0.21	9.66 ± 0.09	47.74 ± 0.21	99.06 ± 0.10
S1	0.30 ± 0.03	1.33 ± 0.02	5.21 ± 0.08	9.63 ± 0.07	48.85 ± 0.22	98.95 ± 0.11
S2	0.48 ± 0.07	1.35 ± 0.03	5.17 ± 0.02	9.90 ± 0.09	48.58 ± 0.33	98.92 ± 0.14
S3	1.06 ± 0.06	2.00 ± 0.09	5.49 ± 0.05	10.18 ± 0.06	49.41 ± 0.23	99.00 ± 0.11

Table S2: Peptides of phosphorylase b from rabbit muscle and of BSA (B) used for calculation of the absolute protein quantitation on the column. The three most intense peptides were used. The table includes the average mass and retention time (Rt) calculated from 45-fold analysis. Carbamido methylated methionine residue is denoted as C*.

No.	Calc.[MH]$^+$	Exp. [MH]$^+$	Δ ppm*	Rt [min]	Rt RSD [%]	Sequence	Sumformula
P1	1853.9644	1853.9734	4.9	50.62	0.5	LLSYVDDEAFIRDVAK	$C_{84}H_{132}N_{20}O_{27}$
P2	1886.9031	1886.9120	4.7	45.46	0.6	GYNAQEYYDRIPELR	$C_{84}H_{123}N_{23}O_{27}$
P3	1678.8646	1678.8759	6.7	46.50	0.6	IGEEYISDLDQLRK	$C_{73}H_{119}N_{19}O_{26}$
B4	1163.6306	1163.6334	2.4	45.96	0.6	LVNELTEFAK	$C_{53}H_{86}N_{12}O_{17}$

B5	1419.6937	1419.7019	5.8	47.64	1.1	SLHTLFGDELC*K	$C_{62}H_{198}N_{16}O_{20}S_1$
B6	1639.9378	1639.9448	4.3	42.62	0.7	KVPQVSTPTLVEV SR	$C_{72}H_{126}N_{20}O_{23}$

Table S3: Peptides of ribulose-1,5-bisphosphate-carboxylase/oxygenases (RuBisCO) LSU (L) and small (S) SSU and RCA2 (R) and lipoxygenase 2 (LO) from *Nicotiana attenuata* and of BSA (B) used for absolute protein quantitation and for calculation of the ^{15}N-incorporation of soil grown plants pulse labeled with $K^{15}NO_3$. The three most intense peptides were taken, except from RuBisCO LSU where the 3th, 6th and 8th most intense peptides were used. The table includes the average mass and retention time (Rt) calculated from 13-fold analysis. Carbamido methylated methionine residue is denoted as C*.

No.	Calc.$[MH]^+$	Exp. $[MH]^+$	Δ ppm*	Rt [min]	Rt RSD [%]	Sequence	Sumformula
L4	1261.7150	1261.7141	0.7	51.88	0.0	DITLGFVDLLR	$C_{58}H_{96}N_{14}O_{17}$
L5	1261.6285	1261.6303	1.4	42.02	0.4	FLFC*AEALYK	$C_{61}H_{88}N_{12}O_{15}S_1$
L6	1546.7358	1546.7371	0.8	41.65	0.0	WSPELAAAC*EV WK	$C_{71}H_{103}N_{17}O_{20}S_1$
S3	933.5152	933.5159	0.8	34.13	0.0	IIGFDNVR	$C_{42}H_{68}N_{12}O_{12}$
S4	1802.8781	1802.8811	1.7	40.22	0.0	QVQC*ISFIAYKPE GY	$C_{83}H_{123}N_{19}O_{24}S_1$
S5	893.4978	893.4964	1.6	32.85	0.1	EVEYLLK	$C_{42}H_{68}N_8O_{13}$
B7	1305.7161	1305.7172	0.8	31.66	0.0	HLVDEPQNLIK	$C_{58}H_{96}N_{16}O_{18}$
B8	1163.6306	1163.6325	1.6	36.52	0.0	LVNELTEFAK	$C_{53}H_{86}N_{12}O_{17}$
B9	1479.7954	1479.7962	0.5	40.81	0.0	LGEYGFQNALIVR	$C_{68}H_{106}N_{18}O_{19}$
LO1	1142.6051	1142.6052	0.0	35.66	0.0	EALPEDLISR	$C_{49}H_{84}N_{13}O_{18}$
LO2	1572.8631	1572.8665	2.2	47.85	0.0	DVLLFETPELLQR	$C_{72}H_{117}N_{17}O_{22}$
LO3	1629.8370	1629.8397	1.7	34.99	0.0	LDPEIYGPPESAIT K	$C_{74}H_{116}N_{16}O_{25}$
R4	1882.9697	1882.9745	2.5	49.83	0.0	IVDTFPGQSIDFFG ALR	$C_{88}H_{131}N_{21}O_{25}$
R5	1706.7980	1706.8001	1.2	35.78	0.0	GLVQDFSDDQQDI AR	$C_{71}H_{111}N_{21}O_{28}$
R6	1332.6794	1332.6796	0.2	34.05	0.0	WVSGTGIEAIGDK	$C_{59}H_{93}N_{15}O_{20}$

***Δ ppm=10^6 *(M_{tn}-M_{exp})*M_{tn}^{-1}**

LEGENDS:

Figure S1: Fertilization scheme of a) permanent labeling experiment and b) pulse labeling experiment. a) 12 days after germination plants were transferred to 50 mL single pots with different concentrations of $Ca(^{15}NO_3)_2$ (see Material and Methods). 10 days later they were put into 1 L single pots with the same concentrations of ^{15}N in the form of $K^{15}NO_3$. Ten days later plants were harvested. b) 7 days after transfer to 1 L pots, plants were pulse labeled with $K_{15}NO^3$. Three days later was the first time-point of harvest.

Figure S2: LC-MS^E production spectra of selected peptides (Table 1) a-c) for LSU; d-f) for SSU; g-i) for RCA2; j-l) for BSA2; pe = precursor error

Figure S3: Absolute difference between calculated (excel sheet Taubert et al. [19]) and expected ^{15}N-incorporation at different concentrations of partial permanent ^{15}N-labeling. Mean ± SE (n=5) of three peptides of RuBisCO LSU (L1-3) and SSU (S1-3) (for peptides see Table 1).

Figure 4: Absolute differences of the ^{15}N-incorporation of RuBisCO peptides between technical replicates determined with MoLE from leaf extracts of plants grown at different concentrations of partial permanent ^{15}N-labeling. Mean ± SE (n=5) of the difference between two technical replicates is shown (for peptides see Table 1).

Figure S5: Absolute difference between measured and expected ^{15}N-incorporation of total soluble protein determined by IRMS from leaf extracts of plants grown at different concentrations of partial permanent ^{15}N-labeling. The proteins with an expected ^{15}N-incorporation higher than 5 % were mixed with BSA before analysis to dilute the labeling to about 1 At% ^{15}N-labeling. Mean ± SE (n=5) of the differences is shown.

Figure S6: Absolute differences between technical replicates of the ^{15}N-incorporation in TSP measured with IRMS from leaf extracts of plants grown at different concentrations of partial permanent ^{15}N-labeling. Mean ± SE (n=5) of the difference between two technical replicates is shown. Samples with a labeling higher than 5 % were mixed with BSA before analysis to dilute the labeling to about 1 At% ^{15}N-labeling.

Figure S7: ^{15}N-incorporation of LOX2 protein in leaves of ir*LOX3* plants determined with MoLE and total ^{15}N-incorporation of the same leaf measured by IRMS.Arrows indicate days of treatment. Oldest sink leaves at time point of labeling were harvested at indicated time points. For further details see Fig. 7.

Figure S1

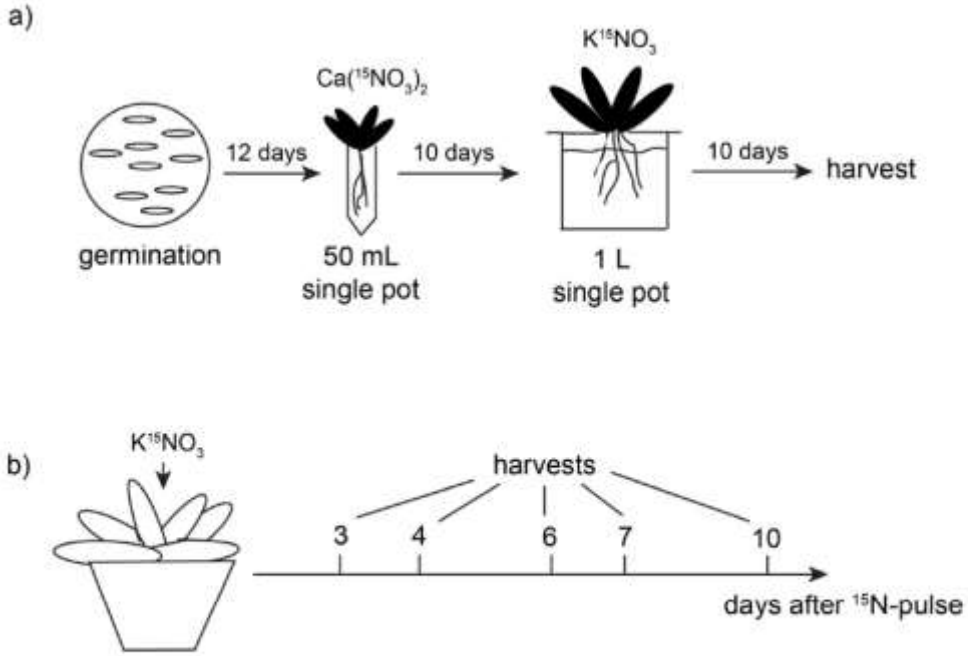
a)
$K^{15}NO_3$
$Ca(^{15}NO_3)_2$
12 days
10 days
10 days
harvest
germination
50 mL
single pot
1 L
single pot
b)
$K^{15}NO_3$
harvests
3
4
6
7
10
days after ^{15}N-pulse

Figure S2

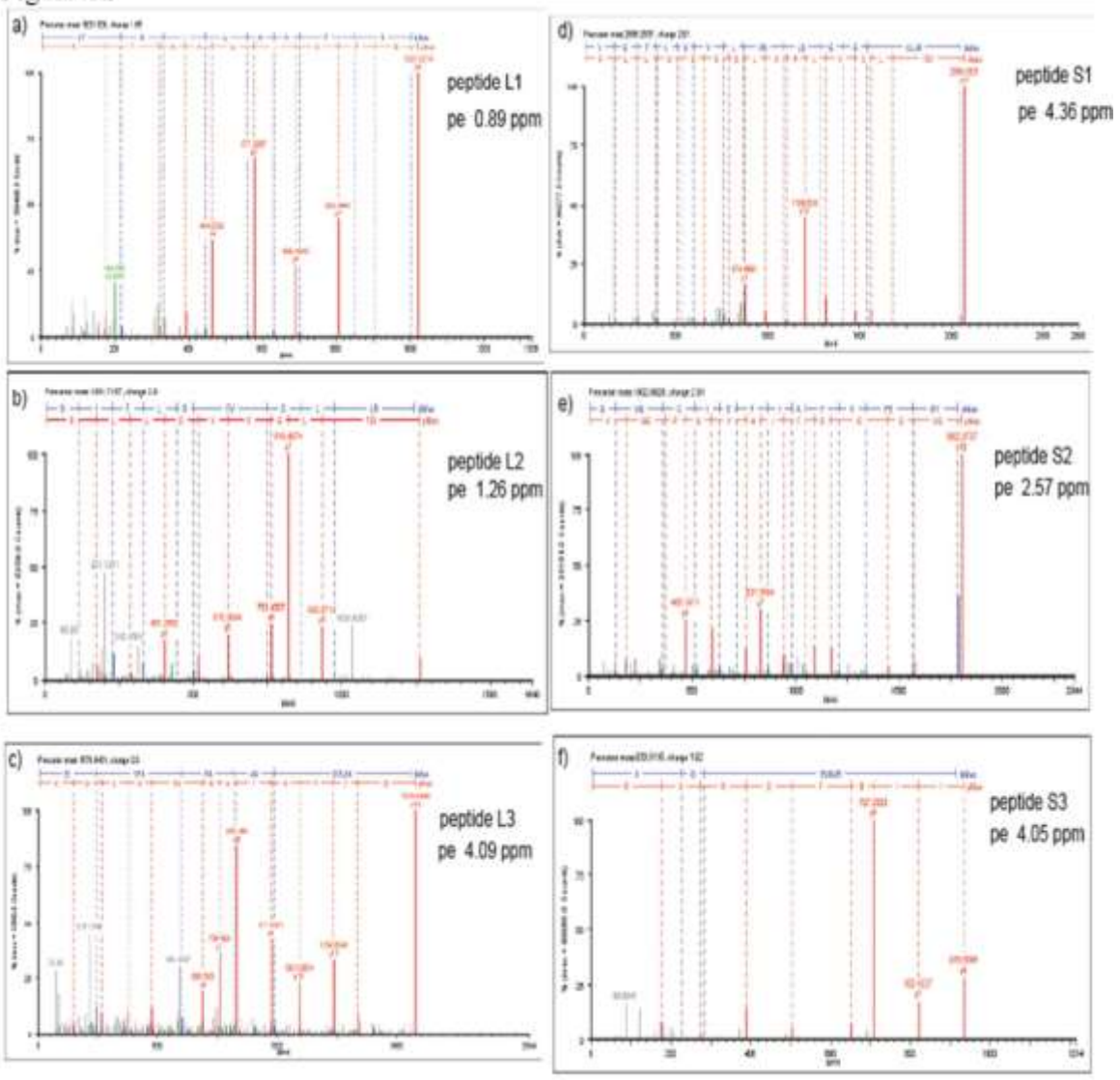
a)
peptide L1
pe 0.89 ppm
d)
peptide S1
pe 4.36 ppm
b)
peptide L2
pe 1.26 ppm
e)
peptide S2
pe 2.57 ppm
c)
peptide L3
pe 4.09 ppm
f)
peptide S3
pe 4.05 ppm

Figure S2 continued

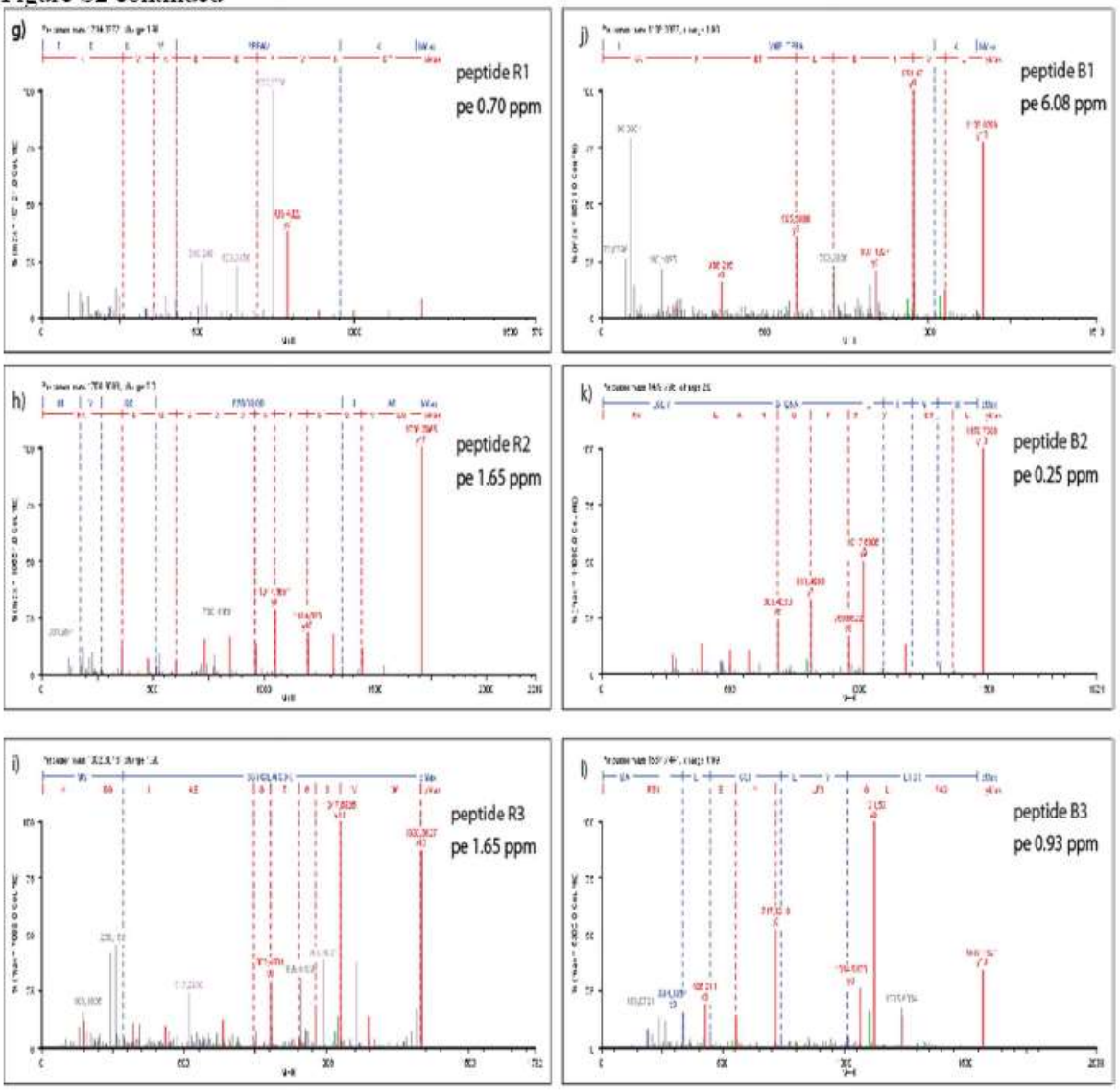

Figure S3

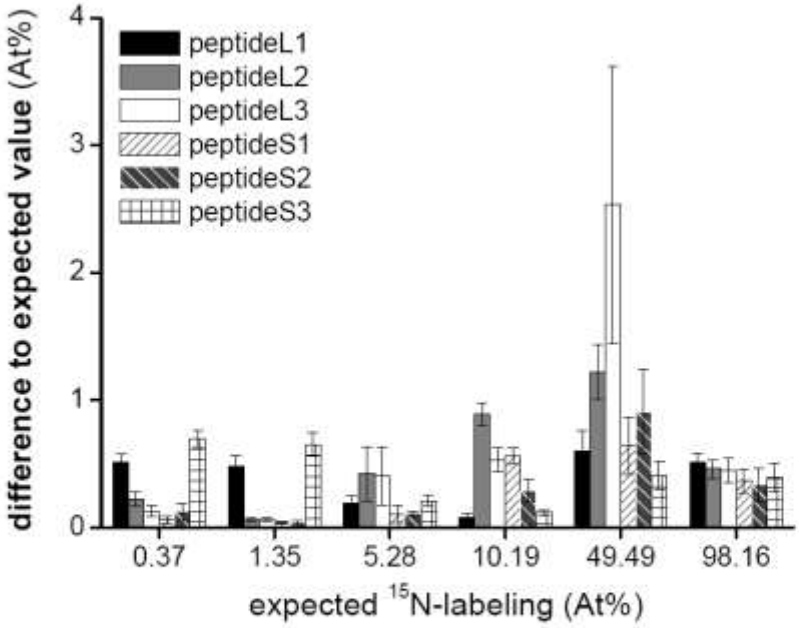
peptideL1
peptideL2
peptideL3
peptideS1
peptideS2
peptideS3
difference to expected value (At%)
0
1
2
3
4
0.37
1.35
5.28
10.19
49.49
98.16
expected 15N-labeling (At%)

Figure S4

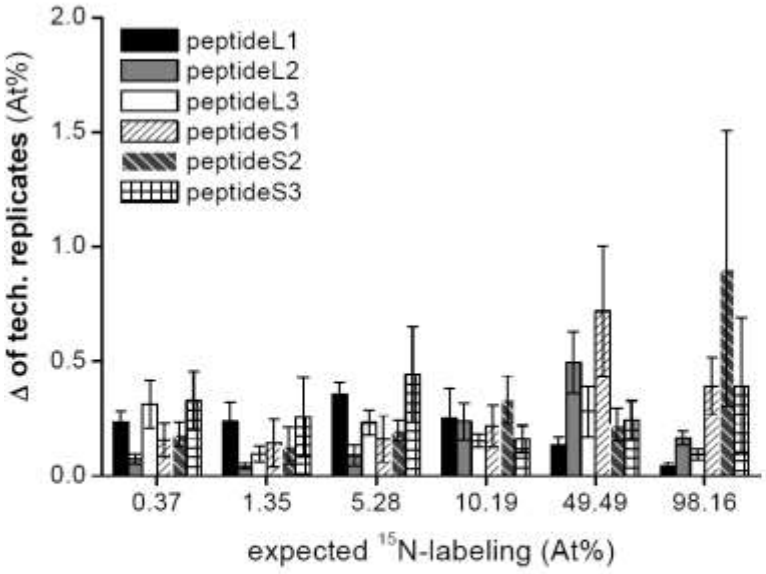
peptideL1
peptideL2
peptideL3
peptideS1
peptideS2
peptideS3
Δ of tech. replicates (At%)
2.0
1.5
1.0
0.5
0.0
0.37
1.35
5.28
10.19
49.49
98.16
expected 15N-labeling (At%)

Figure S5

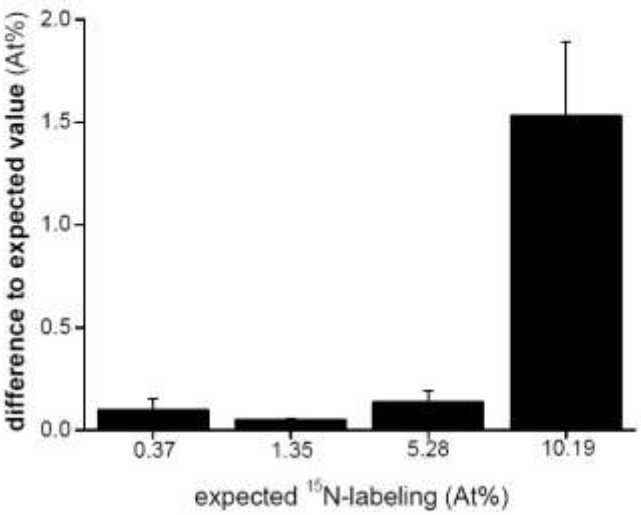
difference to expected value (At%)
2.0
1.5
1.0
0.5
0.0
0.37
1.35
5.28
10.19
expected 15N-labeling (At%)

Figure S6

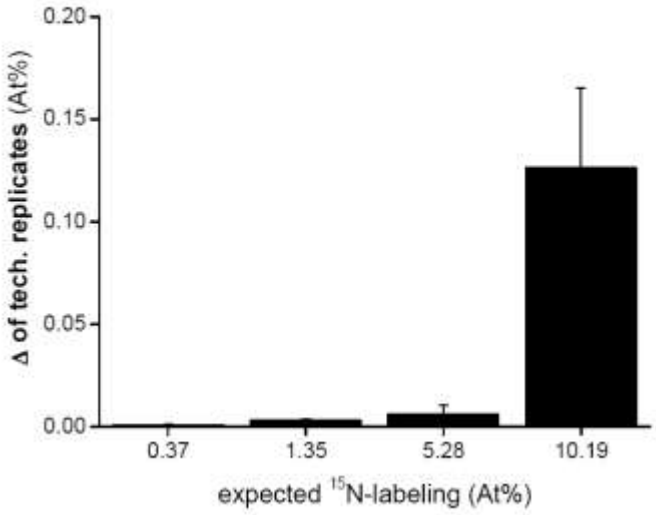
0.20
0.15
0.10
0.05
0.00
Δ of tech. replicates (At%)
0.37
1.35
5.28
10.19
expected 15N-labeling (At%)

Figure S7

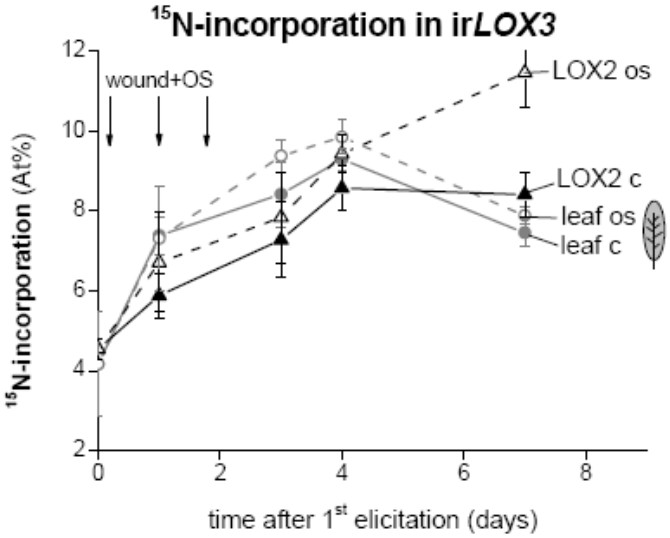
15N-incorporation in irLOX3
wound+OS
LOX2 os
LOX2 c
leaf os
leaf c
15N-incorporation (At%)
time after 1st elicitation (days)
12
10
8
6
4
2
0
2
4
6
8

2.3 Manuscript III

Quantification of growth-defense trade-offs in a common nitrogen (N) currency: phenolamide production mediates herbivory-induced N reallocation to proteins in wild tobacco

Lynn Ullmann-Zeunert[§1], Mariana A. Stanton[§1], Nathalie Wielsch[2], Stefan Bartram[3], Christian Hummert[4], Aleš Svatoš[2], Ian T. Baldwin[1#], Karin Groten[1#]

[§]These authors contributed equally

Author affiliations:

[1] Department of Molecular Ecology, Max Planck Institute for Chemical Ecology, Jena

[2] MS Group, Max Planck Institute for Chemical Ecology, Jena

[3] Department of Bioorganic Chemistry, Max Planck Institute for Chemical Ecology, Jena

[4] Systems Biology/Bioinformatics Research Group, Leibniz Institute for Natural Product Research and Infection Biology, Jena

Running title: Quantification of growth-defense trade-offs

[#]Co-corresponding authors:

Ian T. Baldwin

Karin Groten

Department of Molecular Ecology,

Max Planck Institute for Chemical Ecology,

Hans-Knöll-Straβe 8,

D-07745 Jena,

Germany.

Phone: +49 (0)3641 57 1100

Fax: +49 (0)3641 57 1102

Email: baldwin@ice.mpg.de; kgroten@ice.mpg.de

word count

abstract: 250

Introduction: 1186

Results and Discussion: 3703

Experimental Procedures: 738

Acknowledgements: 43

Supplemental Figure Captions: 122

Figure Legends: 852

Subtotal: 6894

Supplemental Figure Legends (including captions): 225

Total without References: 6997

References: 1892

Abstract

Induced defenses are thought to be economical: allowing fitness-limiting resources to be invested into growth/reproduction when defenses are not needed. To date, this putative growth/defense trade-off has not been quantified in a common currency. Here, a novel quantification method for ^{15}N-labeled proteins enabled a direct comparison of nitrogen (N) flux in a common N currency into proteins, specifically, ribulose-1,5-bisposphate carboxylase/oxygenase (RuBisCO), with that into small N-containing defense metabolites after herbivory with similar accuracy.

After simulated herbivory, total N decreased in shoots of wild type (WT) *Nicotiana attenuata* plants, but not in two transgenic lines impaired in jasmonate defense signaling (ir*LOX3*) and phenolamide biosynthesis (ir*MYB8*). The total N pools in elicited rosette leaves and a systemic stem leaf did not correlate with the genetic background, leaf size or total soluble protein (TSP) pools, indicating that herbivory initiated a reallocation of N among different compounds within the leaf. In elicited WT leaves, a strong decrease in TSP and RuBisCO was accompanied by an increase in defense metabolites; ir*LOX3* plants showed a similar, albeit attenuated pattern. Ir*MYB8* plants were the least responsive to elicitation with overall higher levels of RuBisCO. However, the herbivory-elicited decrease in absolute N-invested in TSP and RuBisCO was much larger than the N-requirements of nicotine and phenolamide biosynthesis. We propose that MYB8, by regulating the production of the metabolically dynamic phenolamides, indirectly regulates TSP and RuBisCO pool sizes after herbivory.^{15}N flux studies revealed that N for phenolamide synthesis originates from recently assimilated N rather than from RuBisCO turnover.

Introduction

Plants have evolved two general direct strategies against herbivory – constitutive and inducible defenses. The biosynthesis of these defenses requires fitness-limiting resources that could otherwise be invested into growth and reproduction. Hence, induced plant defenses are thought to be a cost-saving strategy compared to constitutive defenses (Karban and Baldwin 1997) since they are only produced when needed e.g. after herbivory. This cost-saving model plays a central role in most theoretical treatments of induced defenses (see Stamp 2003) for a review of plant defense hypotheses). Several studies have quantified the costs of induction by measuring photosynthesis rates, plant biomass, size and/or yield associated with an increase in defense metabolites (Bazzaz *et al.* 1987, Karban and Baldwin 1997, Zangerl *et al.* 2002). While measurements of the impact of anti-herbivore defenses on plant yield are important for understanding their ultimate fitness costs, measurements of plant biomass do not discriminate among the relative investments into compounds that function in growth-, storage- and defense processes in the analyzed tissues (Chapin *et al.* 1990) and do not illuminate the mechanisms of the putative allocation costs (Stamp 2003). Therefore, the investment into growth is preferably estimated by measuring components of biomass that directly promote the acquisition of resources for growth, such as photosynthetic proteins (Chapin *et al.* 1990). Additionally, the costs of defense should be measured in a currency of a fitness-limiting resource (Baldwin *et al.* 1998, Mole 1994) as such an approach allows for the direct quantitative comparison of investments into growth- and defense-related compounds, as revealed by changes in allocations into single compounds within plant tissues. However, a lack of suitable methods has thwarted such direct comparisons.

Nitrogen (N) is essential for the biosynthesis of proteins as well as many other molecules including some defense metabolites, and is often a fitness-limiting resource determining the growth and reproduction of plants and the herbivores that eat them. N availability also influences N allocation to defense metabolites (Baldwin *et al.* 1998, Lou and Baldwin 2004, Simon *et al.* 2010), making it an ideal currency to study growth-defense trade-offs in plant-herbivore interactions. Ribulose-1,5-bisphosphate carboxylase/oxygenase (RuBisCO), a protein essential for the dark reaction of photosynthesis, is the most abundant foliar protein in plants, accounting for 30-50% of the total soluble protein (TSP) in C3 plants (Ellis 1979, Makino *et al.* 1984, Stitt and Schulze 1994), and is thus a major N sink in plants, which may function as a potential N storage protein (Millard 1988). Although the amount and activity of RuBisCO are not the only factors controlling growth (Stitt and Schulze 1994),

changes in RuBisCO expression influence growth and lead to complex changes in N metabolism (Matt *et al.* 2002, Stitt and Krapp 1999, Stitt and Schulze 1994), making this enzyme a proxy for defense-related growth costs.

Nicotiana attenuata is a wild tobacco native to the Great Basin Desert in south-western USA that germinates from long-lived seed banks upon exposure to cues from burnt vegetation (Preston and Baldwin 1999). As a pioneer species, *N. attenuata* can take advantage of the abundant, yet ephemeral, pools of inorganic N in burnt soil (Lynds and Baldwin 1998), but is also subject to high intra-specific competition for fitness-limiting resources and attack by a diverse herbivore community, including the specialist tobacco hornworm (*Manduca sexta*). Herbivore attack elicits the jasmonic acid (JA) signaling cascade (Kessler *et al.* 2004), which activates JA-responsive transcription factors that lead to the biosynthesis of a plethora of induced small metabolites (Figure 1a, Woldemariam *et al.* 2011), such as the N-intensive alkaloid, nicotine, and a variety of phenolamides (PAs), which decrease herbivore performance (Baldwin 1999, Kaur *et al.* 2010, Onkokesung *et al.* 2010, Steppuhn *et al.* 2004). The biosynthesis of nicotine and PAs requires the same amino acid precursors (ornithine and arginine for putrescine and spermidine biosynthesis Kaur *et al.* 2010, Steppuhn *et al.* 2004, Takano *et al.* 2012), but the synthesis of nicotine only takes place in the roots (Hibi *et al.* 1994), while PAs are synthesized in the attacked leaf (Kaur *et al.* 2010).

Nicotine is present constitutively in undamaged *N. attenuata* tissues. It is also inducible and foliar concentrations can increase 4- to 10-fold after real or simulated herbivory by repeated wounding (W) and elicitation with *M. sexta* oral secretions (OS) (Baldwin 1999, McCloud and Baldwin 1997). The two major PAs found in *N. attenuata* are the N-acylated polyamines caffeoyl-putrescine (CP) and dicaffeoyl-spermidine (DCS), whose biosynthesis is regulated by the transcription factor, NaMYB8 (hereafter, MYB8, Figure 1a). Both CP and DCS accumulate constitutively in reproductive tissues and are strongly induced by herbivory in leaves (Kaur *et al.* 2010). Herbivory also causes large scale changes in *N. attenuata*'s transcriptome and proteome, decreasing levels of photosynthetic genes and proteins, including RuBisCO (Giri *et al.* 2006, Halitschke *et al.* 2003, Voelckel and Baldwin 2004). Due to the importance of N for its growth and defense, as well as its post-fire germination behavior, *N. attenuata* is an ideal model in which to study growth-defense trade-offs in a N currency.

Here we quantified the N-investments into different plant parts and among different N pools within a tissue to compare the investments into growth and defense in the same currency. A stable isotope labeling technique was used to track N flux among different N

pools in locally-elicited and systemic leaves and seeds. We applied ^{15}N labeled nitrate to the soil because nitrate is the most common form of N taken up by *N. attenuata* in nature, after the soil has been depleted of ammonium (Figure 1, Lynds and Baldwin 1998).

The N-flux into the three major N-intensive small metabolites of *N. attenuata* (nicotine, CP and DCS) were used as proxies for defense investment that could be compared to the N-investment into proteins, and the abundant photosynthetic protein RuBisCO was used as a proxy for growth-related investment. This direct comparison of the growth-defense trade-offs among relatively large molecules, such as proteins, and small N-containing metabolites, has not been previously possible due to a lack of suitable methods. Total soluble protein (TSP) is commonly quantified by spectrophotometry, which, although robust, is not directly comparable with MS-based methods used for metabolite quantification, and not useful for ^{15}N-incorporation analysis. TSP also contains, in addition to RuBisCO, other proteins that perform multiple functions, which confounds comparisons of N allocation to growth and defense. Here we used a novel high-throughput LC-MS^E method for absolute quantitation of proteins and assessment of ^{15}N-incorporation into peptides (Ullmann-Zeunert *et al.* 2012) which allows for the quantification of large proteins with the same accuracy as small defense metabolites quantified by UPLC tandem UV-ToF-MS (modified from Gaquerel *et al.* 2010).

To further disentangle the effects of induced defenses on N allocation after herbivory, we compared two previously described transgenic lines, one deficient in JA signaling, ir*LOX*3 (Allmann *et al.* 2010), and one deficient in the biosynthesis of PAs, ir*MYB8* (Kaur *et al.* 2010), with wild type (WT) plants (Fig. 1a). This design allows for a direct comparison of N-flux into specific classes of defense compounds with that into growth-related proteins measured in the same N currency, and an evaluation of the hypothesis that RuBisCO is used as N-storage compound for defense responses.

Results and Discussion

Anti-herbivore defense elicitation alters shoot N contents

Herbivory is known to change resource allocation within plants (Bazzaz *et al.* 1987, Frost and Hunter 2008, Gomez *et al.* 2010); an example is the allocation of recently assimilated N into alkaloids such as nicotine (Baldwin *et al.* 1994) and the increased allocation of N away from the attacked tissue into storage tissues (Frost and Hunter 2008, Gomez *et al.* 2012, Hanik *et al.* 2010). To estimate the impact of the biosynthesis of N-

containing defense metabolites on N accumulation in *N. attenuata*, we compared the shoot N contents (% dry mass) of the two transgenic lines impaired in defense responses with WT plants after repeated simulated herbivory. Additionally, we estimated the N pool sizes of the shoots by multiplying shoot dry mass by the shoot N content (Fig. S1a). The IRMS measurements revealed that elicitation by *M. sexta* OS reduced the N concentration of WT shoots (Welch two sample T-test, df=7.24, p=0.032), but not of the transgenic lines (Fig. 2), while the N pool sizes were slightly reduced after elicitation for all three genetic backgrounds (Fig. S1b). Changes in the N pool sizes of elicited ir*LOX3* and ir*MYB8* plants were due to a reduction in shoot dry mass (Fig. S1), while elicited WT showed both reduced shoot dry mass and reduced shoot N content, suggesting a possible N reallocation within the plant caused by the biosynthesis of N-containing defense metabolites.

Plants can allocate N to roots to protect their resources from consumption by herbivores and to reduce the nutritional value of the attacked tissues, which, together with increased defenses, can slow herbivore growth and increase their exposure to natural enemies (Trumble *et al.* 1993). Previous studies on tomato demonstrated that N allocation in the form of amino acids from the shoot to the roots was rapidly induced by methyl jasmonate (MeJA) (Gomez *et al.* 2010) and *M. sexta* feeding (Gomez *et al.* 2012, Steinbrenner *et al.* 2011). In *N. attenuata*, herbivory has been shown to cause a rapid allocation of carbon from the shoot to the roots, which can later be used for regrowth (Schwachtje *et al.* 2006). The reduced N concentration of WT shoots in our experiment suggests that this species can also allocate N from the shoot to the roots after herbivory. This inference is consistent with the observation that N contents of WT roots increased after elicitation, as measured in a separate experiment (Welch two sample t-test, df=4.71, p=0.054; inset, Fig. 2). An alternative explanation is that the increased N content of roots may have resulted from increased N assimilation, but previous ^{15}N labeling experiments in this species have found no evidence for changes in N assimilation rate after herbivory (Lynds and Baldwin 1998). Therefore, we conclude that the induced biosynthesis of N-containing metabolites after OS-elicitation alters whole-plant N partitioning.

OS-elicitation causes large changes in leaf protein and N-containing metabolites not reflected in total N pools

To analyze the influence of anti-herbivore defense induction, especially PA biosynthesis, on within-shoot N allocation, we determined the absolute N pools of different

leaf types (hereafter, total N pools) and N allocation to seeds by IRMS. Expressing resource allocation as concentrations reveals proportional allocations within an organ; however, total pool sizes allow for comparisons among organs, since they are a function of both organ size and concentration (Chapin *et al.* 1990). We analyzed locally elicited older (oRL) and younger (yRL) rosette leaves to explore the influence of leaf development on N reallocation after elicitation, and the first stem leaf (S1) to examine systemic effects.

Overall, there was no clear effect of genotype or elicitation on the leaf total N pools. Total N pools varied among genotypes only in the S1 leaf (ANOVA, $F_{1,27}$=4.86, p=0.036), whereby OS-elicitation only reduced the total N pool of ir*LOX3* (Two sample t-test, df=8, p=0.006) and WT (Two sample t-test, df=8, p=0.021) in the yRL (ANOVA, $F_{1,28}$=7.40 , p=0.011). The N pool size in oRL was unaffected by genotype and elicitation (Fig. 3). As N pool size correlates with biomass at the whole-plant scale (Baldwin and Hamilton 2000), we evaluated if the observed changes in total N pools of single leaves could be explained by changes in growth. Although the leaf size of yRL was reduced after elicitation (ANOVA, $F_{1,24}$=12.33, p=0.002) (Fig. S2a), it did not correlate with total N pools (ANCOVA, p = 0.187). Similarly, the change in total N pools of S1 leaves was not correlated with changes in leaf size (ANCOVA, p=0.406).

It is possible that changes in the total N pool of a leaf reflect changes in the pool of proteins within the leaf. TSP has been previously shown to decrease dramatically after herbivory (Brütting 2012), as they did in this experiment in yRL after elicitation. However, the TSP pool size did not correlate with the total N pool size in the yRL (ANCOVA, p=0.122; Fig. 3). Thus, we conclude that although both pools are reduced by elicitation, the total N pool of the rosette leaves does not reflect the changes in TSP pool size or leaf size. This result is consistent with the hypothesis that total leaf N content and TSP (RuBisCO content) are controlled by different mechanisms, as has been shown for rice (Ishimaru *et al.* 2001).

TSP pools differed between the transgenic lines in all three leaf types (ANOVA, oRL: $F_{1,27}$=8.70, p=0.007; yRL: $F_{1,27}$=12.95, p=0.001; S1: $F_{1,27}$=44.77 , p=3.5*10^{-07}; Fig. 3). The TSP of ir*LOX3* and ir*MYB8* in the yRL was reduced by about 50% after OS-elicitation, while WT TSP pools were reduced by 91%. Additionally, both transgenic lines had 2.5 to 3 times larger pools of TSP in the S1 leaf than did WT after elicitation (Fig. 3) suggesting that the biosynthesis of N-containing metabolites affect protein pool sizes.

The recently developed method for the absolute quantification of single proteins allowed us to quantitatively compare the investment in defense metabolites with that in

growth-related compounds, specifically, the photosynthetic protein RuBisCO, with a similar accuracy (Ullmann-Zeunert *et al.* 2012). Being the most abundant soluble protein in plants, the total amount of RuBisCO reflected the TSP pattern in the different leaves independent of genotypes (ANCOVA, oRL: $p<0.0001$; yRL: $p<0.0001$; S1: $p=0.42$; Fig. 3, Fig.S3a). Overall, the data revealed a decrease in RuBisCO LSU and SSU pool sizes after OS-elicitation (Fig. S3a), which coincided with an increase in N-containing defense metabolites (Fig. S3b), but the effects differed among lines. The two transgenic lines with reduced (ir*LOX3*) and no detectable levels of CP and DCS (ir*MYB8*; Fig. S3b) showed a smaller decrease of RuBisCO LSU and SSU than did WT in the locally elicited yRL (47-59% in ir*MYB8*/ir*LOX3* compared to 95 (LSU)/92 % (SSU) in WT; Fig. S3a). RuBisCO LSU and SSU levels were unaltered after elicitation in the systemic S1 leaf of ir*MYB8*, but strongly declined in WT and ir*LOX3*. Overall, ir*LOX3* showed an intermediate phenotype between WT and ir*MYB8*. The nicotine pool sizes showed similar induction patterns for all lines, except in the yRL, where the OS-elicited nicotine levels were higher in WT than in the transgenic lines. These data suggest that the growth-defense trade-offs at the leaf scale are influenced by the biosynthesis of PAs or the level of their induction; and they also affect the systemic S1 leaf. Since all transgenic lines used in this study accumulated similar amounts of nicotine, it is unclear whether the biosynthesis of this alkaloid might affect N allocation to proteins (Fig. S3b). To answer this question rigorously, experiments with transgenic lines completely silenced in the flux of N into nicotine biosynthesis are needed. In the nicotine-silenced transgenic lines we have produced in our laboratory by silencing putrescine N-methyl transferase (ir*PMT*), nicotine biosynthesis is silenced, but the elicited flux of N into other alkaloids (anatabine) is not (Steppuhn *et al.* 2004).

A comparison of the two locally elicited leaves revealed differences in their defense and growth pool sizes: while oRL accumulated the largest defense metabolite pools with only slight reductions in TSP and both RuBisCO subunits after elicitation, the yRL had the strongest reductions in protein pools, with smaller increases in N-containing defense metabolite levels than the oRL (Fig. 3, Fig. S3). The optimal defense (OD) theory predicts that the allocation of defense metabolites correlates positively with the fitness value of different plant parts (McKey 1974, McKey 1979, Rhoades 1979) and many studies have demonstrated that younger leaves in *N. attenuata* contain higher defense metabolite levels which presumably have a higher fitness value than do older leaves (Kaur *et al.* 2010, Onkokesung *et al.* 2012, Zavala *et al.* 2004) as has been experimentally demonstrated in *N.*

sylvestris (Ohnmeiss and Baldwin 2000). These results appear to contradict our findings, because oRL contained higher metabolite levels than did yRL. However, the previous studies compared concentrations of metabolites in rosette leaves at different stages of development, while here we analyzed metabolite pool sizes of two locally elicited rosette leaves of different ages harvested simultaneously from the same plant. Since the plants were just beginning stalk elongation at the time of OS-elicitation, both oRL and yRL are likely comparably important tissues for later plant growth and reproduction. Several scenarios are possible. The larger defense metabolite pools of oRL may reflect their larger nutrient pools, which are probably important for regrowth capacity. Alternatively, the smaller pools of TSP and RuBisCO in the yRL may reflect a lower N allocation to proteins in younger leaves, which could enhance their defense status by reducing the food quality for herbivores. Regardless of their ultimate explanations, these data demonstrate that growth-defense trade-offs are dependent on leaf development.

Previous studies demonstrated the importance of leaf N pools for reproduction in *N. sylvestris* (Ohnmeiss and Baldwin 2000), thus, growth-defense trade-offs at the leaf scale can affect the N allocation to capsules. However, the N pools of seeds in our experiment did not change with elicitation or genetic background (Fig. S2b). This could be due to species-specific differences or differences in the experimental design. *N. sylvestris* produces a single reproductive stalk after rosette growth and extensive root storage, while *N. attenuata* develops multiple floral stalks, and lacks extensive root storage. Alternatively, plants of this experiment may have been too young or the W+OS treatment too weak to elicit changes in allocation to seeds. Previously, strong alterations in N allocation to reproductive units in *N. attenuata* were only found when control plants grew in direct competition with MeJA-elicited plants under low fertilization rates (Van Dam and Baldwin 2001, Baldwin 1998). Additional experiments with plants grown in competition are necessary to explore the impact of growth-defense trade-offs within the leaf on plant fitness.

MYB8 indirectly affects N-investments into proteins

The pool sizes of growth and defense-related compounds of the two transgenic lines indicated an influence of N-containing metabolite biosynthesis on the observed growth-defense trade-offs, but did not allow for a direct comparison of the N demand of metabolite biosynthesis and the decreased N partitioned into TSP and RuBisCO after herbivory. By calculating the N-investment into growth and defense per mg of fresh tissue mass after

elicitation for all three lines, we were able to further explore the role of PA biosynthesis on N reallocation. We combined this approach with ^{15}N pulse labeling to follow the investment of a defined N pool into both plant functions.

After elicitation, WT had higher concentrations of N in nicotine, CP and DCS, and less in TSP, RuBisCO LSU and SSU per mg fresh mass, while ir*MYB8* plants showed only slight effects of elicitation on N-concentrations (Fig. 4a). Ir*LOX3* plants showed similar, but attenuated, N-allocation patterns as WT did after elicitation. These patterns are consistent with the correlation analysis of all measured N pools (Fig 4a, heatmaps). Correlating all genotype/treatment groups with each other revealed that OS-elicited WT plants had a strong negative correlation with the other genotype/treatment groups in all three leaf types. Only OS-elicited ir*LOX3* plants showed a weak positive correlation to WT-OS. In contrast, irMYB8-OS did not correlate with any other genotype by treatment group.

Interestingly, the observed N-investment pattern is congruent with previous results on the patterns of *MYB8* transcript accumulation in *N. attenuata* as *LOX3* plants (which are comparable to ir*LOX3* (Allmann *et al.* 2010, Halitschke *et al.* 2004)). After elicitation, as*LOX3* have 4 times lower transcript levels, while ir*MYB8* have 10 times lower levels than do WT leaves (Onkokesung *et al.* 2012; Kaur et al. 2010). Hence, the observed intermediate phenotype of LOX3-silenced plants is consistent with their respective *MYB8* transcript levels. MYB8 functions downstream of JA signaling - OS-elicited JA levels are not altered in ir*MYB8* plants (Kaur *et al.* 2010) - leading to the conclusion that the observed changes in N allocation after simulated herbivory do not directly require JA signaling, and are likely caused by differences in *MYB8* expression and the MYB8-regulated synthesis of PAs.

MYB8 is rapidly elicited and thought to play a regulatory role in later stages of defense deployment (Galis *et al.* 2010), and is still induced 1-2 days after OS-elicitation (Kaur *et al.* 2010). This time-frame agrees with our experimental time-frame, with the strongest changes 1 day after the last treatment (4 days after first elicitation, see Fig. 1b). One explanation of how MYB8 could regulate defense induction at the later time-points is by playing a role in N assimilation and allocation. In other plants and algae, members of the R2R3-MYB transcription factor family, to which NaMYB8 belongs, have been shown to be crucial for increases in the abundance of transcripts of N assimilation genes (Imamura *et al.* 2009, Miyake *et al.* 2003). Furthermore, a R2R3-MYB transcription factor of *Pinus sylvestris* which regulates lignin biosynthesis, interacts with the glutamine synthetase promoter and has been suggested to play a role in N recycling after lignin production (Gomez-Maldonado *et al.*

2004). To further elucidate the putative role of MYB8 in N reallocation, more detailed expression and enzyme activity studies targeting N metabolism at later time-points after herbivory are necessary.

Based on our data we cannot differentiate if MYB8 itself or the synthesis of PAs, in particular CP and DCS, mediate the changes in N-investment into growth and defense. In other studies, PAs have been shown to regulate abiotic and biotic stress responses (Waie and Rajam 2003, Walters 2003) and apparently play an important role in growth (Imai *et al.* 2004). Silencing *MYB8*also silences genes further downstream of the transcription factor, and in addition to CP and DCS, the synthesis of at least 29 different coumaroyl-, caffeoyl- and feruloyl containing metabolites (Onkokesung *et al.* 2012). It is difficult to pinpoint the effects of single compounds in the complex biosynthetic network of a leaf. Applying PAs in different amounts to control and elicited leaves of ir*MYB8* plants, and evaluating their effect on protein (RuBisCO) levels, or using mutants for single genes affecting PA biosynthesis downstream of MYB8 can help to evaluate if either MYB8 or PAs alone or MYB8 indirectly through PAs biosynthesis mediate the changes in N-investment into proteins.

A comparison of the total N-investment with the ^{15}N-investment per mg fresh mass revealed a similar pattern, with increased ^{15}N in defense compounds and decreased ^{15}N in LSU and SSU after elicitation. One major difference was that WT and ir*LOX3* plants allocated proportionally more ^{15}N than total N into CP and DCS, and less into nicotine, after elicitation (Fig. 4b; for a clearer comparison of N- and ^{15}N-investment, see Fig. S4). These data suggest that recently assimilated N, i.e. ^{15}N, is more rapidly invested into the PA pathway after elicitation by *M. sexta* OS, while another unmeasured previously assimilated N pool is the major source for nicotine biosynthesis. These findings seemingly contradict previous results showing the rapid incorporation of recently assimilated ^{15}N into nicotine after elicitation, but these results were obtained from plants that were N-starved for 24h before application of the ^{15}N pulse, and ^{15}N was applied at the same time as MeJA to the roots (Baldwin *et al.* 1994, Lynds and Baldwin 1998). These differences in experimental design probably led to different source-sink relationships within the plant, resulting in different patterns of ^{15}N-investments: N-starved plants are known to transport N preferentially to the strongest sink (Ohtake *et al.* 2001); MeJA is a stronger elicitor than OS elicitation (Voelckel *et al.* 2001), and in contrast to our experiments, only roots were treated and not leaves. Larger investments of recently assimilated ^{15}N into CP and DCS compared to nicotine makes

ecological sense, because the OS used was from *M. sexta* larvae, which are nicotine-tolerant but are negatively affected by PAs (Kaur *et al.* 2010).

The shift in ^{15}N- and total N-investment patterns is not observed in the relative N allocation to growth, because the ^{15}N-investment into RuBisCO LSU and SSU was proportionally similar to the total N-investment in both control and elicited leaves (Fig 4b, Fig S4). However, a comparison of the decrease in total N-investment into RuBiSCO and TSP after OS-elicitation with the N-requirements of nicotine and phenolamide biosynthesis (Fig. 4a) suggested that RuBisCO metabolism could be a source of reallocated N to defense metabolite biosynthesis. Based on concentrations in the yRL, about 54% of N from RuBisCO or 13% of N from TSP could have been invested into PAs and nicotine (Fig. S4).This comparison does not take into account the N-requirements of biosynthetic enzymes, hence the N demands for defense metabolite biosynthesis is likely underestimated.

N invested into phenolamides does not originate from RuBisCO after herbivory

To investigate if RuBisCO N is used as a source of N for CP and DCS biosynthesis after OS-elicitation, the ^{15}N-incorporation (At%) into N-containing metabolites and RuBisCO was determined in a time course experiment (see Fig 1b for details). This approach allows one to follow the N flux of a known amount of ^{15}N, independently of within-leaf N pool sizes. The experiment was carried out with the yRL, because this leaf showed the greatest differences in N-investment after elicitation (Fig. 4a,b). It is important to note that during the experimental period, the ^{15}N-incorporation of the whole leaf was constant in all three lines, independent of elicitation (Fig. S5), indicating that N is mainly redistributed within the leaves and that there is no increased net N-influx into the leaf after elicitation.

As the ^{15}N-incorporation into RuBisCO LSU and SSU was similar, we only report the incorporation into LSU. Incorporation into RuBisCO increased at a constant rate until it reached a maximum of about 8 At% between 4 and 7 days after the 1st elicitation in all three lines, independent of elicitation (Fig. 5). In contrast, ^{15}N was rapidly incorporated into CP and DCS in elicited leaves until these compounds attained a maximum of about 10-12 At%, 4 days after the 1st elicitation in WT and ir*LOX3* plants. Had RuBisCO degradation provided the precursors for PA biosynthesis, it should have a similar or higher ^{15}N-incorporation as did both PAs, since precursor pools will have similar or higher labeled isotope incorporation rates as their derived compounds. The large differences in ^{15}N-incorporation between CP and DCS and LSU make it unlikely that N derived from RuBisCO was used for CP and DCS

biosynthesis. In contrast, the data indicates that ^{15}N is more rapidly invested into PAs instead of RuBisCO (Fig. 4b). PA biosynthesis requires arginine and ornithine (Kaur *et al.* 2010, Takano *et al.* 2012) both of which are derived from glutamine, the first amino acid produced after N assimilation (Fig. 1a). After elicitation, recently assimilated N in glutamine might be directly channeled into PA biosynthesis by the preferential synthesis of arginine. An increase in arginine levels after herbivory has not yet been reported. Studies on tomato and *N. tabacum* only revealed an early, rapid and transient increase in phenylalanine and tyrosine after elicitation (Gomez *et al.* 2012, Hanik *et al.* 2010). A kinetic analysis of ^{15}N-incorporation into amino acids and their quantification combined with the analysis of PAs and RuBisCO in the same tissues at later time-points will help to elucidate which precursors are used for defense metabolite biosynthesis in *N. attenuata*. Additionally, turnover studies with labeled glutamine or arginine may provide further insights into N-allocation between growth and defense.

^{15}N-incorporation into nicotine only increased slightly after elicitation and reached a maximum of around 2 At% in all three lines (Fig. 5), though roots had a labeling of about 8 At%, similar to shoots. Nicotine is a constantly synthesized pool in the roots in *N. attenuata*, which is transported to the shoot, but not metabolized (Baldwin *et al.* 1994) and contains up to 5-8 % of the plant's total N (Baldwin and Hamilton 2000). It is possible that the newly synthesized nicotine might be diluted by the large pool of previously synthesized unlabeled nicotine, resulting in a low ^{15}N-incorporation. Alternatively, it may be derived from previously synthesized (and therefore unlabeled) precursors. Lastly, nicotine pools might incorporate N at a slower rate than N pools which have a constant turnover, such as proteins.

In summary, the ^{15}N-incoporation illustrates the flux of a defined ^{15}N pulse, independent of pool size, and indicates that N invested into CP and DCS is unlikely derived from RuBisCO, but is allocated directly to defense processes after assimilation instead of growth process.

Conclusion

We quantified the investments into growth and defense in a common N currency in intact and in elicited plants. This was possible by combining ^{15}N pulse-labeling with a novel protein quantification method to quantitatively compare the allocation of an important growth-limiting resource, N, to growth (RuBisCO) and small defense-related compounds (nicotine, PAs) after herbivory with comparable accuracy. Our experiments revealed that in the wild tobacco *N. attenuata*, OS-elicitation reconfigures N allocation at multiple scales (Fig.

6). At the whole-plant scale, OS-elicitation likely induces N re-allocation from the shoot to the root and at the within-leaf scale, it dramatically decreases N-investment into growth-related N pools (TSP and RuBisCO) while increasing investment in defense metabolites (nicotine, CP and DCS). The transcription factor Na*MYB8,* by regulating the production of metabolically dynamic, PAs, CP and DCS, indirectly mediates N-investments into TSP and RuBisCO after elicitation. ^{15}N flux studies indicated that the N for PA biosynthesis comes from recently assimilated N rather than RuBisCO turnover. Further experiments will focus on elucidating the mechanism by which MYB8 and PAs influence N metabolism and identification of which compound(s) play regulatory roles.

Experimental Procedures

Plant germination and growth conditions

Seeds of the 31st generation of an inbred WT line of *Nicotiana attenuata* Torr. ex. Watts (Solanaceae) and two stably transformed lines, ir*MYB8* with reduced expression of the transcription factor *NaMYB8(A-08-810,* Kaur *et al.* 2010), and ir*LOX3* silenced in lipoxygenase 3 (*NaLOX3, A-03-562-2,* Allmann *et al.* 2010), were sterilized and germinated according to Kruegel *et al.* (2002). After germination, plants were cultivated as described in Ullmann-Zeunert *et al.* (2012) for the pulse-labeled plants.

Plant treatment

Pre-experiment to determine elicitation time-points:

Seven days after transfer to 1L single pots, rosette-stage plants were pulse-labeled with 5.1 mg ^{15}N in 50 mL of a 0.694 g*L^{-1} solution of $K^{15}NO_3$ (modified from Van Dam and Baldwin 2001) and the oldest sink leaf (hereafter, younger rosette leaf, yRL) and the youngest source leaf (hereafter, older rosette leaf, oRL) were labeled for later sampling (Pluskota *et al.* 2007). The leaves and roots were harvested 0, 4, 12 h, and 4, 7 and 10 days after the ^{15}N-pulse. Roots were washed to remove excess soil and all samples were dried for 48h at 60^{o}C. Between 3 and 10 days after the pulse, the leaves and roots had a constant ^{15}N-concentration (Fig. 1b), indicating that an equilibrium between plants and N-immobilizing microorganisms in the soil had been reached. This time-period was chosen for further experiments (Fig. 1b, indicated by the grey arrows) since a stable ^{15}N-incorporation facilitates the analysis of proportional allocation to single compounds.

Pulse-labeling experiments:

Three days after the ^{15}N pulse, 3 leaves of rosette-staged plants were wounded with a pattern wheel and elicited with oral secretion (OS) of *M. sexta* on 3 consecutive days (Ullmann-Zeunert *et al.* 2012). Unelicited plants were used as controls. For the whole-shoot N analysis, the aboveground biomass of 5 control and elicited plants per genotype was harvested 4 days after the first elicitation and dried as above.

For the N-partitioning analysis, the right leaf blades of the locally elicited yRL and oRL of a different set of replicates were harvested 4 days after the first elicitation and flash-frozen in liquid N_2. After stalk elongation, the right leaf blade of the first stem leaf (S1) was harvested when it reached the source-sink transition stage. Harvest time-points of the S1 leaf differed depending on plant development. The first mature seed capsules were harvested at the day of opening: seeds were counted, weighed and analyzed for N content. For the kinetic analysis, plants received a ^{15}N pulse and were elicited as described above, and the locally elicited yRL was harvested 0, 1, 3, 4 and 7 days after the first elicitation (Fig. 1b).

Protein extraction and quantification:

The TSP and RuBisCO LSU and SSU were extracted and quantified by Bradford assay and LC-MS^E, respectively, as described by Ullmann-Zeunert *et al.* (2012). The ^{15}N-incorporation of RuBisCO was determined with ProSipQuant (Taubert *et al.* 2011).

Metabolite extraction and quantification

Small metabolites were extracted as in Gaquerel *et al.* (2010) and analyzed by UPLC-UV-ToF-MS, using a Dionex RSLC system with a Diode Array Detector (Dionex, Sunnyvale, USA) tandem Micro-ToF Mass Spectrometer (Bruker Daltonik, Bremen, Germany). Further details on instrument parameters and quantification are described in the Supplemental Procedures. Average mass spectra were extracted for^{15}N-incorporations using ProSipQuant (Taubert *et al.* 2011), modified for small metabolites based on compound sum formula.

Isotope Ratio Mass Spectrometry Analysis (IRMS)

The IRMS sample preparation, analysis and following calculations of total N content (% dry mass) and ^{15}N-incorporation were carried out as described in Meldau *et al.* (2012).

Statistical Analysis

The R environment was used for statistical analysis (Team 2009). For ANOVA analyses, if the assumption of homoscedasticity of variances was violated or the residuals did not follow a normal distribution, response variables were transformed prior to the analyses using Box-Cox transformation. The Box-Cox-lambda was estimated using Venables' and Ripley's MASS library for R. All models were simplified to the minimum adequate model using Aikaike's information criterion (Ronchetti 1985). For the correlation analysis (Fig. 4a, heatmaps) the data were imported into the environment and vectors containing the following variables generated: N-rest protein µg/mg, N-RuBisCO LSU µg/mg, N-RuBisCO SSU µg/mg, N-nicotine µg/mg, N-CP µg/mg, and N-DCS µg/mg. These vectors were pairwise correlated, calculating Kendall's τ coefficient (Kendall 1938). In contrast to Pearson's correlation coefficient Kendall's τ is more robust and not sensitive to the data distribution. For a clearer presentation, the heat maps contain both the original and the LOWESS normalized data (Cleveland 1979).

Acknowledgements

The authors thank Franziska Hufsky for bioinformatics help with RuBisCO quantification and Dr. Matthias Schöttner for technical support with metabolite measurements. This research was supported by the Max Planck Society and M.A.S. by a grant of the International Max Planck Research School.

Supporting Information:

Supplemental Procedures

Figure S1: The dry mass and the absolute amount of nitrogen (N) of the shoot (b) do not depend on genotype.

Figure S2: Average leaf size and mass and total N of pooled seeds from the first seed capsule in transgenic (ir*LOX3*, ir*MYB8*) and WT plants with and without W+OS treatment.

Figure S3: Silencing of *LOX3* and *MYB8* alters the absolute pools of N-containing small metabolites and RuBisCO within leaves.

Figure S4: Increased N investment into nicotine, CP and DCS is accompanied by a decreased N investment into RuBisCO.

Figure S5: ^{15}N-incorporation in the yRL does not depend on treatment or genotype.

Figure S6: The decrease of N investment into protein pools is greater than N needed for biosynthesis of defense metabolites

Supplemental Statistical Information

References

Allmann, S., Halitschke, R., Schuurink, R.C. and Baldwin, I.T. (2010) Oxylipin channelling in *Nicotiana attenuata*: lipoxygenase 2 supplies substrates for green leaf volatile production. *Plant Cell Environ.*, **33**, 2028-2040.

Baldwin, I.T. (1999) Inducible nicotine production in native *Nicotiana* as an example of adaptive phenotypic plasticity. *J. Chem. Ecol.*, **25**, 3-30.

Baldwin, I.T., Gorham, D., Schmelz, E.A., Lewandowski, C.A. and Lynds, G.Y. (1998) Allocation of nitrogen to an inducible defense and seed production in *Nicotiana attenuata*. *Oecologia*, **115**, 541-552.

Baldwin, I.T. and Hamilton, W. (2000) Jasmonate-induced responses of *Nicotiana sylvestris* results in fitness costs due to impaired competitive ability for nitrogen. *J. Chem. Ecol.*, **26**, 915-952.

Baldwin, I.T., Karb, M.J. and Ohnmeiss, T.E. (1994) Allocation of ^{15}N from nitrate to nicotine - production and turnover of a damage-induced mobile defense. *Ecology*, **75**, 1703-1713.

Baldwin, I.T. and Ohnmeiss, T.E. (1994) Coordination of photosynthetic and alkaloidal responses to damage in uninducible and inducible *Nicotiana sylvestris*. *Ecology*, **75**, 1003-1014.

Bazzaz, F.A., Chiariello, N.R., Coley, P.D. and Pitelka, L.F. (1987) Allocating rescources to reproducation and defense. *Bioscience*, **37**, 58-67.

Brütting, C. (2012) The role of cytokinins in plant responses to insect attack. In *Fakultät für Biologie, Chemie und Geowissenschaften*. Bayreuth: Universität Bayreuth, pp. 82.

Chapin, F.S., Schulze, E.D. and Mooney, H.A. (1990) The ecology and economics of storage in plants. *Annu. Rev. Ecol. Syst.*, **21**, 423-447.

Cleveland, W.S. (1979) Robust locally weighted regression and smoothing scatterplots. *J. Am. Stat. Assoc.*, **74**, 829-836.

Ellis, R.J. (1979) Most abundant protein in the world. *Trends Biochem. Sci.*, **4**, 241-244.

Frost, C.J. and Hunter, M.D. (2008) Herbivore-induced shifts in carbon and nitrogen allocation in red oak seedlings. *New Phytol.*, **178**, 835-845.

Galis, I., Onkokesung, N. and Baldwin, I.T. (2010) New insights into mechanisms regulationg differential accumulation of phenylpropanoid-polyamine conjugates (PPCs) in herbivore-attached *Nicotiana attenuata* plants. *Plant Signal. Behav.*, **5**, 610-613.

Gaquerel, E., Heiling, S., Schoettner, M., Zurek, G. and Baldwin, I.T. (2010) Development and validation of a liquid chromatography-electrospray ionization-time-of-flight mass spectrometry method for Induced changes in *Nicotiana attenuata* leaves during simulated herbivory. *J. Agric. Food Chem.*, **58**, 9418-9427.

Giri, A.P., Wuensche, H., Mitra, S., Zavala, J.A., Muck, A., Svatos, A. and Baldwin, I.T. (2006) Molecular interactions between the specialist herbivore *Manduca sexta* (Lepidoptera, Sphingidae) and its natural host *Nicotiana attenuata*. VII. Changes in the plant's proteome. *Plant Physiol.*, **142**, 1621-1641.

Gomez-Maldonado, J., Avila, C., de la Torre, F., Canas, R., Canovas, F.M. and Campbell, M.M. (2004) Functional interactions between a glutamine synthetase promoter and MYB proteins. *Plant J.*, **39**, 513-526.

Gomez, S., Ferrieri, R.A., Schueller, M. and Orians, C.M. (2010) Methyl jasmonate elicits rapid changes in carbon and nitrogen dynamics in tomato. *New Phytol.*, **188**, 835-844.

Gomez, S., Steinbrenner, A.D., Osorio, S., Schueller, M., Ferrieri, R.A., Fernie, A.R. and Orians, C.M. (2012) From shoots to roots: transport and metabolic changes in tomato after simulated feeding by a specialist lepidopteran. *Entomol. Exp. Appl.*, **144**, 101-111.

Halitschke, R., Gase, K., Hui, D.Q., Schmidt, D.D. and Baldwin, I.T. (2003) Molecular interactions between the specialist herbivore *Manduca sexta* (Lepidoptera, Sphingidae) and its natural host *Nicotiana attenuata.* VI. Microarray analysis reveals that most herbivore-specific transcriptional changes are mediated by fatty acid-amino acid conjugates. *Plant Physiol.*, **131**, 1894-1902.

Halitschke, R., Ziegler, J., Keinanen, M. and Baldwin, I.T. (2004) Silencing of hydroperoxide lyase and allene oxide synthase reveals substrate and defense signaling crosstalk in *Nicotiana attenuata*. *Plant J.*, **40**, 35-46.

Hanik, N., Gomez, S., Best, M., Schueller, M., Orians, C.M. and Ferrieri, R.A. (2010) Partitioning of new carbon as ^{11}C in *Nicotiana tabacum* reveals insight into methyl jasmonate induced changes in metabolism. *J. Chem. Ecol.*, **36**, 1058-1067.

Hibi, N., Higashiguchi, S., Hashimoto, T. and Yamada, Y. (1994) Gene-expression in tobacco low-nicotine mutants. *Plant Cell*, **6**, 723-735.

Imai, A., Matsuyama, T., Hanzawa, Y., Akiyama, T., Tamaoki, M., Saji, H., Shirano, Y., Kato, T., Hayashi, H., Shibata, D., Tabata, S., Komeda, Y. and Takahashi, T. (2004) Spermidine synthase genes are essential for survival of Arabidopsis. *Plant Physiol.*, **135**, 1565-1573.

Imai, K., Suzuki, Y., Mae, T. and Makino, A. (2008) Changes in the synthesis of rubisco in rice leaves in relation to senescence and N influx. *Ann. Bot.*, **101**, 135-144.

Imamura, S., Kanesaki, Y., Ohnuma, M., Inouye, T., Sekine, Y., Fujiwara, T., Kuroiwa, T. and Tanaka, K. (2009) R2R3-type MYB transcription factor, CmMYB1, is a central nitrogen assimilation regulator in *Cyanidioschyzon merolae*. *Proc. Natl. Acad. Sci. USA*, **106**, 12548-12553.

Ishimaru, K., Kobayashi, N., Ono, K., Yano, M. and Ohsugi, R. (2001) Are contents of Rubisco, soluble protein and nitrogen in flag leaves of rice controlled by the same genetics? *J. Exp. Bot.*, **52**, 1827-1833.

Karban, R. and Baldwin, I.T. (1997) *Induced responses to herbivory* Univ. of Chicago Press: Chicago u.a.

Kaur, H., Heinzel, N., Schoettner, M., Baldwin, I.T. and Galis, I. (2010) R2R3-NaMYB8 regulates the accumulation of phenylpropanoid-polyamine conjugates, which are essential for local and systemic defense against insect herbivores in *Nicotiana attenuata*. *Plant Physiol.*, **152**, 1731-1747.

Kendall, M. (1938) A new measure of rank correlation. *Biometrika*, **30**, 81-89.

Kessler, A., Halitschke, R. and Baldwin, I.T. (2004) Silencing the jasmonate cascade: Induced plant defenses and insect populations. *Science*, **305**, 665-668.

Kruegel, T., Lim, M., Gase, K., Halitschke, R. and Baldwin, I.T. (2002) Agrobacterium-mediated transformation of *Nicotiana attenuata*, a model ecological expression system. *Chemoecology*, **12**, 177-183.

Lou, Y.G. and Baldwin, I.T. (2004) Nitrogen supply influences herbivore-induced direct and indirect defenses and transcriptional responses to *Nicotiana attenuata*. *Plant Physiol.*, **135**, 496-506.

Lynds, G.Y. and Baldwin, I.T. (1998) Fire, nitrogen, and defensive plasticity in *Nicotiana attenuata*. *Oecologia*, **115**, 531-540.

Makino, A., Mae, T. and Ohira, K. (1984) Relation between nitrogen and ribulose-1,5-bisphosphate carboxylase in rice leaves from emergence through senescence. *Plant Cell Physiol.*, **25**, 429-437.

Matt, P., Krapp, A., Haake, V., Mock, H.P. and Stitt, M. (2002) Decreased Rubisco activity leads to dramatic changes of nitrate metabolism, amino acid metabolism and the levels of phenylpropanoids and nicotine in tobacco antisense RBCS transformants. *Plant J.*, **30**, 663-677.

McCloud, E.S. and Baldwin, I.T. (1997) Herbivory and caterpillar regurgitants amplify the wound-induced increases in jasmonic acid but not nicotine in *Nicotiana sylvestris*. *Planta*, **203**, 430-435.

McKey, D. (1974) Adaptive patterns in alkaloid physiology. *Am. Nat.*, **108**, 305-320.

McKey, D. (1979) *Distribution of secondary compounds within plants*.

Meldau, S., Ullmann-Zeunert, L., Govind, G., Bartram, S. and Baldwin, I.T. (2012) Basal and herbivory-induced defense trade-offs are mediated by mitogen-activated protein kinases, jasmonic acid and salicylic acid in the native tobacco, *Nicotiana attenuata*. *BMC Plant Biol.*, **in press**.

Millard, P. (1988) The accumulation and storage of nitrogen by herbaceous plants. *Plant Cell Environ.*, **11**, 1-8.

Miyake, K., Ito, T., Senda, M., Ishikawa, R., Harada, T., Niizeki, M. and Akada, S. (2003) Isolation of a subfamily of genes for R2R3-MYB transcription factors showing up-regulated expression under nitrogen nutrient-limited conditions. *Plant Mol. Biol.*, **53**, 237-245.

Mole, S. (1994) Trade-offs and constraints in plant-herbivore defense theory - a life-history perspective. *Oikos*, **71**, 3-12.

Ohnmeiss, T.E. and Baldwin, I.T. (2000) Optimal Defense theory predicts the ontogeny of an induced nicotine defense. *Ecology*, **81**, 1765-1783.

Ohtake, N., Sato, T., Fujikake, H., Sueyoshi, K., Ohyama, T., Ishioka, N.S., Watanabe, S., Osa, A., Sekine, T., Matsuhashi, S., Ito, T., Mizuniwa, C., Kume, T., Hashimoto, S., Uchida, H. and Tsuji, A. (2001) Rapid N transport to pods and seeds in N-deficient soybean plants. *J. Exp. Bot.*, **52**, 277-283.

Onkokesung, N., Galis, I., von Dahl, C.C., Matsuoka, K., Saluz, H.-P. and Baldwin, I.T. (2010) Jasmonic acid and ethylene modulate local responses to wounding and simulated herbivory in *Nicotiana attenuata* leaves. *Plant Physiol.*, **153**, 785-798.

Onkokesung, N., Gaquerel, E., Kotkar, H., Kaur, H., Baldwin, I.T. and Galis, I. (2012) MYB8 controls inducible phenolamide levels by activating three novel hydroxycinnamoyl-coenzyme A:polyamine transferases in *Nicotiana attenuata*. *Plant Physiol.*, **158**, 389-407.

Pluskota, W.E., Qu, N., Maitrejean, M., Boland, W. and Baldwin, I.T. (2007) Jasmonates and its mimics differentially elicit systemic defence responses in *Nicotiana attenuata*. *J. Exp. Bot.*, **58**, 4071-4082.

Preston, C.A. and Baldwin, I.T. (1999) Positive and negative signals regulate germination in the post-fire annual, *Nicotiana attenuata*. *Ecology*, **80**, 481-494.

Rhoades, D.F. (1979) *Evolution of plant chemical defense against herbivores*.

Ronchetti, E. (1985) Robust model selection in regression. *Stat. Probab. Lett.*, **3**, 21-23.

Schwachtje, J., Minchin, P.E.H., Jahnke, S., van Dongen, J.T., Schittko, U. and Baldwin, I.T. (2006) SNF1-related kinases allow plants to tolerate herbivory by allocating carbon to roots. *Proc. Natl. Acad. Sci. USA*, **103**, 12935-12940.

Simon, J., Gleadow, R.M. and Woodrow, I.E. (2010) Allocation of nitrogen to chemical defence and plant functional traits is constrained by soil N. *Tree Physiol.*, **30**, 1111-1117.

Stamp, N. (2003) Out of the quagmire of plant defense hypotheses. *Q. Rev. Biol.*, **78**, 23-55.

Steinbrenner, A.D., Gomez, S., Osorio, S., Fernie, A.R. and Orians, C.M. (2011) Herbivore-induced changes in tomato (*Solanum lycopersicum*) primary metabolism: A whole plant perspective. *J. Chem. Ecol.*, **37**, 1294-1303.

Steppuhn, A., Gase, K., Krock, B., Halitschke, R. and Baldwin, I.T. (2004) Nicotine's defensive function in nature. *PLoS Biol.*, **2**, 1074-1080.

Stitt, M. and Krapp, A. (1999) The interaction between elevated carbon dioxide and nitrogen nutrition: the physiological and molecular background. *Plant Cell Environ.*, **22**, 583-621.

Stitt, M. and Schulze, D. (1994) Does Rubisco control the rate of photosynthesis and plant-growth - an exercise in molecular ecophysiology. *Plant Cell Environ.*, **17**, 465-487.

Takano, A., Kakehi, J.I. and Takahashi, T. (2012) Thermospermine is not a minor polyamine in the plant kingdom. *Plant Cell Physiol.*, **53**, 606-616.

Taubert, M., Jehmlich, N., Vogt, C., Richnow, H.H., Schmidt, F., von Bergen, M. and Seifert, J. (2011) Time resolved protein-based stable isotope probing (Protein-SIP)

analysis allows quantification of induced proteins in substrate shift experiments. *Proteomics*, **11**, 2265-2274.

Team, R.D.C. (2009) R: A language and environment for statistical computing (Vienna: R Foundation for Statistical Computing). *http://www.r-project.org*.

Trumble, J.T., Kolodnyhirsch, D.M. and Ting, I.P. (1993) Plant compensation for arthropod herbivory. *Annu. Rev. Entomol.*, **38**, 93-119.

Ullmann-Zeunert, L., Muck, A., Wielsch, N., Hufsky, F., Stanton, M.A., Bartram, S., Böcker, S., Baldwin, I.T., Groten, K. and Svatos, A. (2012) Determination of ^{15}N-Incorporation into plant proteins and their absolute quantitation: A new tool to study nitrogen flux dynamics and protein pool sizes elicited by plant–herbivore interactions. *J. Proteome Res.* 11, 4947-4960.

Van Dam, N.M. and Baldwin, I.T. (2001) Competition mediates costs of jasmonate-induced defences, nitrogen acquisition and transgenerational plasticity in *Nicotiana attenuata*. *Funct. Ecol.*, **15**, 406-415.

Voelckel, C. and Baldwin, I.T. (2004) Herbivore-induced plant vaccination. Part II. Array-studies reveal the transience of herbivore-specific transcriptional imprints and a distinct imprint from stress combinations. *Plant J.*, **38**, 650-663.

Voelckel, C., Krugel, T., Gase, K., Heidrich, N., van Dam, N.M., Winz, R. and Baldwin, I.T. (2001) Anti-sense expression of putrescine N-methyltransferase confirms defensive role of nicotine in *Nicotiana sylvestris* against *Manduca sexta*. *Chemoecology*, **11**, 121-126.

Waie, B. and Rajam, M.V. (2003) Effect of increased polyamine biosynthesis on stress responses in transgenic tobacco by introduction of human S-adenosylmethionine gene. *Plant Sci.*, **164**, 727-734.

Walters, D.R. (2003) Polyamines and plant disease. *Phytochemistry*, **64**, 97-107.

Woldemariam, M.G., Baldwin, I.T. and Galis, I. (2011) Transcriptional regulation of plant inducible defenses against herbivores: a mini-review. *J. Plant Interact.*, **6**, 113-119.

Zangerl, A.R., Hamilton, J.G., Miller, T.J., Crofts, A.R., Oxborough, K., Berenbaum, M.R. and de Lucia, E.H. (2002) Impact of folivory on photosynthesis is greater than the sum of its holes. *Proc. Natl. Acad. Sci. USA*, **99**, 1088-1091.

Zavala, J.A., Patankar, A.G., Gase, K. and Baldwin, I.T. (2004) Constitutive and inducible trypsin proteinase inhibitor production incurs large fitness costs in *Nicotiana attenuata*. *Proc. Natl. Acad. Sci. USA*, **101**, 1607-1612.

Figure Legends:

Figure 1: Overview of experimental strategy used to study growth-defense trade-offs in *Nicotiana attenuata* in a common nitrogen (N) currency.

a) The biosynthesis of nicotine, caffeoyl-putrescine (CP) and dicaffeoyl-spermidine (DCS) is induced after simulated herbivory in wild type (WT) by wounding (W) with a pattern wheel and application of oral secretions (OS) of *Manduca sexta*, but is impaired in the transgenic plants silenced in the expression of lipoxygenase 3 (LOX3) or MYB8 by RNAi with inverted-repeat (ir) constructs. The concentration of ribulose-1,5-bisphosphate carboxylase/oxygenase (RuBisCO) decreases in WT after W+OS, but the effects of jasmonic acid (JA) on N-investment into RuBisCO are unclear. Amino acids serve as precursors for putrescine and spermidine and for nicotinic acid (NA), which provide N for the synthesis of these metabolites. Amino acids are derived from nitrate (NO_3^-) reduction, followed by assimilation catalyzed by glutamine synthetase (GS) and glutamate synthase (GOGAT), and are also used as precursors for RuBisCO synthesis. JA-Ile=JA- isoleucine; NR=nitrate reductase; NiR=nitrite reductase.

b) ^{15}N-incorporation into roots, younger (yRL) and older rosette leaves (oRL) following pulse-labeling with $K^{15}NO_3$ 27 days after germination was determined by isotope-ratio mass spectrometry (IRMS) (n = 5). Grey arrows indicate elicitation time-frame. During this time-frame ^{15}N-incorporation was stable.

Figure 2: Total N content in WT shoots decreases after simulated herbivory.

N content of shoots of ir*LOX3*, ir*MYB8* and WT (n = 5) was determined by IRMS 4 days after the first W+OS elicitation. Three rosette leaves of transgenic lines (ir*LOX3*, ir*MYB8*) and WT plants were wounded with a pattern wheel and treated with 10µL 1:5 diluted *M. sexta* OS for 3 days in a row. Unelicited plants were taken as controls. Asterisks represent significant differences between treatments (*: $p \leq 0.05$; n = 5). Inset: The N content of WT roots was determined in a separate experiment at the same time-point. DM=dry mass

Figure 3: Silencing of *LOX3* and *MYB8* alters the N distribution between and within leaves.

The N pools and total soluble protein (TSP) of leaves (oRL, yRL, S1) of ir*LOX3*, ir*MYB8* and WT, calculated based on leaf mass. The N content was determined by IRMS and the TSP was measured by the Bradford assay. Plants were elicited as described for Figure 2. yRL and oRL were harvested 4 days after the first W+OS elicitation and when S1 leaves

underwent the source-sink transition. Asterisks indicate differences among treatments (*: $p \leq 0.05$; **: $p \leq 0.01$; ***: $p \leq 0.001$). Letters represent significant differences found using the minimum adequate model (n=5). FM=fresh mass. For other abbreviations see Figure 1.

Figure 4: Increased N-investment in nicotine, CP and DCS is accompanied by a decreased N-investment in protein.

a) N-investment in residual TSP (TSP - (SSU + LSU)), RubisCO large (LSU) and small (SSU) subunit, nicotine, CP and DCS in oRL, yRL and S1 was calculated by multiplying the proportion of N in each compound with the concentration of the compound for each leaf. The amount of TSP was quantified by the Bradford assay, RuBisCO LSU and SSU were determined by LC-MS^E and the defense metabolites by UPLC-UV-ToF-MS. Plants were elicited as described for Figure 2 and leaves were harvested as described for Figure 3 (n = 5). For abbreviations see Figure 1 and 3. Heatmaps represent pairwise correlation z-scores for N-investment in all of the above compounds among all genotype/elicitation groups.

b) ^{15}N-investment in RuBisCO LSU and SSU and defense metabolites was calculated as ^{15}N-incorporation multiplied by the N-investment. Plants were pulse-labeled with $K^{15}NO_3$ 3 days before the first treatment. ^{15}N-incorporation was determined based on the MS-spectra with ProSipQuant (Taubert *et al.* 2011).

Figure 5: Dynamics of ^{15}N-incorporation into nicotine, CP, DCS and LSU demonstrates that recently assimilated N, not N derived from LSU metabolism, is rapidly invested into CP and DCS biosynthesis after elicitation.

Three days before the first W+OS treatment plants were pulse labeled with $K^{15}NO_3$ (see Fig. 1a). The yRL at the time of labeling was harvested at indicated time points. ^{15}N-incorporation (n =5) of RuBisCO LSU, nicotine, CP and DCS was determined as described for Figure 4. For abbreviations see Figure 1, 3 and 4.

Figure 6: Herbivory-induced trade-offs of N-investment into growth and defense are mediated by MYB8.

N-investment in defense causes a reallocation of N from the shoot to the root. We suggest that the synthesis of phenolamides (CP, DCS) regulated by MYB8 is involved in the reallocation of N within the local leaf. N invested in phenolamides and in the root-synthesized alkaloid nicotine increases after herbivory, while the N-investment in TSP and RuBisCO

strongly decreases, but it is unlikely that N invested into phenolamides originates from RuBisCO metabolism. The relative changes in N-pool sizes without (C) and with W+OS elicitation (OS) are depicted by quadrangles; the height of the left and right side of the quadrangle represent relative changes in N-pool sizes of C and OS-elicited plants, respectively. All N-pools within the depicted leaf show the ratios of measured values per mg fresh mass. Shoot, root and whole-leaf N-pools depicted outside the plant represent ratios of N determined per mg dry mass. For abbreviations see Figure 1, 3 and 4.

Figures

Figure 1a:

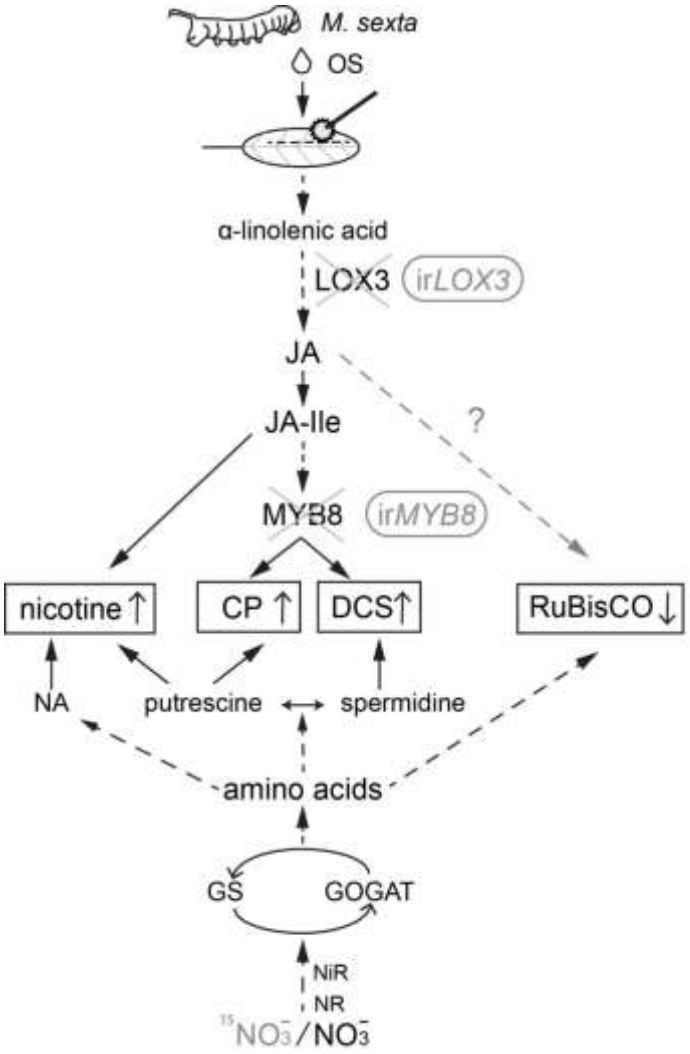

Figure1b:

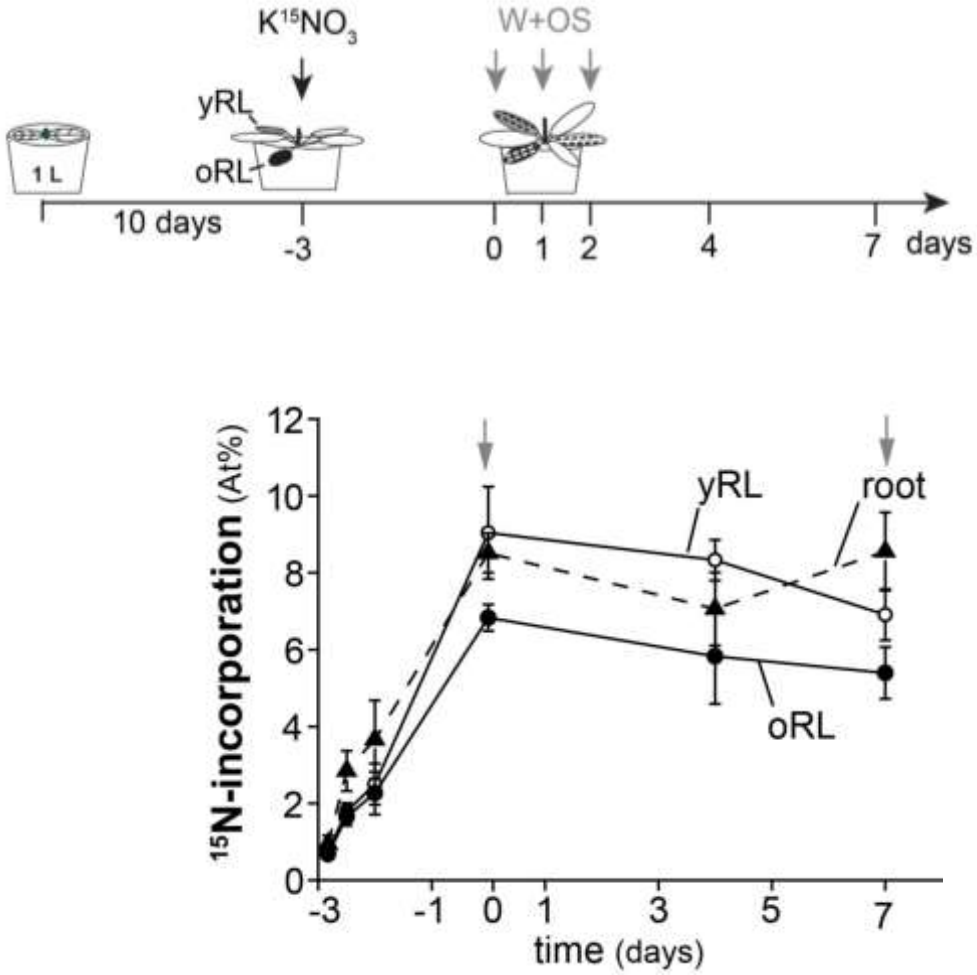
K15NO3
W+OS
yRL
oRL
1 L
10 days
-3
0 1 2
4
7 days
15N-incorporation (At%)
12
10
8
6
4
2
0
yRL
root
oRL
-3 -1 0 1 3 5 7
time (days)

Figure 2:

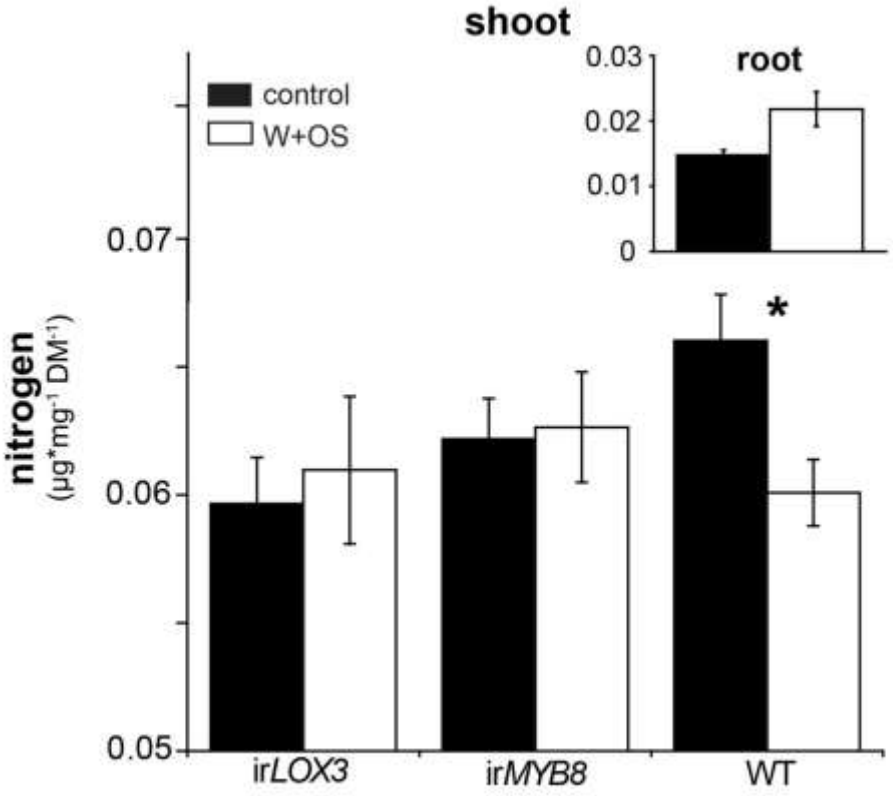
shoot
root
control
W+OS
nitrogen
(µg*mg-1 DM-1)
0.07
0.06
0.05
0.03
0.02
0.01
0
*
irLOX3
irMYB8
WT

Figure 3:

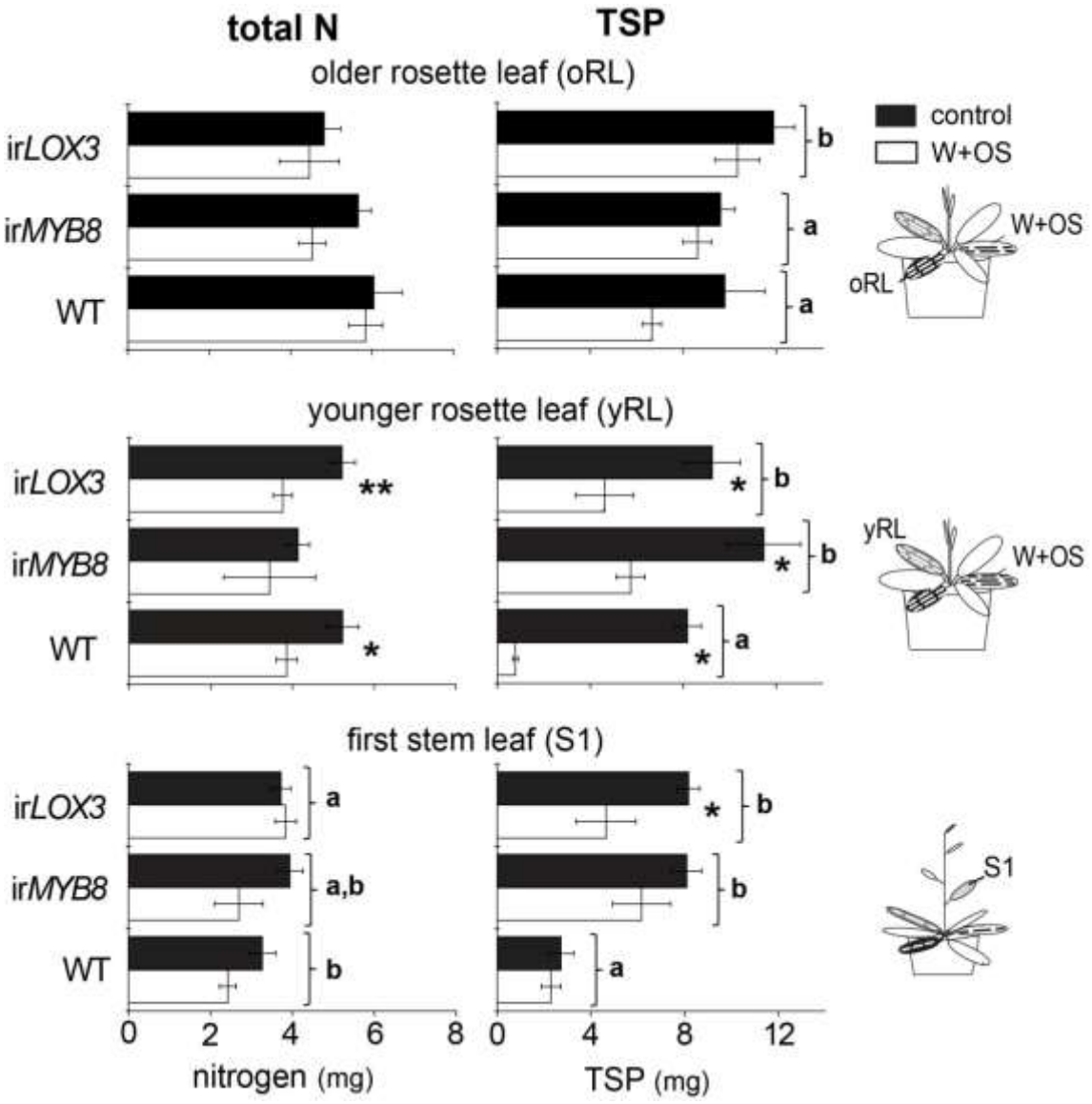
total N
TSP
older rosette leaf (oRL)
irLOX3
irMYB8
WT
b
a
a
control
W+OS
W+OS
oRL
younger rosette leaf (yRL)
irLOX3
irMYB8
WT
**
*
b
*
b
*
a
yRL
W+OS
first stem leaf (S1)
irLOX3
irMYB8
WT
a
a,b
b
*
b
b
a
S1
0 2 4 6 8
nitrogen (mg)
0 4 8 12
TSP (mg)

Figure 4a:

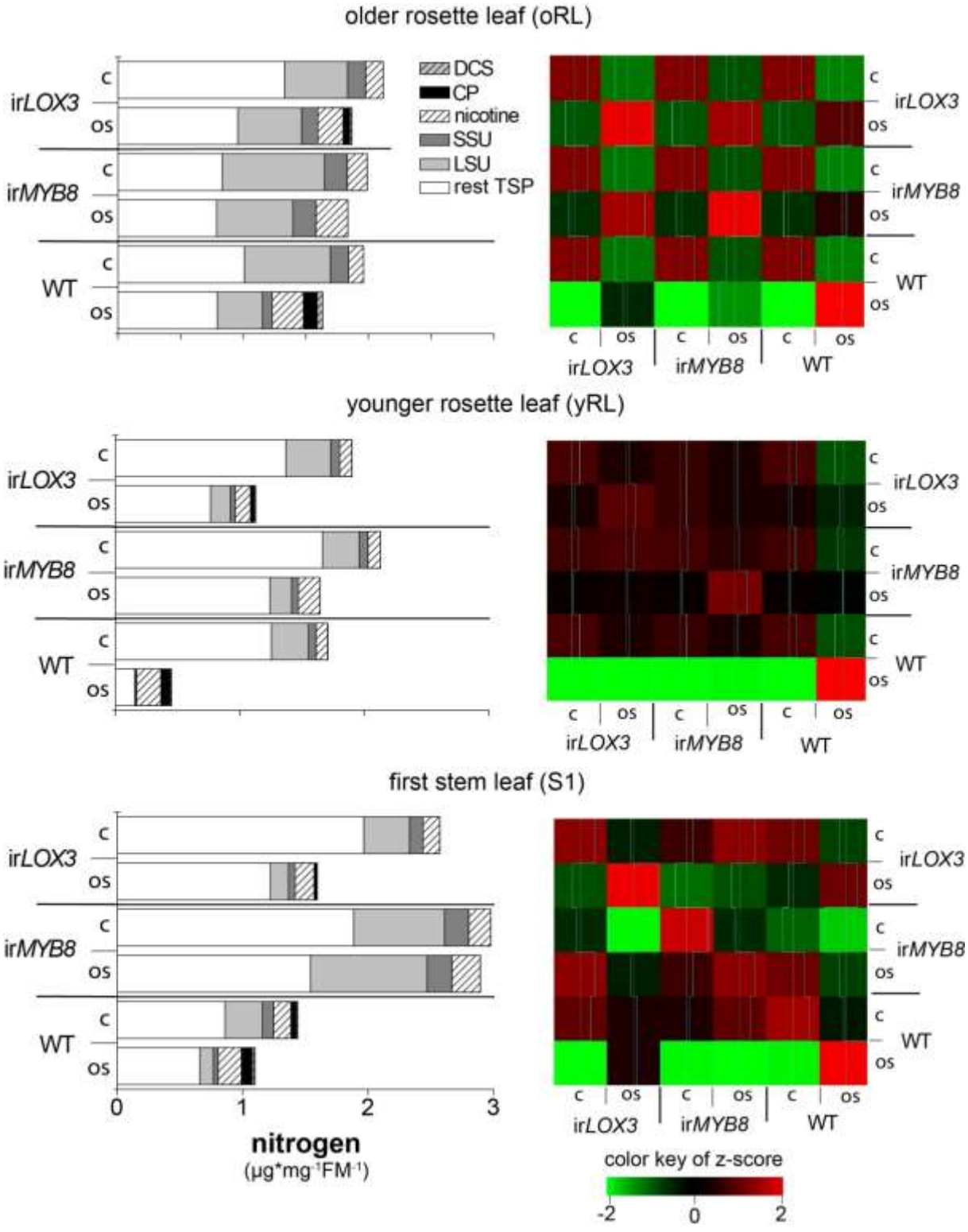
older rosette leaf (oRL)
younger rosette leaf (yRL)
first stem leaf (S1)
irLOX3
irMYB8
WT
c
os
DCS
CP
nicotine
SSU
LSU
rest TSP
0
1
2
3
nitrogen
(µg*mg-1FM-1)
color key of z-score
-2
0
2

Figure 4b:

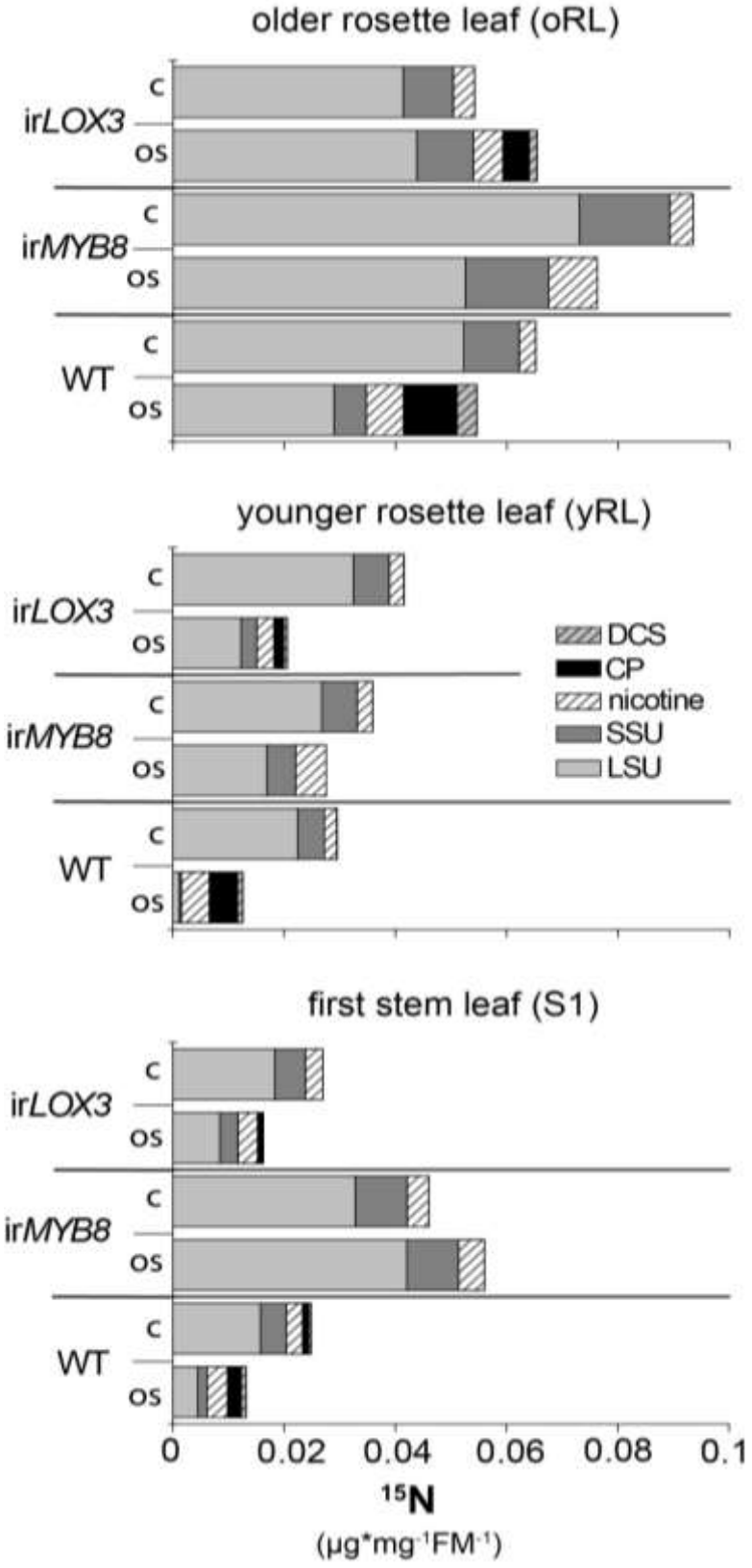
older rosette leaf (oRL)
irLOX3
irMYB8
WT
c
os
younger rosette leaf (yRL)
DCS
CP
nicotine
SSU
LSU
first stem leaf (S1)
0
0.02
0.04
0.06
0.08
0.1
15N
(µg*mg-1FM-1)

Figure 5:

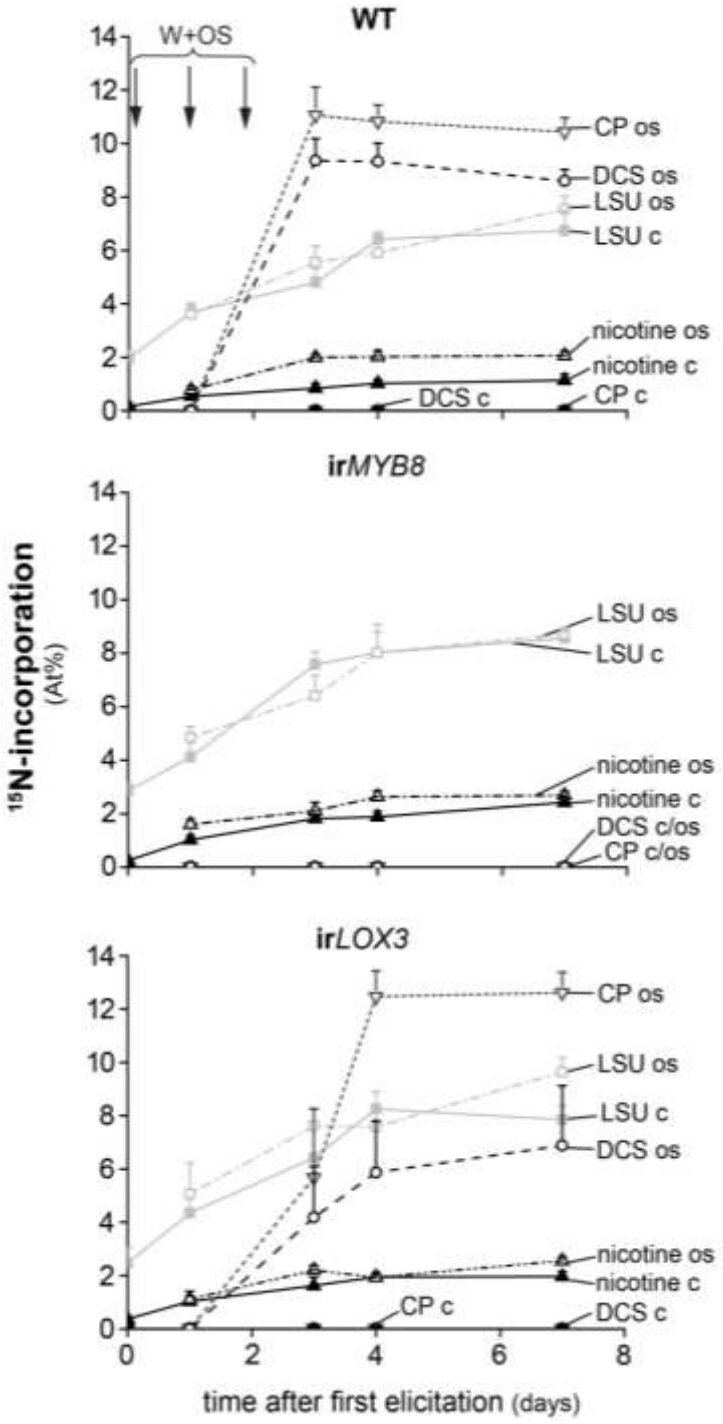
WT
W+OS
CP os
DCS os
LSU os
LSU c
nicotine os
nicotine c
DCS c
CP c
irMYB8
LSU os
LSU c
nicotine os
nicotine c
DCS c/os
CP c/os
irLOX3
CP os
LSU os
LSU c
DCS os
nicotine os
nicotine c
CP c
DCS c
15N-incorporation (At%)
time after first elicitation (days)

Figure 6:

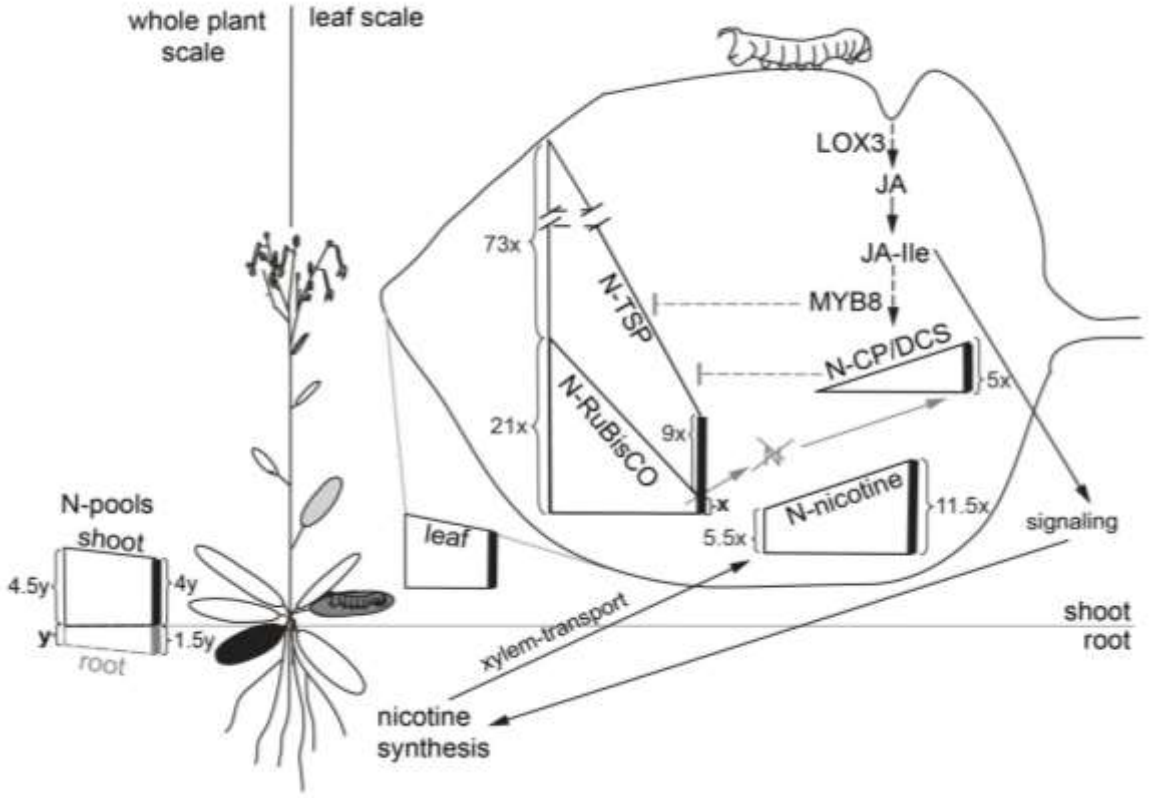
whole plant scale
leaf scale
LOX3
JA
JA-Ile
MYB8
N-TSP
73x
N-CP/DCS
5x
N-RuBisCO
21x
9x
x
N-nicotine
11.5x
5.5x
signaling
leaf
N-pools
shoot
4.5y
4y
y
1.5y
root
xylem-transport
shoot
root
nicotine
synthesis

Supplemental Figures:

Figure S1:

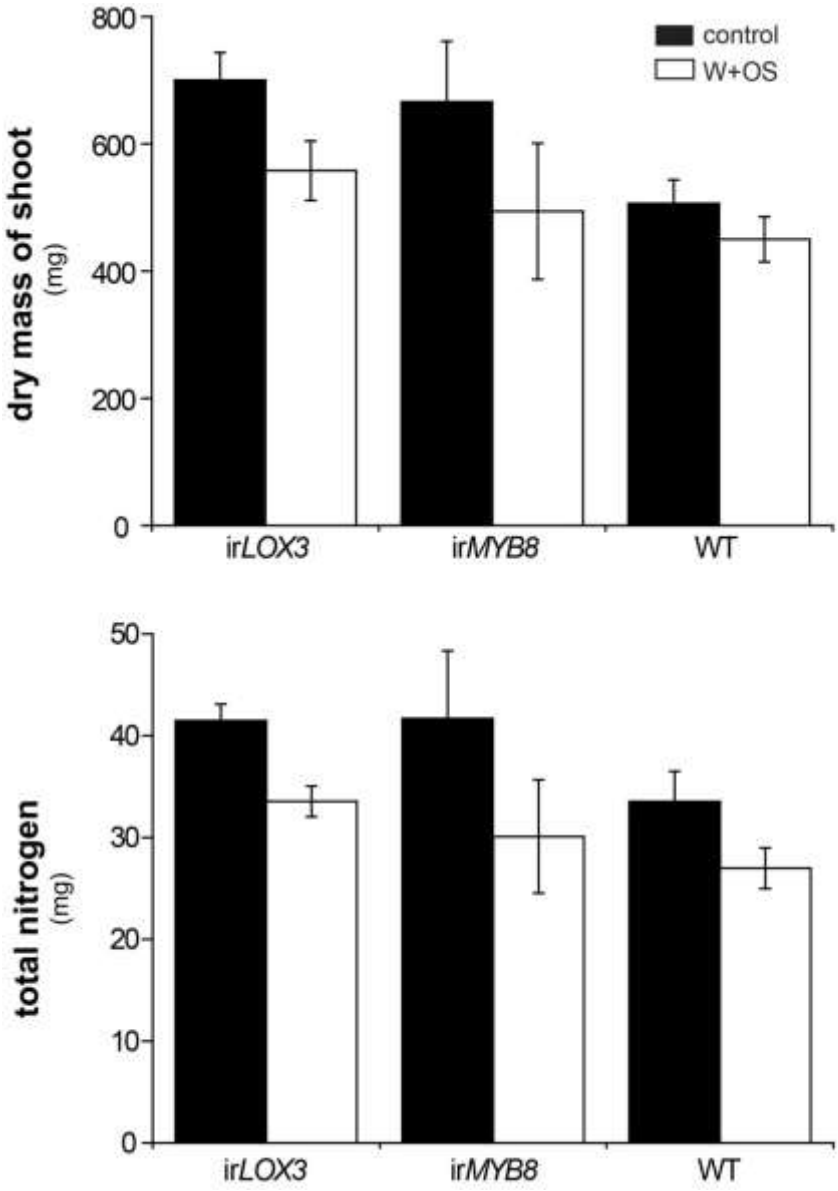

Figure S1: The dry mass and the absolute amount of nitrogen (N) of the shoot do not depend on genotype.

The total N content of the shoot was calculated by multiplying the N content with shoot dry mass.

Figure S2a:

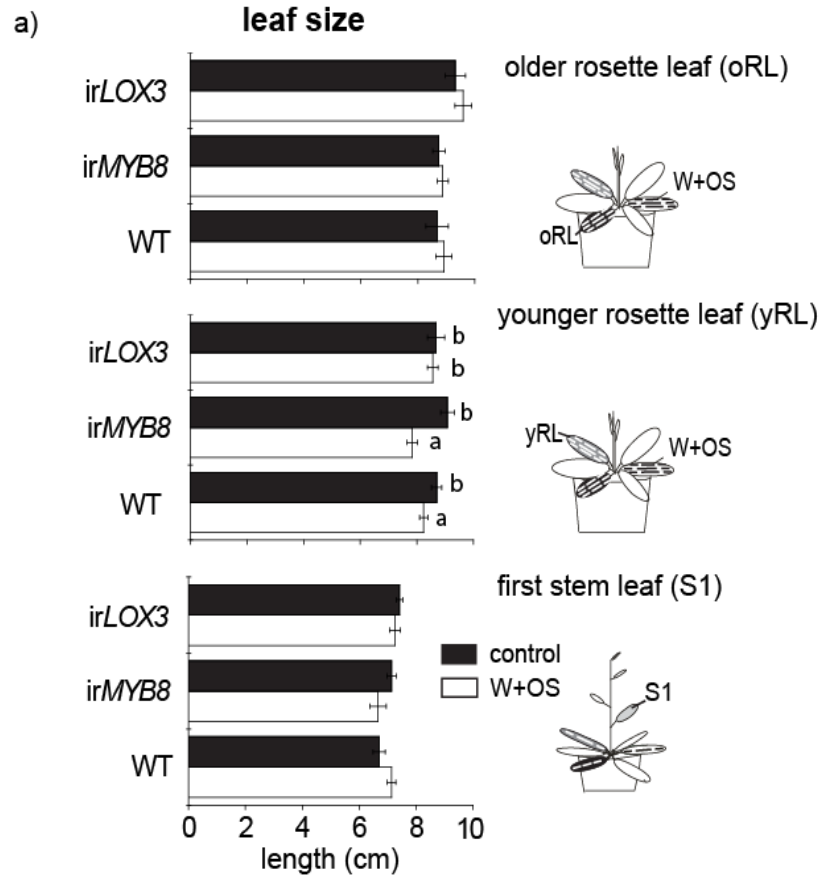

Figure S2b)

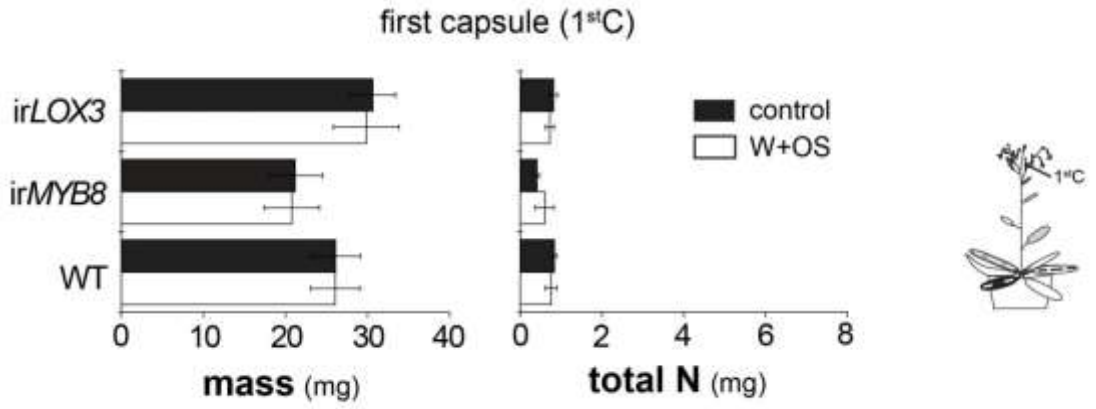

Figure S2: Average leaf size and mass and total N of pooled seeds from the first seed capsule in transgenic (ir*LOX3*, ir*MYB8*) and WT plants with and without W+OS treatment.

Absolute N content of capsules was calculated by multiplying the N concentration by the mass of the pooled seeds of the first capsule.

Figure S3a:

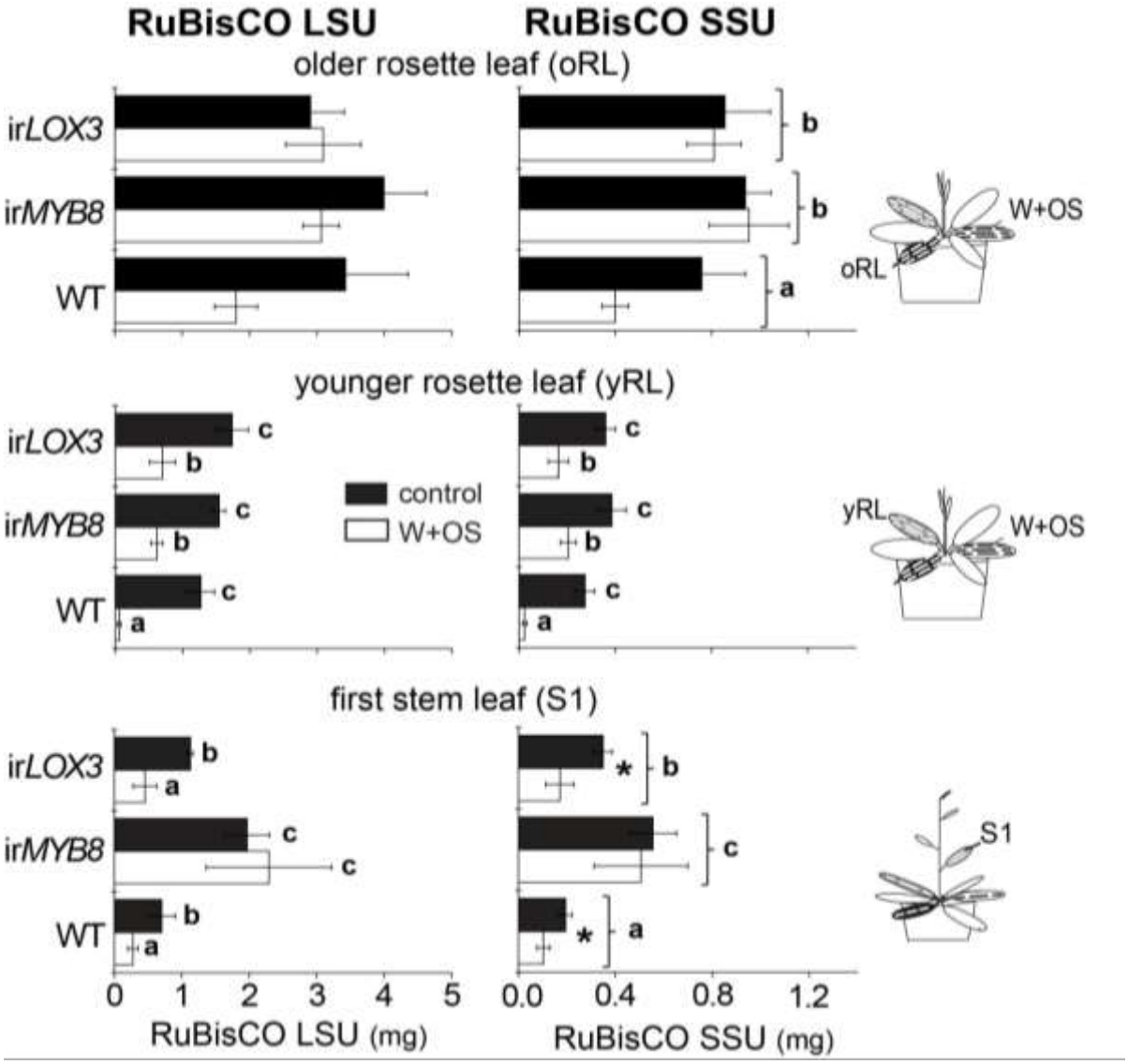
RuBisCO LSU
RuBisCO SSU
older rosette leaf (oRL)
irLOX3
irMYB8
WT
b
b
a
W+OS
oRL
younger rosette leaf (yRL)
c
b
a
control
W+OS
yRL
W+OS
first stem leaf (S1)
*
S1
0 1 2 3 4 5
RuBisCO LSU (mg)
0.0 0.4 0.8 1.2
RuBisCO SSU (mg)

Figure S3b:

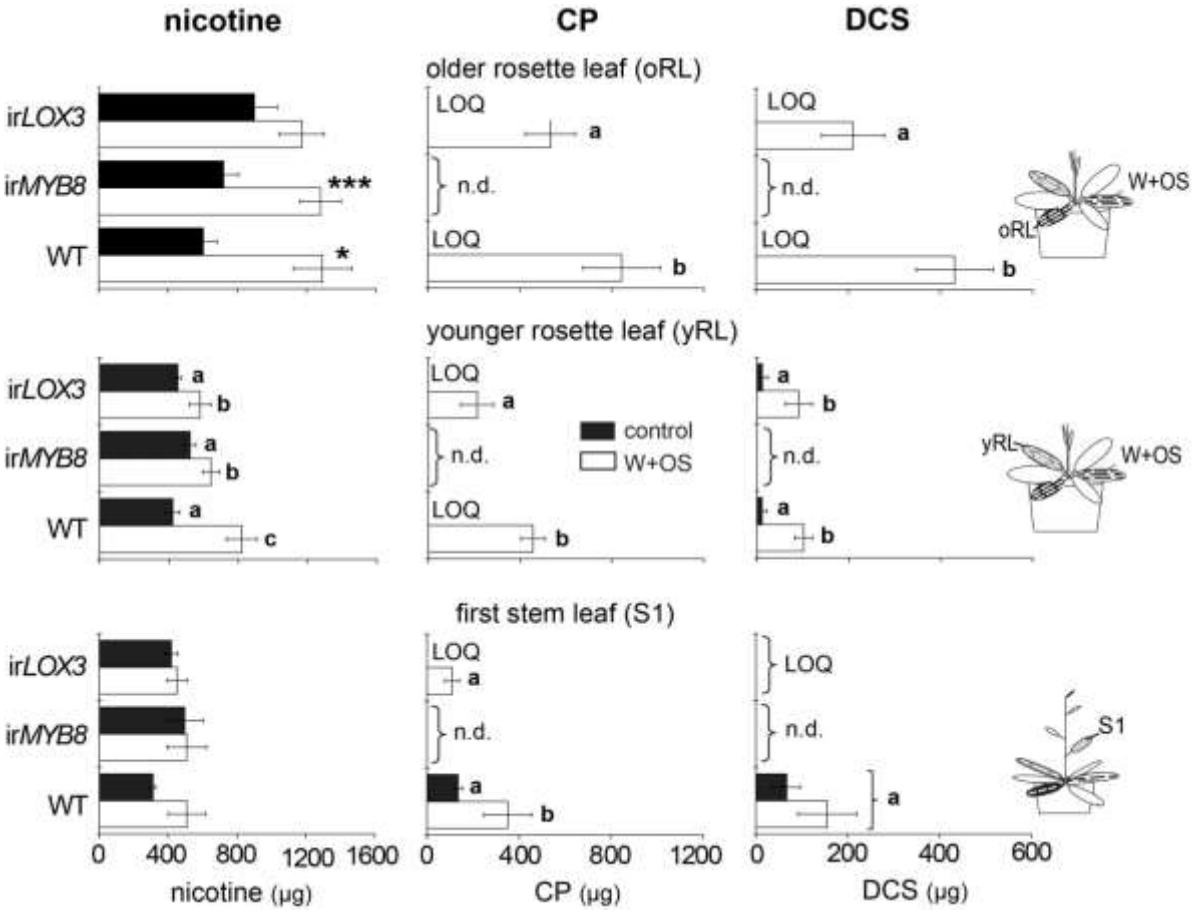

Figure S3: Silencing of *LOX3* and *MYB8* alters the absolute pools of N-containing small metabolites and RuBisCO within leaves.

The absolute pool sizes were calculated by multiplying the concentration of the compounds with the leaf mass. Asterisks indicate differences between treatments, letters significant differences in the minimum adequate model. LOQ=below limit of quantification; n.d.=not detectable.

Figure S4:

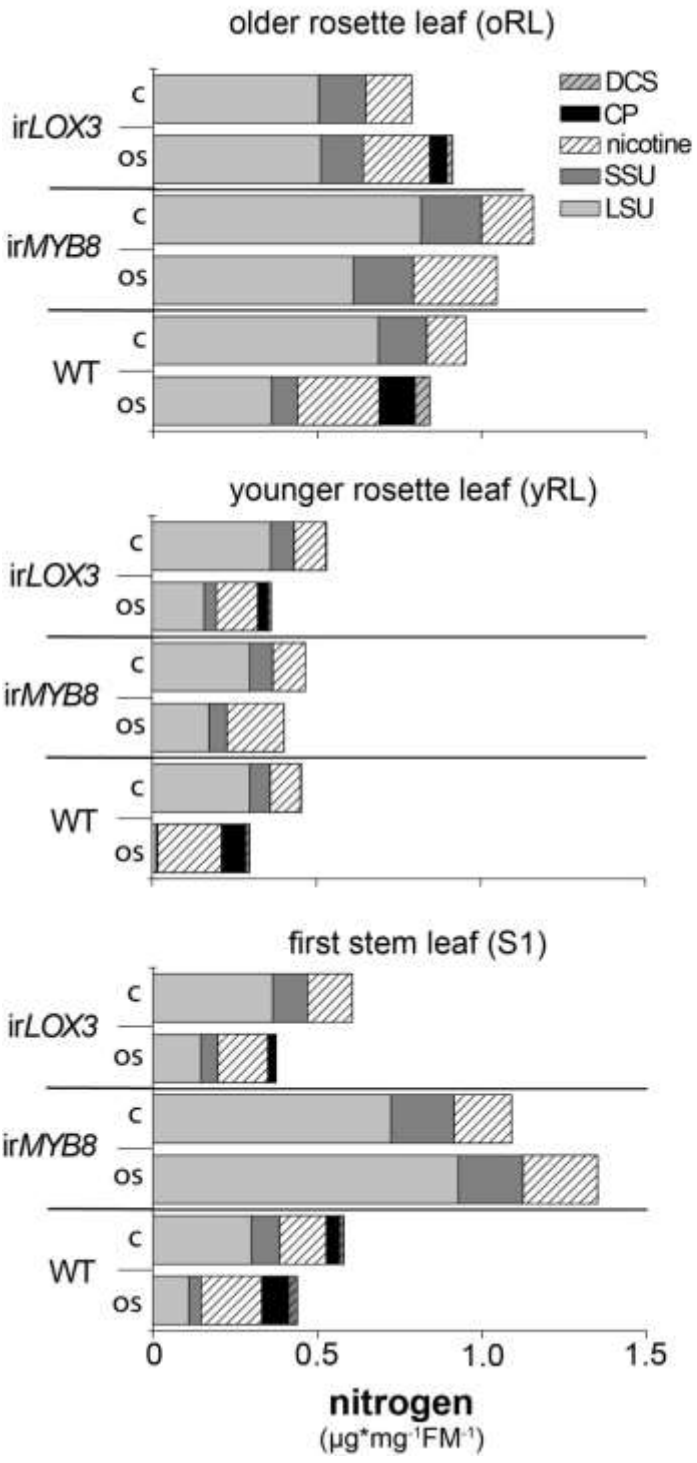

Figure S4: Increased N investment into nicotine, CP and DCS is accompanied by a decreased N investment into RuBisCO.

Same data as for Figure 4a without TSP.

Figure S5:

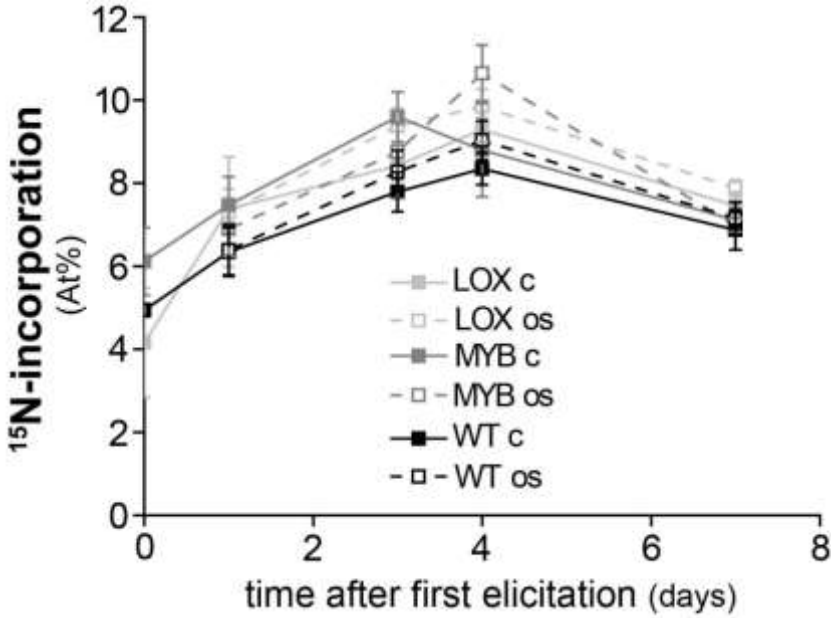

Figure S5: ^{15}N-incorporation in the yRL does not depend on treatment or genotype

Figure S6:

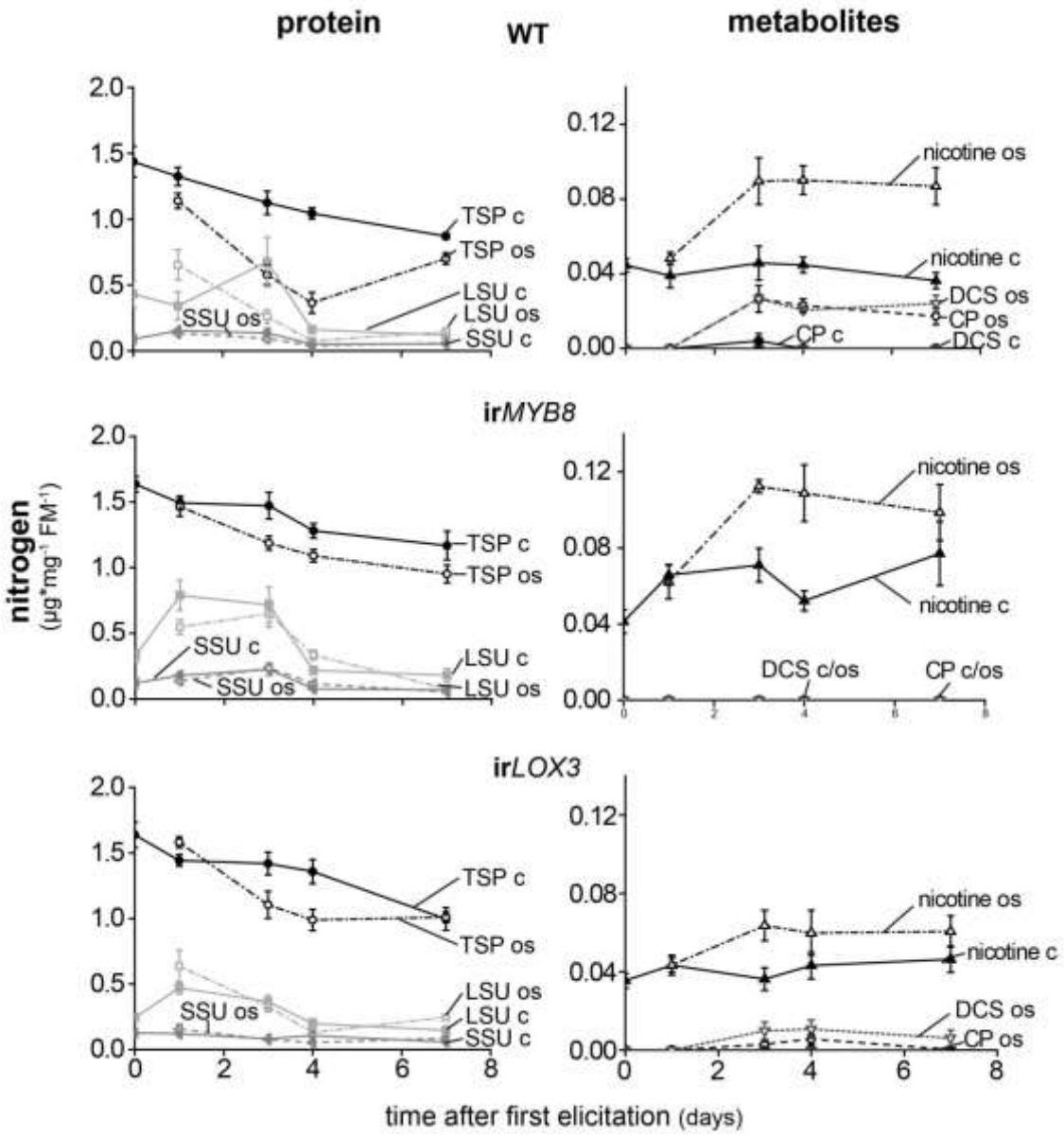

Figure S6: The decrease of N investment into protein pools is greater than N needed for biosynthesis of defense metabolites

N-investments were calculated by multiplying the proportion of N present in each compound with the concentration of the compound.

Supplemental Statistical Information on Supplemental Figures

Figure S1: ANOVA, a) Treatment, $F_{1,28} = 4.68$, $p = 0.039$; b) Treatment, $F_{1,28} = 7.28$, $p = 0.011$.

Figure S2: a) ANOVA, oRL: non-significant (n.s.); yRL: $F_{1,28} = 14.60$, $p = 6.762*10^{-4}$; S1: n.s.), b) ANOVA, mass: n.s.; total N: n.s.

Figure S3: ANOVA, a) RuBisCO LSU: oRL: n.s.; yRL: $F_{2,27} = 78.25$, $p = 5.81*10^{-12}$; S1: $F_{2,26} = 30.084$, $p = 1.719*10^{-7}$; RuBisCO SSU: oRL: Line: $F_{1,28} = 7.91$, $p = 0.009$; yRL: $F_{2,27} = 44.65$, $p = 2.74*10^{-9}$; S1: Line: $F_{2,26} = 13.76$, $p = 8.37*10^{-5}$; Two sample T-test: ir*LOX3*: $p = 0.035$, WT: $p = 0.040$;b) nicotine: oRL: Treatment: $F_{1,28} = 27.77$, $p = 1.32*10^{-5}$; Two sample T-test: irLOX3: $p = 0.053$; ir*MYB8*: $p = 0.009$; WT: $p = 0.020$; yRL: $F_{2,27} = 14.69$, $p = 4.82*10^{-5}$; S1: n.s.; CP: oRL: $F_{2,27} = 44.537$, $p = 2.81*10^{-9}$; yRL: $F_{1,28} = 77.69$, $p = 6.31*10^{-12}$; S1: $F_{2,25} = 31.89$, $p = 1.32*10^{-7}$; DCS: oRL: $F_{2,27} = 36.09$, $p = 2.35*10^{-8}$; yRL: $F_{2,27} = 24.64$, $p = 8.15*10^{-7}$; S1: Line: $F_{2,25} = 11.66$, $p = 2.65*10^{-4}$.
Significance level indicated by asterisks: *: $p \leq 0.05$; **: $p \leq 0.01$; ***: $p \leq 0.001$, n=5.

Figure S5: n = 121; ANOVA, Line:Treatment:Time: $F_{2,109} = 0.201$, $p = 0.98$

Supplemental Procedures

Detection and Quantification of small N-containing metabolites

Eluted compounds were detected using a Diode Array Detector and subsequently by MicroToF Mass Spectrometer (BrukerDaltonik, Bremen, Germany), with the conditions described in Gaquerel *et al.*(2010).

Quantification was based on the UV trace at the wavelengths 254 nm (nicotine) and 320 nm (CP and DCS) using an external standard curve (20, 40, 80, 160, 320, 480 and 640 ng on column for nicotine and 10, 20, 40, 80 and 160 ng on column for CP and DCS). Extracted ion chromatograms for each compound were generated from raw data using Data Analysis software (BrukerDaltonik, Bremen, Germany).

4. General Discussion

Induced defense has been postulated to have evolved as a cost-saving strategy (Simms and Fritz, 1990), but as outlined in the introduction this defense is still costly for the plant. The associated defense costs are defined as a fitness disadvantage, and are assumed to arise as a consequence of resource allocation. While JA caused defense costs are well studied, knowledge about early signaling in arbitrating costs has been lacking. In this thesis, the role of MAPK signaling in mediating fitness consequences of defense has been demonstrated for the first time. The data clearly reveal that MAPKs are involved in the regulation of JA-induced defense trade-offs. In addition, these enzymes are shown to incur costs for inducibility in non-elicited plants. Furthermore, I demonstrated that SA partially masks benefits caused by lower JA-levels **(Manuscript I)**.

In order to study the role of resource allocation in mediating growth-defense trade-offs, a new method for simultaneous protein quantification and determination of ^{15}N-incorporation has been developed **(Manuscript II).** The new method enabled the direct comparison between the N quantity demanded by defense and the loss of N available for growth. The data revealed that the increase of N in phenolamides and nicotine is smaller than the amount of N no longer present in RuBisCO, which was defined as proxy for growth. Furthermore, the respective level of labeling demonstrates that N for phenolamide biosynthesis is not coming from RuBisCO. The use of transgenic plants impaired in N-intensive metabolite biosynthesis revealed, that N-intensive metabolite biosynthesis indirectly regulates the resource allocation to growth, and proteins respectively (RuBisCO) **(Manuscript III).**

Inducible and constitutive costs of early herbivore defense signaling

In Manuscript I, I analyzed the costs of early herbivore defense signaling by growing plants silenced in the MAPKs SIPK and WIPK which are induced shortly after herbivore attack (Wu, 2007) in competition with WT plants. Both kinases regulate herbivory-induced JA-levels and JA-mediated defense metabolite accumulation. Since JA decreases the plants' growth and fitness (Agrawal et al., 2006; Cipollini, 2002; Redman et al., 2001), *SIPK* and *WIPK* silenced plants were expected to grow better than WT, as has been shown for plants with reduced JA-levels (Meldau, personal communication). In the experiments, *WIPK* silenced plants had a similar growth and fitness benefit as *LOX3* silenced plants and expressed

a similar reduction in JA levels, leading to the conclusion that costs of WIPK signaling are mediated by JA.

As demonstrated in earlier studies *LOX3* and *WIPK* silenced plants have reduced JA-mediated defense metabolite accumulation (Halitschke and Baldwin, 2003; Meldau et al., 2009), so that these plants invest less resources into defense than WT. These resources are likely to be allocated to growth and reproduction, resulting in better growth and fitness. Furthermore, JA has been shown to downregulate photosynthesis related genes (Halitschke et al., 2003) and limit the competitive ability for N (Van Dam and Baldwin, 2001), which are important factors for growth. Thus, the lower JA levels of the transgenic plants might have caused alterations of these two plant traits, leading to the plants' better growth and fitness. But the data of Manuscript I did not show any correlation between photosynthesis or the competitive ability for N with JA-levels (Manuscript I). This suggests, that the growth and fitness benefit of both transgenic plants caused by their lower JA levels are independent of these two plant traits, and that other factors have to be involved.

Surprisingly, *WIPK* and *LOX3* silenced plants not only showed benefits after induction, but also resulted in fitness improvements under non-elicited conditions. The constitutive fitness improvement indicates that the plants pay a high cost for having inducible defense ability. One explanation might be constitutive reduced nicotine levels which is permanently synthesized in *Nicotiana* species (Baldwin, 1999) and/or alterations of basal TPI levels, which have been shown to reduce the plant's fitness without induction (Zavala et al., 2004). Since *LOX3* silenced plants have lower basal TPI levels than WT (Allmann et al., 2010), this can explain the observed constitutive fitness benefit of non-elicited plants. In contrast, *WIPK* silenced plants only had lower nicotine and TPI levels than WT after induction (Meldau et al., 2009), leading to the conclusion that in these plants other factors are responsible for the constitutive fitness benefit.

Changes in resource allocation might be such a factor because growth and fitness performance are a result of resource allocation processes (Baldwin, 2001). In the experiments described in Manuscript I both transgenic plants had a 4-12x times higher N-content in rosette leaves before elicitation. These results lead to the hypothesis that an altered N metabolism or N allocation of *LOX3* and *WIPK* silenced plants, which is independent of herbivory, supports their constitutive fitness and growth benefit. Although the N allocation in *WIPK* silenced plants has not been studied in detail yet, changes in N allocation in these plants are likely. A microarray analysis revealed that *WIPK* downregulates enzymes important for amino acid

biosynthesis (Meldau, unpublished data), indicating that silencing of *WIPK* likely results in increased amino acid levels, and thus in changes of N allocation.

Nevertheless, in the experiments of Manuscript I the ^{15}N-incorporation into leaves and seeds was unaltered in *LOX3* and *WIPK* silenced plants independent of treatment. Since the ^{15}N-pulse was given during later rosette growth, the time period for ^{15}N accumulation in the rosette leaves might have been too short to show the same patterns as of total N. Furthermore, changes in N allocation of these transgenic plants might be more pronounced between different N-pools than in the absolute N values of leaves and seeds under these growth conditions. Thus, a ^{15}N-pulse labeling experiment with a parallel analysis of different N-pools important for growth, defense and reproduction could give better insights into the role of WIPK and LOX3 in N allocation under competitive growth. In such an experiment, *WIPK* silenced plants will likely have higher protein levels than WT generated by increased amino acid biosynthesis and possibly resulting in higher N contents of leaves.

Contrary to the data of Manuscript I, in the experiments of Manuscript III *LOX3* silenced plants did not have a growth or fitness benefit and did not show higher N values in leaves of non-elicited plants. These contrary results were likely due to different growth conditions (Manuscript I: competition; Manuscript III: single pots), because *N. attenuata* shows fitness differences only when grown under competition (Baldwin et al., 1998; Van Dam and Baldwin, 2001) and N allocation within the plant is influenced by competition and resource availability (Lynds and Baldwin, 1998; Van Dam and Baldwin, 2001) . Furthermore, earlier studies demonstrated that competition for limited resources results in fitness differences being more pronounced (Baldwin and Hamilton, 2000; Van Dam and Baldwin, 2001; Zavala et al., 2004). Overall this suggests that plants only benefit from *LOX3* silencing under competitive growth conditions.

In contrast to *WIPK*-silenced plants, silencing *SIPK* resulted in a constitutive growth and fitness deficit, indicating that *SIPK* silenced plants did not benefit from their lower JA-levels as assumed. The data of Manuscript I suggests that in *SIPK* silenced plants the benefits of lower JA-levels are partially masked by higher SA levels, but this masking is not a result of a SA impact on resource availability, e.g. photosynthesis or N assimilation (Manuscript I). Since fitness optimization is a process of resource allocation (Baldwin, 2001), SA might overrule the benefits of reduced JA-levels through influencing a plants' resource partitioning. For example, the higher SA levels might enhance the N allocation from the shoot to root even in non-elicited plants, leading to a constitutive growth and fitness deficit after *SIPK* silencing.

In Manuscript III, a transport of N from the shoot to the root in response to herbivory is indicated for WT plants. Similar experiments as already described for *WIPK* silenced plants would have to be carried out to explore if 1. N allocation is responsible for the SA mediated fitness deficit of SIPK silenced plants and 2. to investigate if SIPK in general regulates N allocation with and without herbivory. In such experiments, the use of crosses between *SIPK* silenced plants and *NahG* overexpressing plants which have comparable SA levels to WT and homozygous *NahG* overexpressing plants which have lower SA levels than WT, would help to untangle the role of SA in N allocation.

An additional explanation for the role of SA in masking JA-mediated growth trade-offs in *SIPK* silenced plants might be the interaction with other phytohormones. For example, in Arabidopsis an ET mediated cross talk of SA and JA was recently described (Leon-Reyes et al., 2009). Since SIPK activates ET biosynthesis (Wu, 2007), SIPK silenced plants likely have lower ET values, so that an ET mediated cross-talk in this context is unlikely. Nevertheless, SA can regulate plant development over other hormonal pathways. For example, a positive cross-talk between SA and cytokinins has been demonstrated in pathogen resistance (Choi et al., 2011; Naseem et al., 2012). As both phytohormones also influence growth, a cross-talk in this context might be possible. Different to SA, cytokinins have been shown to increase growth by increasing cell numbers (Xia et al., 2009) and to regulate nutrient homeostasis of N, phosphorus and sulfur (Rubio et al., 2009). Therefore, a downregulation of cytokinin levels by SA might explain the lack of a SIPK growth impact. Furthermore, SA causes a repression of auxin responsive genes in Arabidopsis by stabilizing Aux/IAA repressor proteins, resulting in an inhibition of auxin responses (Wang et al., 2007). As auxin is a growth promoting phytohormone (Leopold, 1955), a similar mechanism in *N. attenuata*, might account for the growth deficit of *SIPK* silenced plants. In soybean a decreased expression of genes involved in the auxin signaling pathway already have been demonstrated to reduce growth (Liu et al., 2011). A detailed phytohormone profiling of *SIPK* silenced plants and their crosses which have similar SA levels as WT may reveal such phytohormonal mechanisms. The application of SA to crosses of *SIPK* silenced plants and *NahG* overexpressing plants, which have similar SA levels than WT, combined with measurements of different phytohormones would allow testing the hypothesis; if SA in *SIPK* silenced plants influences other phytohormone levels, such as cytokinins or auxin. A parallel gene expression analysis of genes may help to elucidate if and how SA directly influences phytohormone biosynthesis (levels) or phytohormone signaling pathways.

Phenolamide biosynthesis mediates growth-defense trade-offs in a common N currency

Previous studies have analyzed the costs induced by JA signaling on a plant's growth and defense, but the study of the influence of individual plant traits has had little attention. Since phenolamides have a high impact on the plant defense against herbivores (Kaur et al., 2010), I hypothesized that the biosynthesis of these N-intensive metabolites causes changes in the N allocation. Through the use of different transgenic lines, one impaired in JA signaling (ir*LOX3*) and one in phenolamide biosynthesis (ir*MYB8*), the differentiation of trade-offs mediated by JA or by a single plant trait, e.g. production of N-intensive metabolites, was possible. The data demonstrate herbivore-induced changes in N allocation throughout the plant and within leaves influenced by phenolamide biosynthesis.

Analysis of the N content of the whole shoot and WT roots indicated a N transport from the shoot to the root for WT, but not for the transgenic lines. Hanik et al. (Hanik et al., 2010) hypothesized that a N allocation from the shoot to the root is driven by nicotine biosynthesis in the roots. My data does not support this hypothesis because the nicotine levels in the transgenic lines were not lower than in WT (Manuscript III) and they do not show signs of N transport to the root. Previously, for tomato a methyljasmonate (MeJA) induced N allocation to roots was described (Gomez et al., 2010). Since *LOX3* silenced plants have lower JA levels (Allmann et al., 2010), but *MYB8* silenced plants do not, in *N. attenuata* JA is unlikely a direct trigger of the N-transport. However, the phenolamide levels are reduced in both transgenic lines, which leads to the conclusion that phenolamide biosynthesis supports the allocation of N from shoots to roots. As the phenolamide biosynthesis is regulated by JA over the transcription factor MYB8, JA might indirectly influence the N transport over phenolamide biosynthesis. Nevertheless, the analysis of the transgenic lines' roots still needs to be carried out.

Phenolamide biosynthesis could alter the transport of amino acids or nitrate resulting in the observed N distribution or influence N assimilation. In tomato a N allocation in the form of amino acids to the roots after induction has recently been described (Gomez et al., 2010). In contrast, a transport of nitrate is unlikely because there is only restricted loading of nitrate into the phloem (Schobert and Komor, 1992), and if nitrate is transported into the phloem, it is transported from older to younger leaves (Fan et al., 2009). Furthermore a higher N assimilation in response to elicitation is unlikely, since previous studies have shown neither changes in N assimilation after herbivory (Baldwin and Ohnmeiss, 1994; Lynds and Baldwin, 1998), nor an increase in nitrate reductase activity in roots (Baldwin et al., 1993). Thus, on the

whole plant perspective phenolamide biosynthesis most likely influences amino acid transport resulting in higher N contents of roots.

In the leaves, the data (Manuscript III) showed a different N partitioning between N pools in the lines and WT. While plants silenced in *MYB8* accumulated no phenolamides as expected, and invested similar amounts of N into protein (TSP and RuBisCO) before and after treatment, WT plants had the highest phenolamide levels and showed the highest reduction of protein levels after elicitation. *LOX3* silenced plants had an intermediate phenotype. The dependency of phenolamide levels and protein levels found in the data supports the conclusion that phenolamides act as the mediator. As phenolamides are scavengers of toxic radicals, they have already been proposed to be components of defense systems against different stresses (Edreva et al., 1995). In transgenic tobacco plants increased spermidine and putrescine concentrations and their conjugates have been demonstrated to increase tolerance to salinity, drought as well as to fungal infection (Waie and Rajam, 2003). Thus, they potentially also increase the tolerance to herbivores by regulating resource allocation within the herbivore defense. If an application of phenolamides to control and elicited leaves of *MYB8* silenced plants would recover the phenotype of WT, e.g. decreased N-investment into proteins, the conclusion would be supported.

Since *MYB8* expression levels and phenolamides accumulation followed a similar pattern, MYB8 likely influences the N allocation based growth-defense trade-offs within the leaves to proteins. This transcription factor was proposed to play a regulatory role in later herbivore defense responses (Galis et al., 2010) because *MYB8* is also induced 1-2 days after elicitation (Kaur et al., 2010). In *Pinus sylvestris,* a R2R3-MYB transcription factor was suggested to regulate N-recycling after lignin biosynthesis (Gomez-Maldonado et al., 2004) because of its interaction with the glutamine synthetase promoter. Similar to proteins, phenolamide biosynthesis requires amino acids synthesized from glutamine, such as arginine and ornithine (Kaur et al., 2010; Takano et al., 2012; Vogt, 2010). Thus, I hypothesize that MYB8 might affect N investment into proteins by influencing amino acid biosynthesis, possibly by encouraging glutamine channeling into phenolamides through the preferential synthesis of arginine. Amino acid profiling of the samples used in Mansucript III could not reveal differences in glutamine, arginine or any other proteinogenic amino acid concentration between WT and *MYB8* silenced plants before and after herbivory (Ullmann-Zeunert, unpublished data). While changes in arginine levels after herbivory have not been reported yet, an increase of glutamine concentration in the stem of tomato plants was described

(Steinbrenner et al., 2011) and phenyalanine and tyrosine increased transiently in the wild tobacco after herbivory (Kim et al., 2011a). These changes of amino acid concentration appeared shortly after herbivore attack, and showed partly a dependency on the diurnal rhythm (Hanik et al., 2010; Kim et al., 2011a; Steinbrenner et al., 2011). Therefore, in my study the sampling interval might have been too long and/or sampling too late after elicitation to be able to detect differences in amino acid pools in WT and the transgenic plants. An additional experiment including earlier sampling time points shortly after herbivore attack and sampling at different times of the day, may reveal changes in amino acids abundances. Furthermore, a following activity analysis of genes involved in the amino acid biosynthesis pathways would shed light on the/help to find genes regulated by MYB8.

However, the data of this thesis do not answer the question, if N allocation to proteins is regulated by MYB8 or directly by phenolamides. Beside several genes with a potential role in phenolamide biosynthesis, MYB8 activates genes encoding enzymes of the phenolpropanoid metabolism and enzymes involved in the biosynthesis of polyamines shortly after herbivore attack (Kaur et al., 2010). MYB8 influences the abundance of at least 29 further coumaric acid-, caffeic acid- and ferulic acid-containing metabolites 1 day after herbivory (Onkokesung et al., 2012), demonstrating that this transcription factor is involved in different processes that could influence the N allocation patterns shown in my work. The activity and partly the abundance of phenylalanine ammonia-lyase, whose coding gene is regulated by MYB8 (Kaur et al., 2010), has for example been demonstrated to regulate the resource flux into multiple pathways and is involved in developmental processes that require N and thus influences N flux within leaves and the plant (Jones, 1984). In that manner also other enzymes of the phenolpropanoid and phenolamide biosynthesis might influence N allocation. Furthermore, polyamines and their conjugates can interact with DNA, so that small amounts of other MYB8 influenced metabolites could regulate the N allocation pattern via DNA interactions (Blagbrough et al., 2003). In order to study the role of other metabolites or regulatory elements of phenolamide biosynthesis in N distribution within leaves, transgenic lines impaired at different positions of the pathway downstream of MYB8 would be required.

Beside phenolamides and nicotine, the wild tobacco has other N-intensive defenses, such as TPIs, that might influence the N distribution. In *N. attenuata*, transgenic lines impaired in TPI biosynthesis are proposed to have an altered N partitioning to fitness (Zavala et al., 2004), but knowledge about their influence on N partitioning within and to other plant parts is lacking.

RuBisCO degradation, is not a precursor pool for defense metabolite biosynthesis

In this thesis, the dynamics of RuBisCO after herbivory has been demonstrated in detail for the first time. The N-investment data of Manuscript III demonstrated a decrease in RuBisCO levels after herbivory, but does not allow for a differentiation between increased degradation or a reduction in synthesis as a result of elicitation, which are both likely taking place. Since the N freed up by RuBisCO degradation is greater than the amount of the N-invested into defense metabolites after elicitation, the data allows for the hypothesis that RuBisCO N is used for phenolamide biosynthesis. In order to test, the hypothesis, a ^{15}N-labeling kinetic experiment was carried out, and the ^{15}N-incorporation into RuBisCO and phenolamides was determined after herbivory. At the time point when phenolamides had their maximum ^{15}N-incorporation, the ^{15}N-incorporation in RuBisCO LSU and SSU was only half the value (Manuscript III). If the phenolamides were acquiring their N from the degraded RuBisCO, the ^{15}N-incorporation levels would be expected to be the same or smaller. Since this is not the case, the hypothesis is unlikely to be correct.

As mentioned above, an alternative hypothesis is that N might be channeled into phenolamides instead of into RuBisCO by a preferential synthesis of the phenolamide precursor arginine in response to herbivory. Although RuBisCO and phenolamides initially have different ^{15}N-labeling, both compounds reached similar ^{15}N-labeling at the end of the experiment, so that both can be synthesized from the same amino acid pool. The ^{15}N-incorporation of phenolamides shortly after elicitation might be higher than of RuBisCO, due to a faster turnover of the metabolites compared to RuBisCO, which is assumed to have a turnover of 5-7 days depending on the species and experimental conditions (Esquivel et al., 1998; Simpson, 1981). A kinetic analysis of the ^{15}N-incorporation and quantity of amino acids together with RuBisCO and phenolamides within the same tissue would help to elucidate which amino acids are used for phenolamide and RuBisCO biosynthesis after herbivory. Furthermore, N allocation studies with labeled arginine and glutamine during herbivory would help to get further insights into the amino acid flux to both compounds.

Furthermore, the data of this thesis showed different dynamics of RuBisCO LSU and SSU in response to herbivory (Manuscript III) which has already been shown for other environmental stresses (Demirevska et al., 2009; Garciaferris and Moreno, 1994; Prioul and Reyss, 1987). In relative concentrations, plants invested less ^{15}N into RuBisCO LSU than SSU, and a kinetic analysis revealed that only N of RuBisCO LSU, and not N of RuBisCO SSU, deceased after elicitation, indicating a different role of both subunits in response to

herbivory (Manuscript III). Due to the higher abundance of RuBisCO LSU prior to elicitation, the majority is unlikely associated with RuBisCO SSU, thus being more unstable (Cohen et al., 2006) and more susceptible for degradation after herbivory. Therefore, RuBisCO LSU might provide an easily accessible N source after herbivory. Additionally, RuBisCO LSU has been shown to be more sensitive and degrade faster than RuBisCO SSU in response to oxidative stresses (Cohen, 2005; Desimone et al., 1996), which increase after herbivory (Imbiscuso et al., 2009). Therefore, oxidative stresses might be a further reason for RuBisCO LSU's higher dynamic after elicitation (Manuscicrpt III). These data suggest, that the majority of N released from RuBisCO after herbivory is provided by RuBisCO LSU.

A regulation of N-allocation through specific herbivores

In the ^{15}N-labeling experiment (Manuscript III), plants allocated relatively little N into nicotine compared to the total N-investment. These plants were elicited with oral secretion of the nicotine tolerant specialist *M. sexta* whose attack has been demonstrated to reduce investment into nicotine (Voelckel et al., 2001). In contrast, in a previous study using MeJA as a chemical elicitor, plants labeled after wounding demonstrated a rapid allocation of N into nicotine (Baldwin et al., 1998), leading to the hypothesis that plants have elicitor dependent N allocation responses. As herbivores differ in their elicitors (Alborn et al., 2007; Schmelz et al., 2006; Spiteller and Boland, 2003), these data lead to a second hypothesis that plants adapt their resource allocation depending on the type of attacking herbivore. Indeed, a similar mechanism has been found in tomato, which had a variable metabolite allocation in response to different herbivores (Steinbrenner et al., 2011). N allocation studies after the treatment with different elicitors, possibly of different herbivore groups, and the induction by oral secretion of specialists and generalists could help to answer this question.

The adaptation of resource allocation in response to a type of herbivore might be regulated by the herbivore specific induced defense signaling pathways. For example, in *N. attenuata* the generalist *Spodoptera exigua* and the specialist *M. sexta* have been demonstrated to induce different phytohormone profile patterns because of their different elicitor compositions (Diezel et al., 2009b). However, varying N-investment patterns in response to generalist and specialists could also be a secondary consequence of their specific induced defense mechanism instead of an active process. Resource allocation studies of transgenic plants with impaired phytohormone biosynthesis or/and signaling after induction with different oral secretions and elicitors could reveal details of the underlying mechanisms.

A new tool to study N flux and protein dynamics after herbivory

Within this thesis (Manuscript II) I describe the development of a new LC-MS^E based method to determine ^{15}N-incorporation into proteins simultaneously with their absolute quantity in isotopically labeled samples, and demonstrate its applicability for ecological studies (Manuscript III). The newly developed algorithm for ^{15}N-calculation allows the ^{15}N-determination of many peptides in a short period of time. Additionally, the quantification approach enables the absolute quantification of all proteins contained within one sample because it is based on an unlabeled universal internal standard protein. Nevertheless, the labeled peptides identification and their processing needs to carried out manually, which is time consuming. This is necessary because ^{15}N-labeling decreases the efficiency of peptide identification by database searching (Nelson et al., 2007), although this process is well established for peptides of natural isotopic distribution. Therefore, advancement and automation of the peptide identification, processing and extraction to the algorithm MoLE and a following automatic calculation of the TICs based on the ^{15}N-estimations of MoLE would further speed up the quantification procedure.

In Manuscript II and III, I demonstrate the applicability of the method to study ecological questions, while focusing on only a few of the proteins present within the analyzed samples. A number of additional proteins involved in carbohydrate metabolism, amino acid biosynthesis, ATP synthesis and regulatory proteins, such as 14-3-3 proteins, were identified (Ullmann-Zeunert, unpublished data). Recent studies indicate that some of the identified proteins might play role in herbivore defense. For example, the upregulation of genes encoding for carbohydrate transporters, and enzymes involved in carbohydrate synthesis, such as sucrose synthase, were found (Kim et al., 2011b). They are likely involved in abundance and allocation of carbohydrates, which have been shown to be altered after herbivore attack (Kim et al., 2011b; Steinbrenner et al., 2011). Furthermore, the expression of genes coding enzymes of tyrosine and phenolalanine biosynthesis was increased in response to herbivore treatment (Kim et al., 2011b), suggesting their regulatory function in amino acid biosynthesis in response to this biological stress. Also 14-3-3 proteins are likely involved in the signal transduction after herbivore attack because their coding genes and the proteins themselves are responsive to MeJA treatment and wounding (Chen et al., 2006; Roberts et al., 2002).The newly developed method combined with enzyme activity studies could help to investigate the role of these proteins in herbivore defense in more detail. Furthermore, by using extraction methods for membrane (Mirza et al., 2006) and/or cellwall proteins (Boudart et al., 2005), the

dynamic of carbohydrate transporters, other plasma membrane and cell wall proteins could be explored.

Synthesis

In this thesis, I demonstrate that early herbivory-induced defense signaling by SIPK and WIPK reduces the plant's growth and fitness through regulating JA and SA levels, but the mechanism is independent of photosynthesis and N assimilation. If resource allocation is involved in this process, still needs to be investigated. Although SIPK and WIPK are part of the induced herbivore response, they cause a constitutive growth reduction. In contrast, costs induced by phenolamide biosynthesis are expressed as changes in N allocation to growth (RuBisCO) instead of in a total growth reduction and could not be shown to be constitutive. The comparison of plants impaired in JA signaling with plants impaired in phenolamide biosynthesis revealed that the influence of phenolamide biosynthesis on N allocation in response to herbivory depends on the expression of *MYB8*. Overall, this thesis gave first evidence about the role of early defense signaling and metabolite biosynthesis in expressing trade-offs of induced herbivore defense and demonstrated that the underlying mechanisms are complex. Results of this work enable future studies to identify the components of the phenolamide biosynthesis pathway that regulate N allocation and the paramenter(s) which are influenced by JA and SA and responsible for the costs of SIPK and WIPK signaling. Furthermore, I used a new approach to study defense related trade-offs that can be applied to other experimental set-ups to study N but also C-investments into single compounds..

5.1 Summary

Plants and herbivores have coevolved for 350 million years. During that time plants developed a plastic defense mechanism which is only induced after herbivore feeding and is regulated by a sophisticated signaling cascade: Shortly after herbivore perception by insect-derived elicitors, mitogen acitvated protein kinase (MAPK) signaling is induced. Herbivory induced MAPKs, such as salicylic-acid protein kinase (SIPK) and wound-induced protein kinase (WIPK), activate the rapid accumulation of jasmonic acid (JA), which induces further downstream defenses. An example of a JA-induced defense is the biosynthesis of nitrogen (N)-intensive metabolites such as nicotine, caffeoylputrecine (CP) and dicaffeoylspermidine (DCS). The inducible defense has been proposed to have evolved as a cost-saving strategy, but depending on the environmental conditions the defense is still costly for the plant because defense requires resources that otherwise could be invested into growth or reproduction. These costs have been mainly shown by manipulating JA-levels, but costs induced upstream of JA still needed to be explored. Furthermore, little was known about the effect of early defense signaling on resource allocation.

In my thesis, the costs induced by SIPK and WIPK and their underlying mechanisms were analyzed for the first time. *N. attenuata* plants silenced in *SIPK* and *WIPK* were expected to grow better than WT as they have lower JA-levels. In contrast, experiments revealed that silencing of *WIPK* resulted in a growth benefit, but *SIPK* silenced plants grew worse than WT. Phytohormone profiling of leaves revealed higher salicylic acid (SA) levels of *SIPK* silenced plants, likely causing their growth phenotype by masking the JA-deficiency mediated growth benefit. Decreasing SA levels by genetic modification recovered the growth and fitness deficits of the plants, supporting the hypothesis. By further exploring the JA and SA mediated growth-defense trade-offs, no evidence was found that the trade-offs are mediated by changes in N assimilation or photosynthesis, indicating that resource allocation is involved as resource assimilation was unchanged.

Resource allocation is optimally studied by quantifying the investment of a fitness-limited resource into the different plant functions. Previous studies determined changes in growth by measuring biomass accumulation, but did not take into account that biomass does not discriminate among investments into compounds functioning in growth, storage or defense. Thus, plant biomass is not an accurate proxy for plant growth. In contrast, components of biomass accumulation that directly promote acquisition of resources for

growth, such as photosynthetic proteins, are a better measure of investment into growth. N is an important nutrient for the plant's growth and defense and thus a good resource to study growth-defense trade-offs in a common currency. In this thesis, N-intensive metabolites were defined as proxy for defense, and total soluble protein (TSP) and specifically ribulose-1,5-bisphosphatecarboxylase/oxygenase (RuBisCO) as proxy for growth.

Since a suitable method for determining simultaneously N-investment, ^{15}N-incorporation into proteins and their absolute quantity was lacking, in this thesis, the development of a new LC-MS^{E} based method for isotopically labeled protein quantification is described. Phosphorylase b spiked into leaf protein extracts could reliably be quantified. In addition the ^{15}N-incorporation of protein extracts of plants grown at different concentration of ^{15}N-labeled nitrate was determined with a high accuracy and precision. The experiments demonstrated the accurate analysis of multiple proteins of different abundance within one sample based on one universal internal standard protein. The applicability of the method to ecologically realistic set-ups was shown with plants grown in soil with unknown ^{15}N-incorporation levels. The analysis of proteins relevant for antiherbivore defense demonstrated that the approach is suitable to study protein dynamics and ^{15}N-flux elicited during herbivore-insect interaction.

Based on the new method, analysis of growth defense trade-offs and the direct comparison of N-investment into growth and defense in a common N currency were possible for the first time. In order to further disentangle effects of single induced defense responses and defense signaling on N allocation, transgenic lines impaired in JA-signaling and the biosynthesis of phenolamides (N-intensive defense metabolites), were used. In response to elicitation the N content of WT shoots decreased, but not of the transgenic lines. In a separate analysis of WT roots, the root's N-content increased after elicitation, indicating a transport of N from the shoot to roots. At the leaf scale the absolute N-pool size did not correlate with leaf size or changes in a single big N-pool, suggesting that herbivory also causes a reallocation of N among different compounds within the leaf. In WT leaves, TSP and RuBisCO showed a strong decrease, while the accumulation of CP, DCS and nicotine increased. Plants impaired in JA signaling had a similar, albeit attenuated phenotype. In contrast, transgenic lines impaired in phenolamide biosynthesis showed almost no decrease in protein amounts and only a small accumulation of nicotine. However, the decrease in the N-investment into proteins was much larger than N that was invested into defense metabolites. The data strongly suggest that phenolamide biosynthesis mediates the N allocation to proteins. Nevertheless,

^{15}N-flux studies revealed that N used for phenolamide biosynthesis was unlikely coming from RuBisCO.

The results of this thesis led to new open research questions that future work will have to answer. It is still unclear, if high SA values reduce the plants fitness by changing the resource allocation or by regulating other phytohormones. Secondly, it has to be elucidated which element of phenolamide biosynthesis pathway regulates N-distribution within the leaf after herbivory. Furthermore, I could identify multiple proteins which are hypothesized to play a role in the herbivore defense response, but which have not been studied yet due to the lack of a suitable method. The newly developed method of this work is going to be automated and will enable studying the role of those proteins and allow analysis in a high through put manner.

5.2 Zusammenfassung

Die Koevolution von Pflanzen und Pflanzenfressern existiert seit 350 Millionen Jahren. Während dieser Zeit entwickelten Pflanzen eine dynamische Verteidigungsstrategie, die nur nach Pflanzenfraß induziert wird und durch eine ausgeklügelte Signalkaskade reguliert wird. Kurz nach der Wahrnehmung des Insekts durch die Pflanze wird eine MAP-Kinase-Kaskade induziert. Im wilden Tabak, *Nicotiana attenuata,* stehen an dessen Ende SIPK und WIPK, zwei MAP-Kinasen, die die Synthese der Jasmonsäure (JA) aktivieren. Der schnelle Anstieg der JA-Konzentration induziert weitere Verteidigungsmechanismen wie zum Beispiel die Synthese von N-haltigen Sekundärmetaboliten wie Nicotine, Caffeoylputrecine (CP) oder Dicaffeoylspermidin (DCS). Obwohl sich diese Verteidigungsstrategie vermutlich Ressourcen spart, weil sie nur induziert wird, wenn sie benötigt werden, kann sie trotzdem nach Induktion abhängig von den Umweltbedingungen zu einem Fitnessnachteil der Pflanze führen. Nachteile für die Pflanze, die durch die Signalwirkung von JA entstehen, sind gut untersucht, aber Kosten, die in der Signalkaskade oberhalb von JA entstehen, waren unbekannt.

In meiner Doktorarbeit habe ich daher die Kosten, die durch die frühe Signalwirkung von SIPK und WIPK entstehen, und deren unterliegende Mechanismen untersucht. Gentechnisch veränderte Pflanzen mit reduzierter *SIPK* und *WIPK* Expression wurden erwartet besser zwachsen als der Wildtyp, weil sie geringere JA-Konzentrationen haben. In Experimenten wuchsen WIPK Pflanzen wie erwartet besser, aber SIPK Pflanzen waren kleiner als der Wildtyp. Phytohormonanalysen zeigten, dass Pflanzen mit reduzierter *SIPK* Expression konstitutiv hehrere Salicylsäurekonzentrationen (SA) haben, was zu dem Wachstumsphänotyp der SIPK Pflanzen geführt haben kann. Nach der Reduzierung der SA Konzentrationen durch genetische Modifikation wuchsen die SIPK Pflanzen fast so gut wie WIPK Pflanzen. Diese Ergebnisse deuten darauf hin, dass die hohen SA-Konzentrationen dazu führen, dass die Fitnessvorteile, die durch die geringeren JA-Konzentrationen hervorgerufen werden, überdeckt werden. Weitere Untersuchungen zeigten, dass die Wirkung von SA Konzentrationen auf den Wachstumsphänotyp nicht über Veränderungen der Photosynthese oder der Stickstoffassimilation erfolgt. Basierend auf den Daten folgerte ich, dass eine Signalweiterleitung durch MAP-Kinasen Kosten für die Pflanze verursacht. Diese Kosten werden durch JA und SA vermittelt, aber nicht durch ihre Wirkung auf Photosynthese oder Stickstoffassimilation beeinflusst. Weil Änderungen der Ressourcenbereitstellung als

Ursache ausgeschlossen werden können, könnten Unterschiede der Ressourcenverteilung für die Kosten verantwortlich sein

Ressourcenverteilung wird am besten durch die Quantifizierung der Investition einer Fitness-limitierenden Ressource in die verschiedenen Pflanzenfunktionen untersucht. Frühere Studien haben Wachstum in Form von Biomasse quantifiziert, haben dabei aber nicht berücksichtigt, dass Biomasse kein genaues Maß für Wachstum ist, weil dieser Parameter auch von Investitionen in die Speicherung und Verteidigung beeinflusst wird. Im Gegensatz dazu sind Bestandteile der Biomasse, die die Akquisition von Ressourcen fördern, wie zum Beispiel photosynthetische Proteine, ein besseres Maß für Investitionen in Wachstum. Stickstoff (N) ist ein wichtiger Nährstoff für das Wachstum und die Verteidigung der Pflanze und damit eine gute Ressource, um Trade-offs zwischen Wachstum und Verteidigung in einer gemeinsamen Währung zu untersuchen. Innerhalb dieser Arbeit wurden N-intensive Metabolite als Maß für die Verteidigung und das gesamte lösliche Protein (TSP) und speziell Ribulose-1 ,5-bisphosphate Carboxylase/Oxygenase (Rubisco) als Maß für das Wachstum definiert. Um die N-Investitionen in Wachstum zu messen, fehlte eine geeignete Methode zur gleichzeitigen Bestimmung der ^{15}N-Einbaurate und der absoluten Menge von Proteinen.

In dieser Arbeit wurde eine neuen LC-MS^{E} basierende Methode für die Quantifizierung isotopenmarkierter Proteine entwicklent, weil ein geeignetes Verfahren zur gleichzeitigen Bestimmung der N-Investition und ^{15}N-Einbaurate in Proteine fehlte. Phosphorylase b, das in bekannten Konzentrationen in Blattproteinextrakte gegeben wurde, konnte zuverlässig quantifiziert werden. Des Weiteren wurde die ^{15}N-Einbaurate von Proteinen mit unterschiedlichem bekanntem ^{15}N-Labeling mit einer hohen Genauigkeit und Präzision bestimmt. Darüber hinaus zeigten die Experimente, dass die genaue Analyse mehrerer Proteine unterschiedlicher Konzentration innerhalb einer Probe möglich ist, weil der Ansatz auf einem universellen internen Standardprotein basiert. Die Anwendbarkeit der Methode unter ökologische relevanten Bedingungen wurde mit in Erde gewachsenen Pflanzen getestet, die eine unbekannte ^{15}N-Einbaurate hatten. Darüber hinaus wurde mit der Analyse verteidigungsrelevanter Proteine gezeigt, dass der Ansatz zum Untersuchen von Proteindynamiken und N-Flussänderungen, die durch/während einer Pflanzen-Insekten-Interaktion entstanden sind, geeignet ist.

Durch die Anwendung der neuen Methode, war es zum ersten Mal möglich, Investitionen in Wachstum und Verteidigung in einer gemeinsamen Einheit zu vergleichen. Um die Auswirkungen der einzelnen Abwehrreaktionen auf die N-Verteilung besser

unterscheiden zu können, wurden transgene Pflanzen verwendet, die entweder in der JA-Synthese oder in der von Phenolamiden, N-intensive Verteidigungsmetabolite, beeinträchtigt waren. Nach simuliertem Pflanzfraß zeigten die Wildtypflanzen einen reduzierten N-Gehalt im Spross, nicht jedoch die transgenen Linien. Eine Einzelanalyse der Wildtypwurzel zeigte, einen Anstieg ihres N-Gehalts nach der Behandlung, was auf einen N-Transport vom Spross zur Wurzel nach Pflanzenfraß hindeutet. Der Stickstoffgehalt der Blätter korrelierte nicht mit ihrer Größe oder mit Änderungen eines einzigen großen N-Pools, was zeigt, dass Pflanzenfraß zu einer N-Umverteilung innerhalb der Blätter zwischen unterschiedlichen N-Pools führt. Eine Analyse der N-Pools ergab, dass im Wildtyp ein starker Rückgang der TSP- und RuBisCOgehalte von einem Anstieg der Verteidigungsmetabolite begleitet wurde. Pflanzen mit beeinträchtiger JA-Synthese hatten einen ähnlichen Phänotyp wie der Wildtyp nur leicht abgeschwächt. Im Gegensatz dazu zeigten Pflanzen mit geschwächter Phenolamidsynthese kaum eine Änderung nach simuliertem Pflanzenfraß. Dementsprechend gingen die N-Investition in Proteine mit einem Anstieg der N-Investition in die Verteidigungmetabolite zurück. Die Daten legen nahe, dass Phenolamidbiosynthese die N-Allokation zu Proteinen beeinflussen oder sogar reguliert. Dennoch zeigte ein ^{15}N-Flussexperiment, dass N für die Phenolamidbiosynthese unwahrscheinlich aus RuBisCO kommt.

Die Ergebnisse dieser Arbeit haben zu neuen offenen Fragen geführt, die Teil zukünftiger Arbeit sein werden. Es ist zum einen ungeklärt ob hohe SA-Werte die Fitness von Pflanzen über Änderungen der Ressourcenverteilung oder die Beeinflussung anderer Phytohormone beeinflussen. Zum anderen ist immer noch offen, welcher Teil der Phenolamidbiosynthese die N-Verteilung nach Pflanzenfraß reguliert. Des Weiteren wurden in dieser Thesis viele Proteine identifiziert, von denen angenommen wird, dass sie eine Rolle in der Pflanzenverteidigung spielen. Die in dieser Arbeit neu entwickelte Methode könnte vor allem nach ihrer geplanten Automatisierung dabei helfen, die Rolle dieser Proteine in der Verteidigung im Detail zu untersuchen.

6. References

Abiko, T., Wakayama, M., Kawakami, A., Obara, M., Kisaka, H., Miwa, T., Aoki, N. and Ohsugi, R. (2010). Changes in nitrogen assimilation, metabolism, and growth in transgenic rice plants expressing a fungal NADP(H)-dependent glutamate dehydrogenase (gdhA). *Planta (Berlin)* **232**, 299-311.

Agrawal, A. A., Lau, J. A. and Hamback, P. A. (2006). Community heterogeneity and the evolution of interactions between plants and insect herbivores. *Quarterly Review of Biology* **81**, 349-376.

Alborn, H. T., Hansen, T. V., Jones, T. H., Bennett, D. C., Tumlinson, J. H., Schmelz, E. A. and Teal, P. E. A. (2007). Disulfooxy fatty acids from the American bird grasshopper *Schistocerca americana*, elicitors of plant volatiles. *Proceedings of the National Academy of Sciences of the United States of America* **104**, 12976-12981.

Allmann, S., Halitschke, R., Schuurink, R. C. and Baldwin, I. T. (2010). Oxylipin channelling in *Nicotiana attenuata*: lipoxygenase 2 supplies substrates for green leaf volatile production. *Plant Cell and Environment* **33**, 2028-2040.

Baldwin, I. T. (1998). Jasmonate-induced responses are costly but benefit plants under attack in native populations. *Proceedings of the National Academy of Sciences of the United States of America* **95**, 8113-8118.

Baldwin, I. T. (1999). Inducible nicotine production in native *Nicotiana* as an example of adaptive phenotypic plasticity. *Journal of Chemical Ecology* **25**, 3-30.

Baldwin, I. T. (2001). An ecologically motivated analysis of plant-herbivore interactions in native tobacco. *Plant Physiology* **127**, 1449-1458.

Baldwin, I. T., Gorham, D., Schmelz, E. A., Lewandowski, C. A. and Lynds, G. Y. (1998). Allocation of nitrogen to an inducible defense and seed production in *Nicotiana attenuata*. *Oecologia* **115**, 541-552.

Baldwin, I. T. and Hamilton, W. (2000). Jasmonate-induced responses of *Nicotiana sylvestris* results in fitness costs due to impaired competitive ability for nitrogen. *Journal of Chemical Ecology* **26**, 915-952.

Baldwin, I. T., Karb, M. J. and Ohnmeiss, T. E. (1994a). Allocation of N-15 from nitrate to nicotine – production and turnover of a damaged-induced mobile defense. *Ecology* **75**, 1703-1713.

Baldwin, I. T. and Morse, L. (1994). up in smoke 2. germniation of *Nicotiana attenuata* in response to smoke-derived cues and nutrients in burned and unburned soils. *Journal of Chemical Ecology* **20**, 2373-2391.

Baldwin, I. T., Oesch, R. C., Merhige, P. M. and Hayes, K. (1993). Damage-induced root nitrogen-metabolism in *Nicotiana-sylvestris* - testing C/N predictions for alkaloid production. *Journal of Chemical Ecology* **19**, 3029-3043.

Baldwin, I. T. and Ohnmeiss, T. E. (1994). Coordiation of photosynthetic and alkaloidal responses to damage in uniducible and inducible *Nicotiana sylvestris*. *Ecology* **75**, 1003-1014.

Baldwin, I. T., Staszakkozinski, L. and Davidson, R. (1994b). Up in smoke .1. smoke-derived germination cues for postfire annual, *Nicotiana attenuata* Torr ex Watson. *Journal of Chemical Ecology* **20**, 2345-2371.

Berenbaum, M. R., Zangerl, A. R. and Nitao, J. K. (1986). Constraints on chemical coevolution-wild parsnips and the parsnip webworm. *Evolution* **40**, 1215-1228.

Blagbrough, I. S., Geall, A. J. and Neal, A. P. (2003). Polyamines and novel polyamine conjugates interact with DNA in ways that can be exploited in non-viral gene therapy. *Biochemical Society Transactions* **31**, 397-406.

Boudart, G., Jamet, E., Rossignol, M., Lafitte, C., Borderies, G., Jauneau, A., Esquerre-Tugaye, M. T. and Pont-Lezica, R. (2005). Cell wall proteins in apoplastic fluids of *Arabidopsis thaliana* rosettes: Identification by mass spectrometry and bioinformatics. *Proteomics* **5**.

Brand, W. A. (1996). High precision isotope ratio monitoring techniques in mass spectrometry. *Journal of Mass Spectrometry* **31**, 225-235.

Brenna, J. T., Corso, T. N., Tobias, H. J. and Caimi, R. J. (1997). High-precision continuous-flow isotope ratio mass spectrometry (vol 16, pg 227, 1997). *Mass Spectrometry Reviews* **16**, 382-382.

Brütting, C. (2012). The role of cytokinins in plant responses to insect attack. In *Fakultät für Biologie, Chemie und Geowissenschaften*, vol. Master, pp. 82. Bayreuth: Universität Bayreuth.

Chapin, F. S., Schulze, E. D. and Mooney, H. A. (1990). The ecology and economics of storage in plants. *Annual Review of Ecology and Systematics* **21**, 423-447.

Chen, F., L, i. Q., Sun, L. and He, Z. (2006). The rice 14-3-3 gene family and its involvement in responses to biotic and abiotic stress *DNA research* **13**, 53-63.

Chini, A., Fonseca, S., Fernandez, G., Adie, B., Chico, J. M., Lorenzo, O., Garcia-Casado, G., Lopez-Vidriero, I., Lozano, F. M., Ponce, M. R. et al. (2007). The JAZ family of repressors is the missing link in jasmonate signalling. *Nature* **448**, 666-U4.

Choi, J., Choi, D., Lee, S., Ryu, C. M. and Hwang, I. (2011). Cytokinins and plant immunity: old foes or new friends? *Trends in Plant Science* **16**, 388-94.

Cipollini, D. (2007). Consequences of the overproduction of methyl jasmonate on seed production, tolerance to defoliation and competitive effect and response of Arabidopsis thaliana. *New Phytologist* **173**, 146-153.

Cipollini, D. F. (2002). Does competition magnify the fitness costs of induced responses in *Arabidopsis thaliana*? A manipulative approach. *Oecologia* **131**, 514-520.

Cohen, I., Knopf, J. A., Irihimovitch, V., and Shapira, M. . (2005). A proposed mechanism for the inhibitory effects of oxidative stress on rubisco assembly and its subunit expression. *Plant Physiology* **137**, 738-746.

Cohen, I., Sapir, Y. and Shapira, M. (2006). A conserved mechanism controls translation of rubisco large subunit in different photosynthetic organisms. *Plant Physiology* **141**, 1089-1097.

Demirevska, K., Zasheva, D., Dimitrov, R., Simova-Stoilova, L., Stamenova, M. and Feller, U. (2009). Drought stress effects on Rubisco in wheat: changes in the Rubisco large subunit. *Acta Physiologiae Plantarum* **31**, 1129-1138.

Desimone, M., Henke, A. and Wagner, E. (1996). Oxidative stress induces partial degradation of the large subunit of ribulose-1,5-bisphosphate carboxylase/oxygenase in isolated chloroplasts of barley. *Plant Physiology* **111**, 789-796.

Diezel, C., von Dahl, C. C., Gaquerel, E. and Baldwin, I. T. (2009a). Different lepidopteran elicitors account for cross-talk in herbivory-induced phytohormone signaling. *Plant Physiology* **150**, 1576-1586.

Diezel, C., von Dahl, C. C., Gaquerel, E. and Baldwin, I. T. (2009b). Different lepidopteran elicitors account for cross-talk in herbivory-induced phytohormone signaling. *Plant Physiology* **150**, 1576-1586.

Doares, S. H., Narvaezvasquez, J., Conconi, A. and Ryan, C. A. (1995). Salicylic-acid inhibits synthesis of proteinase-inhibitors in tomato leaves induced by systemin and jasmonic acid. *Plant Physiology* **108**, 1741-1746.

Doherty, H. M., Selvendran, R. R. and Bowles, D. J. (1988). The wound response of tomato plants can be inhibited by aspirin and related hydroxybenzoic acids. *Physiological and Molecular Plant Pathology* **33**, 377-384.

Edreva, A. V. Y., Kardjieva, R., Hadjiiska, E. and Gesheva, E. (1995). Expression of phenylamides in abiotic stress conditions. *Bulgarian Journal of Plant Physiology* **21**, 15-23.

Ellis, R. J. (1979). Most abundant protein in the world. *Trends in Biochemical Sciences* **4**, 241-244.

Erb, M., Meldau, S. and Howe, G. A. (2012). Role of phytohormones in insect-specific plant reactions. *Trends in Plant Science* **17**, 250-259.

Esquivel, M. G., Ferreira, R. B. and Teixeira, A. R. (1998). Protein degradation in C3 and C4 plants with particular reference to ribulose bisphosphate carboxylase and glycolate oxidase. *Journal of Experimental Botany* **49**, 807-816.

Fan, S. C., Lin, C. S., Hsu, P. K., Lin, S. H. and Tsay, Y. F. (2009). The Arabidopsis nitrate transporter NRT1.7, expressed in phloem, is responsible for source-to-sink remobilization of nitrate. *Plant Cell* **21**, 2750-61.

Frost, C. J., Hunter, M.D. (2008). Herbivore-induced shifts in carbon and nitrogen allocation in red oak seedlings. *New Phytologist* **178**, 835-845.

Galis, I., Onkokesung, N. and Baldwin, I. T. (2010). New insights into mechanisms regulationg differential accumulation of phenylpropanoid-polyamine conjugates (PPCs) in herbivore-attached *Nicotiana attenuata* plants. *Plant Signaling & Behavior* **5**, 610-613.

Gaquerel, E., Heiling, S., Schoettner, M., Zurek, G. and Baldwin, I. T. (2010). Development and validation of a liquid chromatography-electrospray ionization-time-of-flight mass spectrometry method for Induced changes in *Nicotiana attenuata* leaves during simulated herbivory. *Journal of Agricultural and Food Chemistry* **58**, 9418-9427.

Garciaferris, C. and Moreno, J. (1994). Oxidative modification and breakdown of Ribulose-1,5-bisphosphate carboxylase oxygenase in *Euglena gracilis* by nitorgen starvation. *Planta* **193**, 208-215.

Giri, A. P., Wuensche, H., Mitra, S., Zavala, J. A., Muck, A., Svatos, A. and Baldwin, I. T. (2006). Molecular interactions between the specialist herbivore *Manduca sexta* (Lepidoptera, Sphingidae) and its natural host *Nicotiana attenuata*. VII. Changes in the plant's proteome. *Plant Physiology* **142**, 1621-1641.

Gomez-Maldonado, J., Avila, C., de la Torre, F., Canas, R., Canovas, F. M. and Campbell, M. M. (2004). Functional interactions between a glutamine synthetase promoter and MYB proteins. *Plant Journal* **39**, 513-526.

Gomez, S., Ferrieri, R. A., Schueller, M. and Orians, C. M. (2010). Methyl jasmonate elicits rapid changes in carbon and nitrogen dynamics in tomato. *New Phytologist* **188**, 835-844.

Gomez, S., Steinbrenner, A. D., Osorio, S., Schueller, M., Ferrieri, R. A., Fernie, A. R. and Orians, C. M. (2012). From shoots to roots: transport and metabolic changes in tomato after simulated feeding by a specialist lepidopteran *Entomologia Experimentalis Et Applicata* **144**, 101-111.

Gouw, J. W., Krijgsveld, J. and Heck, A. J. R. (2010). Quantitative proteomics by metabolic labeling of model organisms. *Molecular & Cellular Proteomics* **9**, 11-24.

Green, T. R. and Ryan, C. A. (1972). Wound-induced proteinase inhibitores in plant leaves - possible defense mechanism against insects. *Science* **175**, 776-&.

Halitschke, R. and Baldwin, I. T. (2003). Antisense *LOX* expression increases herbivore performance by decreasing defense responses and inhibiting growth-related transcriptional reorganization in *Nicotiana attenuata*. *Plant Journal* **36**, 794-807.

Halitschke, R., Gase, K., Hui, D. Q., Schmidt, D. D. and Baldwin, I. T. (2003). Molecular interactions between the specialist herbivore *Manduca sexta* (Lepidoptera, Sphingidae) and its natural host *Nicotiana attenuata*. VI. Microarray analysis reveals that most herbivore-specific transcriptional changes are mediated by fatty acid-amino acid conjugates. *Plant Physiology* **131**, 1894-1902.

Halitschke, R., Schittko, U., Pohnert, G., Boland, W. and Baldwin, I. T. (2001). Molecular interactions between the specialist herbivore *Manduca sexta* (Lepidoptera, Sphingidae) and its natural host *Nicotiana attenuata*. III. Fatty acid-amino acid conjugates in herbivore oral secretions are necessary and sufficient for herbivore-specific plant responses. *Plant Physiology* **125**, 711-717.

Hanik, N., Gomez, S., Schueller, M., Orians, C. M. and Ferrieri, R. A. (2010). Use of gaseous 13NH(3) administered to intact leaves of *Nicotiana tabacum* to study changes in nitrogen utilization during defence induction. *Plant Cell and Environment* **33**, 2173-2179.

Hegnauer, R. (1988). Biochemistry, distribution and taxonomic relevance of higher plant alkaloids. *Phytochemistry* **27**, 2423-2427.

Heiling, S., Schuman, M. C., Schoettner, M., Mukerjee, P., Berger, B., Schneider, B., Jassbi, A. R. and Baldwin, I. T. (2010). Jasmonate and ppHsystemin regulate key malonylation steps in the biosynthesis of 17-hydroxygeranyllinalool diterpene glycosides, an abundant and effective directdefense against herbivores in *Nicotiana attenuata*. *Plant Cell* **22**, 273-292.

Imai, K., Suzuki, Y., Mae, T. and Makino, A. (2008). Changes in the synthesis of rubisco in rice leaves in relation to senescence and N influx. *Annals of Botany* **101**, 135-144.

Imbiscuso, G., Trotta, A., Maffei, M. and Bossi, S. (2009). Herbivory induces a ROS burst and the release of volatile organic compounds in the fern *Pteris vittata* L. *Journal of Plant Interactions* **4**, 15-22.

Jansen, J. J., Allwood, J. W., Marsden-Edwards, E., van der Putten, W. H., Goodacre, R. and van Dam, N. M. (2009). Metabolomic analysis of the interaction between plants and herbivores. *Metabolomics* **5**, 150-161.

Jehmlich, N., Schmidt, F., Hartwich, M., von Bergen, M., Richnow, H. H. and Vogt, C. (2008). Incorporation of carbon and nitrogen atoms into proteins measured by protein-based stable isotope probing (Protein-SIP). *Rapid Communications in Mass Spectrometry* **22**, 2889-2897.

Jones, D. H. (1984). Phenylalanine ammonia-lyase: regulation of its induction and its role in plant development. *Phytochemistry* **23**, 1349-1359.

Kahl, J., Siemens, D. H., Aerts, R. J., Gabler, R., Kuhnemann, F., Preston, C. A. and Baldwin, I. T. (2000). Herbivore-induced ethylene suppresses a direct defense but not a putative indirect defense against an adapted herbivore. *Planta* **210**, 336-342.

Kallenbach, M., Alagna, F., Baldwin, I. T. and Bonaventure, G. (2010). *Nicotiana attenuata* SIPK, WIPK, NPR1 and fatty acid-amino acid conjugates participate in the induction of JA biosynthesis by affecting early enzymatic steps in the pathway. *Plant Physiology* **152**, 96-106.

Kant, M. R., Bleeker, P. M., Van Wijk, M., Schuurink, R. C. and Haring, M. A. (2009). Plant volatiles in defence. In *Plant Innate Immunity*, vol. 51 (ed. L. C. VanLoon), pp. 613-666.

Kant, M. R., Sabelis, M. W., Haring, M. A. and Schuurink, R. C. (2008). Intraspecific variation in a generalist herbivore accounts for differential induction and impact of host plant defences. *Proceedings of the Royal Society B-Biological Sciences* **275**, 443-452.

Karban, R. (1997). Induced responses to herbivory. Univ. of Chicago Press: Chicago u.a.

Karban, R. and Baldwin, I. T. (1997). Induced responses to herbivory.

Kaur, H., Heinzel, N., Schoettner, M., Baldwin, I. T. and Galis, I. (2010). R2R3-NaMYB8 Regulates the accumulation of phenylpropanoid-polyamine conjugates, which are essential for local and systemic defense against insect herbivores in *Nicotiana attenuata*. *Plant Physiology* **152**, 1731-1747.

Kerchev, P. I., Fenton, B., Foyer C.H., Hancock R.D. . (2011). Plant responses to insect herbivory: interactions between photosynthesis, reactive oxygen species and hormonal signalling pathways. *Plant Cell and Environment* **35**, 441-53.

Kessler, A. and Baldwin, I. (2001). Defensive function of herbivore-induced plant volatile emissions in nature. *Science* **291**, 2141-2144.

Kim, S.-G., Yon, F., Gaquerel, E., Gulati, J. and Baldwin, I. T. (2011a). Tissue specific diurnal rhythms of metabolites and their regulation during herbivore attack in a native tobacco, *Nicotiana attenuata*. *Plos One* **6**.

Kim, S. G., Yon, F., Gaquerel, E., Gulati, J. and Baldwin, I. T. (2011b). Tissue specific diurnal rhythms of metabolites and their regulation during herbivore attack in a native tobacco,
Nicotiana attenuata. *Plos One* **6**, e26264.

Kline, K. G. and Sussman, M. R. (2010). Protein quantitation using isotope-assisted mass spectrometry. In *Annual Review of Biophysics, Vol 39*, eds. D. C. Rees K. A. Dill and J. R. Williamson), pp. 291-308: Annual Reviews.

Koo, A. J. K. and Howe, G. A. (2009). The wound hormone jasmonate. *Phytochemistry* **70**, 1571-1580.

Krischik, V. A. and Denno, R. F. (1983). Individual, population, and geographic patterns in plant defense.

Laudert, D. and Weiler, E. W. (1998). Allene oxide synthase: a major control point in Arabidopsis thaliana octadecanoid signalling. *Plant Journal* **15**, 675-684.

Leon-Reyes, A., Spoel, S. H., De Lange, E. S., Abe, H., Kobayashi, M., Tsuda, S., Millenaar, F. F., Welschen, R. A. M., Ritsema, T. and Pieterse, C. M. J. (2009). Ethylene modulates the role of NONEXPRESSOR OF PATHOGENESIS-RELATED GENES1 in cross talk between salicylate and jasmonate signaling. *Plant Physiology* **149**, 1797-1809.

Leopold, A. C. (1955). Auxin and plant growth. Berkeley and Los Angeles: Universitiy of California.

Li, Q., Xie, QG., Smith-Becker, J., Navarre, DA., Kaloshian I. (2006). Mi-1-mediated aphid resistance involves salicylic acid andmitogen-activated protein kinase signaling cascades. *Molecular Plant-Microbe Interactions* **19**, 655-64.

Lindsey, K. and Yeoman, M. M. (1983). The relationship between growth-rate, differentiation and alkaloid accumulation in cell-cultures. *Journal of Experimental Botany* **34**, 1055-1065.

Liu , J., Horstman, H., Braun, E., Graham, M., Zhang, C., Navarre, D., Qiu, W., Lee, Y., Nettleton, D., Hill, J. et al. (2011). Soybean homologs of MPK4 negatively regulate defense responses and positively regulate growth and development. *Plant Physiology* **157**, 1363-78.

Lou, Y. G. and Baldwin, I. T. (2004). Nitrogen supply influences herbivore-induced direct and indirect defenses and transcriptional responses to *Nicotiana attenuata*. *Plant Physiology* **135**, 496-506.

Lynds, G. Y. and Baldwin, I. T. (1998). Fire, nitrogen, and defensive plasticity in *Nicotiana attenuata*. *Oecologia* **115**, 531-540.

MacCoss, M. J., Wu, C. C., Matthews, D. E. and Yates, J. R. (2005). Measurement of the isotope enrichment of stable isotope-labeled proteins using high-resolution mass spectra of peptides. *Analytical Chemistry* **77**, 7646-7653.

Makino, A., Mae, T. and Ohira, K. (1984). Relation between nitrogen and ribulose-1,5-bisphosphate carboxylase in rice leaves from emergence through senescence. *Plant and Cell Physiology* **25**, 429-437.

Meldau, S., Wu, J. and Baldwin, I. T. (2009). Silencing two herbivory-activated MAP kinases, SIPK and WIPK, does not increase *Nicotiana attenuata*'s susceptibility to herbivores in the glasshouse and in nature. *New Phytologist* **181**, 161-173.

Meloni, F., Lopes, N. P. and Varanda, E. M. (2012). The relationship between leaf nitrogen, nitrogen metabolites and herbivory in two species of Nyctaginaceae from the Brazilian Cerrado. *Environmental and Experimental Botany* **75**, 268-276.

Mendelsohn, R. and Balick, M. J. (1995). The value of undiscovered pharmaceuticals in tropical forests. *Economic Botany* **49**, 223-228.

Millard, P. (1988). The accumulation and storage of nitrogen by herbaceous plants . *Plant Cell and Environment* **11**, 1-8.

Millard, P. and Catt, J. W. (1988). The influence of nitrogen supply on the use of nitrate and ribulose 1,5 bisphosphate carboxylase oxygenase as leaf nitrogen sotres for growth of potato tubers (*Solanum tuberosum* L). *Journal of Experimental Botany* **39**, 1-11.

Mirza, S. P., Halligan, B. D., Greene, A. S. and Olivier, M. (2006). Improved method for the analysis of membrane proteins by mass spectrometry *Physiological Genomics* **30**, 89-94.

Mole, S. (1994). Trade-offs and constrains in plant herbivore defnse theory – a life-history perspective. *Oikos* **71**, 3-12.

Naseem, M., Philippi, N., Hussain, A., Wangorsch, G., Ahmed, N. and Dandekar, T. (2012). Integrated systems view on networking by hormones in *Arabidopsis* immunity reveals multiple crosstalk for cytokinin *The Plant Cell* **24**, 1793-1814.

Nelson, C. J., Huttlin, E. L., Hegeman, A. D., Harms, A. C. and Sussman, M. R. (2007). Implications of N-^{15}-metabolic labeling for automated peptide identification in *Arabidopsis thaliana*. *Proteomics* **7**, 1279-1292.

Ohnmeiss, T. E. and Baldwin, I. T. (1994). The allometry of nitrogen allocation to growth and an inducible defense under nitrogen limited growth. *Ecology* **75**, 995-1002.

Onkokesung, N., Gaquerel, E., Kotkar, H., Kaur, H., Baldwin, I. T. and Galis, I. (2012). MYB8 Controls inducible phenolamide levels by activating three novel hydroxycinnamoyl-coenzyme A:polyamine transferases in *Nicotiana attenuata*. *Plant Physiology* **158**, 389-407.

Orians, C. M., Thorn, A. and Gomez, S. (2011). Herbivore-induced resource sequestration in plants: why bother? *Oecologia* **167**, 1-9.

Pan C., F. C. R., Hyatt D., Bowen B. P., Hettich R. L., Banfield J. F. (2011). Quantitative tracking of isotope flows in proteomes of microbial communities. *Molecular & Cellular Proteomics*.

Pena-Cortes, H., Albrecht, T., Prat, S., Weiler, E. W. and Willmitzer, L. (1993). Aspirin prevents wound-induced gene-expression in tomato leaves by blocking jasmonic acid biosynthesis. *Planta* **191**, 123-128.

Pieterse, C. M. J., Leon-Reyes, A., Van der Ent, S. and Van Wees, S. C. M. (2009). Networking by small-molecule hormones in plant immunity. *Nature Chemical Biology* **5**, 308-316.

Pohnert, G., Jung, V., Haukioja, E., Lempa, K. and Boland, W. (1999). New fatty acid amides from regurgitant of lepidopteran (Noctuidae, Geometridae) caterpillars. *Tetrahedron* **55**, 11275-11280.

Prioul, J. L. and Reyss, A. (1987). Acclimation of ribulose bisophosphate carboxylase and messenger-RNAs to changing irridiance in adult tobacco-leaves-differential expression in LSU and SSU and messenger-RNA. *Plant Physiology* **84**, 1238-1243.

Redman, A. M., Cipollini, D. F. and Schultz, J. C. (2001). Fitness costs of jasmonic acid-induced defense in tomato, *Lycopersicon esculentum*. *Oecologia* **126**, 380-385.

Roberts, M. R., Salinas, J. and Collinge, D. B. (2002). 14-3-3 proteins and the response to abiotic and biotic stress *Plant Molecular Biology* **50**, 1031-1039.

Rubio, V., Bustos, R., Irigoyen, M., Cardona-Lo´pez, X., Rojas-Triana, M. and Paz-Ares, J. (2009). Plant hormones and nutrient signaling. *Plant Molecular Biology* **69**, 361-373.

Schaff, J. E., Mbeunkui, F., Blackburn, K., Bird, D. M., and Goshe, M. B. (2008). SILIP: a novel stable isotope labeling method for in planta quantitative proteomic analysis. *Plant Journal* **56**, 840-854.

Schmelz, E. A., Carroll, M. J., LeClere, S., Phipps, S. M., Meredith, J., Chourey, P. S., Alborn, H. T. and Teal, P. E. A. (2006). Fragments of ATP synthase mediate plant perception of insect attack. *Proceedings of the National Academy of Sciences of the United States of America* **103**, 8894-8899.

Schmelz, E. A., LeClere, S., Carroll, M. J., Alborn, H. T. and Teal, P. E. A. (2007). Cowpea chloroplastic ATP synthase is the source of multiple plant defense elicitors during insect herbivory. *Plant Physiology* **144**, 793-805.

Schobert, C. and Komor, E. (1992). Transport of nitrate and ammonium into the phloem and the xylem of *Ricinus communis* seedlings. *Plant Physiology* **140**, 306-309.

Schulze, W. X. and Usadel, B. (2010). Quantitation in mass-spectrometry-based proteomics. *Annual Review of Plant Biology, Vol 61* **61**, 491-516.

Schwachtje, J., Minchin, P. E. H., Jahnke, S., van Dongen, J. T., Schittko, U. and Baldwin, I. T. (2006). SNF1-related kinases allow plants to tolerate herbivory by allocating carbon to roots. *Proceedings of the National Academy of Sciences of the United States of America* **103**, 12935-12940.

Simms, E. L. and Fritz, R. S. (1990). The ecology and evolution of host-plant resistance to insects. *Trends in Ecology & Evolution* **5**, 356-360.

Simon, J., Gleadow, R. M. and Woodrow, I. E. (2010). Allocation of nitrogen to chemical defence and plant functional traits is constrained by soil N. *Tree Physiology* **30**, 1111-1117.

Simpson, E. (1981). Measurement of protein degradation in leaves of *Zea mays u*sing [3H acetic anhydride and tritiated water. *Plant Physiology* **67**, 1214-1219.

Snijders, A. P. L., de Vos, M. G. J. and Wright, P. C. (2005). Novel approach for peptide quantitation and sequencing based on N-^{15} and C-^{13} metabolic labeling. *Journal of Proteome Research* **4**, 578-585.

Spiteller, D. and Boland, W. (2003). N-(15,16-Dihydroxylinoleoyl)-glutamine and N-(15,16-epoxylinoleoyl)-glutamine isolated from oral secretions of lepidopteran larvae. *Tetrahedron* **59**, 135-139.

Spiteller, D., Oldham, N. J. and Boland, W. (2004). N-(17-phosphonooxylinolenoyl)glutamine and N-(17-phosphonooxylinoleoyl)glutamine from insect gut: The first backbone-phosphorylated fatty acid derivatives in nature. *Journal of Organic Chemistry* **69**, 1104-1109.

Stamp, N. (2003). Out of the quagmire of plant defense hypotheses. *Quarterly Review of Biology* **78**, 23-55.

Steinbrenner, A. D., Gomez, S., Osorio, S., Fernie, A. R. and Orians, C. M. (2011). Herbivore-induced changes in tomato (*Solanum lycopersicum*) primary metabolism: A whole plant perspective. *Journal of Chemical Ecology* **37**, 1294-1303.

Steppuhn, A., Gase, K., Krock, B., Halitschke, R. and Baldwin, I. T. (2004). Nicotine's defensive function in nature. *Plos Biology* **2**, 1074-1080.

Stitt, M. and Schulze, D. (1994). Does Rubisco control the rate of photosynthesis and plant-growth - an exercise in molecular ecophysiology. *Plant Cell and Environment* **22**, 583-621.

Takano, A., Kakehi, J. I. and Takahashi, T. (2012). Thermospermine is not a minor polyamine in the plant kingdom. *Plant Cell Physiology* **53**, 606-616.

Taubert, M., Jehmlich, N., Vogt, C., Richnow, H. H., Schmidt, F., von Bergen, M. and Seifert, J. (2011). Time resolved protein-based stable isotope probing (Protein-SIP) analysis allows quantification of induced proteins in substrate shift experiments. *Proteomics* **11**, 2265-2274.

Thines, B., Katsir, L., Melotto, M., Niu, Y., Mandaokar, A., Liu, G., Nomura, K., He, SY., Howe, GA., Browse, J. (2007). JAZ repressor proteins are targets of the SCF(COI1) complex during jasmonate signaling. *Nature* **448**, 661-65.

van Dam, N. M. and Baldwin, I. T. (1998). Costs of jasmonate-induced responses in plants competing for limited resources. *Ecology Letters* **1**, 30-33.

Van Dam, N. M. and Baldwin, I. T. (2001). Competition mediates costs of jasmonate-induced defences, nitrogen acquisition and transgenerational plasticity in *Nicotiana attenuata*. *Functional Ecology* **15**, 406-415.

Voelckel, C., Krugel, T., Gase, K., Heidrich, N., van Dam, N. M., Winz, R. and Baldwin, I. T. (2001). Anti-sense expression of putrescine N-methyltransferase confirms defensive role of nicotine in *Nicotiana sylvestris* against *Manduca sexta*. *Chemoecology* **11**, 121-126.

Vogt, T. (2010). Phenylpropanoid Biosynthesis. *Molecular Plant* **3**, 2-20.

Waie, B. and Rajam, M. V. (2003). Effect of increased polyamine biosynthesis on stress responses in transgenic tobacco by introduction of human S-adenosylmethionine gene. *Plant Science* **164**, 727-734.

Wang, D., Pajerowska-Mukhtar, K., Culler, A. and Dong, X. (2007). Salicylic acid inhibits pathogen growth in plants through repression of the auxin signaling pathway. *Current Biology* **17**, 1784-1790.

Winz, R. A. and Baldwin, I. T. (2001). Molecular interactions between the specialist herbivore *Manduca sexta* (Lepidoptera, Sphingidae) and its natural host *Nicotiana attenuata*. IV. Insect-induced ethylene reduces jasmonate-induced nicotine accumulation by regulating putrescine N-methyltransferase transcripts. *Plant Physiology* **125**, 2189-2202.

Wu, J. and Baldwin, I. T. (2010). New Insights into plant responses to the attack from insect herbivores. *Annual Review of Genetics, Vol 44*, vol. 44 eds. A. Campbell M. Lichten and G. Schupbach), pp. 1-24.

Wu, J., Hettenhausen, C., Meldau, S., Baldwin, IT. (2007). Herbivory rapidly activates MAPK signaling in attacked and unattacked leaf regions but not between leaves of *Nicotiana attenuata*. *Plant Cell* **19**, 1096-122.

Wünsche, H. (2005). Comparative proteome analysis of herbivore-induced *Nicotiana attenuata* leaves. Diploma thesis, pp. 91. Jena: Jena.

Xia, J., Zhao, H., Liu, W., Li, L. and He, Y. (2009). Role of cytokinin and salicylic acid in plant growth at low temperatures. *Plant Growth Regulation* **57**, 211-221.

Yan, J., Zhang, C., Gu, M., Bai, Z., Zhang, W., Qi, T., Cheng, Z., Peng, W., Luo, H., Nan, F. et al. (2009). The Arabidopsis CORONATINE INSENSITIVE1 protein is a jasmonate receptor. *Plant Cell* **21**, 2220-2236.

Yoshinaga, N., Aboshi, T., Ishikawa, C., Fukui, M., Shimoda, M., Nishida, R., Lait, C. G., Tumlinson, J. H. and Mori, N. (2007). Fatty acid amides, previously identified in caterpillars, found in the cricket *Teleogryllus taiwanemma* and fruit fly *Drosophila melanogaster* larvae. *Journal of Chemical Ecology* **33**, 1376-1381.

Zavala, J. A. and Baldwin, I. T. (2004). Fitness benefits of trypsin proteinase inhibitor expression in *Nicotiana attenuata* are greater than their costs when plants are attacked. *BMC Ecology* **4**, 11-Article No.: 11.

Zavala, J. A., Patankar, A. G., Gase, K. and Baldwin, I. T. (2004). Constitutive and inducible trypsin proteinase inhibitor production incurs large fitness costs in *Nicotiana attenuata*. *Proceedings of the National Academy of Sciences of the United States of America* **101**, 1607-1612.

7. Danksagung

Jetzt bin ich endlich am Ende meiner Doktorarbeit angekommen und möchte an dieser Stelle all den Menschen danken, die mich dabei unterstützt haben diesen Punkt zu erreichen. Rückblickend kann ich nur sagen, dass meine Beschreibung einer Doktorarbeit als emotionale Achterbahnfahrt voll zutrifft. Ich glaube am Anfang ist es gut, dass man nicht 100%ig weiß worauf man sich einlässt, aber abschließend kann ich auch bestätigen, dass es eine gute Erfahrung war. Man lernt während dieser Zeit nicht nur viel über die Wissenschaft, sondern man lernt auch sich selbst besser kennen und entwickelt sich als Mensch weiter. Ich danke all denen, die mich in diesem Entwicklungsprozess begleitet haben.

Ich danke **Ian Baldwin** dafür, dass er mir die Möglichkeit gegeben hat an einem solch großartigen Institut meine Doktorarbeit zu machen. Ohne die Zusammenarbeit der unterschiedlichen Abteilungen wäre meine Arbeit in dieser Form nicht möglich gewesen. Er stand mir stets mit Rat zur Seite und war selbst im fernen Utah über Email immer erreichbar.

Anschließen möchte ich **Karin Groten** danken, um die mich viele andere Doktoranden beneidet haben. Karin ist/war eine großartige Betreuerin, die es immer geschafft hat allem etwas Positives abzugewinnen, waren die Ergebnisse auch noch so schlecht. Sie stand mir immer mit Rat und Tat zur Seite und hat mich in allem unterstützt. Selbst in ihrer Elternzeit konnte sie nicht ganz von der Wissenschaft lassen.

Mariana Stanton danke ich für ihre Unterstützung, lustigen Kommentare und auch fachliche Kritik. Wir haben gerade in der Anfangszeit dieser Doktorarbeit viel gemeinsame Zeit im Gewächshaus verbracht und zahlreiche Pflanzen gemessen, verwundet und wieder gemessen und uns dabei öfters gefragt, warum wir eigentlich Biologie studiert haben. Aber ohne ihren Beitrag wäre das große Fluxprojekt nicht möglich gewesen.

Des Weiteren wäre ich ohne meinen Mann **Mike** und **meine Eltern** in manch einer Situation sehr mutlos gewesen. In Zeiten, in denen die Doktorarbeit kein Ende nehmen wollte und es einfach nicht vorwärts ging, waren sie für mich da. Meinem Mann möchte ich danken, dass er nach Deutschland gekommen ist, so dass ich hier am MPI meine Doktorarbeit machen konnte. Er hat mich in dieser Zeit hoch jauchzend und tief betrübt erlebt, war aber immer für mich da und hat mir geholfen den Horizont nicht t aus den Augen zu verlieren. Außerdem hat er mich während des Schreibprozesses dieser Arbeit geduldig mit seinem Englisch unterstützt. Meinen Eltern haben mir Kraft gegeben und mir sehr dabei geholfen, Fructose aus meiner Nahrung zu eliminieren, was oft nicht einfach war. Von der Diagnose bis zur Umstellung war

es ein weiter Weg, aber ohne meine Eltern hätte ich manchmal nicht die Kraft gehabt ihn weiter zu gehen. Mein Mann hat mir in dieser schweren Zeit geholfen, indem er alle meine Launen ausgehalten hat und für mich da war, wenn mich der Zucker mal wieder außer Gefecht gesetzt hatte.

Ales Svatos, Alex Muck und **Natalie Wielsch** danke ich für ihre Unterstützung, die zur Entwicklung einer genialen Methode geführt hat. Es war ein langer steiniger Weg mit einigen Umwegen, der aber am Ende zum Ziel geführt hat. Schade, dass ich die Automatisierung der Methode nicht mehr mitbekomme, denn sie hat viel Potential.

Stefan Batram möchte ich für seine Hilfe bei den IRMS-Messungen danken. Er hat mir dabei geholfen tausende von Samples zu starten und auszuwerten. Zusätzlich war er immer für eine fachliche Diskussion offen und hatte für unsere IRMS-Ansätze gute Ideen.

Stefan Meldau war immer für fachliche Dikussionen zu haben und unsere Zusammenarbeit hat schließlich zum Abschluss eines Projektes mit vielen vielen Pflanzen geführt. Ihm und vor allem **Christian Hettenhausen** danke ich für gute Kommentare, die zur Verbesserung dieser Arbeit geführt haben.

Ich möchte außerdem **Danny Kessler**, **Celia Diezel**, **Martin Schäfer** und einigen anderen danken mit denen ich über die Jahre das Büro geteilt habe und mit denen es nie langweilig wurde. Nicht zu vergessen sind **die Gärtner**, die in den Jahren bestimmt an die 1000 oder mehr Pflanzen für mich groß gezogen und betreut haben. Auch **Stefan Schuck** und **Melkamu Woldemarian** müssen hier erwähnt werden, denn im Institut und privat hatten wir viel Spaß und man konnte das Labor mal vergessen. Ich möchte auch all den anderen Menschen danken, die mich währen dieser Zeit begleitet haben, und hier nicht namentlich erwähnt sind. Dazu gehören alle Mitglieder der **Abteilung Molekulare Ökologie** und meine **Freunde aus Jena**, **Osnabrück** und dem **Rheinland**.

8. Selbständigkeitserklärung

Ich erkläre, entsprechend § 5 Abs. 3 der Promotionsordnung der Biologisch-Pharmazeutischen Fakultät der Friedrich Schiller Universität Jena, dass mir die geltende Promotionsordnung der Fakultät bekannt ist. Ich habe die Dissertation selbstständig und nur unter Zuhilfenahme der im Text angegebenen Quellen und Hilfsmittel angefertigt, wobei alle von Dritten übernommenen Textabschnitte entsprechend gekennzeichnet wurden. Personen, die zu den Experimenten, der Datenauswertung oder der Verfassung der einzelnen Manuskripte beigetragen haben, sind in den „Manuscript Overviews“ unter Angabe ihrer jeweiligen Beitrage zur Arbeit aufgeführt, oder werden, im Falle von Beitragen geringeren Ausmaßes, in den Danksagungen am Ende der entsprechenden Manuskripte genannt. Gemäß Anlage 5 zum § 8 Abs. 3 wurde die Beschreibung des von mir geleisteten Eigenanteils von Prof. Ian T. Baldwin, dem Betreuer der Dissertation, mit Unterschrift bestätigt und der Fakultät bei Einreichung dieser Dissertation vorgelegt. Ich habe weder die Hilfe eines Promotionsberaters in Anspruch genommen, noch haben Dritte unmittelbar oder mittelbar geldwerte Leistungen von mir für Arbeiten erhalten, die im Zusammenhang mit dem Inhalt der vorgelegten Dissertation stehen. Diese Dissertation wurde von mir niemals zuvor als Prüfungsarbeit für eine staatliche oder andere wissenschaftliche Prüfung eingereicht. Desweiteren habe ich keine in wesentlichen Teilen ähnliche oder eine andere Abhandlung bei einer anderen Hochschule als Dissertation eingereicht.

Lynn Ullmann-Zeunert, Jena den